BERICHTE
aus dem Fachbereich Geowissenschaften
der Universität Bremen

No. 263

Bohrmann, G., Spiess, V., B. Böckel, A. Boetius, M. Boles, M. Brüning, S. Buhmann, C. Cruz Melo, M. Dalthorp-Moorhouse, K. Dehning, F. Ding, E. Escobar-Briones, K. Enneking, J. Felden, N. Fekete, T. Freidank, A. Gassner, A. Gaytan, J. Geersen, K.-U. Hinrichs, J. Hohnberg, S. Kasten, H. Keil, S. Klar, I. Klaucke, J. Kuhlmann, I. MacDonald, G. Meinecke, C. Mortera, T. Naehr, N. Nowald, C. Ott, J. Pacheco Muñoz, J. R. Pelaez, V. Ratmeyer, J. Renken, M. Reuter, V. Sackmann, H. Sahling, F. Schubotz, F. Schewe, S. Stephan, J. Thal, A. Trampe, T. Truscheit, M. Viehweger, T. Wilhelm, G. Wegner, F. Wenzhöfer, M. Zabel

CRISTOBAL - TAMPICO, 14 MARCH - 31 MARCH 2006, TAMPICO - BRIDGETOWN, 3 APRIL - 25 APRIL 2006. FLUID SEEPAGE IN THE GULF OF MEXICO.

Berichte, Fachbereich Geowissenschaften, Universität Bremen, No. 263, 119 pages, Bremen 2008

ISSN 0931-0800

The "Berichte aus dem Fachbereich Geowissenschaften" are produced at irregular intervals by the Department of Geosciences, Bremen University.

They serve for the publication of experimental works, Ph.D.-theses and scientific contributions made by members of the department.

Reports can be ordered from:

Monika Bachur

Forschungszentrum Ozeanränder, RCOM

Universität Bremen

Postfach 330 440

D 28334 BREMEN

Phone: (49) 421 218-65516

Fax: (49) 421 218-65515

e-mail: MBachur@uni-bremen.de

Citation:
Bohrmann, G., Spiess, V., and cruise participants
Report and preliminary results of R/V Meteor Cruise M67/2a and 2b, Balboa - Tampico - Bridgetown,
15 March - 24 April, 2006. Fluid seepage in the Gulf of Mexico.
Berichte, Fachbereich Geowissenschaften, Universität Bremen, No. 263, 119 pages. Bremen, 2008.

ISSN 0931-0800

R/V METEOR
Cruise Report M67/2

Fluid Seepage in the Southern Gulf of Mexico (Campeche Bay)

M67, Leg 2a
Cristobal – Tampico, 14 March - 31 March, 2006

M67, Leg 2b
Tampico – Bridgetown, 3 April – 25 April 2006

Cruise within the framework of the DFG financed Research Center Ocean Margins, project area E: "Fluid and gas seepage"

Edited by
Gerhard Bohrmann, Volkhard Spiess and Greta Ohling

The cruise was performed by
MARUM Center for Marine Environmental Sciences

Universität Bremen

marum

Table of Contents **Page**

Preface

R/V METEOR Cruise M67/2 investigated fluid and gas venting in relation to asphalt volcanism in the southern Gulf of Mexico. The expedition was strongly related to the previous cruise of R/V SONNE SO-174, during which asphalt volcanoes have been found for the first time (MacDonald et al. 2004). The R/V METEOR cruise was separated into two legs (Legs 2a and 2b) because of the heavy scientific equipment. Both legs were planned together as part of research area E of the DFG Research Center Ocean Margins at the University of Bremen.

During Leg M 67/2a selected knolls were planned to map by high-resolution multichannel seismic and DTS sidescan sonar. The focus of Leg M 67/2b was the detailed investigation using ROV QUEST on the asphalt deposits of the seafloor. With the help of the ROV the asphalt flows will be mapped and sampled in great detail in order to reveal how asphalt volcanoes originate and what relevance these structures have in the light of their geological setting.

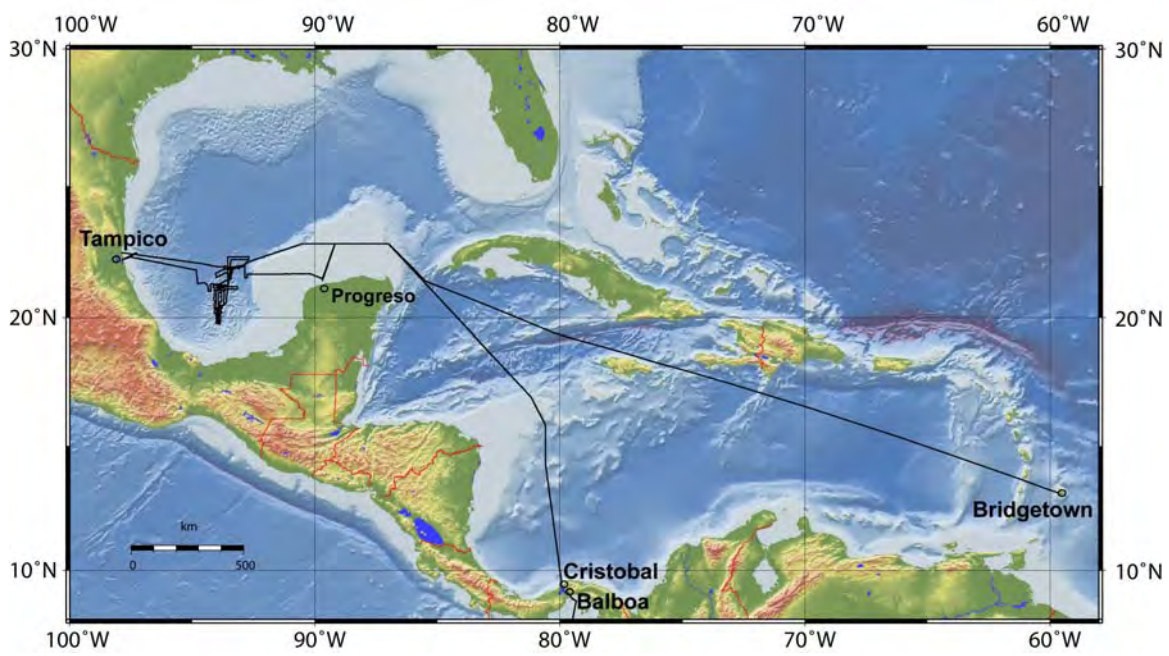

Fig. 1: Cruise track of R/V METEOR cruise M67/2 (March 14 – April 25, 2006; Cristobal – Tampico – Bridgetown).

Twenty-two morphological highs (knolls) have been mapped in the Campeche Bay off Mexico at water depth of more than 3000 m during R/V SONNE 174 in 2003 (Bohrmann und Schenck 2004). They are connected to salt diapirism which is related to massive salt deposits of Jurassic age. Yet unknown processes have shaped the morphology of the knolls, which have crater-like structures and show signs of mass wasting processes. Towed TV-sled observations during the former R/V SONNE cruise at two knolls revealed evidence for lava-like asphalt flows with different generations of asphalt flows and chemosynthetic communities. The origin and processes leading to these asphalts at the seafloor can not be explained by any of the known mechanisms leading to fluid seepage, i.e. mud volcanism or diapirism.

The investigation of the asphalt volcanism took place in a collaborative action between Germany, Mexico (Prof. Dr. Elva Escobar Briones, UNAM) and the USA (Prof. Dr. Ian MacDonald, TAMU). The national petroleum company of Mexico PEMEX (Petróleos Mexicanos) helped in the preparation of scientific targets. The cruise and the research programs were planned,

coordinated and carried out by the Department of Earth Sciences and the MARUM Center for Marine Environmental Sciences of the University of Bremen.

Fig. 2: R/V METEOR during Cruise M67/2 in the Campeche Bay in Mexican Waters (left). Positioning of the multichannel seismic streamer on the working deck (right).

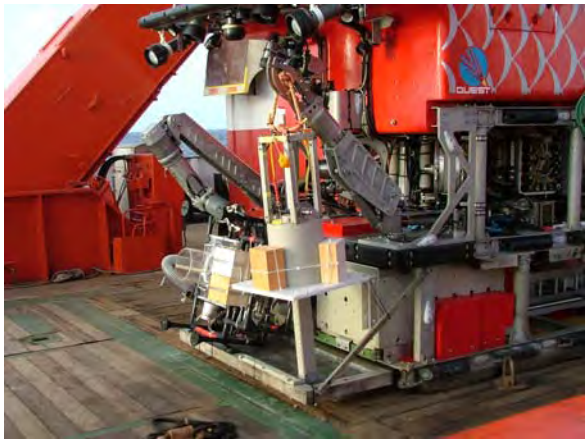

Fig. 3: ROV QUEST heavily laden by scientific tools on the working deck before deployment (left). Sediment sampling of a gravity core in the core lab onboard of R/V METEOR (right).

The scientific parties aboard R/V METEOR M67/2a and 2b gratefully acknowledge the friendly cooperation and efficient technical assistance of Martin Kull and his crew. We are indebted to the Federal Foreign Ministry (Auswärtiges Amt; Referat 405; Wolfgang Mahrle) in Berlin and the German diplomatic representatives in Mexico, who helped to clear necessary allowances from national authorities. Special thanks go to Arne Wolf at the German Embassy in Mexico for his support to achieve the permission to carry out the research in Mexican waters. Arne Wolf sadly died at the age of 49 years on February 27, 2008 in Hongkong. His visit and participation in the reception on Sunday April 2 held in the harbour of Tampico onboard of R/V METEOR will stay in our mind.

We also appreciate the most valuable help of Captain Michael Berkenheger at the Leitstelle METEOR, Hamburg and both shipping companies, RF Reederei Forschungsgemeinschaft GmbH, Bremen and Reederei F. Laeisz GmbH, Bremerhaven. Shipping operator RF was responsible in 2005 for planning and implementation and the new shipping operator F. Laeisz took over the vessel with the year 2006. Financial support for the cruise was supplied by the Deutsche Forschungsgemeinschaft (Research Center 15).

Table 1: Personnel aboard R/V METEOR M67/2.

Name	Discipline	Legs	Institute
Böckel, Babette	Water column work	a	RCOM, Bremen
Boetius, Antje	Biogeochemistry	b	MPI, Bremen
Bohrmann, Gerhard	Chief scientist	a+b	RCOM, Bremen
Boles, Marshall	Geology	b	UOG, USA
Brüning, Markus	Geophysics	a+b	RCOM, Bremen
Buhmann, Sitta	ROV team	b	RCOM, Bremen
Cruz Melo, Carlos	Water column work	a	IG-UNAM, Mexico
Dalthorp-Moorh., Margaret	Geology	a	TAMU, USA
Dehning, Klaus	ROV team	b	RCOM, Bremen
Ding, Feng	Geophysics	a+b	RCOM, Bremen
Escobar-Briones, Elva	Biology	a+b	ICML-UNAM, Mexico
Enneking, Karsten	Geochemistry	a	RCOM, Bremen
Felden, Janine	Biogeochemistry	b	MPI, Bremen
Fekete, Noemi	Geophysics	a	RCOM, Bremen
Freidank, Thorben	Geophysics	a	RCOM, Bremen
Gassner, André	Geochemistry	b	RCOM, Bremen
Gaytan, Adriana	Biology	b	ICML-UNAM, Mexico
Geersen, Jacob	Geophysics	a	RCOM, Bremen
Hinrichs, Kai-Uwe	Biogeochemistry	b	RCOM, Bremen
Hohnberg, Jürgen	Geology	b	RCOM, Bremen
Kasten, Sabine	Geochemistry	a+b	AWI, Bremerhaven
Keil, Hanno	Geophysics	a	RCOM, Bremen
Klar, Steffen	ROV team	b	RCOM, Bremen
Klaucke, Ingo	Geophysics	a	IFM-GEOMAR, Kiel
Kuhlmann, Jannis	Geophysics	a	RCOM, Bremen
MacDonald, Ian	Geology	b	TAMU, USA
Meinecke, Gerrit	ROV team	b	RCOM, Bremen
Mortera, Carlos	Geophysics	a	IG-UNAM, Mexico
Naehr, Thomas	Geology	b	TAMU, USA
Nowald, Nicolas	ROV team	b	RCOM, Bremen
Ott, Carola	Water column work	a	RCOM, Bremen
Pacheco Muñoz, Jorge	Geophysics	b	PEMEX/IMP, Mexico
Pelaez, Juan Ramòn	Geophysics	a	UNAM, Mexico
Ratmeyer, Volker	ROV team	b	RCOM, Bremen
Renken, Jens	Geophysics	a	RCOM, Bremen
Reuter, Michael	ROV team	b	RCOM, Bremen
Sackmann, Volker	Technician	a	STN, Bremen
Sahling, Heiko	Geology	b	RCOM, Bremen
Schubotz, Florence	Biogeochemistry	b	RCOM, Bremen
Schewe, Felix	Geology	a	RCOM, Bremen
Spiess, Volkhard	Chief Scientist	a+b	RCOM, Bremen
Stephan, Sebastian	Geophysics	a	RCOM, Bremen
Thal, Janis	Geology	a	RCOM, Bremen
Trampe, Anna	Geophysics	a	RCOM, Bremen
Truscheit, Thorsten	Meteorology	a+b	DWD, Hamburg
Viehweger, Marc	ROV team	b	MPI, Bremen
Wilhelm, Torsten	Geochemistry	a	AWI, Bremerhaven
Wegner, Gunter	Biogeochemistry	b	MPI, Bremen
Wenzhöfer, Frank	Biogeochemistry	b	MPI, Bremen
Zabel, Matthias	Geochemistry	b	RCOM, Bremen

AWI	Alfred-Wegener-Institut für Polar- und Meeresforschung, 27570 Bremerhaven, **Germany**
DWD	Deutscher Wetterdienst, Geschäftsfeld Seeschifffahrt, Bernhard-Nocht-Straße 76, 20359 Hamburg, **Germany**
ICML-UNAM	Instituto de Ciencias del Mar y Limnología, Universidad Nacional Autónoma de México, A.P. 70-305 Ciudad Universitaria, 04510 México, **D.F. México**
IFM-GEOMAR	Leibniz-Institut für Meeresforschung an der Christian-Albrechts Universität, Wischhofstr. 1-3, 24148 Kiel, **Germany**
IG-UNAM	Instituto de Geofísica, Universidad Nacional Autónoma de México, Ciudad Universitaria, 04510 México, **D.F. México**
MPI	Max-Planck-Institut für Marine Mikrobiologie, Celsiusstr. 1, 28359 Bremen, **Germany**
PEMEX/IMP	PEMEX Exploración y Explotación/Instituto Mexicano del Petróleo, **México**
RCOM/MARUM	MARUM / DFG-Forschungszentrum Ozeanränder University of Bremen, Postfach 30440, 28334 Bremen, **Germany**
STN	STN Elektronik GmbH, Sebaldsbrücker Heerstr. 235, 28309 Bremen, **Germany**
TAMU	Texas A&M University Corpus Christi, 6300 Ocean Dr. PALS ST320, Corpus Christi, TX 78412, **USA**
UOG	Department of Marine Sciences, University of Georgia, Athens, GA 30602-3636, **USA**

Fig. 4: Scientists, technicians and guests sailed onboard R/V METEOR during M67/2a.

Fig. 5: Scientists and technicians from Germany, Mexico and USA sailed onboard R/V METEOR during M67/2b.

Table 2: Crew members onboard R/V METEOR.

Name	Work onboard	Name	Work onboard
Martin Kull	Master	Kai Rabenhorst	A.B.
Walter Baschek	Chiefmate	Günther Ventz	A.B.
Uwe-Klaus Klimek	1st Officer	Günther Stängl	A.B.
Haye Diecks	2nd Mate	Manfred Gudera	A.B.
Anke Walther	Surgeon	Bernd Neitzsch	A.B.
Peter Neumann	Chief Engineer	Pjotr Bussmann	A.B.
Thomas Fischer	2nd Engineer	Michael Both	Chief Steward
Ralf Heitzer	3rd Engineer	Rainer Götze	2nd Steward
Ernst Krabbe	Electrician	Jan Hoppe	2nd Steward
Gerhard Lange	Motorman	Peter Eller	2nd Steward
Hermann Rademacher	Motorman	Franz Grün	Chief Cook
Frank Sebastian	Motorman	Willi Braatz	2nd Cook
Jörg Walter	Chief Electr. Engineer	Ulrich Schreiber	Nautical Assistant
Werner Dimmler	Electr. Engineer	Thomas Weber	Technical Assistant
Katja Pfeiffer	System Manager	Arne Simmen	Trainee
Werner Sosnowski	Fitter	Stefan Möller	Trainee
Karl-Heinz Lohmüller	Bosun	Nan Sng Lee	Laundryman

Participating Companies

Reederei F. Laeisz GmbH	"Haus der Schifffahrt", Lange Str. 1a, D-18055 Rostock, **Germany**
FIELX	Gesellschaft für wissenschaftliche Datenverarbeitung mbH, Schifferstrasse 10 -14, 27568 Bremerhaven, **Germany**

1 Research Program

(G. Bohrmann)

Based on the instruments used for the investigation of the asphalt volcanoes in the Campeche Bay the research program was splitted into two sub-legs 2a and 2b. Sub-leg 2a was planned to use geophysical methods like multibeam mapping, seismic and sediment echosounding to get more information about the distribution of asphalt volcanism. Bathymetric mapping of the Campeche Knolls was a first target of the expedition and the area south and southwest of the so-far mapped region was supposed to be covered. This work should reveal whether or not other knolls show also evidence for crater-like structures and mass wasting process, which may be indicative for the potential of asphalt occurrences. It was planned to study three working areas as representatives for a larger area in detail. The selection of the areas was based on bathymetry and seismic data as well as satellite data of oil slicks and the unpublished work provided by our colleagues from TAMU. The seismic overview profiles should provide important information as to which area will be selected for detailed seismic surveys. Detailed surveys were planned in two or three areas. The survey strategy depended on the dimension of the structures and was adjusted on board. For the selection of targets the multibeam mapping will provide additional information. The DTS sidescan sonar survey was planned to cover knolls with pronounced crater-like structures and slide scars. A major objective was to map, beside the mass wasting processes, the asphalt flows. DTS deployments were planned to alternate with seismic work and/or sampling. At selected locations gravity corer were planned to deploy in order to test whether or not the sediments are influenced by the flow of asphalt or hydrocarbon seepage.

The work in the water column included the mapping of hydroacoustic anomalies with echosounder and the measurement of hydrocarbons and their isotopes based on samples taken by a CTD equipped with a rosette. These investigations should reveal which knolls are actively seeping hydrocarbons at present. Furthermore, the investigations should answer what is the fate of hydrocarbons in the water column? Are they oxidized or diluted? Do they reach, finally, the sea surface and the atmosphere?

The ROV QUEST was planned to serve during sub-leg 2b as a platform for surveys, mapping and sampling as well as for launching and recovering of autonomous tools. The deployment of the ROV QUEST at the asphalt flows was of fundamental relevance in order to reveal how these systems developed. Individual flows and faults were mapped in order to find the conduits through which the asphalt escaped. Flows of different structures and ages were mapped to identify the dynamic of the system and the evolution through time. With the ROV-mounted cameras details of the seafloor seepage were planned to document in order to provide basic information about sampling strategies and in situ measurements. The ROV was used to sample, survey and conduct measurements on a very small scale. Besides temperature measurements, samples of asphalts, chemosynthetic organisms and sediment cores were planned to sample. Another important aspect was covered by autonomous tools. These techniques carry out measurements of chemical gradients and fluid flow as well as incubation experiments. In order to transport the autonomous tools to the seafloor and samples back to the ship an elevator was developed. TV-guided multicorer (TV-MUC) and gravity corer (GC) were used to recover all those samples, which are difficult to be obtained by ROV.

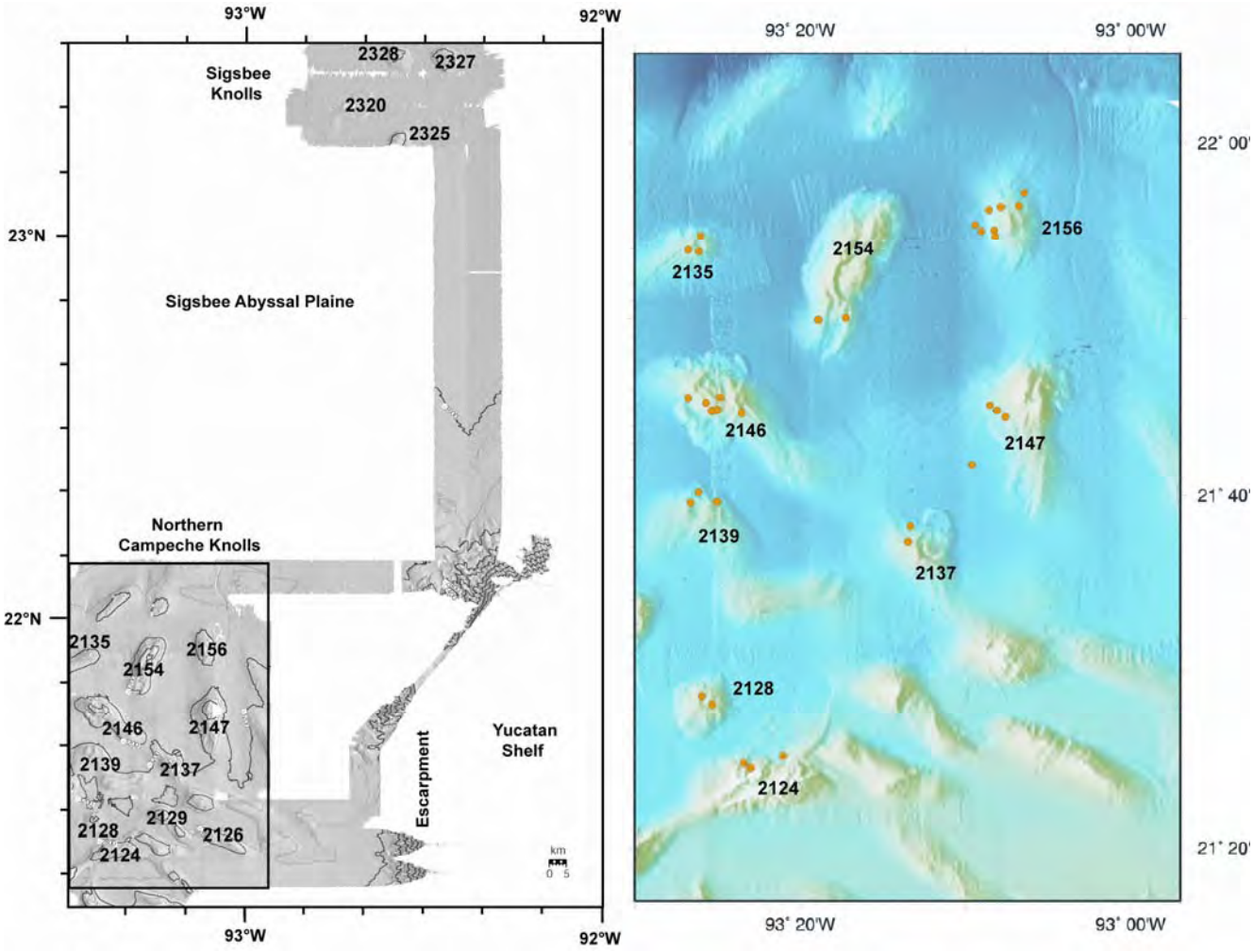

Fig. 6: High-resolution bathymetry obtained during R/V SONNE Cruise SO 174-2. Overview map (left) and detail map (right) of the northern Campeche Knolls. The knolls are numbered according to the geographic position of their highest summits. The locations of oil slicks at the sea surface are indicated as dots. Those were detected by RADASAT-Satellite pictures (I. MacDonald unpublished) and indicate that oil seepage occurs at most knolls.

2 Cruise Narrative and Weather

2.1 Cruise Narrative

(G. Bohrmann, V. Spiess)

The R/V METEOR sailed from Pier 8 in Cristobal harbor, Panama at 6 pm on March 15 to transit through the Caribbean Sea to the Gulf of Mexico. The time required by the R/V METEOR in the port of Cristobal was short after crossing the Panama Canal through Balboa on the Pacific side; time at which 5 participants of the Cruise M67/2 had boarded the ship. The crossing through the Panama Canal started on March 14. The METEOR reached the Caribbean Sea after leaving the last lock at Gatun on March 15 to come alongside the port of Cristobal. A container of the previous cruise leg belonging to the research institution 574 in Kiel was unloaded and 5 new containers from Bremen were loaded. All 27 scientists and technicians from Germany, Mexico, Colombia, China, Hungary and the US arrived onboard after midday and in this way we were able to sail from the port of Cristobal on the same day as planned.

The over four day transit period into the Gulf of Mexico was used on board to set the laboratories, and in part to feel acquainted with the new techniques on the R/V METEOR and in the frame of daily thematic seminars and work meetings to introduce the upcoming research activities to all participants. In the first week most of the time of the M67/2a cruise was spent in activities on the harbor, transit and preparation to collect and analyze samples. The second week was characterized by a dense program that included the geophysical survey with multichannel seismic, sidescan sonar, bathymetry and sediment, followed by the sampling of the water column and the seafloor.

The CTD with a 22 bottle rosette was the first equipment used on March 20 to support nanoplankton studies in the top 250 m depth in the water column and to determine the Barium tracer and the dissolved methane concentration in the deeper layers, its descent was used to calibrate the swath mapping echosounder with a sound profile characteristic for the Campeche Bay as well. This first equipment was the only successful action of the cruise for a while. The fate of the days onboard not only seemed to be bewitched by technical difficulties and misshapen but it seemed problem-bearing for the gadget's first action. An intensive search for problems included the contacts, the cables and the software of all, the multichannel seismic, the sidescan sonar and the new echosounder as well, the new navigation sensors or the proficiency of the upgraded PARASOUND system.

Several short circuits were recognized in the connectors of the sidescan sonar and the housing that had equal level of importance as the ongoing strong noise in the imaging of the seismic and that made it impossible to initiate the measurements. Over two days were devoted to find the errors, change the cables and connectors of the sidescan sonar and the cleaning of the seismic streamer connecting plugs was added on Thursday, after being exposed to saltwater, until the two equipments were considered fit to perform the tasks.

We were able to extend the bathymetry accomplished in the study area of the R/V SONNE Cruise SO 174 (Bohrmann and Schenck, 2004) at sites with recorded asphalt and seepage by carrying out profiles successfully with the PARASOUND. The first measurements with the updated PARASOUND revealed several limitations that were overcome by the new capabilities and functions added and will provide an important tool with time in this study. Measurements and survey within the water column, imaging of gas bubbles or optimal diagrams and form of signals are only a small glance of

the required capabilities that this cruise will slowly require available for us to work in the upcoming days.

The bathymetric data of the new SIMRAD EM120 echosounder gave us several things to wish among which a broader swath band is available through the availability of the box located in the keel that allows to record high quality data while sailing at more than 10 knots and allows to search in station and measure systematically with more comfort. In this way we concentrated in the area studied during SO 174 and accompanied the geophysical repairs with activities on station such as the sampling of the water column with the CTD/Rosette. It is in this way that we retrieved the first 5 m long gravity core sample with pelagic deep sea mud from the upper crater rim of the deep sea knoll “Chapopote”, sampling that took on this occasion from the stern on March 21.

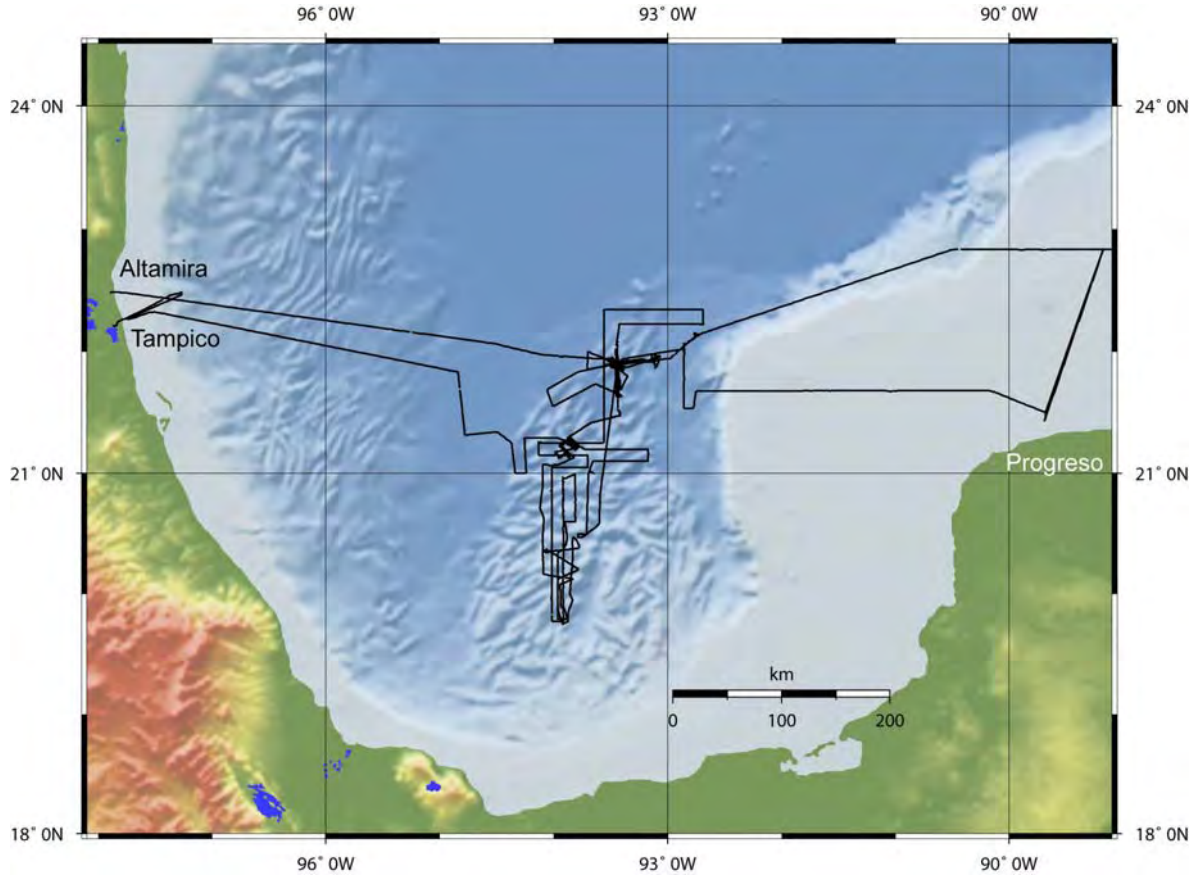

Fig. 7: Track lines of R/V METEOR during Cruise M67/2 in the Campeche Bay area.

While sailing in the area we could directly confirm the presence of oil drops and oil slicks in the surface. The surface mapping with PARASOUND/Echosounder should at the same time help to provide additional profiles to establish a basis and optimize the upcoming measurements and help to overcome the forecasted storm-phase of winds of strength of 10 while the sidescan sonar and seismic equipments are being repaired. This allowed us to recognize the infallible characteristics of the equipments that carry out hydrographic measurements under rough sea conditions that have greatly improved as in contrast with the past. With the right speed these measurements could be accomplished successfully even during the storm forecasted to reach wave heights of 4 m, which is a great step for future work onboard the R/V METEOR.

It was over night from March 23 to 24 that the weather conditions improved and that the diminishing strength of winds throughout the day that we could get the seismic equipment back in

water on the evening of March 24. We could then accomplish diverse profiles over seep locations in order to understand the complex geological conditions on the seafloor represented by the salt diapirism, sliding and strong deformation to interpret jointly with the oil and gas outflow to the superficial sediment layers.

Although there was little time to complete the geophysical survey work for the following ROV dives, we were able to produce overall very satisfying results. The untiring efforts of system operator and electronics technicians enabled the multibeam and PARASOUND systems to collect data of excellent quality and system failures common on previous METEOR cruises seem to be a thing of the past.

From March 27 to March 31 morning, the scheduled date for our arrival in Tampico, work focused on the acquisition of multi-channel seismic data in the Campeche Knolls area, which is characterized by asphalt deposits and sea surface oil slicks. In a renewed attempt to collect side-scan sonar data we successfully deployed the instrument and collected several hours worth of data on two interesting seafloor features before communication to the deep-towed fish ceased. Unable to resolve whether the source of the failure was located in the deep-sea wire, connectors, or electronics, we had to refrain from further deployments.

On the other hand, a suite of multi-channel seismic data were successfully acquired that, at least in the Chapopote area, will allow to characterize the area of asphalt deposition identified during R/V SONNE Cruise SO 174. In addition, seismic data allowed us to identify sites of fluid flow and asphalt deposition on other knolls and ridges in the study area.

While preparing the side-scan sonar we had the opportunity to deploy a CTD cast with water sampler and a gravity core in an area of visible oil slicks on the sea surface on March 28. To our surprise, water samples contained traces of higher hydrocarbons and shore-based investigations will show if the sediments also contain a record of active seepage.

The remaining hours of M67/2a were spent on systematically documenting a number of oil slicks with seismic, multibeam, and PARASOUND surveys. All instruments were back on deck at 9:00 a.m. on March 30 and we concluded our scientific program with shallow water sampling in support of a coccolithophores study before we reached the pilot station at 7:00 a.m. on Friday March 31.

Due to problems with customs processing, we chose the port of Altamira, about 30 nautical miles north of Tampico (Fig. 7), for container loading and unloading, which we completed late Friday morning March 31. Several hours later we reached the dock in Tampico after steaming upriver and enjoying the view of a city shaped by the oil industry – shipyards, oil rig construction, and factories alternated with austere settlements, all embedded in a tropical jungle. The evening saw the beginning of a 4-day port call in Tampico to exchange personnel - only six scientists from M67/2a stayed on board - and to conduct necessary repairs and maintenance work to the front thruster and bathymetry systems.

After most new cruise participants for M67/2b had boarded METEOR in Tampico on Saturday, April 1, scientists from Mexico and the United States arrived during Sunday, April 2. On board, installation of the QUEST ROV system continued and a number of analytical instruments were set up in the laboratories. Numerous guests from the Tampico area, as well as from the German embassy in Mexico City participated in a reception on board METEOR on Sunday as well. Tours of the ship followed and from conversations with our guests it became obvious that there was a great deal of interest in the German research vessel and in our research activities in the Gulf of Mexico. Local media reported in great detail about the visit of R/V METEOR to Tampico.

METEOR's scheduled departure for Leg M67/2b from Tampico on Monday, April 3 was delayed to 4:00 p.m. due to the late arrival of airfreight. In addition to cruise participants from Germany, Mexico, and the United States, seven engineers and technicians for bow thruster, dynamic positioning system, PARASOUND, and the multibeam system had joined us on board to conduct much needed repairs. These repairs and upgrades had become necessary after the many changes to the ship's systems during its time in the shipyard and will probably continue to affect subsequent legs as well.

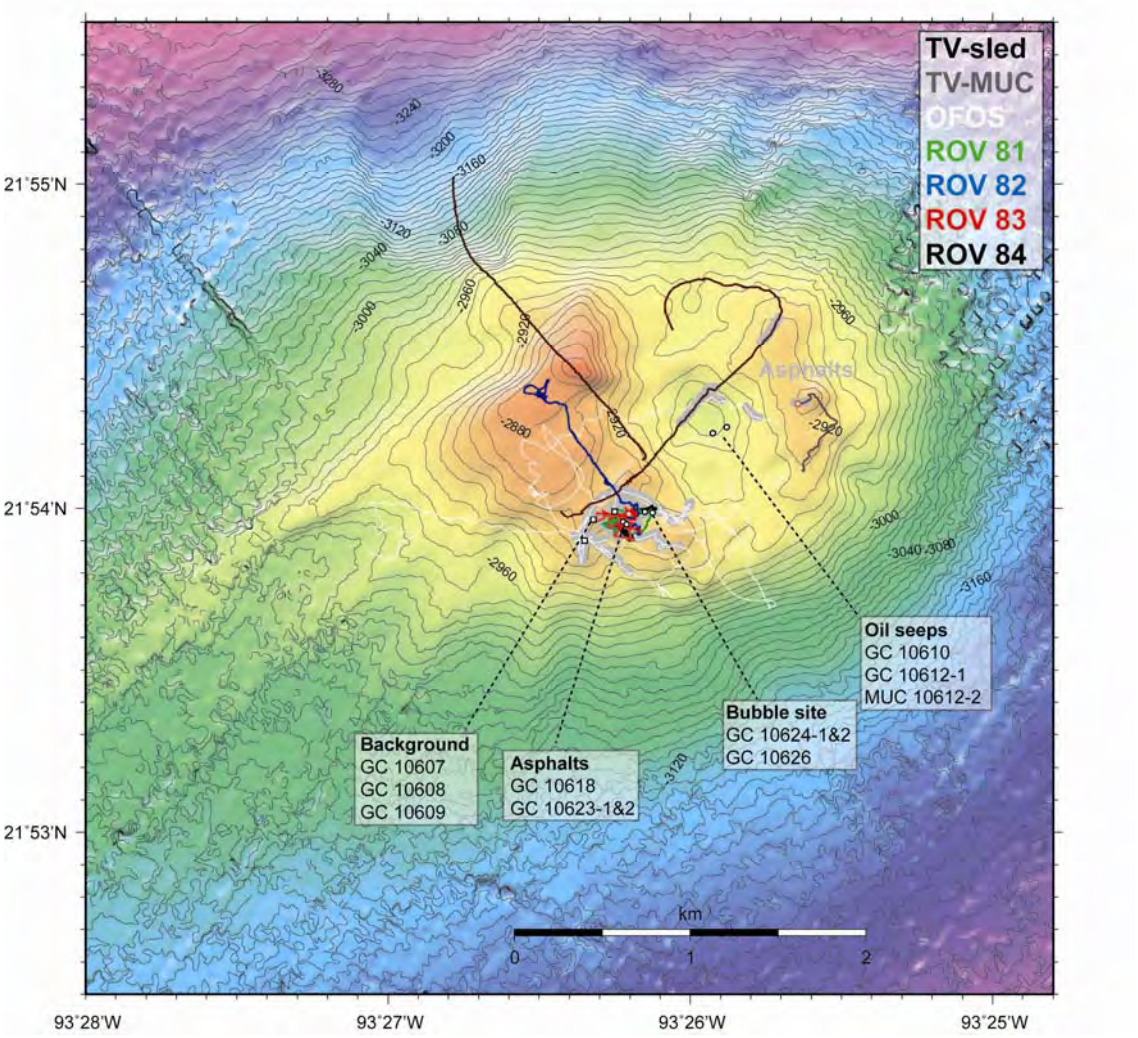

Fig. 8: Chapopote Knoll with major sampling sites (GC = Gravity Corer; MUC = Multicorer), ROV tracks and TV-observation lines at the seafloor (TV-sled and TV-MUC).

Maintenance tasks to the vessel were completed late, after the technicians had disembarked at the pilot's station in Tampico at midnight, the vessel continued its transit to our study area in the northern Bay of Campeche. Underway collection of PARASOUND and multibeam bathymetry data continued until the morning of April 5. Sediments from an approximately 40 km long ridge characterized by numerous sea surface oil slicks were recovered at our first multi-corer station from a water depth of 2200 m. A first series of ROV dives with QUEST was scheduled for the two following days. However, strong winds (6 to 7 Beaufort) in combination with a still nonfunctional bow thruster forced us to conduct alternative sampling activities. In addition, the program was curtailed by a failure of the video telemetry system, which led to a fairly extensive use of the

gravity corer on Thursday, April 6. Excitement grew with recovery of the final sediment core, which contained patches and stringers of heavy oil in its core catcher. Pore water and gas analyses revealed geochemical gradients typical for anaerobic methane oxidation in the lower portion of the core.

Detailed multibeam mapping of the Chapopote deep-sea mound with a reduced beam width of 2 km and overlapping tracks followed during the night. The result, a much more detailed morphological map of Chapopote (Fig. 8), convinced us to survey a second deep-sea mound similar to Chapopote and another potential dive target during the following day. However, a ROV dive scheduled for Saturday had to be cancelled due to technical problems with the vehicle. Excellent weather and calm seas allowed us instead to survey a natural sea-surface oil slick covering an area of 1.5-4 km^2 in the northeastern section above Chapopote. The slick was caused by rising droplets of oil originating from a water depth of almost 3000 m. We took advantage of the calm seas for documenting rising drops of oil and areas of increased occurrences of gas bubbles on the sea surface. Below the sea surface, we were able to document acoustic anomalies caused by ascending oil and gas bubbles in the water column using the new PARASOUND system. During the night, we finally succeeded in deploying the repaired TV-sled and received the first video images from the seafloor of knoll 2139. Previous side-scan sonar surveys had indicated the presence of asphalt deposits at this knoll, which was confirmed by the TV-sled. We have now documented asphalt deposits on four of the Campeche Knolls, which is an important step towards our goal of documenting the presumably large regional extent of asphalt volcanism. Gravity coring and deployments of the multi-corer completed our program for the weekend.

Technical problems with the ROV once again prevented a dive on Sunday, April 9 but were overcome by the end of the day thanks to a dedicated, all-day repair effort of the entire ROV team. The week before the Easter Weekend (April 10-14) focused completely on the deployment of ROV QUEST realizing daily dives to the Chapopote asphalt volcano. Due to technical problems with the ROV, Monday's dive on April 10 was limited to only a little more than one hour of bottom time but already demonstrated the vast opportunities the vehicle has to offer to science. Cold vents, previously known to us only from black and video images of rather poor quality, were now finally visible in great detail on high-resolution color video. An animal trap belonging to our Mexican colleagues was quickly deployed on the seafloor moments before the vehicle was forced to return to the surface.

The final breakthrough came with the second dive to the targeted asphalt volcano on Tuesday April 11. Several east-west transects across the central area of the previously discovered asphalt discharge site allowed to document details of the asphalt landscape, both in picture and by taking samples with QUEST's two robotic arms. For the first time, we were able to grasp the three-dimensional geometry of the asphalt deposits, including branching flows and stacked layers as well as their bizarre colonization by communities of chemosynthetic organisms. The asphalt flows are extremely heterogeneous in nature. Similar to features known from flowing lava, there are blocky and fractured asphalt layers indicating varying degrees of alteration, which are covered by younger, less altered sheets showing clear indications for liquid flow. While the consistency of the, according to stratigraphic principles, older flows appears hard and brittle, younger layers are viscous and soft and proved difficult to sample with the ROV's robotic arms. Petrographic and geochemical analyses of the asphalt samples will now contribute to a better understanding of asphalt volcanism as a geologic phenomenon.

Following this first dive (Fig. 9), we successfully sampled one of the asphalt layers using the gravity corer, which recovered a 70 cm long cylinder 10 cm in diameter containing asphalt in association with gas hydrate. This was an important discovery regarding processes allowing a colonization of the asphalt by chemosynthetic organisms and has implications for the microbially driven alteration of the asphalt deposits. Wednesday's dive on April 11 was focused on the deployment of several large in situ instruments using a specially designed elevator system, which was lowered to the seafloor using the ships deep-sea winch. We had planned to position the instruments with the ROV and return them to the elevator after completion of the measurements. Then, the elevator would have started its buoyancy-driven return to the sea surface. Unfortunately, a heavy rope broke during deployment and the elevator sank to the seafloor, which was documented both by its POSIDONIA navigation unit and the ship's PARASOUND system. Because the elevator had lost part of its flotation material, it did not return to the sea surface and we decided to use Thursday's dive on April 12 for a recovery attempt. During this extremely complex mission the ROV team successfully connected one of METEOR's deep-sea wires to the elevator, which was then hoisted back up to the surface. The second part of the 16 hour-long-dive was used to take short sediment cores, so-called push cores, with QUEST's robotic arm in carefully selected cold seep locations. This allowed us to conduct a variety of interdisciplinary geochemical and microbiological investigations on the first few centimeters of the sedimentary section. In addition to push cores, the ROV also retrieved various organisms as well as water and rock samples from the seafloor.

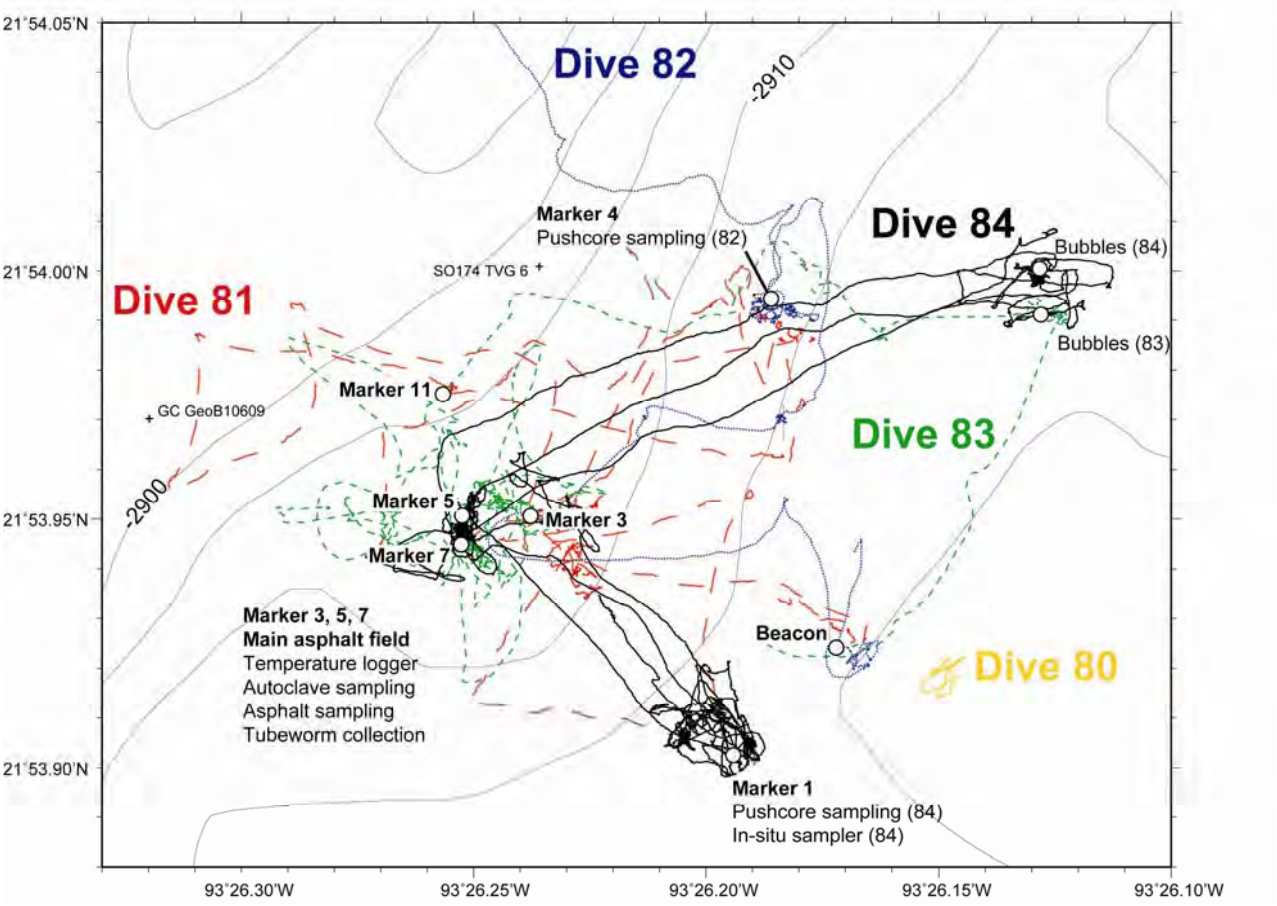

Fig. 9: Track lines, marker and sample positions of ROV dives on Chapopote Knoll.

Wednesday night on April 13/14 was used to conduct a TV-sled survey along two transects near the northeastern crater of Chapopote in order to explore the area for additional dive targets. Asphalt was visible there as well and we decided to visit the area during Thursday's dive. For this dive, the ROV was outfitted with an autoclave tool, which makes it possible to take samples on the seafloor and seal them under in-situ pressure conditions. We successfully sampled a piece of fresh asphalt and were able to determine gas content and composition by degassing the sample after retrieval under controlled conditions in the lab. Just like before, this dive of over 11 hours not only brought numerous samples of asphalt and chemosynthetic organisms, including tubeworms and mussels to the surface, but expanded our understanding of the structure of the asphalt-dominated deep-sea environment of Chapopote. It became clear that the deep-sea asphalt landscape with its bizarre biological communities represents an almost completely novel deep-sea habitat, which is controlled by the just as novel and poorly understood process of asphalt volcanism.

The last week of our research cruise our work was in the beginning quite labour intensive, however, this changed during the transit to Bridgetown and throughout Easter days. First we tried to sample the deeper sediment of the active fluid- and gas seeps on the asphalt volcano Chapopote using the 3 meter long gravity corer on April 14. This happened with different stage of success, in which variable environments of the cold seeps could be sampled down to a depth of 1,5 m. One of the sediment cores contained oil-saturated sediment, which was underlain by clam shell layers. The shells were from chemosynthetic bivalves, which are known from submersible observations to be a characteristic species of the cold seep environments on the seafloor. Another gravity corer deployment recovered a pure 90 cm asphalt core. This core contained throughout pores filled with methane hydrate. Because methane hydrates are not stable under atmospheric conditions on deck, we observed bubbling methane escaping from the pores of the asphalt core.

After finishing the gravity coring, we performed the last dive of the cruise on April 15, which turned out to become the longest dive with more than 18 hours bottom time. Scientific aim of this dive was the investigation of geochemical gradients and fluxes of oily and asphalt-like seep sediments using different in-situ tools. To fulfill this task, ROV QUEST was packed with instruments and scientific payload prior to deployment. Two devices – a benthic chamber and an in-situ pore water sampler, where initially parked at the seafloor to allow QUEST to search for bacterial mats. These are abundant in the marginal areas of asphalt covered zones on the seafloor, and document very active zones. Here the in-situ devices were deployed, and a set of push cores was taken precisely positioned, which can only be achieved with a ROV or submersible. During recovery of the push cores from the sediment, rising oil drops were sometimes observed. During the second half of the dive, the benthic chamber was deployed onto a fresh-looking asphalt surface, being covered with a white bacterial mat. A large portion of oxygen depletion inside the chamber is probably due to a high microbial activity above the fresh asphalt, whereas the flux is most probably due to the asphalt itself.

Continuing the dive, a zone with rising gas bubbles through the water column was investigated. Although this area is situated only some 200 m apart from the last position, it shows a different cold seep habitat. The seafloor here consists of heavily altered asphalt, which is clearly recognizable due to the dark colour. Also, the biological facies of the active seeps is different. Tube worms are dominant aside to clams being known as chemosynthetic organisms, which are mixed with other sessile, coral or sponge-like organisms. Animals, such as crabs, snails or sea cucumbers are abundant in this zone around 3000 m as well. Gas bubbles detected in the water column were

followed until their origin at the seafloor, where surprisingly gas hydrates of some cm thickness were found. Such hydrate structures were found at different gas bubble seeps and are probably connected to the free methane which immediately forms hydrate under high pressure in contact to the cold water.

During ascent of the ROV the rising gas bubbles could be followed at a distance around 20 m, visible as an acoustic anomaly in the sonar, all the way up to 600 m depth. This confirmation of an active gas bubble ascent can be connected with those gas observations at Chapopote performed with the new 18 kHz PARASOUND System. After this exciting and scientifically very successful dive and a short following sampling campaign, we finished the scientific stations and METEOR steamed towards Progreso on Yucatan, where our Mexican and US American colleagues left during the Easter Sunday evening. The seven days lasting transit towards Barbados, where we arrived on schedule on Monday, April 24 the harbour in Bridgetown, we used for examination of the samples and scientific results, for the preparation of the cruise report, and for daily seminars to discuss the scientific results of the cruise. Although both legs M67/2a and 2b where dealing with a variety of technical problems, they where finished with mostly very successful results.

2.2 Weather Conditions During METEOR Cruise M 67/2a and b

(T. Truscheit)

With NE wind of about 4 to 5 Beaufort and isolated rain showers R/V METEOR left the Port of Cristobal/Panama. The transit to the Bay of Campeche, the southern part of the gulf, was estimated to take 5 days with constant winds of Beaufort 4 to 5 and a sea of about 2 meters. It was partly cloudy, at times even only bright or cloudless. Arriving at the Yucatan Channel around March 19th the wind turned to SE and increased to Beaufort 6. On arrival, the Bay of Campeche, on March 20 a low pressure zone had built up over Mexico and Texas with pressure values under 1000 hPa, opposed by a high of 1020 hPa over South Florida. This led to an increase of the wind to Beaufort 7 from SSE and a sea of ca 3 m. Nevertheless it remained partly cloudy and dry. A part of the already described low remained over the Mexican peninsula of Yucatan, but decreased. Simultaneously a North American high widened southwards and was supposed to develop a part of a high of 1036 hPa on 38°N/100°W up to Friday 24. The satellite picture of the 22nd showed weak frontal cloud ribbons from 19.8 °N/97.6°W to Mid-Florida (Fig. 10). The drier cold air on the rear of this cold front had already reached the then current position of METEOR with northeastern winds from North America. A so called Northern was expected until Friday. On Friday in the research area it was still only little breezy and nearly cloudless, when ships in the northern gulf already reported wind forces 7 to 8 from the North. With some delay due to a more southern position of R/V METEOR than expected in the morning, the winds finally reached the Bay of Campeche in the late afternoon of March 24. In the evening the wind had reached Beaufort 7 from the North and in the night to Saturday, March 25 finally Beaufort 8 with gusts of Beaufort 9 were reached, decreasing only very slowly on Saturday again. The sea reached wave heights of ca. 5.5 to 6 m. The temperature dropped to about 21°C and rose only very slowly in the following days. On Sunday, March 26, it was still cloudy in the morning, but the wind had decreased to about Beaufort 4 to 5 again and in the afternoon the clouding diminished. Later on, the wind changed to SE heading again and blew permanently with Beaufort 4 to 5 until R/V METEOR arrived in Tampico/Mexico on March 31. On

transit to Tampico, the wind decrased to about Beaufort 3 during the night of March 31. It remained partly cloudy, at times it was even only little clouded and dry. The port of Tampico/Mexico was reached in the early morning of March 31st 2006.

In the afternoon of April 3 R/V METEOR left the Port Tampico for the second part of Cruise M67/2. During the stay in port it remained almost windless, but already during transit to the coast the wind increased continuously and along the coast finally blew permanently with Beaufort 5. While the sky remained only little cloudy, on the proceeding of the cruise the wind continually gained force until it reached Beaufort 6, in gusts Beaufort 7 until arrival at the northern edge of the Bay of Campeche 93 to 94°W. Due to this there was an increase of swell up to 2.5 to 3 m. Finally on April 8 the synoptic situation was quite similar to the situation 2 weeks prior.

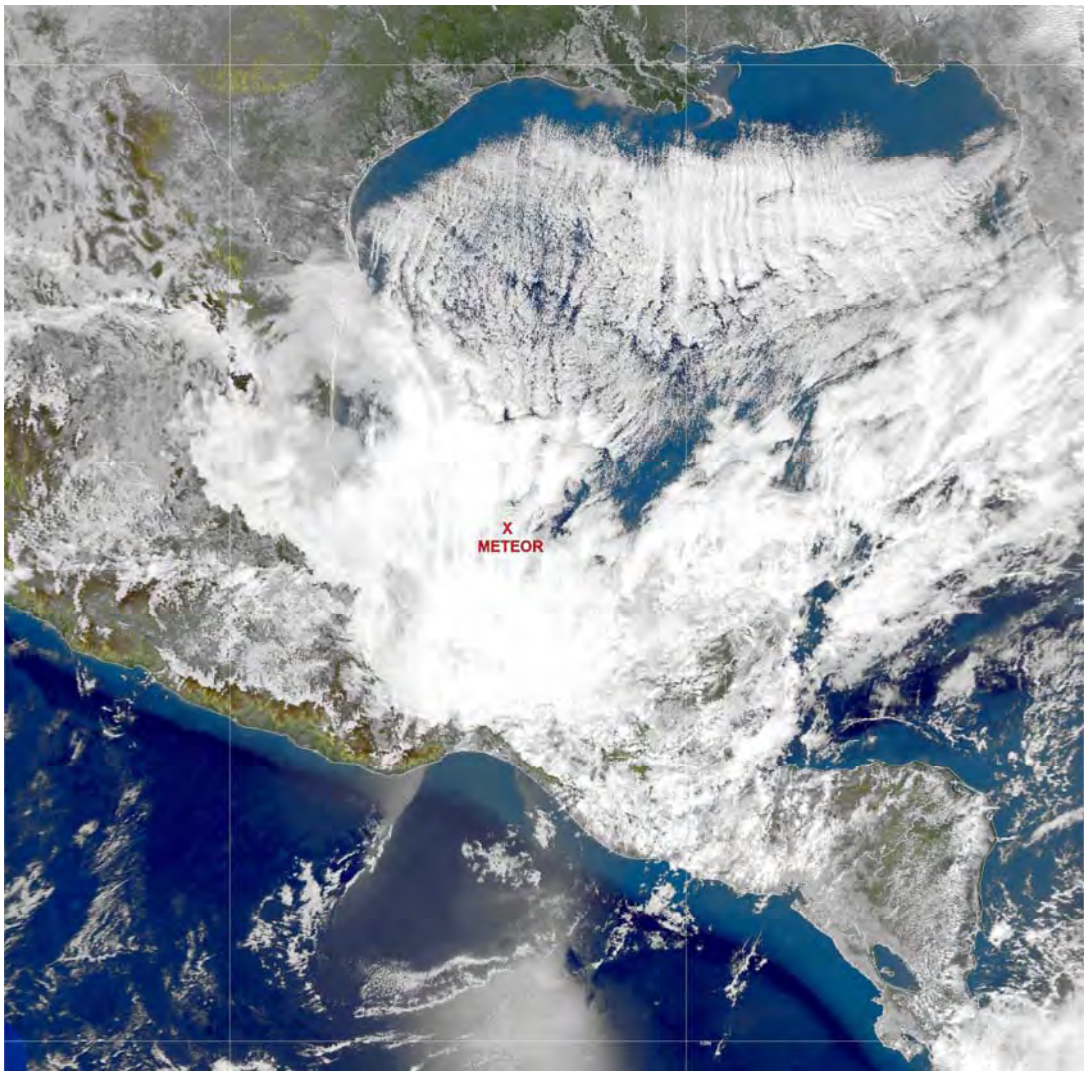

Fig. 10: Satellite image from the southwestern Gulf of Mexico showing R/V METEOR in bad weather conditions on March 24, 2006.

Close to the west of the research area a low of 1006 hPa moved to the Mexican peninsula Yucatan. Simultaneously, the wedge of a high of 1027 hPa widened from central Canada to Mexico and was supposed to reach the field of work on the following day. Another "Northern" announced itself. Even though squalls of Beaufort 8 were expected for the following day, the maximum of the

wind speed and gustiness was already reached during the night with Beaufort 7. The cold front resulting from a low at the East Coast of the USA moved out southeast faster than expected and the atmospheric pressure contrasts in the field of work decreased accordingly. On April 9 the wind force had already decreased to Beaufort 4 to 5, now blowing from northern directions, and - according to the situation two weeks prior - the air temperature had dropped distinctly to about 22°C. The high of 1027 hPa over the Big Lakes moved on eastward and the atmospheric pressure contrasts in the research area of R/V METEOR decreased accordingly until on April 11 it was sometimes nearly windless. An eastwardly moving low of 1008 hPa and an also eastwardly moving high over New Orleans produced a new increase of wind up to Beaufort 6 to 7. In the meantime, the temperatures had risen to about 25 to 26°C again and until April 14 the wind turned back to southeastern directions again and blew with Beaufort 5 to 6 until the arrival of R/V METEOR at Progreso at the northern side of Yucatan. Although with arrival at Progreso in the evening of April 16 wind of Beaufort 5 prevailed, swell was only about one meter in the lee of Yucatan. With the exception of the passing of a cold front in connection with a Northern (it was mainly cloudy on this day) it remained partly cloudy for the whole time after leaving Tampico, sometimes even cloudless. After the disembarking of the Mexican guest scientists on the safe anchorage of Progreso the transit to Barbados began. With the sky nearly cloudless, the wind first blew permanently with about Beaufort 5, later on Beaufort 3 to 4. The low over Mexico widened up to Yucatan. Simultaneously a high over Florida moved further eastward so that the pressure differences hardly changed. With southeastern winds of about Beaufort 4 R/V METEOR passed the Yucatan Channel during the night of April 18. Even though it was only slightly cloudy at dawn of this day, the clouding became more dense/increased in the course of the morning and repeatedly higher reaching swellings passed. From one of those a water hose developed in the morning. As the hose had built up directly ahead of the vessel, the heading was changed slightly to starboard, so that the water hose passed by at a distance of appr. 200 mtrs on the port side and could be watched well. With the arrival in Caribbean waters came an increase of air and water temperature. For the transit to Barbados a course was chosen that passed north of Jamaica and on a direct course between St. Lucia and St. Vincent finally led to Bridgetown. A cold front which moved south-eastwards on April 21 of a low south of Newfoundland was responsible for these conditions. R/V METEOR Cruise M67 ended on April 24 in the port of Bridgetown/Barbados.

3 Multibeam Swath Mapping

Collecting multibeam data in order to cover a large area in addition to the data taken during R/V SONNE Cruise SO174 (Bohrmann and Schenck 2004) in the Campeche Bay was a major goal. We used the new systems which have been installed at the ASMAR shipyard in Talcahuano. There the replacement of the old ATLAS HYDROSWEEP DS multibeam echosounder by new multibeam systems from KONGSBERG MARITIME (formerly SIMRAD) was done. To allow for efficient and economic bathymetric mapping in shallow and in deep water, two systems, a shallow-water EM710 as well as a deep-water EM120 system had been installed. The EM710 installed is a new 1-by-1-degree broadband multibeam echosounder operating in the 70-kHz to 100-kHz band. It uses CW (continuous wave) pulses in shallow modes and FM (chirp) pulses in deep modes. The maximum water depth for this system is up to 1500 m to 2000 m, however, the most efficient depth range for the EM710 is less than 500 m. In this depth it has a better resolution and a slightly wider swath than the EM120. For greater depths, the EM120 was permanently used. As the main area of investigation of Cruise M67/2 had water depths of more than 2000 m the EM710 was operated only in test mode e.g. close to Tampico. Data coverage in the research area is shown in Fig. 11. Details of the new system are described in cruise report of M67/1 (Weinrebe et al. 2006).

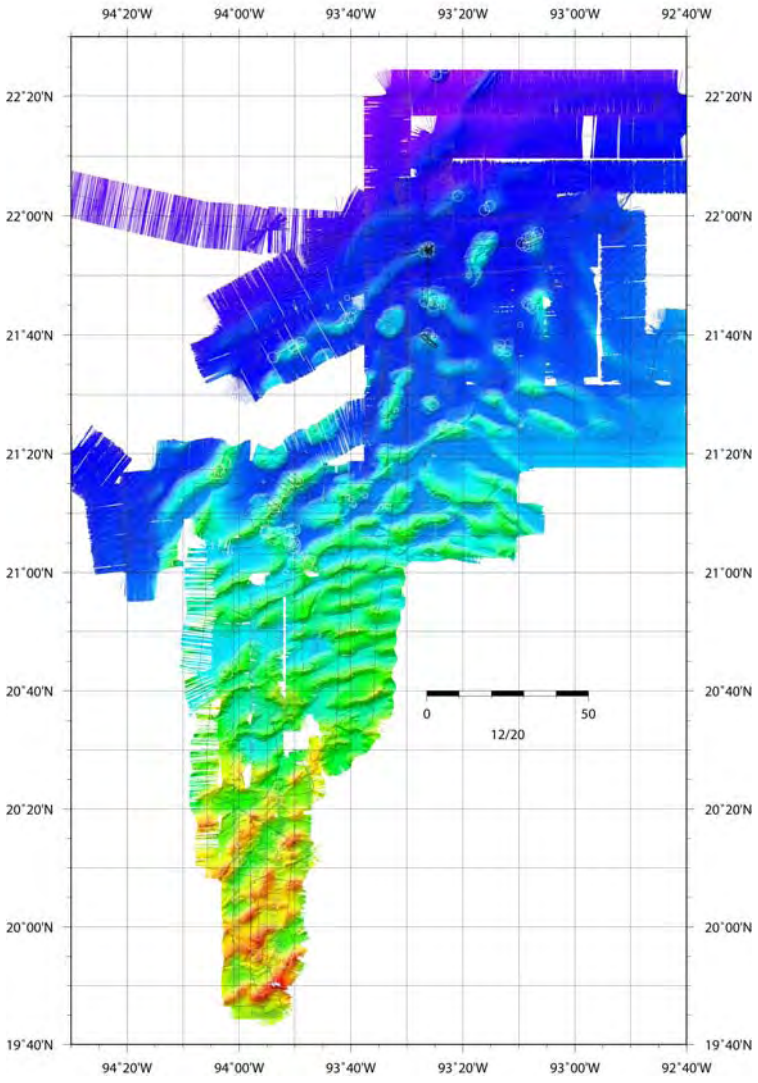

Fig. 11: Coverage of multibeam mapped during R/V METEOR Cruise M67/2 in the Campeche Bay.

4 Sidescan Sonar Operations

(I. Klaucke, J. Renken, M. Brüning)

Detailed geoacoustic mapping of asphalt volcanism and related fluid-escape structures have been targeted using the DTS-1 sidescan sonar system operated by IfM-GEOMAR, Kiel. The DTS-1 sidescan sonar is a dual-frequency, chirp sidescan sonar (*EdgeTech Full-Spectrum*) working with 75 and 410 kHz centre frequencies. The 410 kHz sidescan sonar emits a pulse of 40 kHz bandwidth and 2.4 ms duration (giving a range resolution of 1.8 cm), and the 75 kHz sidescan sonar provides a choice between two pulses of 7.5 and 2 kHz bandwidth and 14 and 50 ms pulse length, respectively. They provide a maximum across-track resolution of 10 cm. With typical towing speeds of 2.5 to 3.0 kn and a range of 750 m for the 75 kHz sidescan sonar, maximum along-track resolution is on the order of 1.5 metres. In addition to the sidescan sonar sensors, the DTS-1 contains a 2-16 kHz chirp subbottom profiler providing a choice of three different pulses of 20 ms pulse length each. The 2-10 kHz, 2-12 kHz or 2-15 kHz pulse gives a nominal vertical resolution between 6 and 10 cm. The sidescan sonar and the subbottom profiler can be run with different trigger modes, internal, external, coupled and gated triggers. Coupled and gated trigger modes also allow specifying trigger delays. The sonar electronics provide four serial ports (RS232) to attach up to four additional sensors. One of these ports is used for a Honeywell attitude sensor providing information on heading, roll and pitch and a second port is used for a pressure sensor. Finally, there is the possibility of recording data directly in the underwater unit through a mass-storage option with a total storage capacity of 30 GByte (plus 30 Gbyte emergency backup).

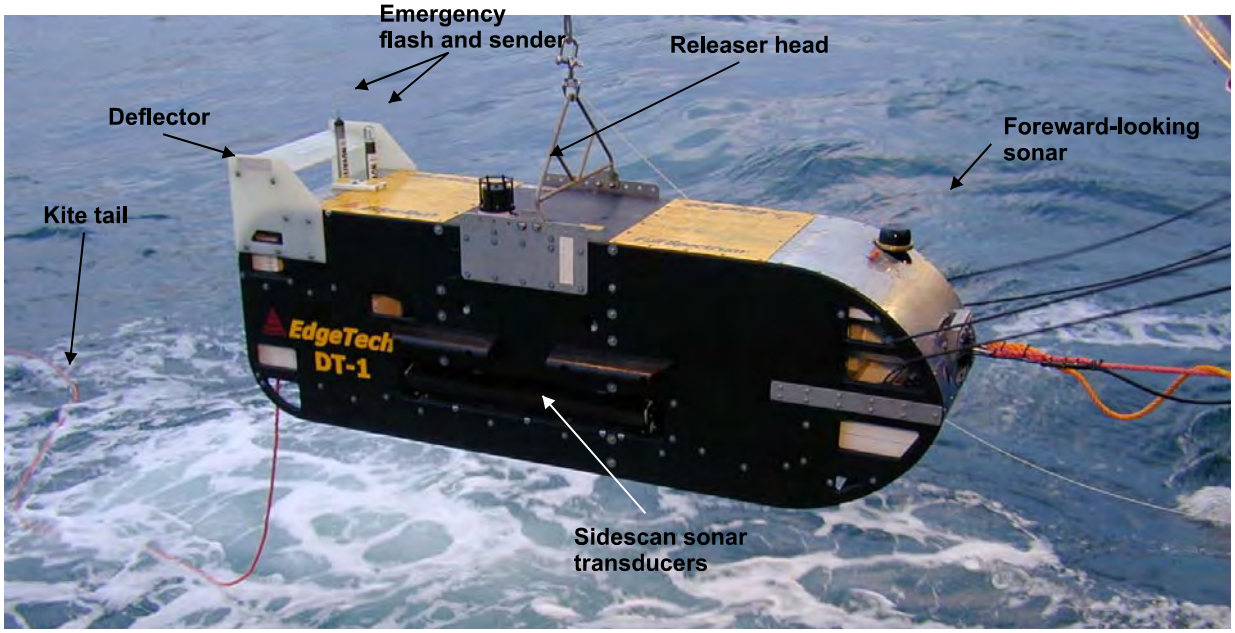

Fig. 12: A picture of the DTS-1 sidescan sonar towfish. The foreward-looking sonar is no longer mounted.

The sonar electronic is housed in a titanium pressure vessel mounted on a towfish of 2.8 m x 0.8 m x 0.9 m in dimension (Fig. 12). The towfish houses a second titanium pressure vessel containing the underwater part of the telemetry system (SEND DSC-Link). In addition, a releaser capable to work with the USBL positioning system POSIDONIA (IXSEA-OCEANO) with separate receiver head, and an emergency flash and radio beacon (NOVATECH) are included in the towfish. The

towfish is also equipped with a deflector at the rear in order to reduce negative pitch of the towfish due to the weight of the depressor and buoyancy of the towfish.

The towfish is connected to the sea cable via the depressor through a 43-m long umbilical cable (Fig. 13). The umbilical cable is tied to a buoyant rope that takes up the actual towing forces. An additional rope has been taped to the buoyant rope and serves to pull in the instrument during recovery.

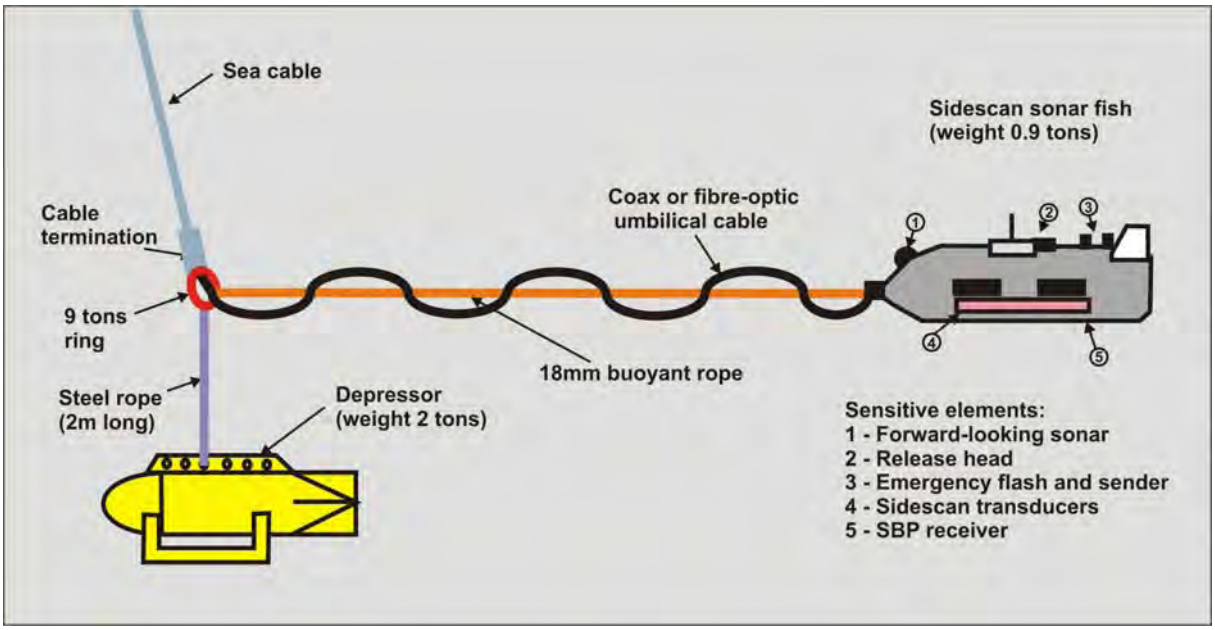

Fig. 13: The DTS-1 towing configuration.

The main operations of the DTS-1 sidescan sonar are run using HydroStar Online, the multibeam bathymetry software developed by ELAC Nautik GmbH and adapted to the acquisition of EdgeTech sidescan sonar data. This software package allows onscreen presentation of the data, of the towfish's attitude, and the towfish's navigation when connected to the POSIDONIA USBL positioning system. It also allows setting the main parameters of the sonar electronics, such as selected pulse, range, power output, gain, ping rate, and range of registered data. HydroStar Online also allows activating data storage either in XSE-format on the HydroStar Online PC or in JSF-format underwater on the full-spectrum deep-water unit FS-DW. Simultaneous storage in both XSE and JSF-formats is also possible. Accessing the underwater electronics directly via the surface full-spectrum interface-unit FS-IU and modifying the sonar.ini file of the FS-DW allows changing additional settings such as trigger mode. The FS-IU also runs JStar, a diagnostic software tool that also allows running some basic data acquisition and data display functions. HydroStar Online creates a new XSE-file when a file size of 10 MB is reached, while a new JSF-file is created every 20 MB. How fast this file size is reached depends on the amount of data generated, which depends on the use or not use of the high-frequency (410 kHz) sidescan sonar. The amount of data generated is also a function of the sidescan sonar and subbottom pulses and of the data window that is specified in the initialisation file (sonar.ini) on the FS-DW. The data window specifies the range over which data are sampled.

4.1 Sidescan Sonar Deployments

Deployments of the DTS-1 sidescan sonar were targeted at imaging seafloor elevations in the Campeche Basin, the so-called Campeche Knolls. These structures with positive relief are related to salt tectonics and upward fluid-flow that brings hydrocarbon-rich fluids and asphaltenes to the seafloor. These structures of asphalt flows and carbonate crusts formed as an end product by the anaerobic oxidation of methane are generally well distinguished from background hemipelagic sedimentation and easily mapped using sidescan sonar.

After several unsuccessful attempts due to broken cables during deployments and unstable data connection to the towfish, a final attempt has been made on 28/03/06 at 23:00 UTC. Although data connection to the towfish was initially again unstable, the data connection subsequently stabilised and about 6 hours of high-quality data have been gathered. At this point data registration in the towfish proved extremely useful, because some of the data has been lost during data transmission, but the full data-set could be uploaded after the deployment. At 29/03/06 at 05:35 UTC, however, data connection to the towfish broke down although the sidescan sonar continued to operate normally, as subsequent analysis of the data registered in the towfish has shown.

The continued bad or even faulty data connection between the sidescan sonar dry end and wet end is rather unusual as these elements have never shown any problems in the past, except for broken cables during deployments. Data connection is via two DSC modems that have to synchronise and agree on a certain data transmission rate depending on the quality of the cable. Once this transmission rate is established the modems normally run very stable. During M67/2a, however, the synchronisation was lost at irregular intervals without signs of major current variations over the cable. This is very unusual and several working hypotheses have been advanced:

a) The sidescan sonar instrument was damaged during the loss of the equipment during METEOR Cruise M66/4a. Since then the instrument has not been back to the institute for detailed verification. The main argument against this hypothesis is the fact that the sonar electronic works without problem and the telemetry system used during M67/2a was installed on the towfish during M66/4a.

b) Since the loss of data connection was only observed when the instrument was in the water (never on deck with both a short direct cable and while using the deep-sea cable), another hypothesis was a problem with the deep-sea cable that was newly installed at the beginning of M66/4a. Measurements of the electric characteristics of the deep-sea cable, however, did not reveal any anomalies.

c) Damages to the telemetry system due to inversion of the current poling on R/V METEOR compared to all other German research vessels are a third possibility. This fact was not taken into account on initial connection of the towfish and inversely poled current was send to the telemetry. Although this did not apparently damage the telemetry system, it might have altered the sensitivity of the modem.

In any case, a detailed fault analysis will take place once the instrument is back at IfM-GEOMAR in Kiel.

4.2 Preliminary Results

During the short 6 hours deployment one of the knolls in the Campeche Bay area was crossed. The sidescan sonar data show one rounded area of 300-400 metres in diameter at the summit of this structure (Fig. 14). This area is characterised by speckled high backscatter intensity and could

represent a zone of asphalt flows at the seafloor. Some isolated spots of high backscatter to the south of the summit show a similar characteristic. In addition, the northwestern part of the sidescan sonar image shows very high backscatter intensity associated with some ridges at the edge of the structures. Whether this high backscatter intensity may result from carbonates at the seafloor is not clear at this point.

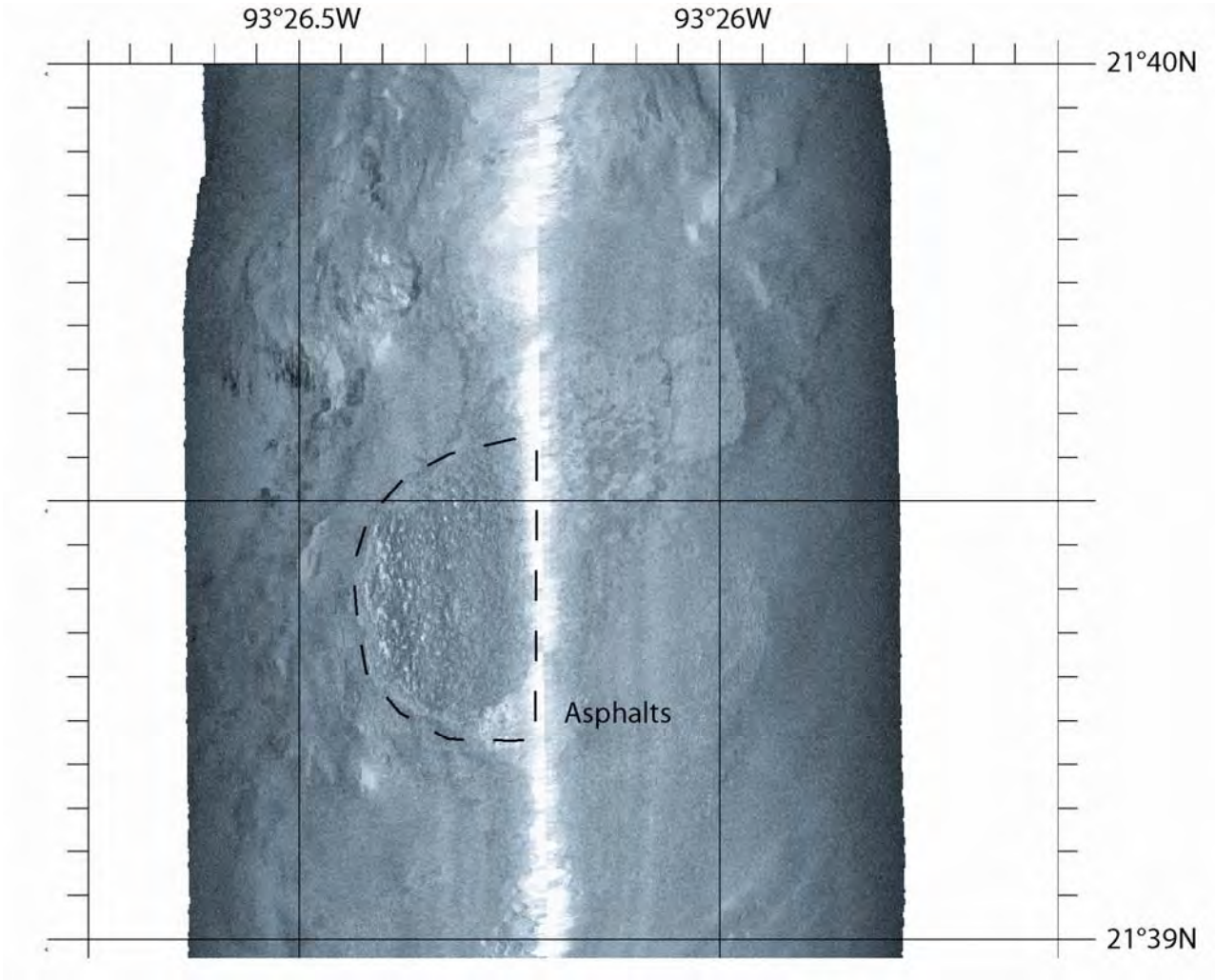

Fig. 14: kHz sidescan sonar swath (1500 metres swath width) across one knoll of the Campeche Knoll area showing possible asphalt flows at the seafloor.

5 Sub-bottom Profiling and Plume Imaging

(V. Spiess, H. Keil, M. Brüning, C. Mortera, M. Pacheo, J. Pelaez)

During the port call in Taicahuano/Chile in January/February 2006, the existing PARASOUND sediment echosounder system was replaced by a fully digital signal acquisition and processing system, the new PARASOUND DS-3 system (Atlas Hydrographics, Bremen). During Cruise M67/2 the new system was used for the first time for scientific investigations, but during subleg 2a functionality was limited and troubleshooting was carried out by technicians of the manufacturer Atlas Hydrographics due to severe malfunctions.

With the arrival in the working area in the southern Gulf of Mexico, a normal operation and watchkeeping could be started, and the system was mostly running reliably with only few technical problems.

Sediment echosounder data during the cruise were collected for several purposes:

1) Reconstruction of depositional processes as turbidity, pelagic and current-controlled sedimentation
2) Identification of near-surface deformation in conjunction with salt diapirism and slumping
3) Identification of vent locations from surface and subsurface amplitude and structural anomalies
4) Investigations of the water columns to search for bubble streams

5.1 The New PARASOUND System

The new PARASOUND system represents the first major system upgrade since 1986 with a complete redesign of hardware and software used, except for the transducers, which remained in place on the ship. While the original system, which was installed on R/V METEOR in 1986, was basically built on analog components, the new system follows a complete digital design. It was installed in parallel on R/V MS MERIAN and R/V METEOR, and for R/V METEOR, Cruise M67/2 was the first to operate the system on a routine basis. In the following chapters, a brief overview on both hardware and software will be given.

Hardware Concept

Fig. 15 summarizes the system design. The 128 (8 x 16) transducer elements are connected to the Analog Electronic Unit (AEU), which handles parametric sound generation and sound recording. It is based on a real-time Linux computer, connected to 8 Transmission Beam Formers (TBF), which carry out the digitization and first phase of signal processing for 16 individual staves each. Via fiberoptic cables as GigaBit network connection, the results are transmitted to the Digital Electronic Unit (DEU), where the digitized signals are further processed. This unit is based on a PC with Windows XP operating system.

At this point, motion sensor data are incorporated to control beam direction and to correct for heave variation. The DEU further processes all commands from the the Hydromap Control Software, running on an Operator-PC, and provides the digital single beam and multibeam data via an ftp service.

AEU and DEU are located close to the transducers in the hull of the ship to minimize the influence of electronic noise. The Operator-PC on METEOR is located in the 'Lotzentrale', where the operation of all echosounders is supervised, mostly on a 24-hour watchkeeping schedule, and connected to AEU/DEU via GigaBit LAN.

Functionality

The basic physical principle of parametric sediment echosounding is the parametric effect, which occur in few media as water or air, when very high (finite) amplitude sound waves are generated. If the emitted energy is close to cavitation (240 to 246 db), energy can be transferred to different frequency band, in particular higher harmonics. If two waves of similar frequency are generated simultaneously, also the sum and the difference of the two primary frequencies are observed, however, with an energy coefficient of less than 1%.

For the PARASOUND System, 18 kHz is one fixed primary frequency, which distributes energy within a beam of 4.5° for a transducer of ~1 m length. The second primary frequency can be varied, now between 18.5 and 24 kHz (before 20.5 to 23.5 kHz), resulting in difference frequencies from 0.5 to 6.0 kHz (before 2.5 to 5.5 kHz). This signal travels within the narrow 18 kHz beam, which is much narrower than e.g. a 4 kHz signal, emitted from the same transducer directly (30°). Therefore, a higher lateral resolution can be achieved, and imaging of small scale structures on the seafloor is superior to conventional systems. As another consequence, the signal bandwidth is also increased, and much shorter signals can be generated with improved vertical resolution. It is now also possible to choose different signal shapes (sine wave, box, triangle, hamming, etc.) or to provide a custom function.

While the old PARASOUND system was designed as an analog system both for screen display (echoscope) and paper recording (DESO), the digital acquisition was added through the ParaDigMA System, developed by the University of Bremen (Spiess, 1993). The signal processing path was not optimized for digital acquisition, and noise level was relatively high. In particular, it had been difficult on R/V METEOR to access the 18 kHz primary signal due to a technical design problem in the adaption.

The new system treats three signals separately: the primary high frequency signal (18 kHz; PHF), the secondary low frequency signal (selectable 0.5 to 6.0 kHz; SLF) and the secondary high frequency (selectable 36.5 to 42 kHz; SHF). All three signals are recorded separately at the DEU, and is made available for download via ftp. Alternatively, also exclusively a low frequency signal (PLF; 3 or 12 kHz) can be emitted at much lower energy levels, where sound emission energy levels have to be limited (e.g. for mammal protection).

While the original digitization is carried out fulfilling the Nyquisit theorem, i.e. the sampling frequency must be greater than the greatest frequency in the signal, a given limited bandwidth, as result of an analog bandpass filter, will allow to shift the signal in the frequency domain towards lower frequencies. This shift is equivalent to a resampling and data volume can be reduced accordingly by saving the complex time series. These data are transferred in the internal ASD data format.

While the old PARASOUND system could only generate sinusoidal signals of 1 to 8 periods, now not only different signal shapes can be generated, but also chirp signal with increasing frequency can be emitted. A barker coded signal, which repeats a waveform at irregular time shifts, is also

available. In both cases, a subsequent correlation with the emitted signal is required, which destroys the phase information, but improves significantly the signal-to-noise ratio.

Due to the very narrow beam, it is necessary to control beam direction to compensate the ship's movement and to send the energy vertically downwards. Beyond this traditional approach, steeper slope angles of the seafloor >2° cause the difficulty that energy is not reflected back to the transducer, but only scatter energy returns. In such circumstances, a steering of the beam perpendicular to the seafloor would be more appropriate. The new feature 'Incidence Angle Control (IAC)' allow both manual and automatic beam steering. For the automatic mode, the topography, i.e. the average slope angle and direction of maximum slope must be known. To determine this, a multibeam mode was implemented, which determines the water depth for an array of up to 9 x 9 beams, covering an angle of +/-7.5° across the ship's axis, and +/-10° along the axis.

Software Concept

The PARASOUND system uses minimum three different computer systems. Two of them control realtime signal generation and data acquisition through a Linux and a Windows XP system. The third PC is available for the operator. This Operator-PC hosts the Hydromap Database Server, the Hydromap Control Software and the ParaStore 3 Software.

The Hydromap Control Software is responsible for all system settings and for communication with the realtime computers. Instrument parameters are set via several windows and acknowledged by the submit button.

For visualization, online processing and storage, the ParaStore Software Package is used. It plays a passive role, i.e. it recognizes notifications by UDP packets, which are sent by the DEU, when data is ready for upload. Then an ASD file, which contains data and all available metadata, is transferred by ftp. ParaStore determines, whether this ASD file is permanently stored or temporarily in a ring buffer. Furthermore, data can be stored in PS3 or SEG-Y Format from each visualization window.

A large number of individual windows can be opened to display different signals (PHF, SLF, SHF) and with different scaling or processing parameters. This allows to optimize windows for specific purposes, as e.g. to image the corable sediment cover of just the upper 20 m, to choose a full penetration plot, which also allows coverage of the topography, or to study the complete water column.

System Performance

At the time of cruise, it had been the first time of a deep sea test, and after a 3-weeks period of testing and troubleshooting, the system could be used in a routine mode. The main operations were the single pulse mode, when a single pulse is emitted and the water column and sediment response are recorded before the next pulse is sent. This operation is most suitable, when signals in the water column, as from plancton, fish or gas bubble are to be identified. Also it is suitable, if the system should be run in an unattended mode without watchkeeping, since it is possible to record the equivalent of several thousand meters in the time series, and the recording window does not have to be adjusted.

The window adjustment is only needed, when the pulse train mode is activated, by which the two-way traveltime of the signal through the water column until the first return is used to emit more

signal at regular intervals. Then, the signal density can be increased by as much as a factor of 16, if the time interval between pings and water depths allow.

With the new system, the pulse train mode is no longer restricted to deep water. While in the old system the time interval was fixed to 400 ms, and main trigger periods were directly connected to a fixed range setting of 10000 m (13.3), 5000 m (8.3), 2000 m (3.3 s), the new system is more flexible. Already on the upper continental slope in water depths of a few hundred meters, the pulse train mode significantly improve the horizontal sampling of the seafloor. In particular on steep slopes, the imaging is now sufficient to trace reflectors and identify coring locations, since a better continuity can be achieved.

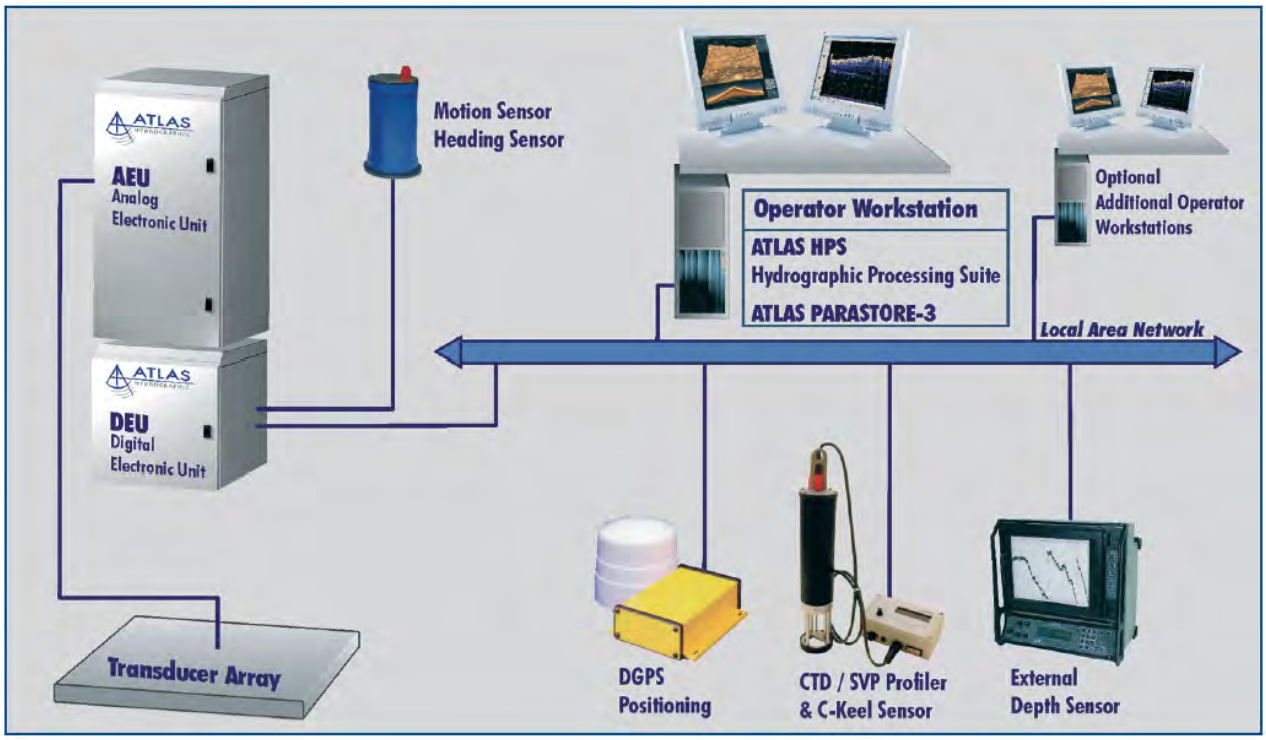

Fig. 15: System Design of the new PARASOUND DS-3 system (from: PARASOUND DS-3 Prospekt, Atlas Hydrographics).

A major deficit of the system had been the depth determination, which was not working reliably. Therefore, all automatic modes, e.g. for a window control in the pulse train mode, or the automatic incidence control in the multibeam mode, did not work. Improvements for better algorithms have been provided to the manufacturer, and improvements were expected for following cruises.

A specific test had been carried out for extreme low secondary frequencies, particular for 0.5 to 2.0 kHz, which were not available for the old systems. For deep sea with water depths beyond 3000 meters, no sufficient energy had been recorded except for the traditional frequencies from 2.5 to 6.0 kHz. A shallow water test of this features had not been carried out.

Successful tests were performed for the chirp and barker coded signals, where correlation was applied. As expected, the signal penetration and signal-to-noise rations were slightly improved. The reliability of the system was not very good and numerous restarts and reboots were necessary, particularly of the DIP boxes, which provided serial interface information to the network.

5.2 Preliminary Results

Sediment Echosounding

The Quaternary sediment cover in the southern Gulf of Mexico is quite uniform and mostly of turbiditic or pelagic origin. Well-stratified sediments are present both in the basins and on the diapirs and knolls, where they had been in some places significantly deformed in recent geologic time.

The selected examples illustrate the general performance of the new system and the overall data quality. Water depths in the survey areas range from 700 m to more than 3300 m, penetration is on average 50 to 80 meters. Figure 16 illustrates distinct, sharp reflectors, originating from the deposition of pelagic sequences draping an underlying small-scale topography. Due to the narrow beam, image quality is superior even in local depressions, where conventional echosounders would show a bow-tie pattern and would partially mask the internal structure.

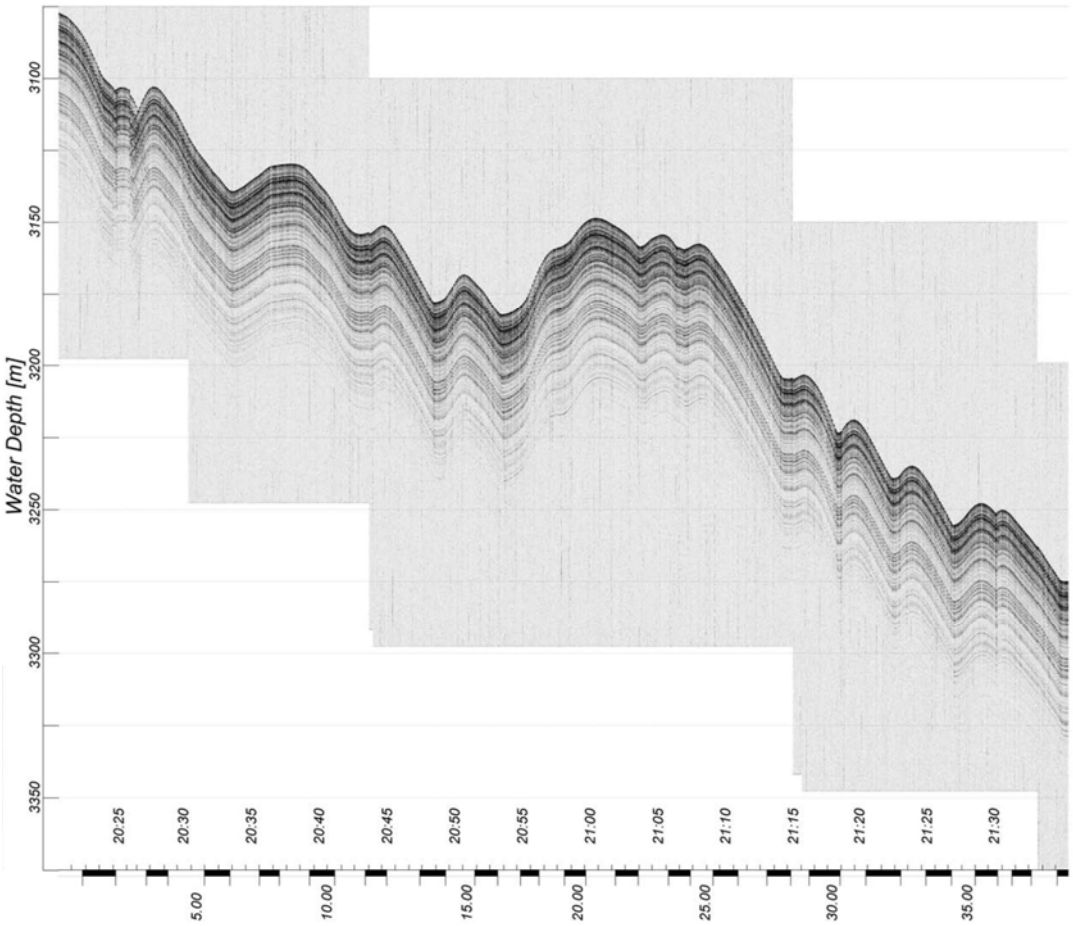

Fig. 16: Wavy topography with uniform sediment cover with distinct layering in the southern Gulf of Mexico west of Chapopote. Horizontal black bars are 1 km long. Vertical exaggeration is ~100.

A second example with a similar reflection pattern is shown in Figure 17. But here, the overall variation in layer thickness may hint to a current-controlled development of mud waves with a visible asymmetry. The wave height is just on the order of 10 meters, and wavelength approximately 2 to 3 km. These waves could also be observed in bathymetric data as linear features, which in turn most likely relate to long-term deep-water current activity.

The example from shallow depth of 700 to 1100 m on the continental slope off Tampico in Figure 18 shows a significantly steeper slope, on average 1.5 degrees, which reveals indications for small scale failure, an intercalated debris flow and some compression resulting in a small scale topography. Otherwise, the sediments seem to be of hemipelagic origin.

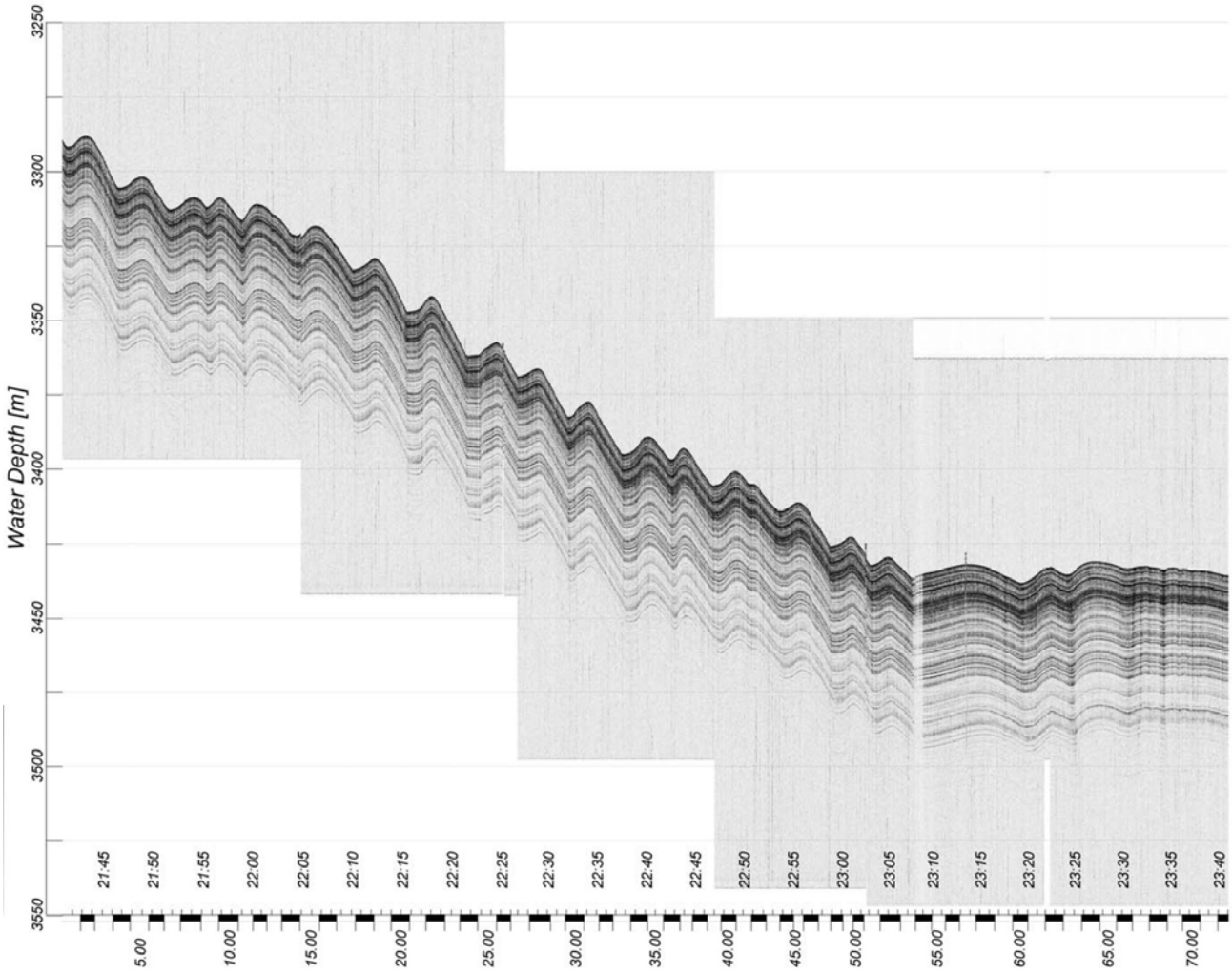

Fig. 17: Mud waves in the southern Gulf of Mexico west of Chapopote. Horizontal black bars are 1 km long. V.E. ~200.

Figure 19 from the steep flank of Oil Ridge contains a much higher proportion of transparent lense-shaped bands, typically interpreted as debris flows. It is quite likely that concurrent with the uplift of the salt diapir, causing the topography of the knoll to develop, frequent mass wasting occurs at the steepest slopes and at places of maximum degree of deformation. To the right, at 06:45, a bow-tie pattern appear in a buried depression or at a crossing of a linear channel at an angle.

Figure 20, recorded on the flank of Chapopote, displays only one debris flow unit at 12:00, while otherwise the layering is pronounced and distinct. The local depression at 11:50 reveals somewhat higher sedimentation rates, probably because it is acting as a sediment trap. Between 11:05 and 11:20, numerous normal faults are present, probably on top of a major, deep reaching fault, which

causes a clockwise tilting of the overlying sediment block. The flank of Chapopote at 12:10 is too steep to provide a clear image of the seafloor reflection, but rather shows scattering.

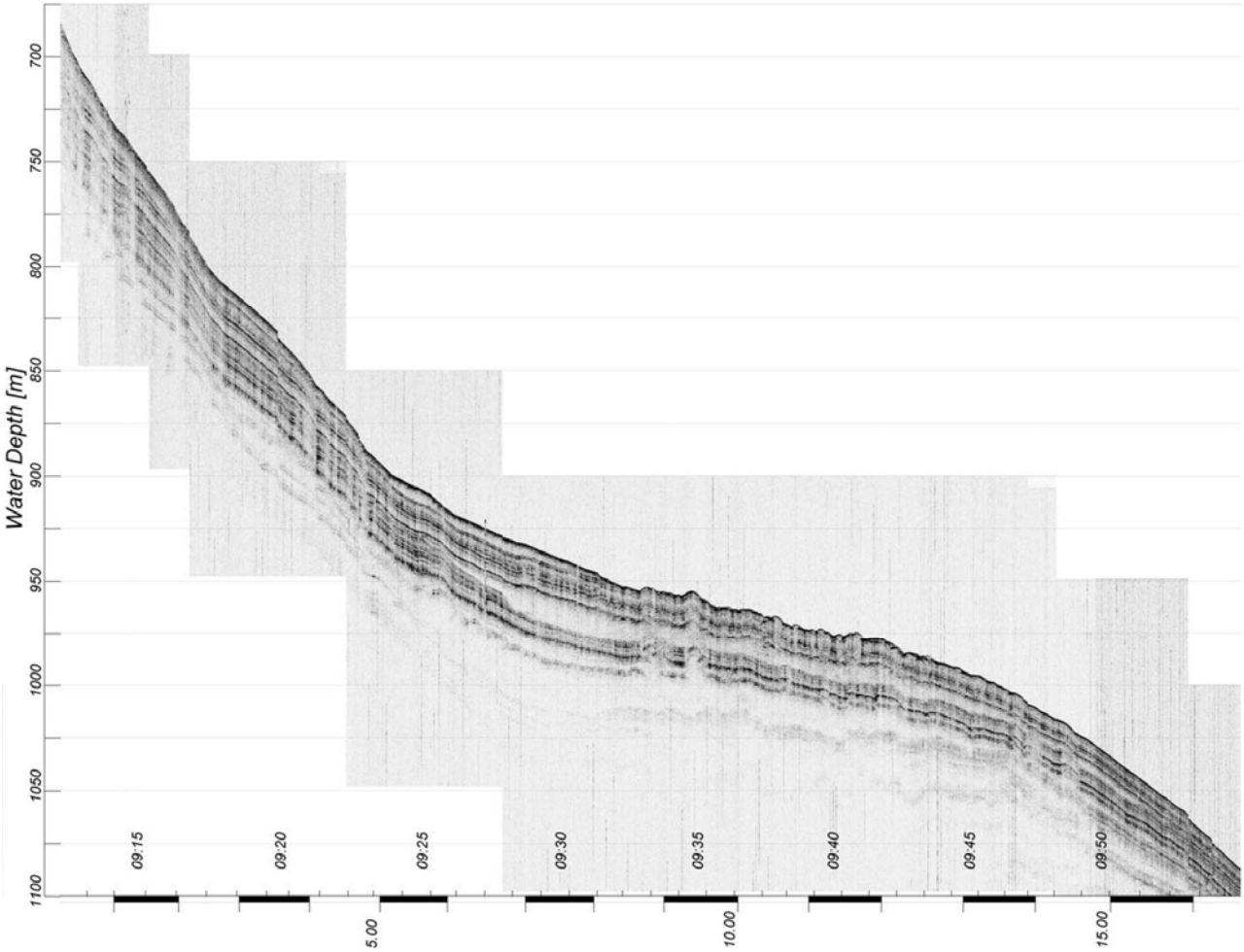

Fig. 18: Mud waves in the southern Gulf of Mexico west of Chapopote. Horizontal black bars are 1 km long. V.E. ~30.

Figure 21 shows a complete crossing of Chapopote Knoll. Flanks are too steep to be properly imaged, but incidence angle control was not functioning properly and could not be tested here. On the other hand, for a vertical beam slope angles of 4 to 5 degrees do not allow to record signals other than backscatter from the surface or any internal reflector, since reflections are directed sideways. Internal reflectors are not identified, which may be the result of strong deformation and/or homogenization in conjunction with the effect of steep slopes. On top of the knoll, topography is so complex and steep that hyperbolic echoes dominate the image, although a sediment cover of several 10 meters can be confirmed. Due to the extreme local variability PARASOUND data could not be used to search for asphalt occurrences at the seafloor. Seismic migration algorithms would have to be applied to derive a true image of surface and internal structures.

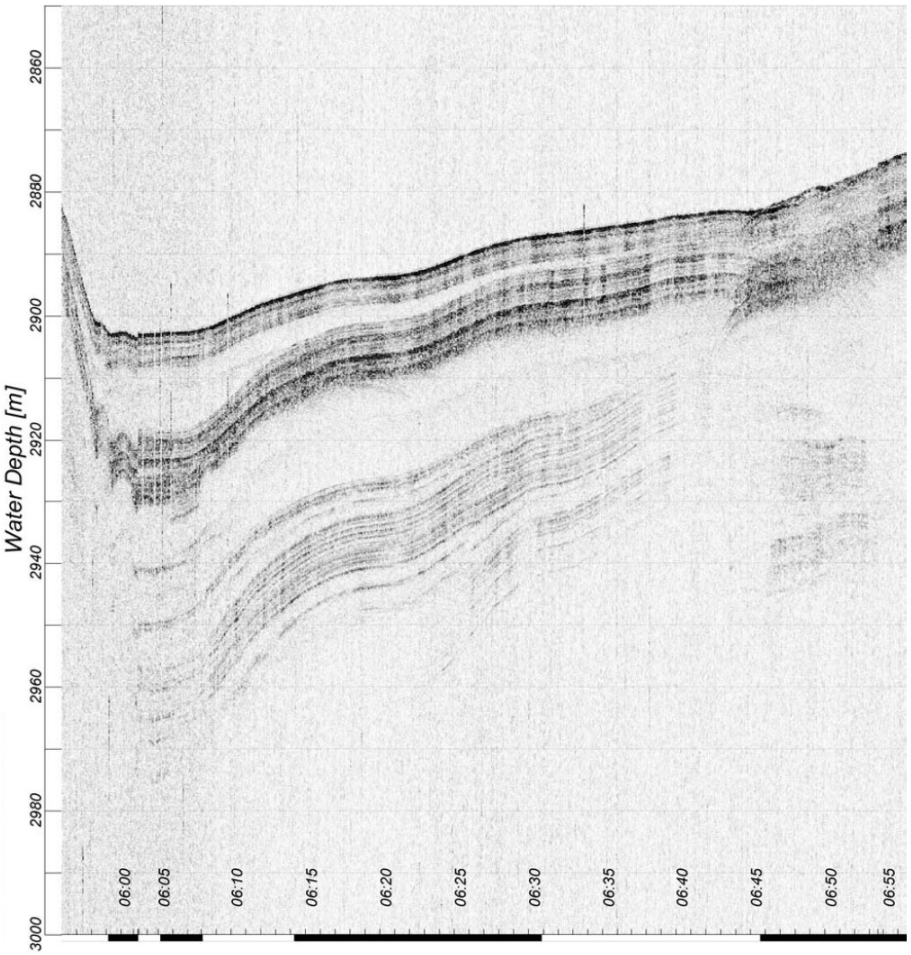

Fig. 19: A sequence of layered and transparent sedimentary units from the flanks of Oil Ridge. Horizontal black bars are 1 km long. V.E. ~30. Acquisition mode was switched at 06:07 from 'single pulse' to 'pulse train'.

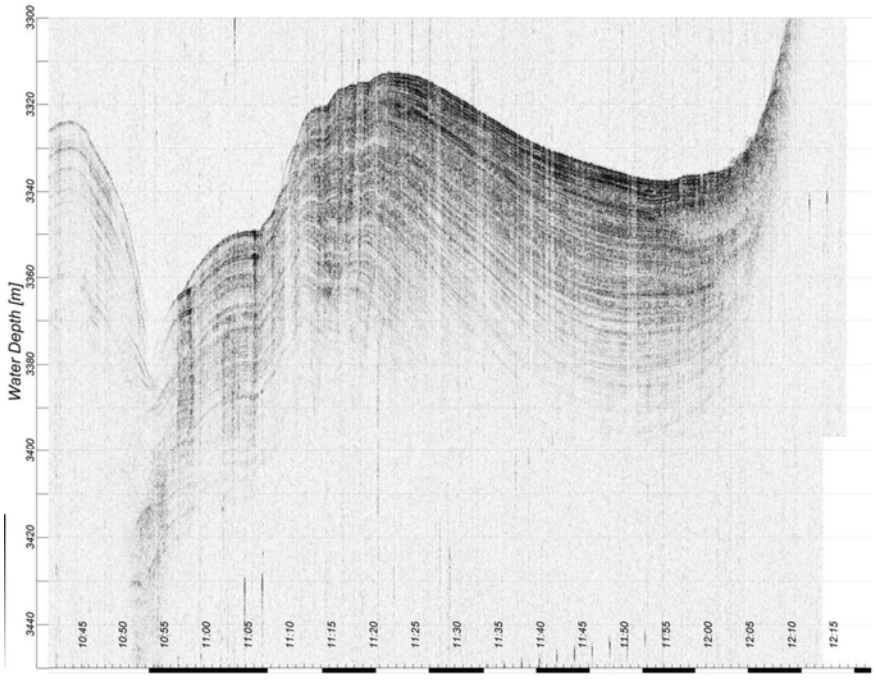

Fig. 20: A sequence of layered and transparent sedimentary units from the flank of Chapopote. Horizontal black bars are 1 km long. Different lengths indicate changes in the number of pulses (pulse train mode) of velocity changes of the ship. V.E. ~30.

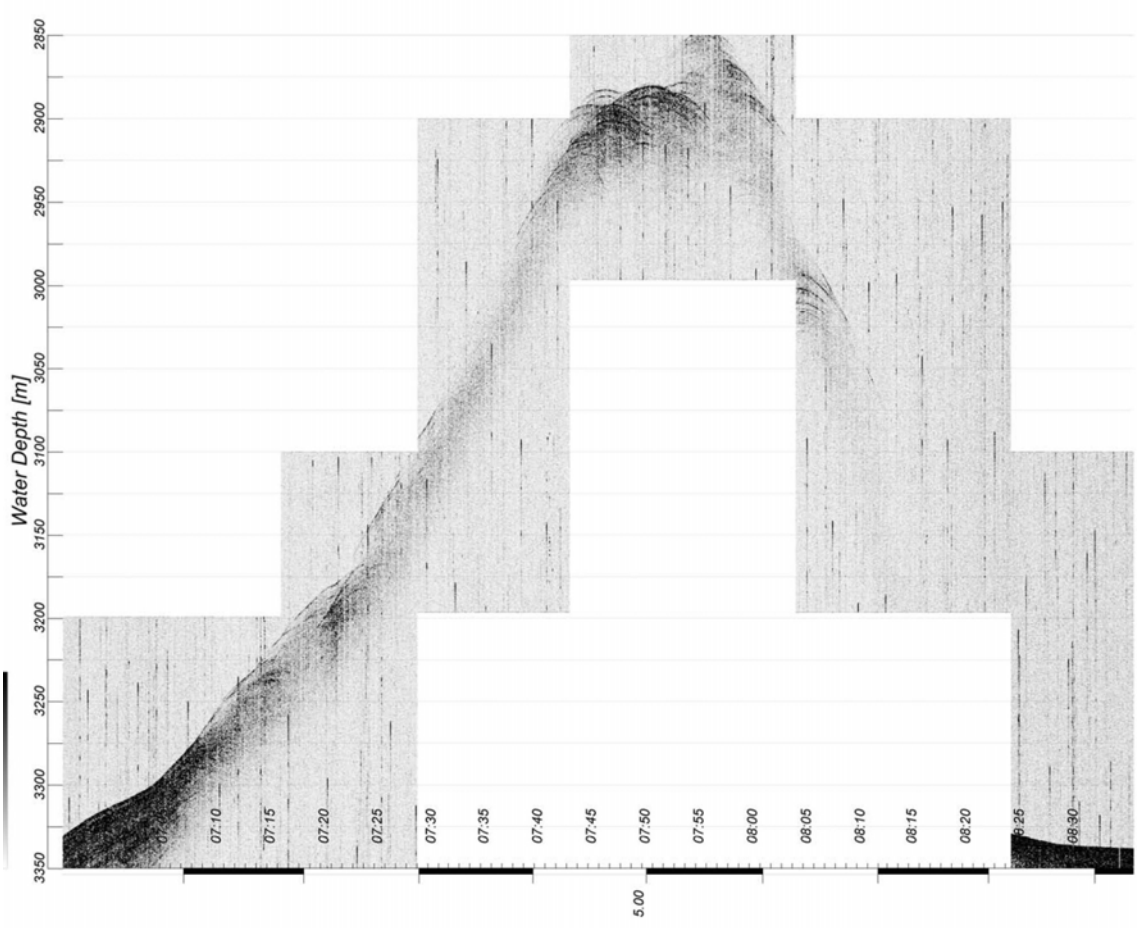

Fig. 21: Digital PARASOUND line across Chapopote Knoll; horizontal black bars are 1 km long. V.E. ~12.

Plume Imaging

As a benefit of the new functionality of the PARASOUND system, we specifically could use it during station work and slow profiling to search for gas bubbles in the water column with the 18 kHz PHF signal. This has already been successfully carried out during previous cruises to the Black Sea and the Gulf of Mexico. However, since the system had not been designed to optimize signal quality for the primary high frequency, data quality had been limited.

With the new PARASOUND hardware, but also with the new capabilities of parallel visualization, a full recording of the water column is possible. Choosing separate windows for different depth interval then gives the opportunity to use an amplitude scaling, which accounts for the spherical spreading loss, and maximum quality was reached for small object detection.

While no evidence for gas bubbles had been found during the first subleg 2a, the slower ship's speed during the second subleg, sometimes only 2 knots on bathymetric surveys and during station work, was favourable to image the bubble streams in several consecutive pings, which would be a minimum requirement to unequivocally identify gas plumes. Typical ship's velocities of 5 knots and higher are not suitable because of the narrow beam of the PARASOUND system, where objects are enlightened by sound only 2 to 4 times in a water depth of 3000 m at a ping interval of 5 seconds.

At slow speed, several gas plumes were found in the water column, some associated with oil slicks at the sea surface. Figure 22 shows an example of the water column record of the PHF 18

kHz signal at 3000 m water depth, acquired on a somewhat irregular course. Ship's speed is variable, but <3 knots. Amplitudes are greyscaled, and scaling is optimized for weak reflections or scatter signal, thus sea floor reflections and the return from plancton clouds in near-surface waters are clipped. Otherwise, amplitudes are corrected for spherical spreading losses.

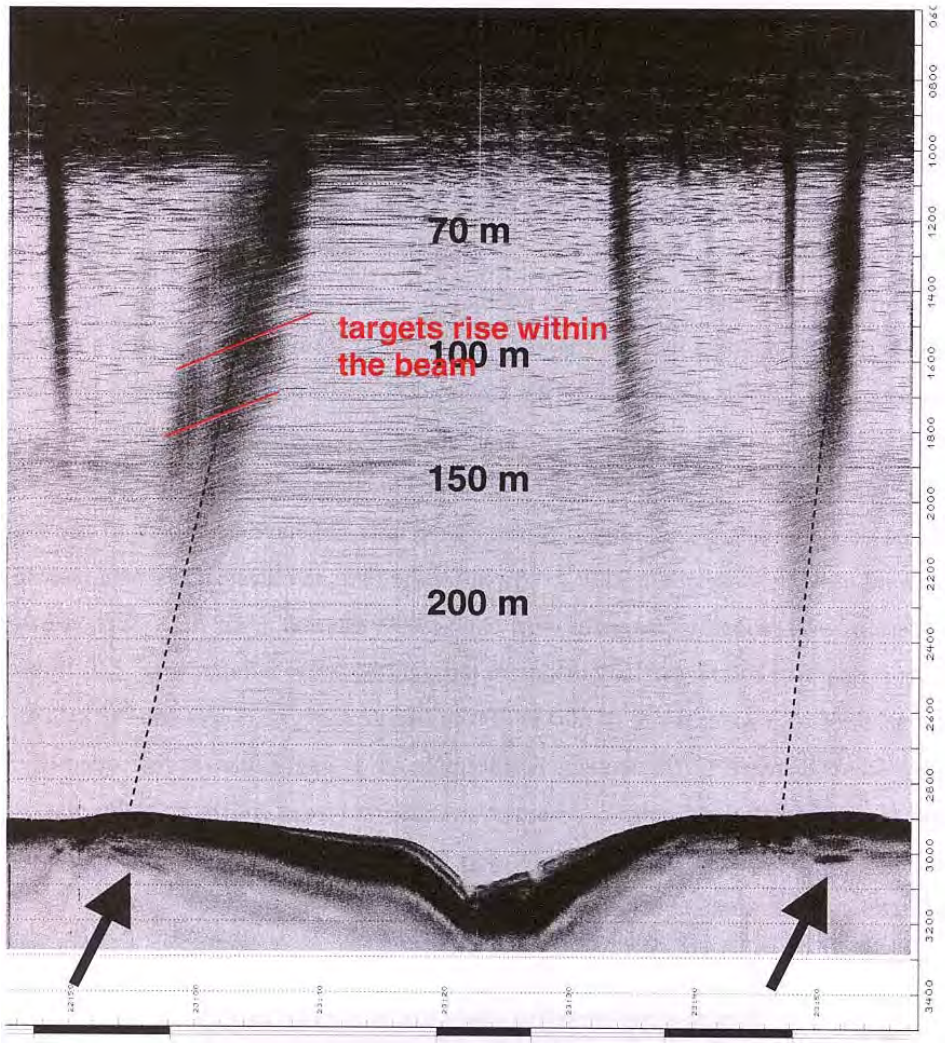

Fig. 22: PHF 18 kHz record from Chapopote, recorded at slow ship's speed across a surface oil slick. Vertical axis is water depth for a sound velocity of 1500 m/s. Numbers give diameter of the PARASOUND sound beam for different water depths. Arrows indicate possible subsurface anomalies, gas flares appear as dark, near-vertical columns. Amplitudes are corrected for spherical spreading losses.

Gas flares appear as dark, near-vertical columns. Internally, they reveal numerous lines with the same slope angle, which originate from bubbles or bubble clusters, which rise at constant speed. Arrows indicate possible subsurface anomalies, which may be the origin of gas flares. The scatter signal from bubbles decrease with water depth, which may partially be caused by a loss of sound energy as well as by a possible increase of bubble size due to decreasing ambient pressure. It is difficult to trace the streams back to the seafloor due to weak returns, but linear extrapolation connects to locations at the seafloor, where a pronounced structural anomaly might be identified in the 18 kHz signal, apparently at some 50 m sub-bottom depth. However, since penetration of this

high frequency signal is known to be low, i.e. on the order of 5 to 20 meters, it is more likely, that the anomalous patches occur within the sound beam from a rugged surface at greater depth.

The width of the plume basically depends on the beam diameter and the ship's speed, and does not provide a measure of the stream size itself. If we can assume that the diagonal lines within the plume originate from scattering of individually rising bubbles or groups, a rising speed can be estimated to appx. 30 centimeter/second.

Based on the onboard compilation of the plume data, we have been able to use the forward-looking sonar of the ROV to search for the flare and locate a site with intense release of big, probably centimeter size bubbles. At the end of a ROV dive it had been possible to follow the bubble stream through the water column (Fig. 23) from the seafloor to a water depth of 600 to 700 m, where navigation was too difficult to keep small distance to the stream. Furthermore, it is likely, that at this depth the hydrate coat of the gas bubbles becomes unstable anyway, and most of the gas is dissolved. The interaction with the strong backscatter signal of the near-surface plancton made it impossible to find out, whether bubbles can reach the surface.

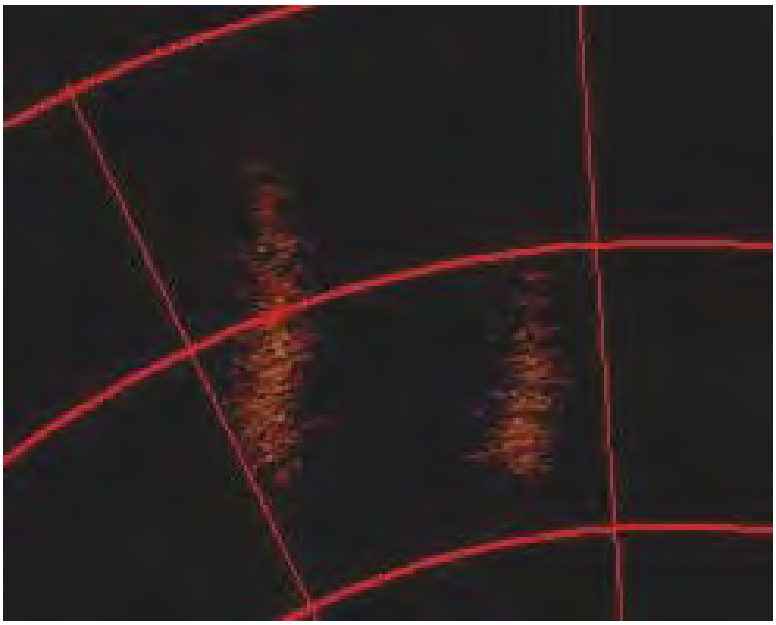

Fig. 23: Two parallel bubble streams in ROV forward looking sonar at Chapopote.

6 Multichannel Seismics

(V. Spiess, N. Fekete, H. Keil, F. Ding, T. Freidank, J. Geersen, J. Kuhlmann, S. Sebastian, A. Trampe)

6.1 Introduction

The Gulf of Mexico has been investigated for its hydrocarbon potential for about 30 years. Reservoirs are associated with salt diapirs, as a continuous sub-surface salt province stretches from the continental slope in the north to the central abyssal plain. Salt diapirism is one of the controlling processes in the entire Gulf, producing seafloor morphological structures up to 1500 m in height.

Until early 2006, twenty-two knolls (morphological highs) had been mapped in the Campeche Bay offshore Mexico, in water depths exceeding 3000 m. These are elongated features of 5 to 10 km in length and 480 to 800 m in height. Several of them display crater-like morphologies and signs of mass wasting in the form of slide scars.

During R/V SONNE Cruise SO 174 in 2003, so-called asphalt volcanoes were discovered at two of the knolls (MacDonald et al., 2004). These included several generations of lava-like asphalt flows with different surface textures, isolated blocks of asphalt in various shapes, and chemosynthetic communities. Seafloor samples from the asphalt revealed clear cooling structures, and contained rock fragments. Retrieved sediments were rich in oil and contained gas hydrates.

The origin of asphalt flows, as well as possible processes leading to their formation, appear hitherto unknown. One hypothesis for their development involves supercritical water from great subsurface depths passing through salt diapirs (Hovland et al., 2005). Hot, liquid asphalt is thought to erupt and cover sediments, to cool down and eventually solidify. While still warm it possibly destabilizes gas hydrates in the sediment and thus may trigger extensive mass wasting.

The asphalt volcanoes became the main focus of R/V METEOR Cruise M67/2. Our main objectives were 1) to determine the extents of the crater, the slides, and the asphalt flows, and identify potential subsurface structures in control of the system; 2) to investigate what is beneath these structures and find a plausible driving mechanism; 3) to find out if asphalt flows are a rarity or wide-spread features; 4) to determine the circumstances at which asphalt flows develop; 5) to explain the large amount of asphalt; 6) to assess the relation of chemosynthetic organisms to both the asphalts and other hydrocarbon seeps; and finally 7) to identify the biogeochemical and biological processes dominating the Campeche Knoll and their relationship to the asphalts. In addition to contributing to the above, a goal of Leg M67/2a was to utilize geophysical methods such as multichannel seismic survey, PARASOUND narrow-beam echosounder profiling, and sidescan sonar imagery, in order to help select prospective targets for the subsequent sampling with the ROV QUEST during Leg M67/2b.

6.2 Multichannel Seismic Equipment

Multichannel seismic surveying was carried out in three study areas during Leg M67/2a, including the vicinity of Chapopote Mound, the Oil Ridge, and the southern area. With the GeoB high-resolution multichannel seismic equipment, small scale subsurface structures are imaged on a meter to sub-meter scale, which can usually not be resolved with conventional seismic systems. During R/V METEOR Cruise M67/2a, a Sodera Generator-Injector (GI) airgun with extended chamber

volume (4.1 L generator and 1.7 L injector, frequency range ca. 30-300 Hz) was used as the main seismic source.

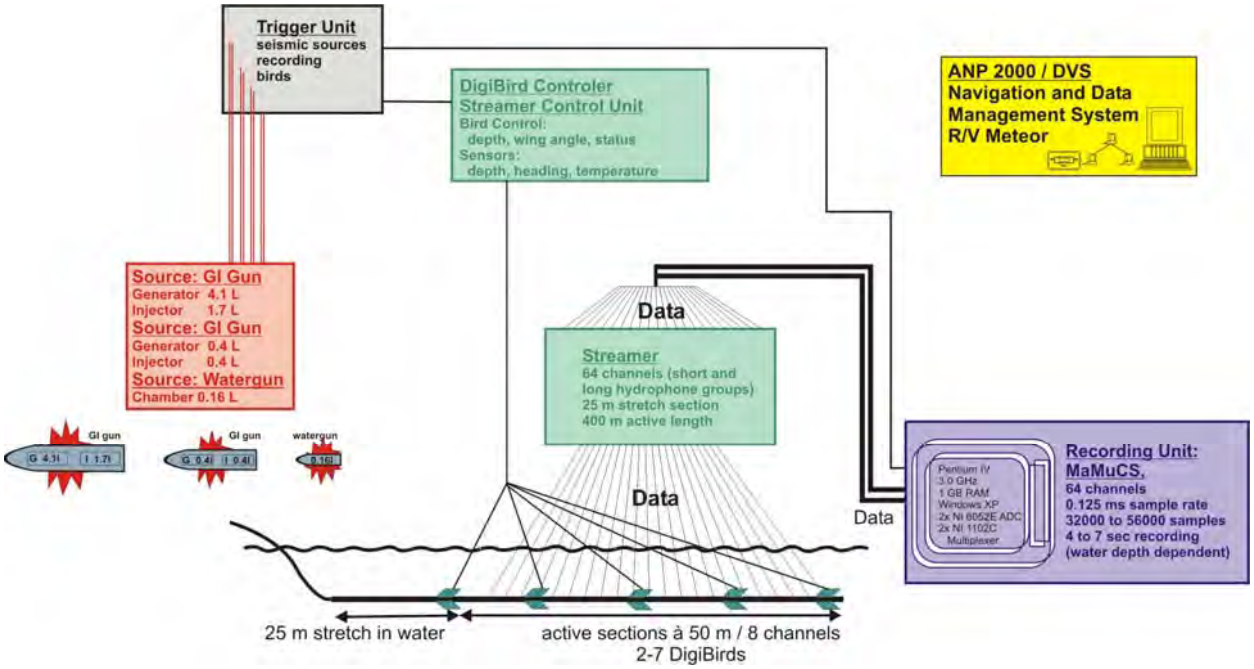

Fig. 24: System setup during M67/2a.

On the majority of profiles (GeoB06-086 to GeoB06-104 and GeoB06-117 to GeoB06-127), a small chamber watergun (Sodera S-15; 0.16 L, 200-1600 Hz) was operated quasi-simultaneously. A small GI gun (both chambers 0.4 L; 100 – 500 Hz) was used as a substitute for the large source during its maintenance (profile GeoB06-117). The alternating operation of guns provided several simultaneous seismic data sets, which are characterized either by greater depth penetration (GI gun source) or higher vertical resolution (watergun source). The active streamer length used was generally 400 m, with one profile (GeoB06-112) acquired with 150 m active length. Onboard processing of seismic data was carried out with custom software as well as with the commercial software package VISTA for Windows (Seismic Image Software Ltd.) and preliminary interpretation with Kingdom Suite (Seismic Micro, Inc.). Figure 24 gives an outline of the system setup as it was used during R/V METEOR Cruise M67/2a.

Seismic Sources and Compressor

During seismic surveying, a single GI gun (all profiles) and a watergun (on profiles GeoB06-086 to GeoB06-104 and GeoB06-117 to GeoB06-127) were used. Whenever more than one gun was operated, they were triggered in a combined mode, with the watergun first and the GI Gun 1.3 to 1.5 seconds later, before the reflections of both were recorded and stored in one seismogram. Shot rate varied depending on the water depth between 6.5 to12 s (see also trigger unit). Owing to an average ship's speed of 4.5 knots, a shot distance between 15 - 28 m was obtained for the alternating mode operation of each gun. The sources were shot at an air pressure of approximately 150 bar. The geometry of source and receiver systems during the measurements is shown in Figures 25 and 26. Ship velocity during deployment and retrieval was between 1.5 and 2.5 knots.

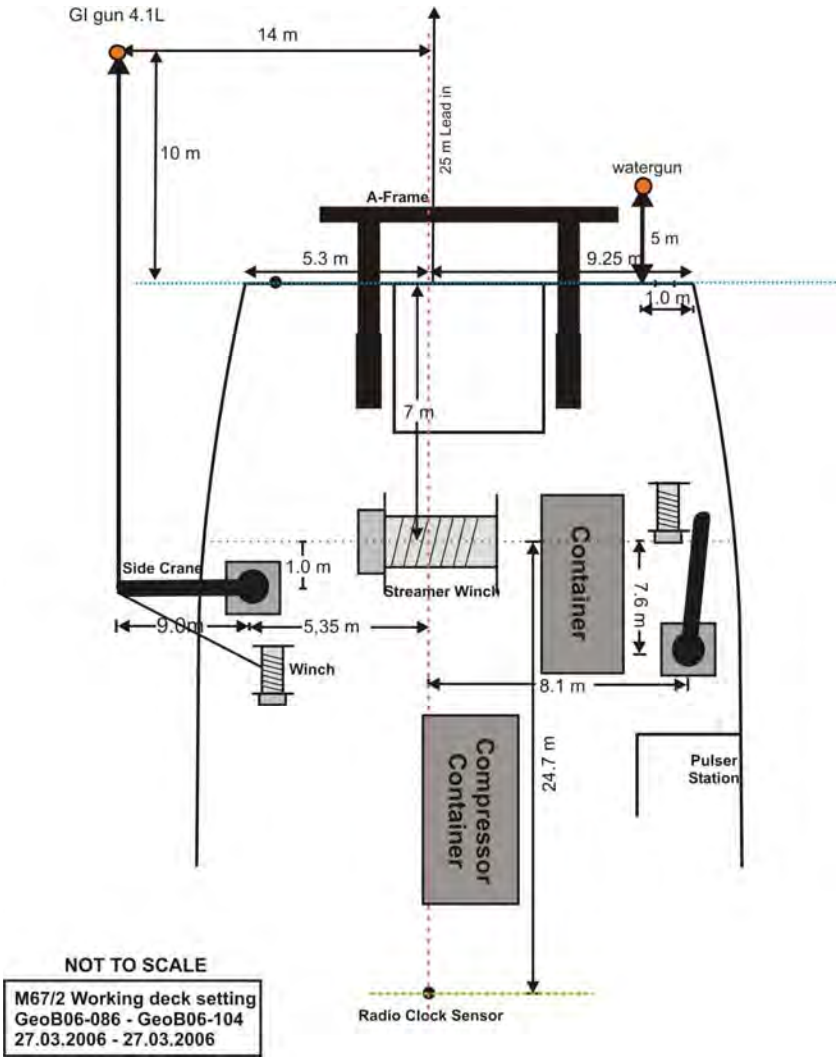

Fig. 25: Deck setting and towing geometry for profiles GeoB06-086 - GeoB06-104, with reference to the radio clock sensor.

One standard GI gun (Generator-Injector gun; Sodera) with extended generator chamber volume (generator: 4.1 L, injector: 1.7 L) and an S15 watergun (0.16 L, Sodera) were towed approximately 10 and 5 m behind the stern, respectively. Their lateral separation was 22 m until profile GeoB06-105 (watergun gun towed on the port side, GI gun from a crane on the starboard side) and 2 m thereafter (both sources towed on the port side, GI gun from a crane). For each gun, the towing wire was connected to a bow with the gun hanging on two chains 40 cm beneath. The watergun was fitted with an elongated buoy at the bow by two rope loops, stabilizing it in a horizontal position at a water depth of 0.5 m. The GI gun was connected to two small buoys which stabilized it in the water column. A large buoy tied directly to the towing cable held the gun at a water depth of 7 m. The injector chamber of this source was triggered with a delay of 50 ms with respect to the generator, basically eliminating the bubble signal.

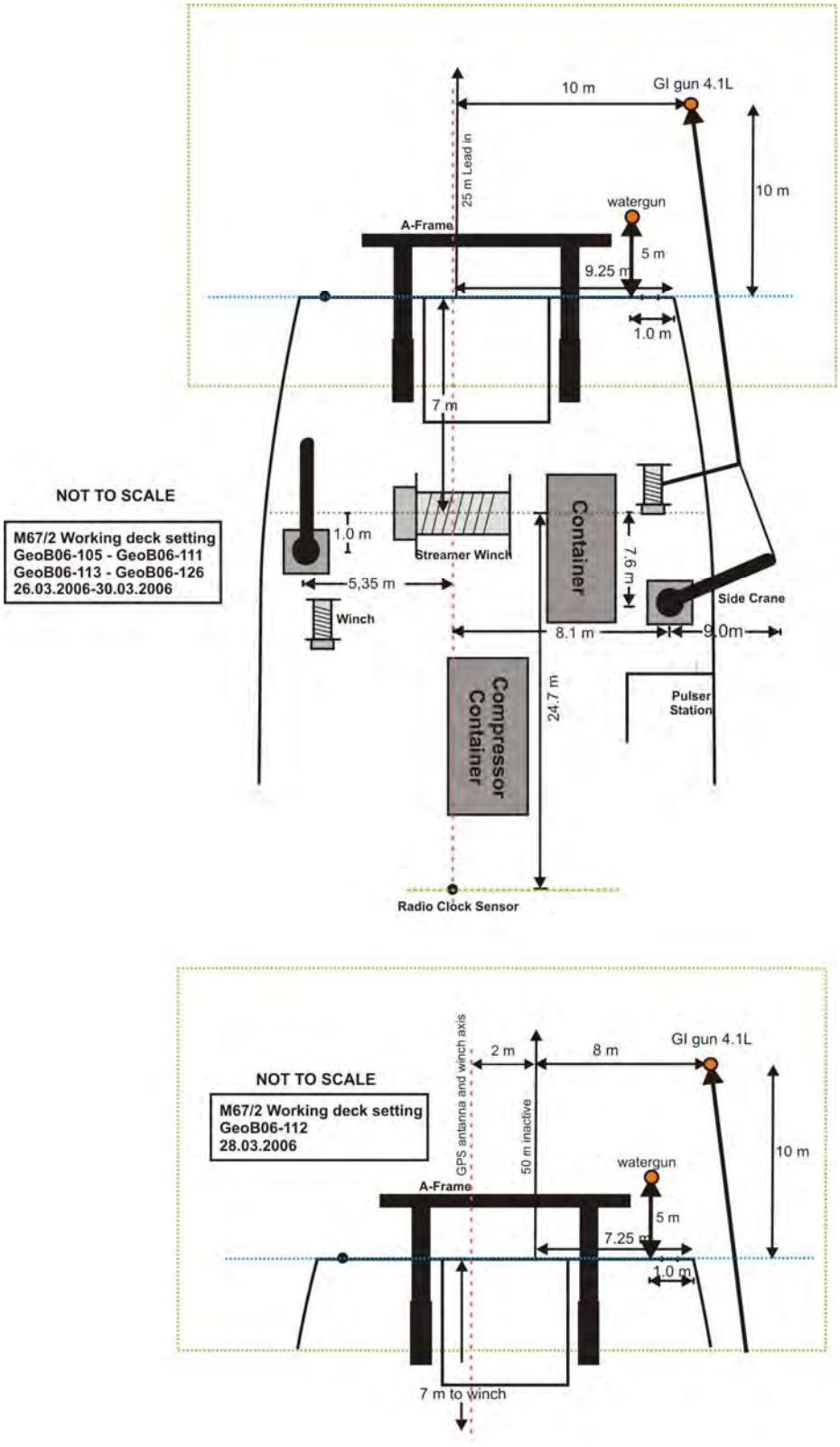

Fig. 26: Deck setting and towing geometry for profiles GeoB06-105 - GeoB06-127, with reference to the radio clock sensor. Note different settings for profile GeoB06-112 (bottom).

Streamer

The multichannel seismic streamer (SYNTRON) used during R/V METEOR Cruise M67/2a included a lead-in (25 m of which was towed in water), one stretch section of 50 m, and up to twelve active sections of 50 m length. However, data from only eight of these were recorded during most of the survey, in order to avoid the usage of two different acquisition units with two very different recording characteristics (see Section "Data acquisition system"). A 50 m long METEOR rope with a buoy at the end was connected to the tail swivel. A 30 m long deck cable connected the streamer to the recording system. Streamer setup is shown in Figure 27.

On profile GeoB06-112, only four streamer sections were deployed, in order to minimize the risk of the streamer being damaged by or tangled up with the cable of the simultaneously operating deep-tow sidescan sonar. Since the first section was partially out of the water, only data from three sections were recorded (24 channels), and streamer altitude was controlled by two DigiBirds only. Streamer section locations, the distance of their front behind the vessel, bird numbers, and bird socket locations in meters from the stern are summarized in the appendix (App. 2).

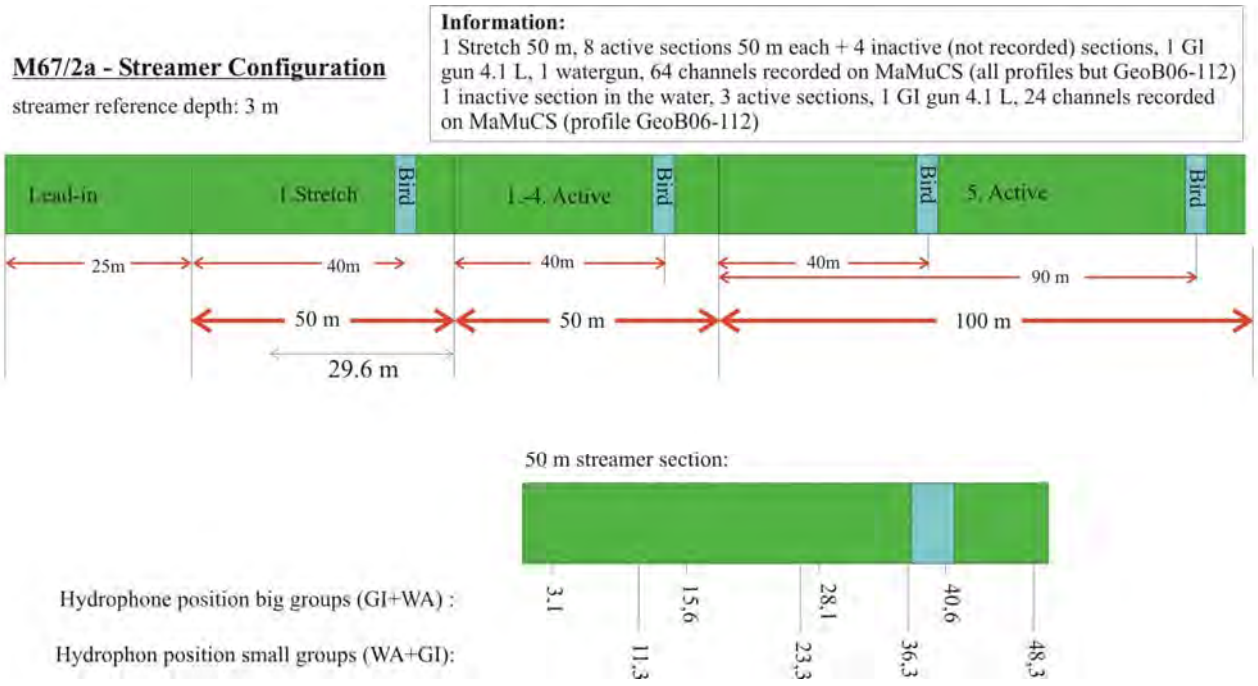

Fig. 27: Streamer setup. Streamer reference depth is 3 m. For bird locations, see Appendix 2.

Active 50-m-sections are subdivided in 8 hydrophone groups. Each of the 6.25 m long hydrophone groups is again subdivided into 5 subgroups of different length. One of the subgroups is a high-resolution hydrophone with pre-amplifier. A programming module distributes the subgroups of 4 hydrophone groups, i.e. a total of 20 groups, to 5 channels. Every second 6.25 m hydrophone subgroup was completely used with all 13 hydrophones, whereas the two additional channels were reduced in length to 2.2 m and 3.3 m, respectively. Locations of individual hydrophone groups are given in Figure 27. During M67/2a, output channels 1 to 64 (all hydrophone groups of 400 m active sections) were connected to the custom-designed MaMuCS recording

system, independent of the hydrophone group length. Single hydrophones were not recorded. Irrespective of the location within the 25 m units, programming modules were hardwired with the two long groups as first and second channel, at 12.5 m spacing, and the shorter groups as third and fourth channel. Accordingly, channels need to be rearranged for proper offset assignment.

Bird Controller

Streamer position is controlled and monitored through cable-levellers, so-called birds. The system consists of a controller computer and several Remote Units. Each RU includes a depth and a heading sensor as well as adjustable wings. Controller and RUs communicate via communication coils nested within the streamer. A twisted pair wire within the deck cable connects controller and coils.

Seven DigiBird RUs (numbers 5, 6, 11, 12, 13, 14, 15) were available and could be configured using the bird controlling unit. In operation, communication with RU 15 failed, therefore depth and heading readings from only six birds are available. However, since the malfunctioning did not appear to influence wing angle, the defective bird was programmed on deck to keep a depth of 3 m, and used at the streamer tail. Birds were positioned along the streamer such that the control of streamer attitude could be maximized (see Appendix 2).

Each shot trigger started the bird scan of water depth, wing angle and heading data. The momentary location of the streamer could be displayed as a depth profile on a screen. Bird parameters including date and time were digitally stored on the trigger PC through a hyperterminal.

Before the streamer was deployed, each RU was programmed in the seismic lab to keep an operating depth of 3 m. The RUs thus forced the streamer to the chosen depth by adjusting the wing angles accordingly. Possible depth variations of the streamer could be checked later during preliminary data processing and depth control appeared to be successful.

Data Acquisition System

For data recording, a new custom-designed and PC-based 64-channel seismograph was used. It is based on a Pentium IV PC (3 GHz, 1 GB RAM) with Windows XP operating system and was operated at a shortest sampling rate of 0.125 ms at 16 bit resolution. It is equipped with two 32-channel multiplexers (NI 1102C) and two analogue-to-digital convertors (NI 6052E). The seismograph provides online data display of shot gathers as well as a brute stack section of the range of channels of the user's choice, and stores data in SEG-Y format on the internal hard disk drive. First back-up copies were created during periods of no seismic acquisition on an external disk, from which DVDs and tape backups could be created subsequently. Data were recorded at a sampling frequency of 8 kHz over time intervals of 4 to 7 s, resulting in up to 64 x 56000 samples of 4 byte per sample. Anti-aliasing was fixed to 10 kHz on the AD converter. Gain for each channel was set to 100 (measurement range 0.1 V). A filter of 55 to 600 Hz was applied to the data displayed on screen during acquisition, which however did not influence the raw seismic recordings.

Radio Clock

A crucial part of seismic data acquisition is that all components run on exactly the same time, within an error of milliseconds. For this purpose, GPS time is used, which is directly acquired from the satellites through a Hopf GPS-DCF77 radio clock apparatus. The apparatus consists of a GPS aerial, a radio clock (Hopf modul 6870), a multi-aerial amplifier (modul 4446), and a radio clock PC card (modul 6039). This last item is built into the trigger PC (see section "Trigger Unit"), making it the time server of the seismic acquisition system. GPS time is then distributed via LAN, and all other PCs are synchronized through the NTP (network time protocol) service. Larger time offsets are adjusted "smoothly" within a few minutes rather than in steps, but subsequently clocks are set every second. The interval of the survey included the switch from normal to daylight saving time. This feature was deactivated in all computers except the bird controller which, despite several attempts to readjust, still returned to summer time. Because of an erronously running Microsoft service, the recording unit finished profile GeoB06-127 with a 26 sec time shift relative to GPS time.

Trigger Unit

The custom trigger unit used during R/V METEOR Cruise M67/2a controls seismic sources, seismographs, and bird controller. The unit is set up on an IBM compatible PC with a Windows XP operating system and includes a real-time controller interface card (SORCUS) with 16 I/O channels, synchronized by an internal clock. The unit is connected to an amplifier unit and a gun amplifier unit. The PC runs a custom software, which allows to define arbitrary combinations of trigger signals, which were used to optimize the available recording time for two seismic sources and to minimize shot distance.

Trigger times can be changed at any time during the survey. Through this feature, the recording delay can be adjusted to water depth without interruption of data acquisition. The amplifier unit converts the controller output to positive or negative TTL levels. The gun amplifier unit, which generates a 60V/8 amp. trigger level, controls the magnetic valves of the individual seismic sources. This was placed in the pulser station close to the gun pressure controls to enable immediate shutdown of gun operation.

The quasi-simultaneous trigger scheme for a varying number of gun shots within a trigger period was relatively complex. Depending on the water depth, shot interval changed, as did the length of recording and the time offset between individual guns. The following constraints were applied: 1) GI gun was triggered 1.5 s after the watergun because of the typical penetration of the latter. 2) Unlike in the case of the watergun, large air volumes needed to operate the GI gun limit its shooting frequency. This allowed shot cycles to contain two watergun shots before a GI gun shot in water depths greater than 2250 m (3 s two-way travel time for the seafloor reflection at an acoustic velocity of 1500 m/s), or even three of them in water deeper than 3375 m (4.5 s TWT). 3) The recording unit was triggered slightly before the seafloor reflection energy of the first watergun shot arrived to the receivers, thus maximizing the useful part of recorded traces (no reflectors above the seafloor were acquired). 4) Shot cycles lasted long enough to allow a minimum of 3 s recording of the GI gun signal as well as a full recharge of the gun itself. 5) In shallow waters, time delay between the gun triggers had to be chosen such as to avoid interference between subsurface

reflections from one shot with the direct wave of the next. 6) The bird controller was usually triggered right at the beginning of the trigger period to avoid interference with seismic recording. Because of the relative complexity of trigger scheme, it had to be adjusted several times during the cruise, and careful processing is needed for properly applying delay times.

The trigger pattern was specifically readjusted for profiles acquired with just one source and during gun maintenance intervals. The resulting trigger schemes are listed in Appendix 3. A sound velocity through water of 1500 m/s TWT is assumed in the calculation of necessary delays. In Appendix 3, delays within individual delay sections are relative to the section beginning, and not from the beginning of the entire trigger cycle.

Apart from its main task, the trigger PC was also used to record navigation data, bird status reports and as time server.

6.3 Onboard Seismic Data Processing

Most of the onboard seismic processing concerned only 4.1 L GI gun data. Brute stack profiles, commonly used to give an immediate evaluation of data quality, were also obtained online during the data acquisition with MaMuCs. In most cases, channels 5 to 15 were summed up (stacked). A relatively narrow bandpass filter of around 20 - 300 Hz is applied during the stacking process. On the other hand, parameters such as the number of channels as well as filter limits may have been subject to change during the acquisition in order to obtain optimum visualization online. The brute stack data were further processed on board to correct trigger jumps and recording time delay. The images were used for preliminary analyses of the seismic data and further planning.

For some selected lines, CMP-stacks for 10 m CMP spacing were carried out on board. Processing was carried out with the Vista software (Seismic Image Software Ltd) on a PC. The processing procedure included trace editing, setting up geometry, static corrections, velocity analysis, normal moveout corrections, bandpass frequency filtering (frequency content: 55/110 - 600/800 Hz), stack and time migration.

To all the GI gun profiles in the Oil Ridge and Chapopote area, a simplified calculation of CMP positions was used on board to quickly produce high quality stack profiles. The procedure assumes that the streamer is constantly straight and parallel to the ship course during profiling. With these conditions, CMP locations relative to the starting points of profiles could be calculated from the absolute shot time using an average ship’s velocity. The determination of relative positions in one dimension allows CMP binning.

A CMP spacing of 10 m was chosen in general for all the profiles, while for several profiles in the Chapopote area, also a smaller spacing of up to 3 meters was tested, in order to compare lateral resolution and data quality. After setting up the geometry, delay and trigger jumps were corrected, and data above the seafloor arrival were cut. The profiles were then resampled to 0.25 ms and a bandpass filter of 20/40 - 600/1200 was applied. NMO correction with a constant velocity of 1500 m/s and CMP stacking were carried out. For most of the profiles across the Chapopote knoll, FD migration with a constant velocity of 1500 m/s and 45° to 60° dip angle was performed. However, due to the limited computational power available on board, data had to be resampled to 1 ms before this migration step.

6.4 Preliminary Results

Working Areas and Survey Strategy

During Leg M67/2a, 42 seismic lines (Appendix 4) were acquired during most of the transit and bathymetric survey profiles as well as for dedicated survey grids around the Northern Knoll (Chapopote and others; Fig. 28) and across the Oil Ridge (Fig. 29). An overview survey was carried out in the southern part of the working area (Fig. 30), providing a complete bathymetric coverage.

The location of the profiles was partially chosen based on the known existence of oil slicks, which had been identified on satellite images. Lines were planned across as many oil slicks as possible to study their sub-seafloor structures. Furthermore, lines were mostly run perpendicular to the knoll structure to avoid side echoes and artifacts due to threedimensional topography and structures.

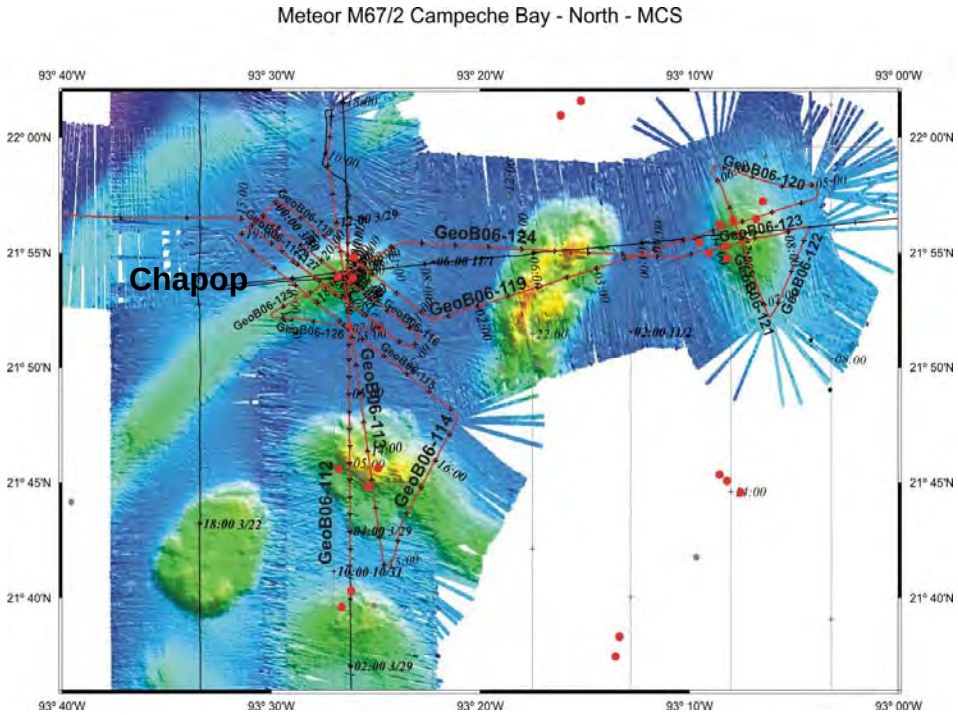

Fig. 28: Bathymetry and seismic lines in the northern working area around Chapopote Knoll. Red and grey dots indicate oil slicks identified in satellite images.

The survey across Chapopote Knoll, which had been visited during R/V SONNE Cruise SO 174, was targeted to the deformational pattern of the sediment cover. Faults running along the axis of the knoll in NE-SW direction were assumed to provide pathways for upward migration of asphalts. Several parallel lines across the known near-surface occurrence of asphalts were shot to analyze the seismic response and signature of asphalts versus normal sediments, particularly using different frequencies of watergun and GI Gun signals and PARASOUND sediment echosounder records.

Another significant structure in the central working area (Fig. 29) was Oil Ridge, which revealed the highest density of first order oil slicks. Also there a number of lines were shot perpendicular to the ridge for mapping of faults systems and subsurface gas and asphalt reservoirs.

The survey in the southern part of the working area was mostly carried out to gain a better overview over the existing knoll and salt diapiric structures and the variability of fluid and gas migration systems and deformational patterns.

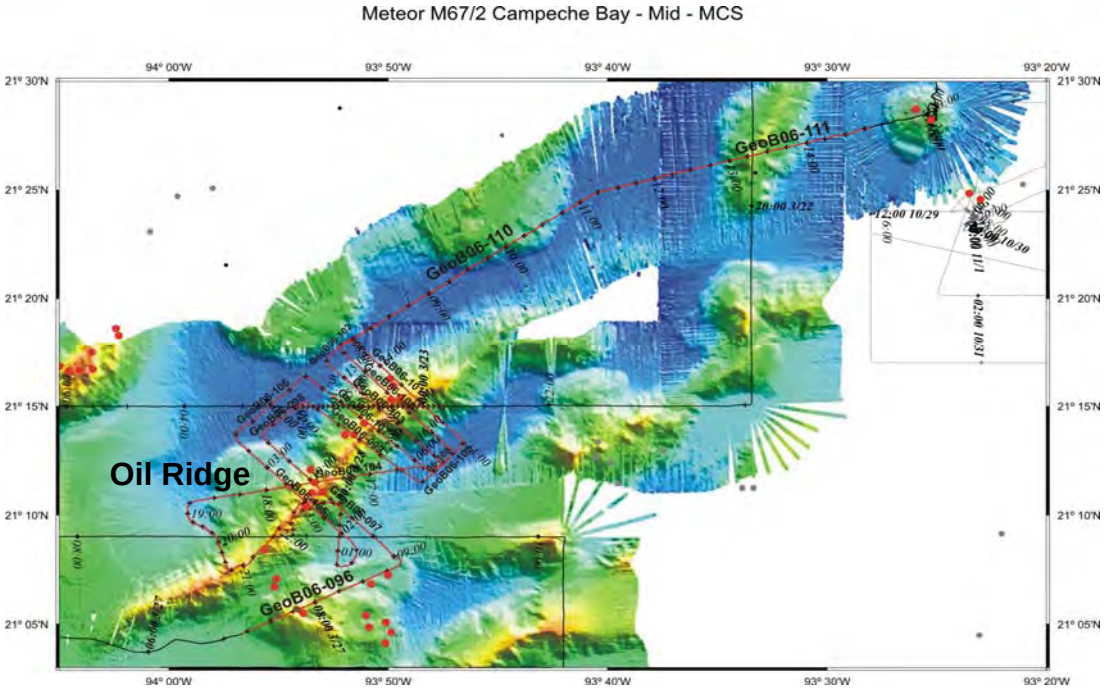

Fig. 29: Bathymetry and seismic lines in the central working area around Chapopote Knoll. Red and grey dots indicate oil slicks identified in satellite images.

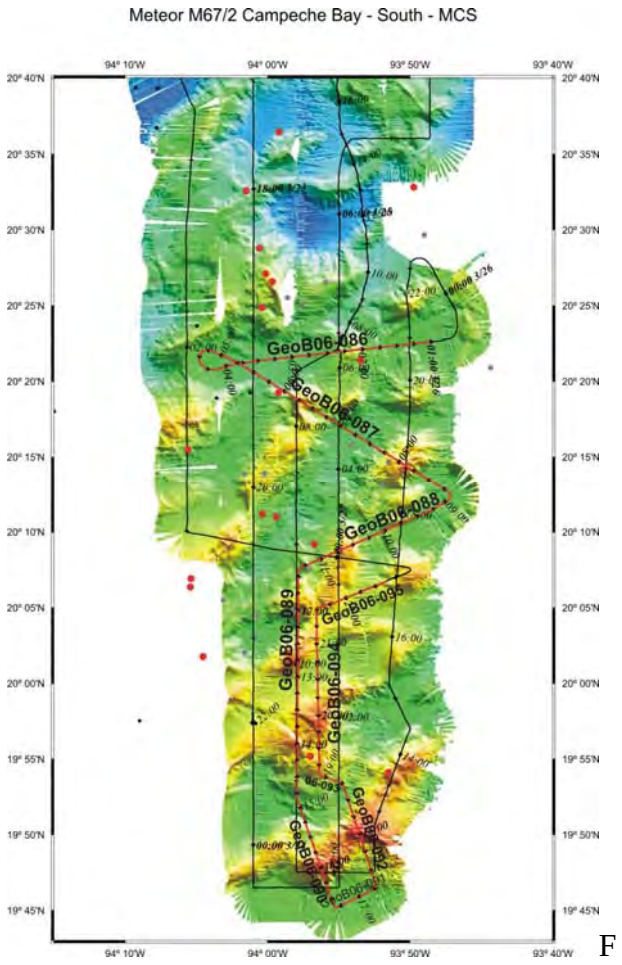

F

Fig. 30: Bathymetry and seismic lines in the southern working area. Red and grey dots indicate oil slicks identified in satellite images.

Southern Working Area

Typical for the southern working area is a pronounced deformation due to salt diapirism, which causes a significant uplift of the sediment cover, associated with faulting and tilting. Furthermore, as shown in Figure 31 for Line GeoB 06-089, high reflection amplitudes are observed a few hundred milliseconds beneath the seafloor in elevated areas. Since these bands appear relatively diffuse, and are not directly following the original layering, they very likely represent reservoirs of trapped shallow gas. Although the sediments are fine-grained and relatively impermeable, most likely the gas is trapped by the presence of gas hydrates. In the local basins, where deformation is moderate to low, gas concentration seems to be insufficient for developing free gas pockets.

Signal penetration is apparently controlled by the amount of shallow gas, as can be evaluated from the comparison of the southernmost ridge and the northern diapir in Figure 31. At ~CMP 1500, penetration reaches 2 seconds TWT, which equals 2000 m or more for sufficiently consolidated sediment. Near the bright spots in the South, penetration is limited to only a few hundred milliseconds. The top of the high-reflectivity band varies in sub-bottom depth, which may indicate either pronounced variations in heat flux or in methane flux. The data will be used to generally characterize and map the distribution of diapirs, shallow gas traps, fault zones and migration pathways.

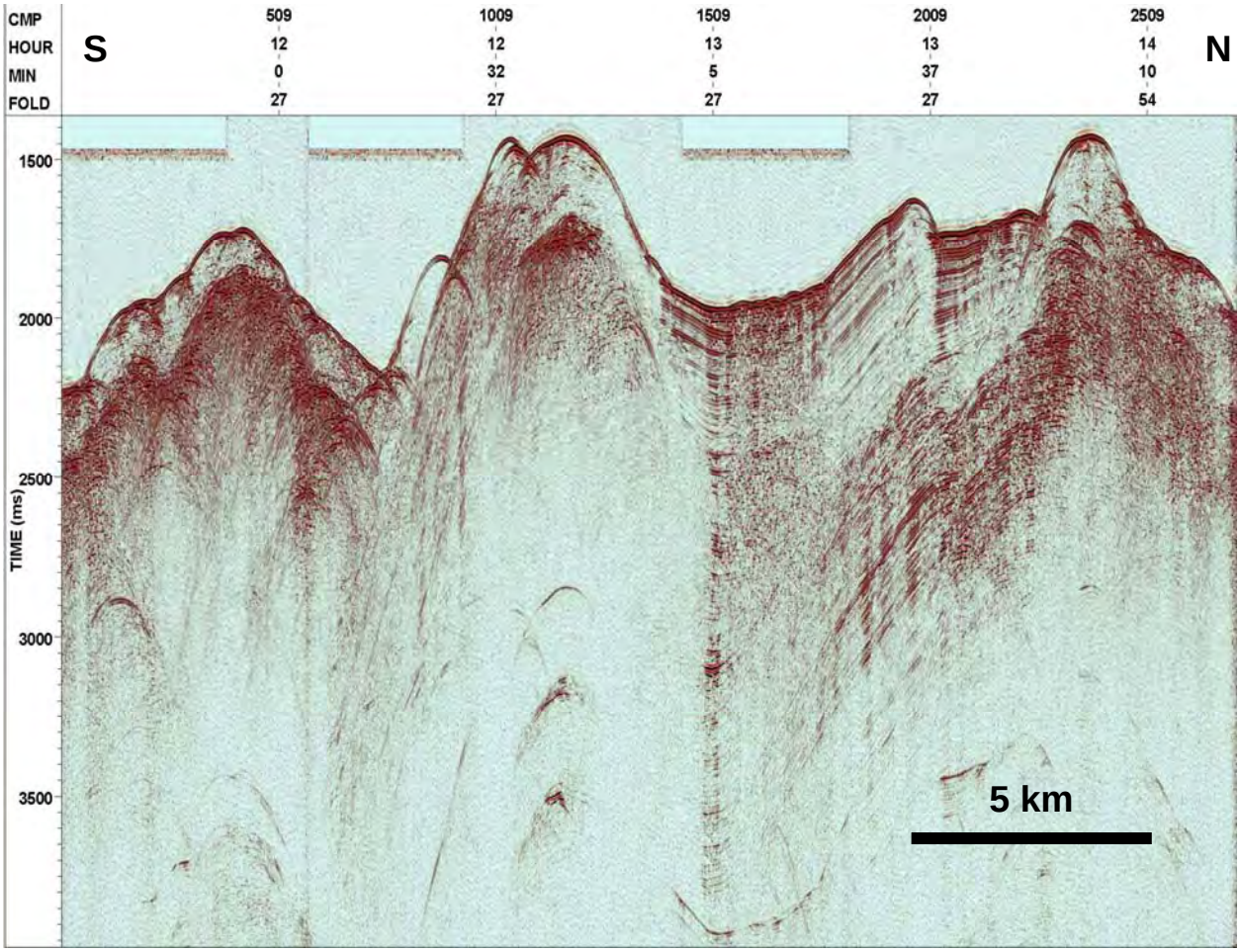

Fig. 31: Multichannel seismic line GeoB 06-089 in the southern part of the working area.

Central Working Area – Oil Ridge

A marked ridge structure had been the target for seismic surveying in the central working area. With respect to oil slicks, the area reveals most dense clustering, particularly above the ridge itself, and dedicated seismic lines were shot perpendicular to the ridge at several locations. Figure 32 shows an E-W line, to which we applied a preliminary processing including stacking at 20 m CDP spacing and FD migration. This relatively time consuming migration had to be applied to account for the extreme complexity of the surface and internal reflectors and the steepness of flanks.

Internally, the ridge is characterized by the absence of distinct layering (Ding et al. subm.). The western flank reveals higher amplitudes than the eastern flank and a wider band of diffuse reflectivity. The eastern flank may be interpreted as a mass wasting structure, but confirmation will require detailed processing and interpretation. Most pronounced is a sub-surface reflector at 200-300 ms TWT, which is sharp and continuous over several kilometers. The lower frequency content and high amplitude together with a negative polarity indicates a shallow gas reservoir, which may be the origin of an oil slick, which was also observed during this cruise. The image reveals a significant lateral variability in structure and amplitude, also steeply inclined reflectors, potentially parts of deep-reaching faults. The penetration of the seismic signals used is, however, insufficient to image the deeper structures due to attenuation. As is true for other diapirs, the ridge and knoll structures seem to be asymmetric in shape and deformation. Further processing may help to image the shallow sub-surface structures, which have been the target of the interdisciplinary research objectives of RCOM and this cruise.

Northern Working Area – Chapopote

During R/V SONNE Cruise SO 174, Chapopote Knoll had been visited for sampling and video and swath mapping. The most striking observation had been the surface occurrences of asphalts. No seismic data had yet been collected and the survey designed across this and other knoll structures was particulary looking for the distribution of asphalt at the surface, but also in the sub-seafloor, and their seismic signatures.

Both the flanks and the top of Chapopote are characterized by a smooth and distinct surface reflection, and a marked topography. In the vicinity of the asphalts, which were originally mapped between ~CMP 2400 and 2500, the amplitude is increased. Furthermore, beneath this surface amplitude anomaly, a turbid zone is found, which connects to another amplitude anomaly at depth at appx. 200-250 ms TWT below seafloor. Towards the south the original layering is preserved, but uplift due to salt diapirism can be observed (Ding et al. 2008). Within the layering, amplitude enhancement appears, which may hint to gas charge along a potential migration pathway. It can be speculated that the asphalt and the venting oil and gas originates from the shallow reservoir, which may be trapped due to impermeability of fine-grained sediments, but also due to the presence of gas hydrates.

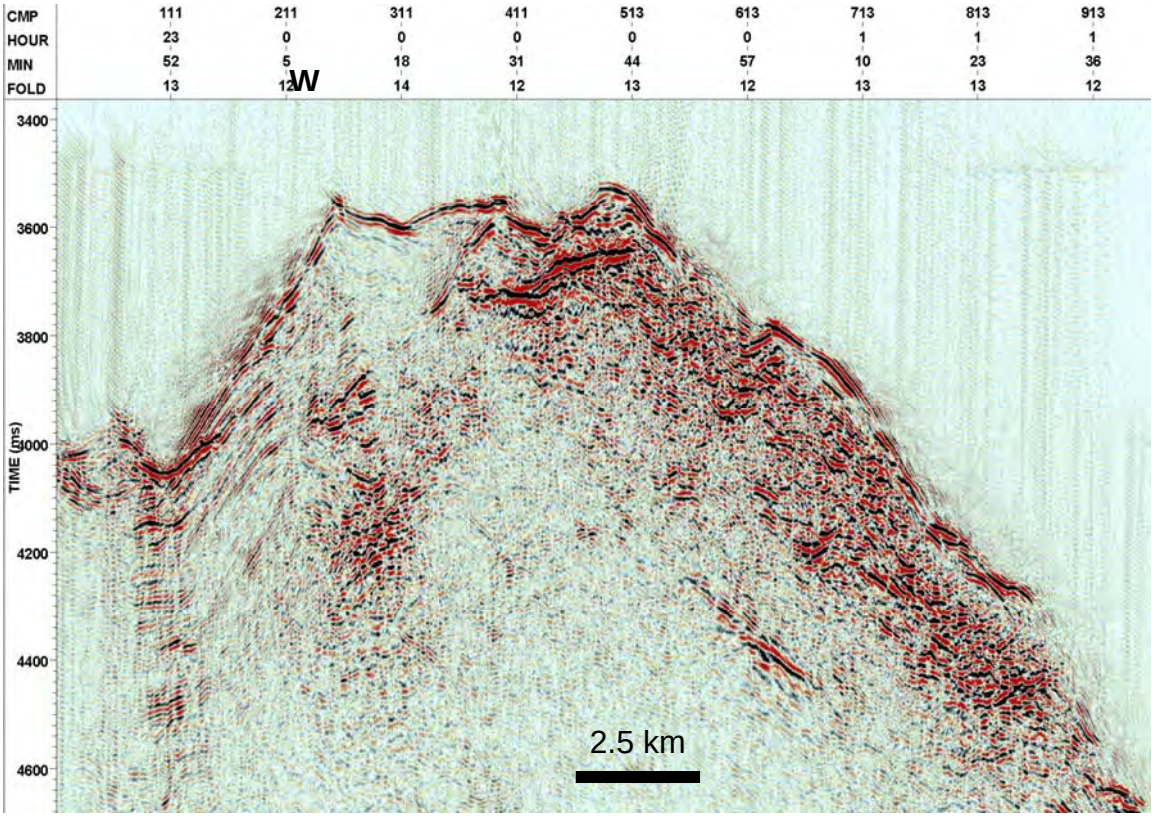

Fig. 32: Multichannel seismic line across Oil Ridge. Profile is stacked and FD-migrated with v=1500 m/s.

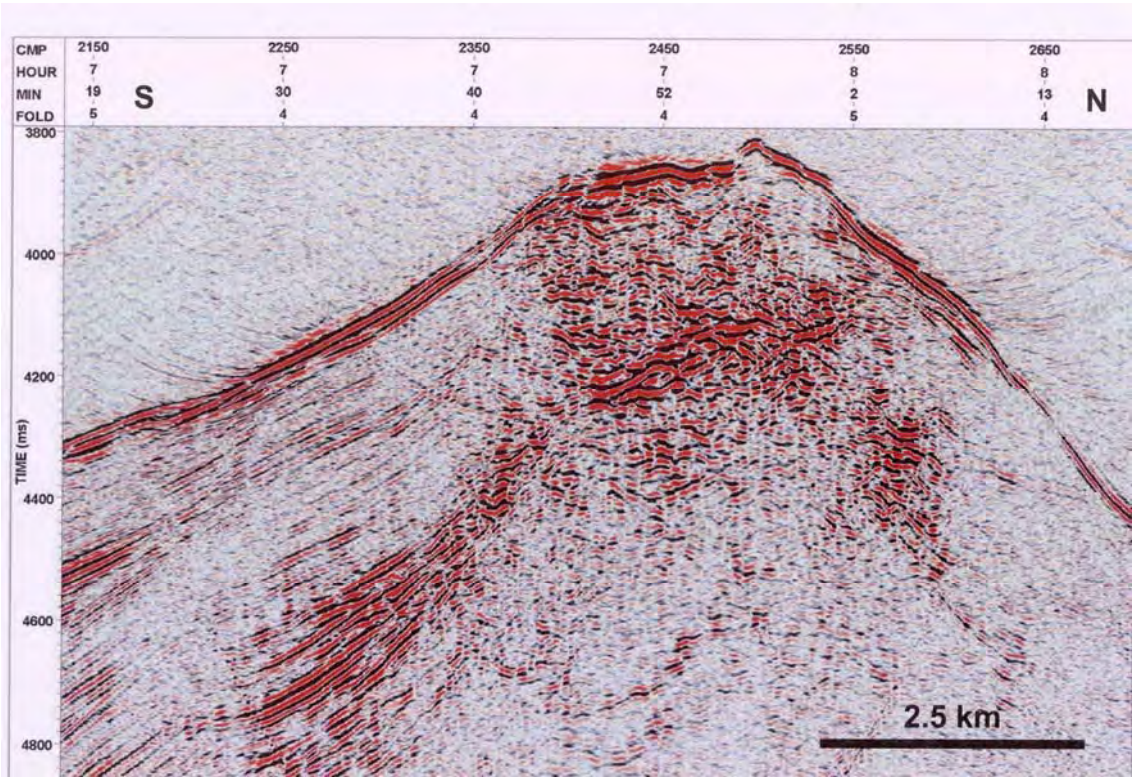

Fig. 33: Multichannel seismic line GeoB06-113 across Chapopote. Data is stacked and FD-migrated.

7 Visual Observations, TV-sled (TV-S) and TV-guided MUC (TV-MUC)

(H. Sahling, M. Brüning, I. MacDonald, T. Naehr, S. Kasten)

TV-sled and TV-MUC were used in order to observe and sample seep sites at the seafloor. The main aim for the TV-sled was to explore potential dive targets. The TV-MUC was thought as sampling tool for sediments influenced by hydrocarbon seepage. It has the advantage of a fast recovery of sediment cores. Asphalts have been found at Chapopote with OFOS 135 and 138 during the Cruise SO174. The occurrence of asphalt was mapped on the OFOS slides by Ian MacDonald and Elva Escobar. Based on these maps the ROV dives, TV-MUC deployments and additional TV-sled tows were planned.

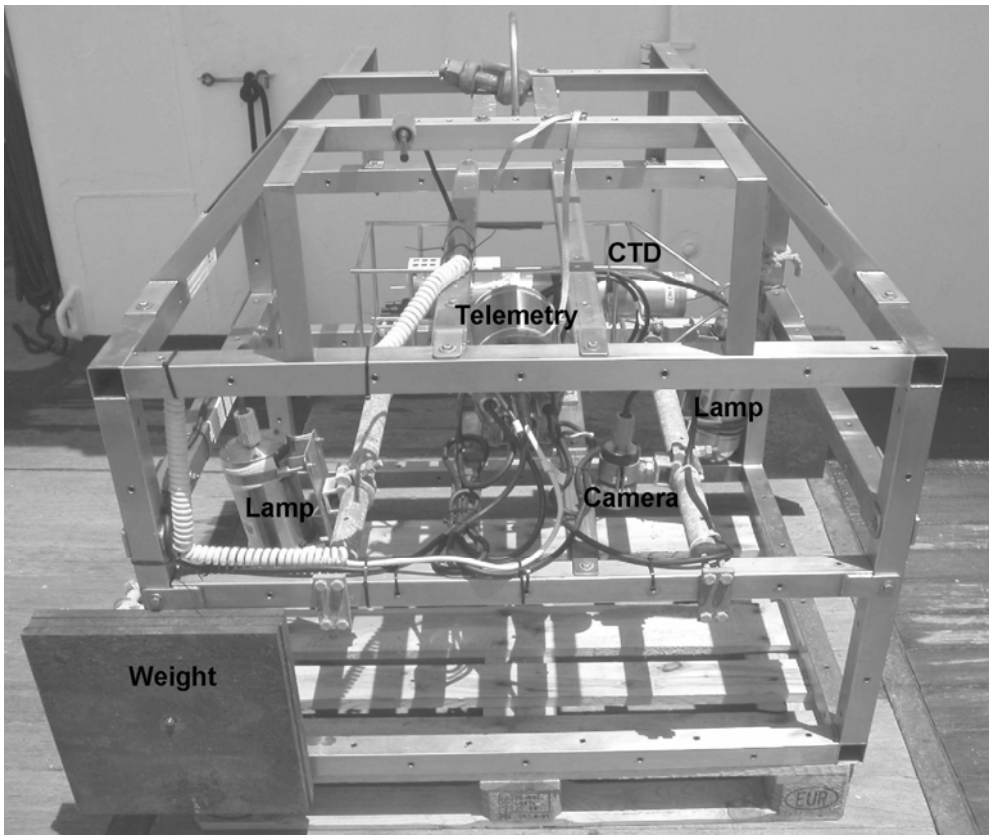

Fig. 34: TV-sled with the OKTOPUS video telemetry used during M67/2b.

7.1 Methods

The video-telemetry from OKTOPUS (SN 002) was used for the sled as well as for the conventional multicorer (MUC). The underwater unit consists of two xenon lamps, a camera, and telemetry. The analogue black-and-white video signal is transmitted via the 8000 m long coax cable of ship (W 12) to the on-board unit. The energy for the underwater components is supplied by the cable. The signal is recorded by a video recorder.

For the deployment of the TV-sled the video telemetry was mounted on the multi-frame (IFM-GEOMAR) together with a memory CTD (SEABIRD, SN 613) and the POSIDONIA transponder provided by the ship. The distance between the vertically down-looking camera and the xenon

lamps was about 60 cm. In most instances only one xenon lamp was turned on. The sled is towed at a speed of about 0.5 knots at the seafloor. A rope with a 13 cm wide shackle was suspended 200 cm below the camera helping the winch operator to manually adjust the distance of the sled to the seafloor.

Table 3: Summary of TV-sled and TV-MUC stations during Cruise M67/2b.

GeoB Station	Tool	Date	Area	Time at bottom (UTC)	Time off bottom (UTC) Sample site	Comments
10611	TV-sled	9 April	Knoll 2139	04:48	08:00:49	1 Video tape Transponder 70 CTD during downcast
10613	TV-MUC	9 April	Chapopote	22:02	00:17 21°54.323'N 93°25.634'W ca. 2920 m	1 Video tape Transponder 70
10614	TV-MUC	10 April	Chapopote	03:55	04:33 21°53.982'N 93°26.221'N ca. 2920 m	1 Video tape Transponder 70
10616	TV-MUC	10 April	Chapopote	22:51	01:18	No samples taken 1 Video tape only ship position
10620	TV-sled	13 April	Chapopote	11:43	14:20:04	1 Video tape Transponder 413 No CTD
10621	TV-sled	13 April	Chapopote	15:56	19:40	1 Video tape Transponder 413 No CTD

The video telemetry with one lamp and the camera was mounted on the small conventional MARUM multicorer. The small cores at one side had to be dismounted in order to give space for the telemetry mounted with a hydraulic cramp. The POSIDONIA system by IXSEA of R/V METEOR was used for underwater navigation. Two transponders are available, a low frequency miniature transponder "mini transponder" (MT861S-R, SN 070) and the duplex steel recoverable transponder "releaser" (RT861B2S, SN 413). A holding similar to that of the pinger was constructed in order to mount the mini-transponder on the sled as well as on the wire itself during the TV-MUC deployments. However, the Li-battery power of the mini-transponder is limited to about 5600 pings and only thought as additional energy supply in case the main power supply via an external source is not available. The much larger releaser is supplied by conventional batteries and last much longer. It was mounted on the sled. Data of POSIDONIA were recorded in two ways. Data output was via the network to the ROV database, where it was later exported and by directly recording the NMEA string with the ship and transponder positions on the POSIDONIA control unit. Data quality was generally excellent. However, the data had to be cleaned by deleting outliers and smoothing with a running mean.

7.2 Preliminary Results

TV-MUC and TV-Sled equipped with the video-telemetry are generally very effective tools which can be deployed by only two people in between, for example, ROV dives, in order to explore new sites or obtain additional sediment samples. During this cruise we encountered several drawbacks that led to a limited use of these systems. The wrong polarity of the underwater plug of the cable damaged the underwater telemetry unit during the very first test on deck. It took about four days to fix all technical problems. The TV-MUC was deployed only three times due to the lack of suitable soft sediments with evidence for being influenced by hydrocarbon seepage in the area of Chapopote.

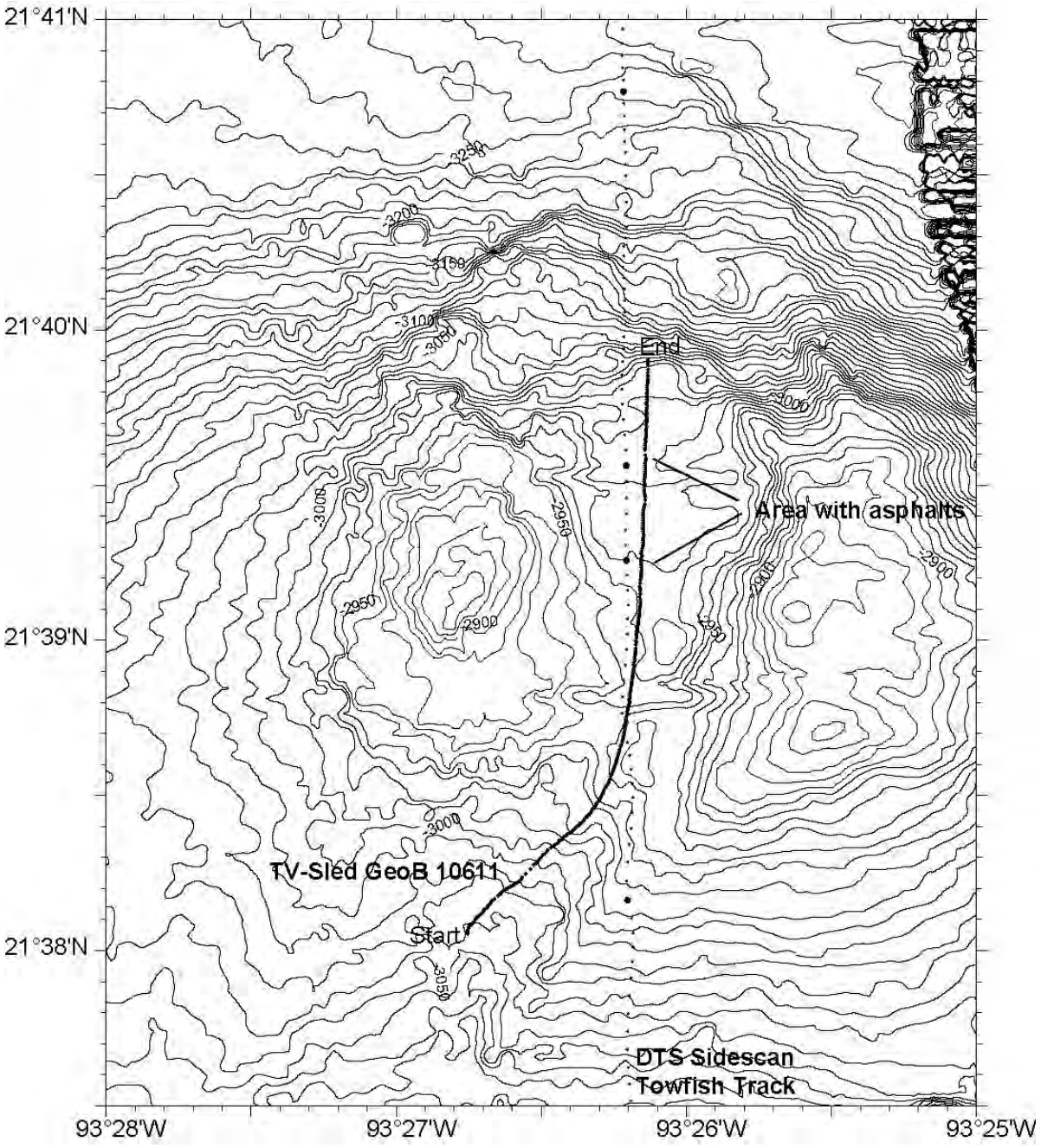

Fig. 35: TV-sled and DTS sidescan sonar tracks at Knoll 2139. In general, there was a good agreement between the sidescan sonar evidence (Fig.14) for asphalt at the seafloor and the observations by the TV-sled.

GeoB 10611 TV-sled

DTS sidescan sonar obtained during Cruise M67/2a revealed backscatter facies that are very likely related to the occurrence of asphalt at the Knoll 2139. In order to test this a TV-sled tow was conducted. It revealed that soft sediment covers the entire surveyed slide area at the southern flank of the knoll. Furthermore, it could be confirmed that eroded looking asphalts occurred in the central depression of the knoll between the summits. The asphalts occur in patches of a few meters. No seep-typical fauna was observed.

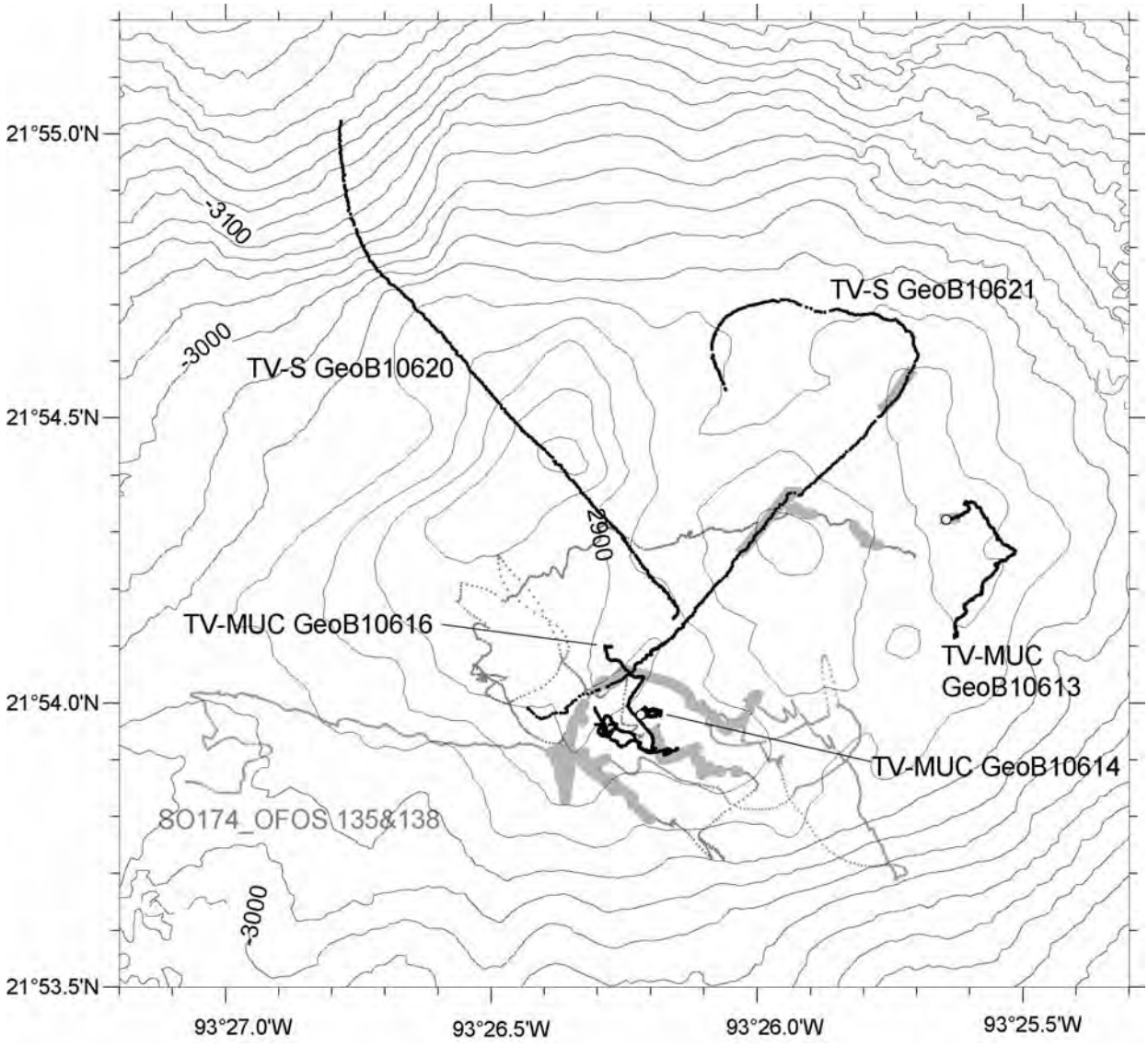

Fig. 36: TV-sled and TV-MUC tows at Chapopote conducted during Cruise M67 (black) and OFOS deployments conducted during Cruise SO174 (gray). Gray areas mark roughly were asphalts have been observed.

GeoB 10613 TV-MUC

Survey of the eastern crest of Chapopote where PARASOUND indicated acoustic anomalies in the water column. Only soft sediments were observed. In the area of the highest summit at the eastern crest some asphalts occurred. The TV-MUC was deployed in sediments close to asphalts, it

probably stood partly with the legs of the MUC on asphalts, therefore multicorer head tilted and only a few cores were filled with sediments. Brownish sediments were overlaying blackish sediments, but the sediments were not sulphidic and indicated a rather regular deep-sea geochemistry.

GeoB 10614 TV-MUC
Starting at SO174 TVG 6 position. Deployment close to asphalts, again recovery of sediments without evidence for hydrocarbon seepage.

GeoB 10616 TV-MUC
Long search track starting at TVG 6 position, no samples were taken due to the lack of interesting targets.

GeoB 10620 TV-sled
From depression going over the NW summit down the slide at NW flank of Chapopote. Mussel fields and asphalts only observed at start at western side of central depression. Only soft sediments in low backscatter region at SE slope of NW summit, soft sediments at summit. Above the slide headwall ripple-like sediment structures are interpreted as slump marks (creeping sediments?). Small scarps at headwall region. Some solid material of less than a few meter in the slide may be asphalts, carbonates or lithified sediments.

GeoB 10621 TV-sled
During this tow the existence of an asphalt field on the NE wall of the central depression discovered already during Cruise SO174 could be confirmed. The asphalts look more eroded compared to the asphalt field farther southwest. In contrast, the biological communities appear to be more extensive, with mussel and tubeworm fields. Another area with even more strongly eroded asphalts was observed at the local north-eastern local summit at the eastern crest. No biological communities were observed.

8 Remotely Operated Vehicle (ROV) QUEST

8.1 Technical Description and Performance

(V. Ratmeyer, S. Buhmann, K. Dehning, S. Klar, G. Meinecke, N. Nowald, M. Reuter, M. Viehweger)

The deepwater ROV (remotely operated vehicle) "QUEST 4000 m" used during M67/2b, is operated and installed at MARUM, Center for Marine Environmental Sciences at the University of Bremen, Germany. The QUEST is a commercially available, but specially adapted, 4000 m rated system designed and built by Schilling Robotics, Davis, USA. Aboard R/V METEOR for the 8th cruise since installation at MARUM in Mai 2003, the system is well adapted to the research vessel and could be handled during all stages of weather encountered during the cruise, with only one exception.

During M67/2b, QUEST performed a total of 5 dives to depths around 2900 m. All dives with a total of 56,5 hours bottom time allowed successful scientific sampling and observation at different sites at the Chapopote Knoll.

The total QUEST system weighs about 45 tons (including the vehicle, control van, workshop van, electric winch, 5000-m umbilical, and transportation vans) and can be transported in four 20-foot vans. Using a MacArtney Cormac electric driven storage winch to manage the 5000 m of 17.6 mm NSW umbilical, no additional hydraulic connections are necessary to host the handling system.

The QUEST uses a Doppler velocity log (DVL, 1200kHz) to perform stationkeep, displacement, and other auto control functions. Designed and operated as a free-flying vehicle, QUEST system exerts such precise control over the electric propulsion system that the vehicle maintained relative positioning accuracy within decimeters. Although these data were not used for absolute navigation, they are an essential tool for vehicle control during flight. The combination of 60-kW power with DVL-based auto control functions provides exceptional positioning capabilities at depth. In addition, absolute GPS positions are obtained using the very new shipboard IXSEA Posidonia USBL positioning system. Performance of the USBL system was limited to an absolute accuracy around 10-20 m.

The QUEST SeaNet telemetry and power system provides an extremely convenient way to interface all types of scientific equipment, with a current total capacity of 16 video channels and 60 RS-232 data channels. The SeaNet connector design allows easy interface to third-party equipment, particularly to prototype sensor and sampling devices, by combining power-, data-, video-distribution plus compensation fluid transport all through one single cable-connector setup. This ease of connection is especially important in scientific applications, where equipment suites and sensors must be quickly changed between dives. When devices are exchanged, existing cables can be kept in place, and are simply mapped to the new devices, which can consist of video, data, or power transmission equipment.

The substantial empty space inside the QUEST 5 frame allows installation of mission-specific marine science tools and sensors. The initial vehicle setup includes two manipulators (7-function and 5-function), five video cameras, a digital still camera (insite SCORPIO, 3.3 Megapixel), a light suite (with various high-intensity discharge lights, HMI lights, lasers, and dimmable incandescent lights), a CTD, a tool skid with drawboxes, an acoustic beacon finder and a 675 kHz scanning sonar. Total lighting power is 5 kW, and additional auxiliary power capacity is 8 kW.

For detailed video closeup filming, a near-bottom mounted broadcast quality (870 TVL) 3CCD video camera was used (Insite ATLAS). Continuous video footage was recorded with the ATLAS

camera and one additional color zoom video camera (Insite PEGASUS or DSPL Seacam 6500). In order to gain a fast overview of the dive without the need of watching hours of video, one video feed is continuously frame-grabbed and digitized at 5sec intervals.

The QUEST control system provides transparent access to all RS-232 data and video channels. The scientific data system used at MARUM feeds all ROV- and ship-based science and logging channels into a commercial, adapted real-time database system (DAVIS-ROV). During operation, data and video are distributed in realtime to minimize crowding in the control van. Using the existing ship's communications network, sensor data is distributed by the real-time database via TCP/IP from the control van into various client laboratories, regardless of the original raw-data format and hardware interface. This allows topside processing equipment to perform data interpretation and sensor control from any location on the host ship.

Table 4: Major data of ROV dives 80 – 84.

	Dive 80	Dive 81	Dive 82	Dive 83	Dive 84
GeoB	**10615**	**10617**	**10619**	**10622**	**10625**
Date	10.04.2006	11.04.2006	12.04.2006	13.04.2006	15.04.2006
Time start at bottom	17:41	05:12	15:50	23:41	01:59
Lat. start at bottom	21°53.920'	21°53.942'	21°54.333'	21°53.949'	21°53.380'
Long. start atbottom	93°26.152'	93°26.131'	93°26.497'	93°26.249'	93°26.131'
Depth start at bottom	2840	2913	2880	2915 m	2935 m
Time left at bottom	18:45	16:08	07:56	11:02	20:04
Lat. left at bottom	21°53.917'	21°53.949'	21°53.926'	21°53.927'	21°53.690'
Long. left at bottom	93°26.146'	93°26.238'	93°26.049'	93° 26.147'	93°26.131'
Depth left at bottom	2904	2910	2925	2923 m	2922 m
Total bottom time	1 hr 5 min	10 hr 56 min	16 hr 06 min	11 hr 21 min	18 hr 5 min
Video tapes	2x 1hr tapes	12 x 1 hr tapes	17 x 1hr tapes	11 tapes	
Scientist	Ian MacDonald	Ian MacDonald	Frank Wenzhöfer	Thomas Nähr	Antje Boetius

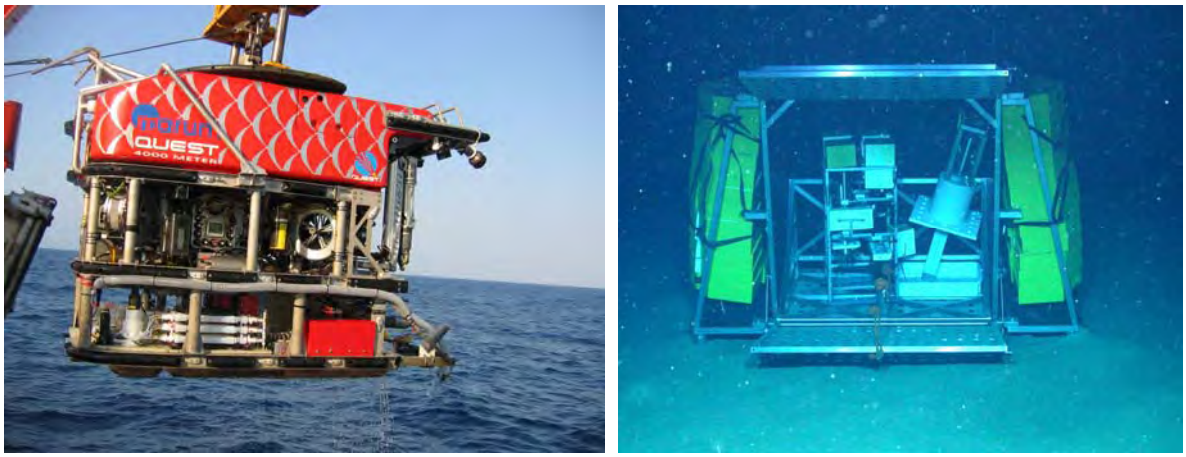

Fig. 37: ROV QUEST aboard R/V METEOR during recovery after a successful dive (left). Lift system on seafloor imaged during ROV Dive 82 (GeoB 10619).

Additionally, the pilot's eight-channel video display is distributed to client stations in labs and bridge on the ship via CAT5 cable. This allows the simple setup of detailed, direct communication between the bridge and the ROV control van. Similarly, information from the pilot's display is distributed to a large number of scientists. During scientific dives where observed phenomena are

often unpredictable, having scientists witness a "virtual dive" from a laboratory rather than from a crowded control van allows an efficient combination of scientific observation and vehicle control.

Post-cruise data archival will be hosted by the information system PANGAEA at the World Data Center for Marine Environmental Sciences (WDC-MARE), which is operated on a long-term base by MARUM and the Foundation Alfred Wegener Institute for Polar and Marine Research, Bremerhaven (AWI).

During M67/2b, additional scientific sampling equipment was installed:

- fluid pump system of 9 x 600ml with remote sampling and temperature probe
- rotary sampler with suction hose and capability of up to 8 discrete samples
- up to 12 pushcores, 2 in-situ tracer pushcores
- various “hand” tools including nets, scoops, markers

In addition, the Kongsberg 625kHz Scanning Sonar head provided acoustic information of bottom morphology and was used to detect and follow gas emissions at distances up to 100 m through 2000 m vertical distance from the seafloor.

8.2 Dive 80 (GeoB 10615)

Responsible scientist:	Ian MacDonald		
Date:	10 April 2006		
Start/end at bottom (UTC):	17:41 / 18:45		
Total bottom:	1 hr, 5 min		
Start at the bottom:	21°53.920’N	93°26.152’W	2840 m water depth
Start ascend:	21°53.917’N	93°26.146’W	2904 m water depth

Table 5: Instruments, tools and samples of Dive 80.

GeoB	Tool/sample	Start	Lat. (°N)	Long. (°W)	Remarks
10615-1	Beacon	18:30	21°53.920’	93°26.152’	deployed
10615-2	Fish trap	18:33	21°53.920’	93°26.149’	deployed

The QUEST developed a leak in the compensation system during descent. There was a hold at about 2000 m to evaluate the rate of leakage. It was determined that the dive could continue, but would be curtailed.

QUEST reached the seafloor at 17:41 UTC near a bottom depth of 2922 m (Fig. 9). Numerous small asphalt outcrops were in view. Shortly after bottom checks, the navigation system developed a problem and had to be restarted. The ROV turned to a heading of 000° to face into the slope. As the navigation problem was being worked on, QUEST was manoeuvred forward to investigate a ~1-m-wide mound. There were about 10 articulated, dead clam shells (possibly lucinid) on the top of the mound, each pair in small grey patch of sediment (Fig. 38, left). A discolored patch in the center of the mound looked like bacterial mat. Several photos were taken as we approached.

We decided to attempt a push core on the mound because time would be limited. The homing beacon was removed and deployed next to the mound. Movement of the ROV created a cloud of suspended sediments. A large brotulid fish appeared - possibly attracted by the baited trap. We deployed the fish trap near the beacon.


Fig. 38: Small elevation at the seafloor close to the beginning of the dive (left).

The pilot announced that we needed to leave the bottom. Before leaving, the ROV arm was poked into a small mound near the larger one. It encountered hard substrate below about 15 cm of sediment. The ROV moved NE toward a large outcrop of asphalt and briefly videoed a healthy aggregation including tube worms and mussels before leaving the seafloor (Fig. 38, right).

8.3 Dive 81 (GeoB 10617)

Responsible scientist:	Ian MacDonald		
Date:	11 April 2006		
Start/end at bottom (UTC):	05:12 / 16:08		
Total bottom:	10 hr, 56 min		
Start at the bottom:	21°53.942’N	93°26.131’W	2913 m water depth
Start ascend:	21°53.949’N	93°26.123’W	2910 m water depth

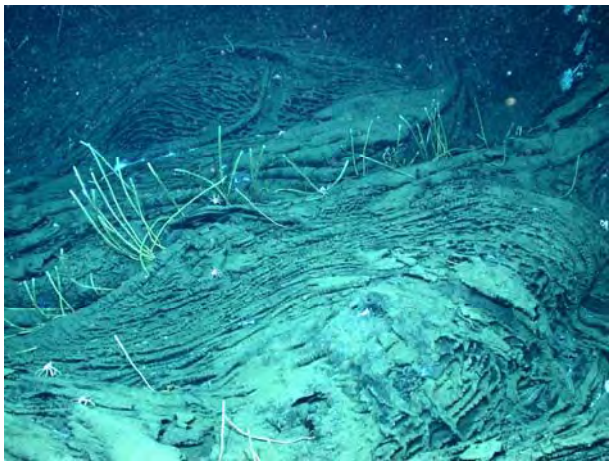
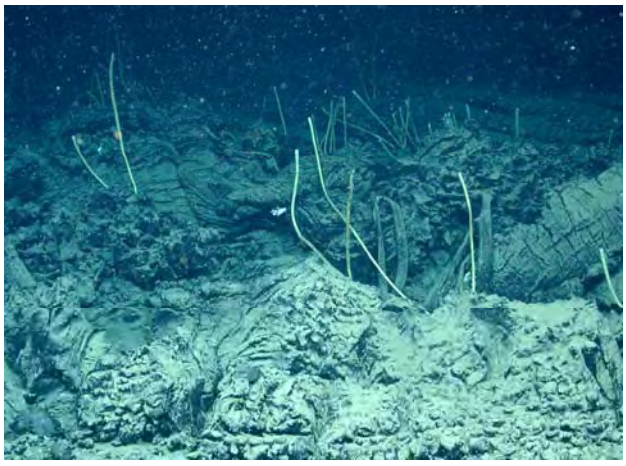

Fig. 39: Seafloor images taken by the ROV.

Dive 81 explored an area of approximated 200 m east-west and 100 m north-south and started at the seafloor close to Dive 80 (Fig. 40). Markers were deployed at prominent habitats (Tab. 6): Marker 3 is a large area of fresh asphalt. Marker 4 is an oily sediment area suitable for push core and in-situ instruments. Marker 11 is a massive asphalt structure that appears to be quite old (Fig. 40).

Table 6: Instruments, tools and samples of Dive 81.

GeoB	Tool/sample	Start	Lat. (°N)	Long. (°W)	Remarks
	Trap	05:30			replaced at beacon
	Marker 3	06:02	21°53.949’	93°26.235’	deployed
	Marker 4	07:23	21°53.989’	93°26.186’	deployed
	Marker 11	08:33	21°53.977’	93°26.253’	deployed
	Marker 1	10:18	21°53.902’	93°26.194’	deployed
10617-1	Niskin-1	11:44	21°53.988’	93°26.181’	at Marker 4
10617-2	Kips-1	11:48	21°53.988’	93°26.180’	at Marker 4
10617-3	Kips-2	12:33	21°53.951’	93°26.228’	
10617-4	Kips-3	13:12	21°53.937’	93°26.228’	
10617-5	Rotary-4	13:52	21°53.940’	93°26.226’	asphalt pieces
10617-6	Rigmaster	14:44	21°53.945’	93°26.229’	asphalt sample
10617-7	Rotary-5	15:55	21°53.953’	93°26.226’	
10617-8	Rotary-6	15:59	21°53.951’	93°26.224’	

The exploration was organized as 5 E-W transects of 200 m separated by approximately 25 m, starting at the beacon (Marker 4) location. Manoeuvring along tracks was some times difficult because the ship was pulling the ROV. During the northern most transect (transect 2), the ROV was pulled about 50 m to the north off the track.

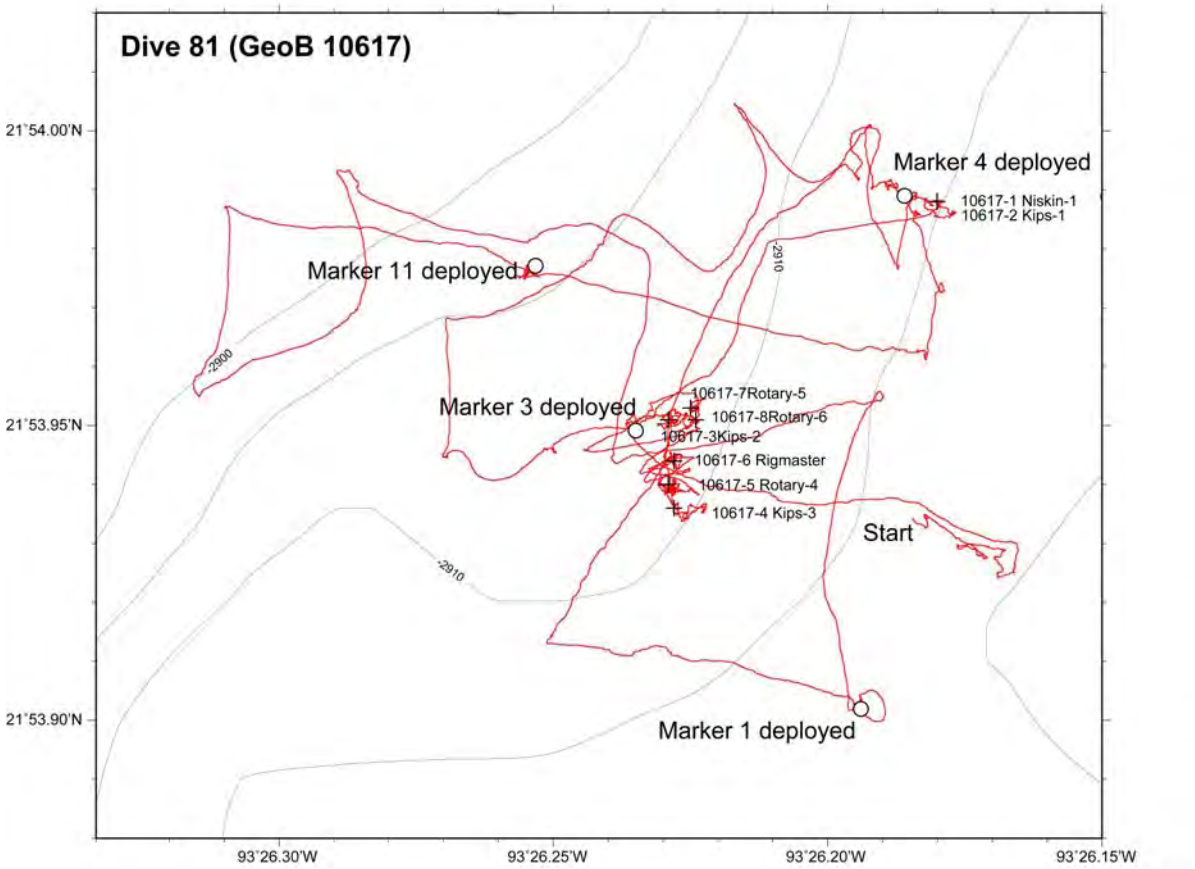

Fig. 40: Track lines and seafloor sampling sites of Dive 81.

The area of Marker 4 was established as a possible site for in-situ instruments and push core sampling. The large, fissured asphalt floe imaged during 2003 was relocated, observed and

documented by video and still images. On a track to the south we explored another seafloor area that would be suitable for push core sampling on a future dive and we deployed Marker 1 on that site (Fig. 9).

A Niskin bottle sample and three Kips water samples were taken at fresh asphalt near Marker 4. In the same area we attempted to drill into the asphalt with the hand corer. This broke off some pieces of asphalt that could be suctioned, but did not produce a clean core of asphalt.

Several pieces of asphalt were sampled at about 15:47 by the rotary sampler (Tab. 6). This material is important because subsequent review would show that it was covered with the "white stuff" that is prevalent on the asphalt. The "white stuff" on this sample was quite thick and well-attached to the asphalt. A mosaic of bacteria mats was flown.

8.4 Dive 82 (GeoB 10619)

Responsible scientist:	Frank Wenzhöfer		
Date:	12 April 2006		
Start/end at bottom (UTC):	15:50 / 07:56		
Total bottom:	16 hr, 6 min		
Start at the bottom:	21°54.333'N	93°26.497'W	2880 m water depth
Start ascend:	21°53.926'N	93°26.049'W	2925 m water depth

Table 7: Instruments, tools and samples of Dive 82.

GeoB	Tool/sample	Start	Lat. (°N)	Long. (°W)	Remarks
10619-1	Insinc x1	01:14	21°53.992'	93°26.189'	
10619-2	Insinc x2	01:31	21°53.991'	93°26.183'	
10619-3	Niskin bottle	01:53	21°53.992'	93°26.181'	
10619-4	Push Core 14	01:54	21°53.992'	93°26.181'	
10619-5	Push Core 6	02:23	21°53.991'	93°26.183'	rhizone core
10619-6	Push Core 9	02:36	21°53.991'	93°26.183'	
10619-7	Push Core 10	02:46	21°53.991'	93°26.183'	
10619-8	Push Core 25	03:21	21°53.991'	93°26.183'	
10619-9	Push Core 32	03:28	21°53.991'	93°26.183'	
10619-10	Push Core 56	03:42	21°53.991'	93°26.183'	
10619-11	Push Core 22	03:47	21°53.993'	93°26.186'	rhizone core
10619-12	Push Core 52	04:03	21°54.000'	93°26.187'	
10619-13	Push Core 36	04:22	21°54.035'	93°26.184'	
10619-14	Push Core 27	04:36	21°53.012'	93°26.176'	
10619-15	Rotary 4	05:54	21°53.969'	93°26.184'	
10619-16	Rotary 5	06:10	21°53.970'	93°26.185'	
10619-17	Rotary 6	06:30	21°53.951'	93°26.229'	
10619-18	Manipulator	06:46	21°53.952'	93°26.231'	tube worms
10619-19	Manipulator	07:40	21°53.925'	93°26.165'	trap exchange

Dive 82 started with the recovery of the lift which got lost the day before. With the help of the Posidonia position we were able to localize the lift at the seafloor approximately 800-900 m NW of the main asphalt area. When we arrived at the lift we saw that the front door was open but all in situ

instruments were still in the lift. After closing the lift door QUEST inspected the lift but no damages were observed. A ship wire, equipped with a Homer beacon, was then send to the seafloor for recovering the lift and placed close to the lift at the seafloor. With QUEST we were able to hook the lift to the ship wire and the lift could be recovered safely. After the lift has been on deck the regular dive program continued.

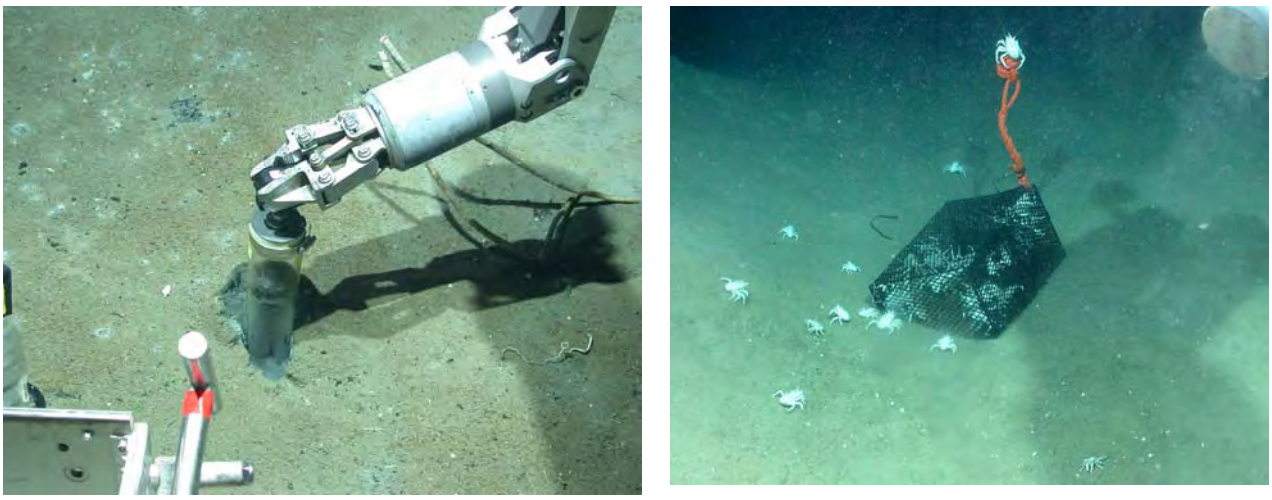

Fig. 41: Push core sampling (left). Bated trap recovered during Dive 82 (right).

When returning to the main asphalt area a survey started to locate asphalt flows but only soft sediments with some dead mussel shells were observed. PARASOUND records detected a gas flare at WP 11 but no gas escape was found by ROV observations at this site. The survey track was then continued and first asphalt flows were found at 21° 54.0710'N/93° 26.2721'W in 2910 m water depth. Sampling of the *Insinc* push cores close to the asphalt flows failed due to a hard layer below the sediment surface. Therefore soft sediment around a tube worm assemblage close to the previous site was sampled. Two *Insinc* push cores (Tab. 7) were taken and after placing them back in the sheaths the tracer was successfully injected allowing the cores to be incubated at in situ pressure for the rest of the dive.

A Niskin bottle was taken before core sampling was continued. A total of 11 push cores were successfully taken around the tube worm assemblage (Tab. 7). When taking the cores a viscous oil string flowing out of the core bottom could be observed indicating that oil is quite close to the sediment surface (Fig. 41, left).

After coring it was decided to collect asphalt samples therefore ROV QUEST was heading towards Marker 3. Weathered asphalt was sampled with the rotary sampler as well as a crab. We were then heading towards a site with fresher asphalts at Marker 3 and spotted a chimney like structure of out flowed tar on the way towards the targeted site. At marker 3 a sample of fine structured fresher asphalt was taken with the rotary sampler. A small tube worm bush was sampled with the manipulator and placed in the ROV drawer. The attempt to sample more fresh asphalt failed and QUEST returned to Marker 1 to recover two traps (Fig. 41, right). After ca. 16 hours at the seafloor ROV QUEST descended to the sea surface.

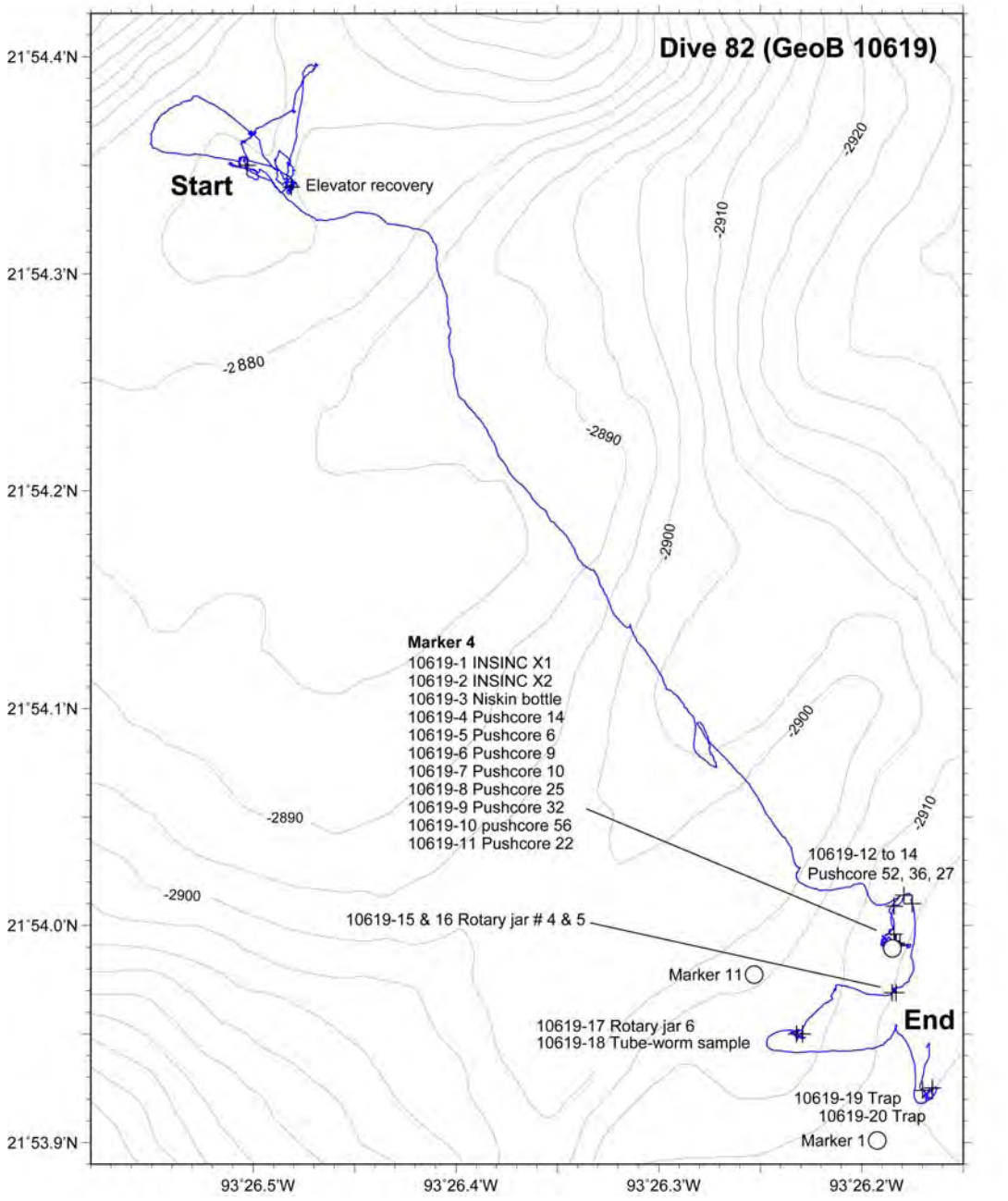

Fig. 42: Track lines and sample locations of Dive 82.

8.5 Dive 83 (GeoB 10622)

Responsible scientist:	Thomas Naehr		
Date:	13 April 2006		
Start/end at bottom (UTC):	23:41 / 11:02		
Total bottom:	11 hr, 21 min		
Start at the bottom:	21°53.949'N	93°26.249'W	2915 m water depth
Start ascend:	21°53.927'N	93°26.147'W	2923 m water depth

Table 8: Instruments, tools and samples of Dive 83.

GeoB	Tool/sample	Start	Lat. (°N)	Long. (°W)	Remarks
	T-logger	00:53	21°53.950’	93°26.239’	deployed
10622-1	Autoclave	02:40	21°53.956’	93°26.247’	asphalt sample
	Marker 5	02:40	21°53.956’	93°26.247’	deployed
	Marker 7	04:54	21°53.950’	93°26.251’	deployed
10622-2	Tubeworm	05:26	21°53.945’	93°26.249’	collection
10622-3	Net sample	10:17	21°53.990’	93°26.124’	asphalt
10622-4	Net sample	10:17	21°53.990’	93°26.124’	clams

Dive 83 reached the seafloor near marker 3 on April 13, 2006 at 23:41 hours. Scheduled tasks for this dive included deployment of traps for biological sampling, testing of the autoclave sampler, asphalt and biology sampling using the ROV’s suction sampler, a survey of possible gas flares in the water column, and exploration of a second area with asphalt flows near the eastern summit of Chapopote.

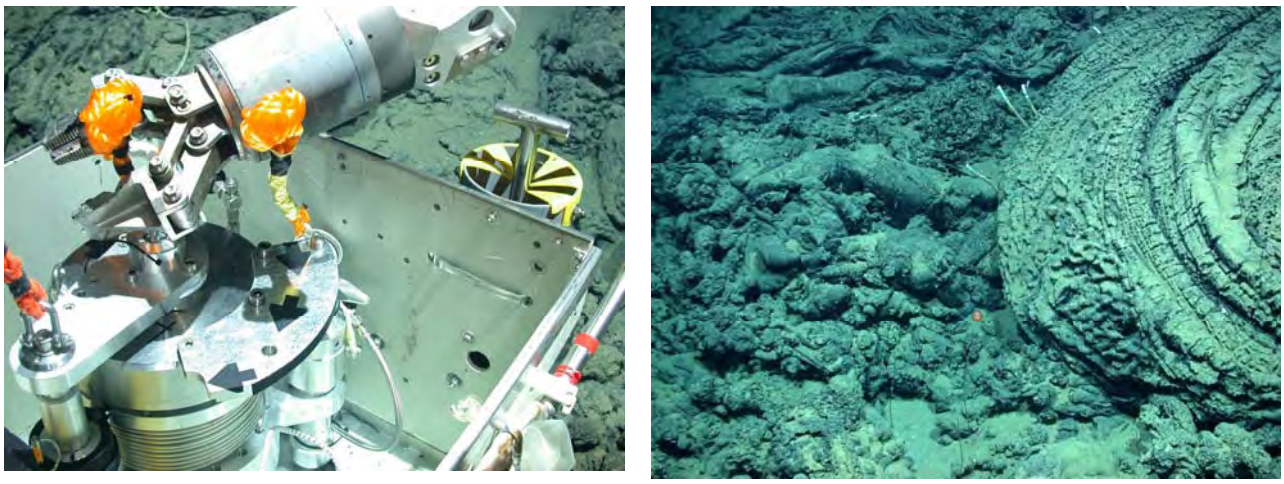

Fig. 43: Closing procedure of the autoclave sampler (left). Less alterated asphalt flow above highly alterated asphalt (right).

Two animal traps and the Antares temperature sensor were deployed near Marker 3 between 00:42 and 01:00 hours on April 14 in an area of fresh-looking asphalt. Testing of the autoclave sampler was performed between 01:40 and 02:40. Initially, there were problems placing a fresh piece of asphalt in the sampler as the asphalt pieces floated out of the sample chamber due to their positive buoyancy. A third attempt succeeded by sticking a piece of asphalt to the bottom of the sample chamber. After closing the lid of the autoclave sampler (Fig. 43, left), the ROV resumed a visual survey of the main area of the asphalt flow, which lasted until approximately 05:00 hours and included the deployment of a second temperature probe at marker 7 (Tab. 8).

Asphalt sheets of varying ages, ranging from fresh to apparently older, more strongly altered flows were encountered during the survey Fig. 43, right). Next, between 05:00 and approximately 5:45, tube worms were sampled slightly north of Marker 7 using the ROV’s manipulator arm. After closing the sample drawer, the ROV had a partial failure of its telemetry system and had to leave the seafloor to correct the problem. We continued at 07:20 with a brief survey of a slightly older asphalt flow we had encountered during one of our OFOS transects in 2003. At 08:13 we decided to move to the presumed location of a large gas flare in visible with the ships PARASOUND system,

located east of Marker 4 (Fig. 9). En route, approximately 50 meters SW of our target location we encountered a 3-4 m wide, solitaire asphalt seep, with several tower-like asphalt extrusions roughly 2 m in height.

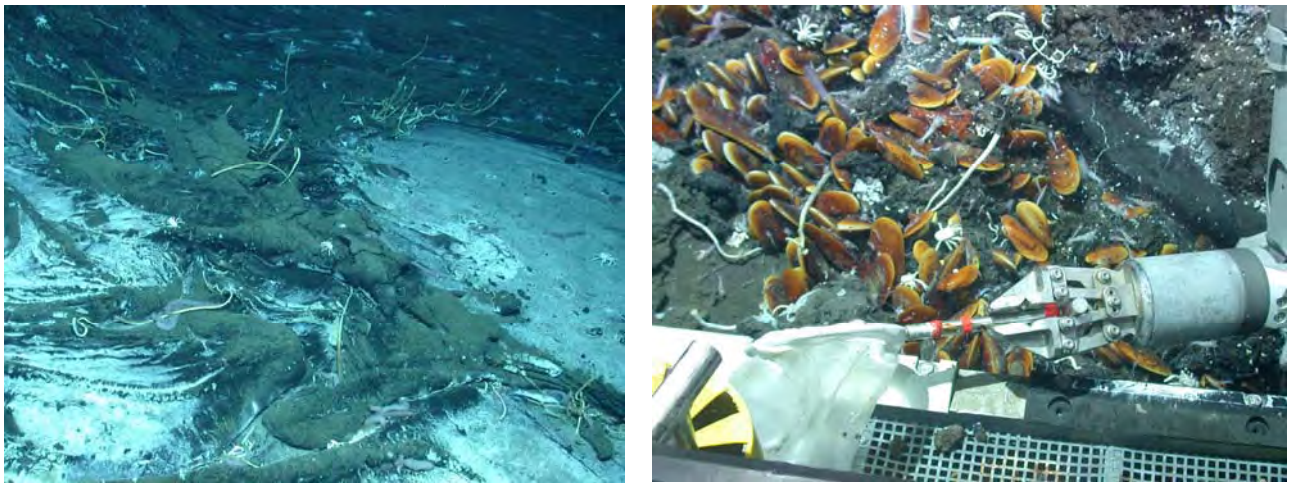

Fig. 44: Bacterial mats on aphalt (left). Sampling of bathymodiolin mussels at a seep site (right).

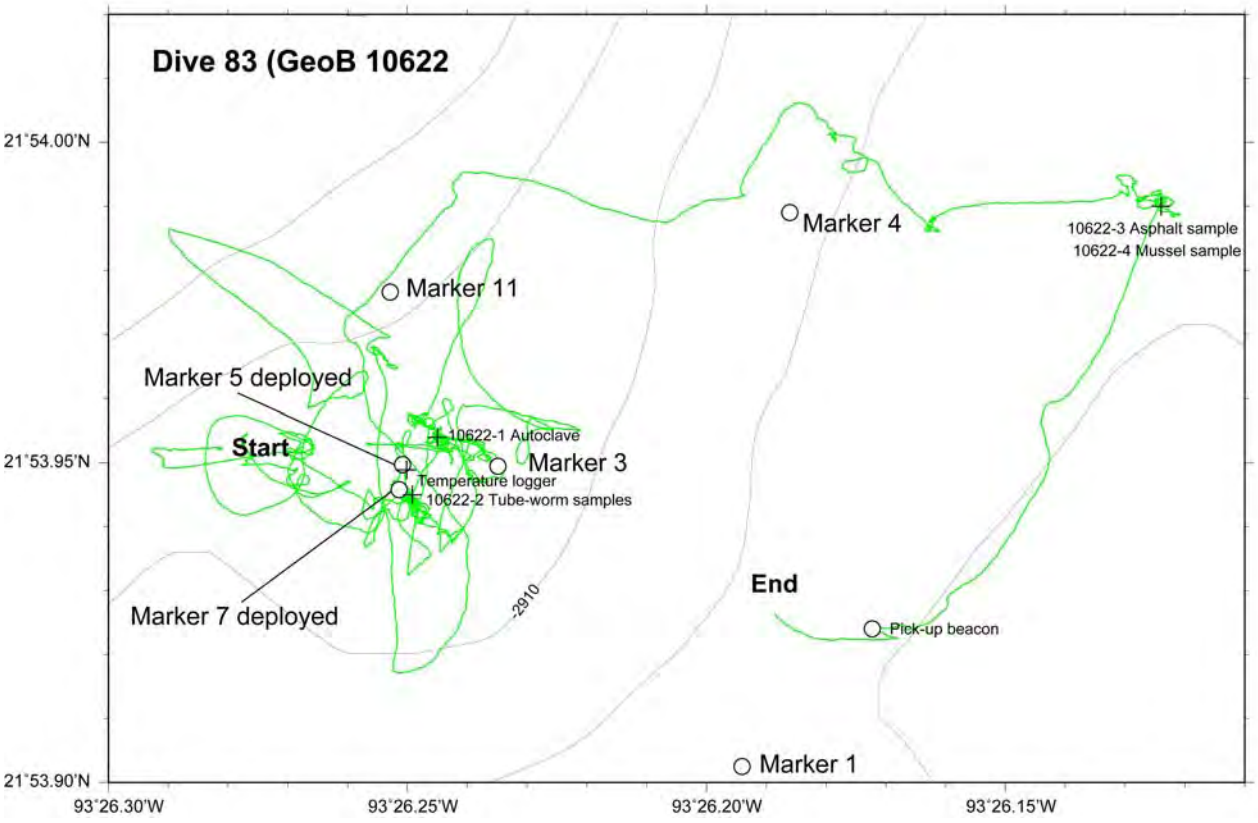

Fig. 45: ROV sampling sites and track lines of Dive 83.

After arriving at the flare position at 09:12, we ascended about 30 meters in the water column and used the ROV's sonar system to look for gas bubbles. We located two small sonar targets and followed the smaller target to the seafloor, where we encountered an area of active gas seepage at 09:43. We marked the area with waypoints and proceeded to collect a number of mussels with one

of the ROV's sampling nets and some small pieces of asphalt covered with a white substance using the vehicles suction sampler. Sampling was complete at 10:17. After investigating a small white mound, which was later confirmed to consist of gas hydrate, we returned to the beacon deployed during earlier dives, which we reached at 10:53. After collecting the beacon, the ROV started to ascend to the surface at 11:02. The lid of the autoclave sampler was sealed at 11:28 in a water depth of 2500 m and the vehicle returned to the surface, concluding Dive 83.

8.6 Dive 84 (GeoB 10625)

Responsible scientist:	Antje Boetius		
Date:	15 April 2006		
Start/end at bottom (UTC):	01:59 / 20:04		
Total bottom:	18 hr, 5 min		
Start at the bottom:	21°53.380'N	93°26.131'W	2935 m water depth
Start ascend:	21°53.690'N	93°26.131'W	2922 m water depth

Table 9: Instruments, tools and samples of Dive 84.

GeoB	Tool/sample	Start	Lat. (°N)	Long. (°W)	Remarks
10625-1	In-situ pore ws	04:35	21°53.905'	93°26.190'	
10625-2	Chamber 1	06:09	21°53.903'	93°26.192'	
10625-3	Push Core 6	06:45	21°53.906'	93°26.190'	rhizone core
10625-4	Push Core 22	06:52	21°53.905'	93°26.190'	rhizone core
10625-5	Push Core 52	06:57	21°53.905'	93°26.190'	rhizone core
10625-6	Push Core 25	07:02	21°53.904'	93°26.191'	
10625-7	Insinc x3	07:51	21°53.907'	93°26.205'	
10625-8	Insinc x4	08:04	21°53.907'	93°26.205'	
10625-9	Push Core 32	08:13	21°53.907'	93°26.205'	
10625-10	Push Core 26	08:26	21°53.907'	93°26.205'	
10625-11	Push Core 14	08:40	21°53.907'	93°26.204'	
10625-12	Chamber 2	10:11	21°53.946'	93°26.251'	
10625-13	Rotary sampler 1	11:44	21°53.999'	93°26.128'	shrimp, gastropodes
10625-14	Rotary sampler 8	12:50	21°53.997'	93°26.129'	close to hydrates
	T-logger (black)	15:44	21°53.948'	93°26.252'	pick-up
10625-15	Rotary sampler 7	16:27	21°53.948'	93°26.253'	3 holothurians
	T-logger (yellow)	17:00	21°53.963'	93°26.239'	pick-up at Marker 3
10625-16	Rotary sampler 6	18:47	21°53.953'	93°26.250'	asphalt
10625-17	Rotary sampler 5	19:02	21°53.950'	93°26.251'	holothirians
10625-18	Rotary sampler 4	19:09	21°53.953'	93°26.249'	white cover

Dive 84 was mainly dedicated to measurements of pore water gradients and element fluxes in oil/asphalt-impacted sediments, as well as to observation of the geo-bio-system at fresh asphalt flows with gas emission (Fig. 9). The dive started with the search for a target site with soft sediments for deployment of the in situ flux chamber and the rhizone sampler as well as the push coring. During Dive 82 we had selected the site around Marker 1 for this task. This site is characterized by patches of bacterial mats on sediments close to the asphalt. After proofing 2

transects between Marker 1 and the area of Markers 5 and 7, we decided on a position close to Marker 1 with 6 patches of mats for deployment of the chamber and the rhizone sampler, which were fixed to the front porch of QUEST.

Unfortunately, sediments were easily stirred up and the visibility strongly decreased by clouds of sediment particles. The bottom currents were too weak to clear visibility rapidly. We lost the chamber in a big cloud and decided to first deploy the rhizone sampler away from the sediment cloud next to WP20. Here we could not observe bacterial mats, but found soft sediments to mount the rhizone sampler. Next we took the in situ chamber from the Marker 1 area and deployed it close to the rhizone push cores (Tab. 9).

We took 3 push cores next to the in situ devices, as well as one core for solid phase analysis (Tab. 9). For the sampling of 2 *Insinc* push cores as well as 4 regular push cores we returned to the bacterial mats around Marker 1. All cores were taken within ca 5 square meter from soft sediments characterized by white precipitates on the seafloor. When we started coring, we observed oil droplets emanating from the seafloor. All but one push core were successfully sampled from the highly oily sediments. The total duration for the sampling task at Marker 1 was 7 hrs (including a 30 min time out in operations due to problems with the wire, and an hour wait for improved visibility).

The second part of the dive was dedicated to another chamber deployment, this time on fresh asphalt covered with white material. Finally the chamber was deployed at WP31 on a large flow of presumably fresh asphalt covered with a thin layer of whitish precipitates (Fig. 46).

Fig. 46: Second deployment of in-situ flux chamber (left) and sampling of white mats (right) in the vicinity of the chamber (Marker 7, WP31).

The dive continued with a transit to the flare and hydrate site, passing Marker 3 for one hour of surveys in eastward/westward transects. Not only the large asphalt flows but also the small asphalt pieces in sedimentary environments were found to be populated by dense aggregations of tubeworms (Fig. 47).

The dive continued with the passage to WP34 for observation of hydrate and gas bubbles. Close to outcropping hydrate a high density of diverse animals was observed with seemed somewhat different from the communities associated with only asphalt. Close to the hydrate, shrimps and gastropods were sampled into the rotary sampler (Tab. 9).

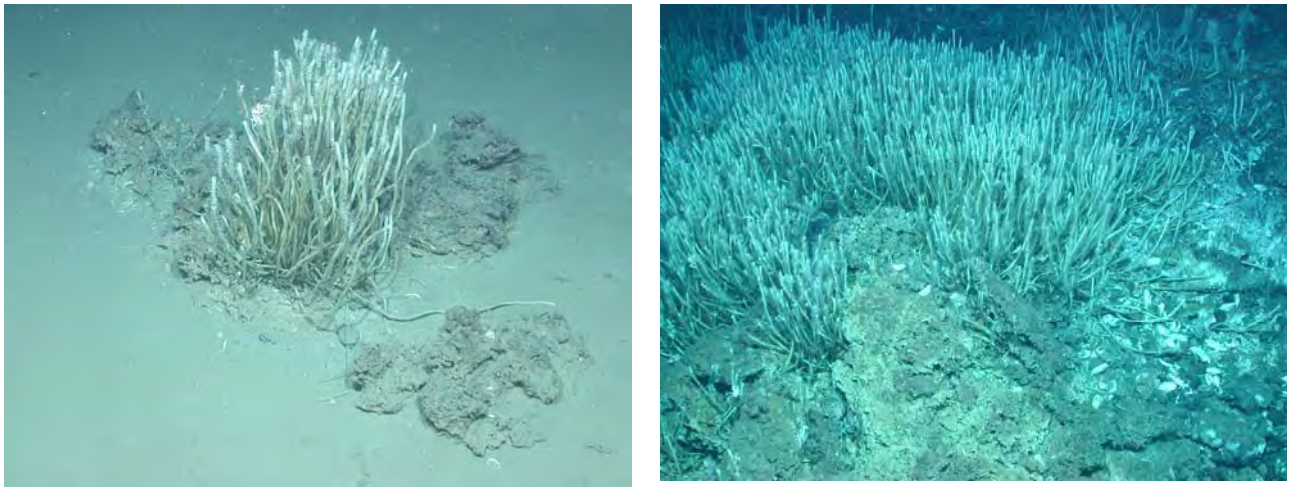

Fig. 47: Tubeworm aggregations associated with carbonates (left), Sedimentary environment (right): large aggregation on asphalt flow.

A sampling of the presumably outcropping hydrate was attempted, and the behaviour of the particles in water confirmed that in this area asphalt is associated with massive hydrate. Also, ebullition of gas bubbles was observed in this area and documented by video footage. The dive continued with 2 hours of transect around Marker 7 and 5, passing again massive asphalt flows. The temperature logger was picked up sea cucumbers were sampled into the rotary sampler, which failed temporarily.

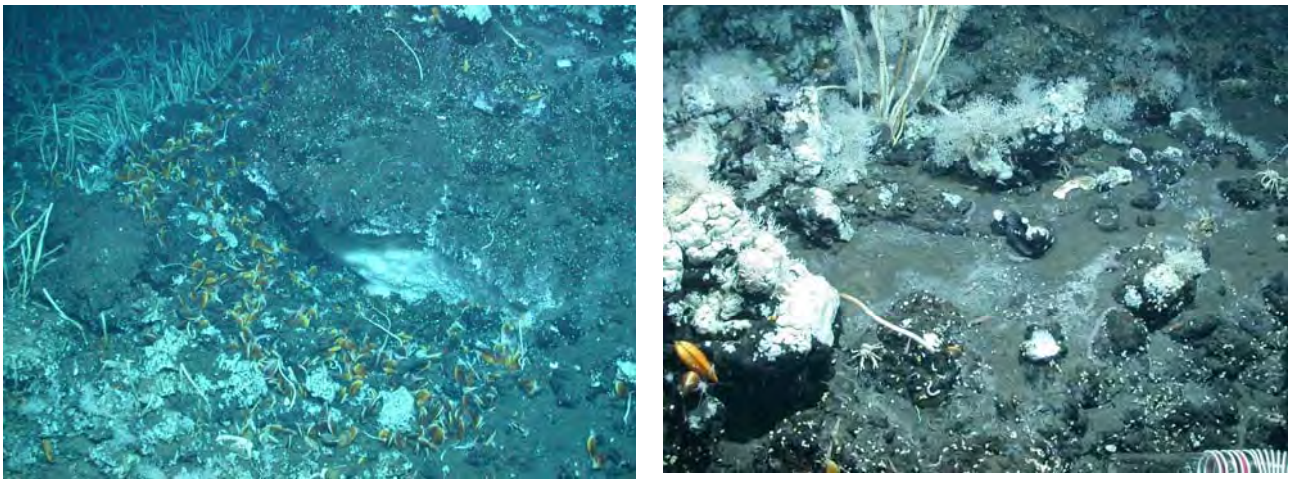

Fig. 48: Outcropping hydrate with dense accumulation of gastropods (A) and association of corals, tubeworms and presumably sponges around hydrate/bubble site (B).

At Marker 3 for pick up of the second temperature logger, and then the transit to WP20 for pick up of the traps and the rhizone sampler. Finally, we returned to WP31 to sample more white precipitates and to pick up the in situ chamber. At the end of the dive, the ROV returned to the flare site and the sonar was used to follow the upward bubble stream during the ascent of the vehicle.

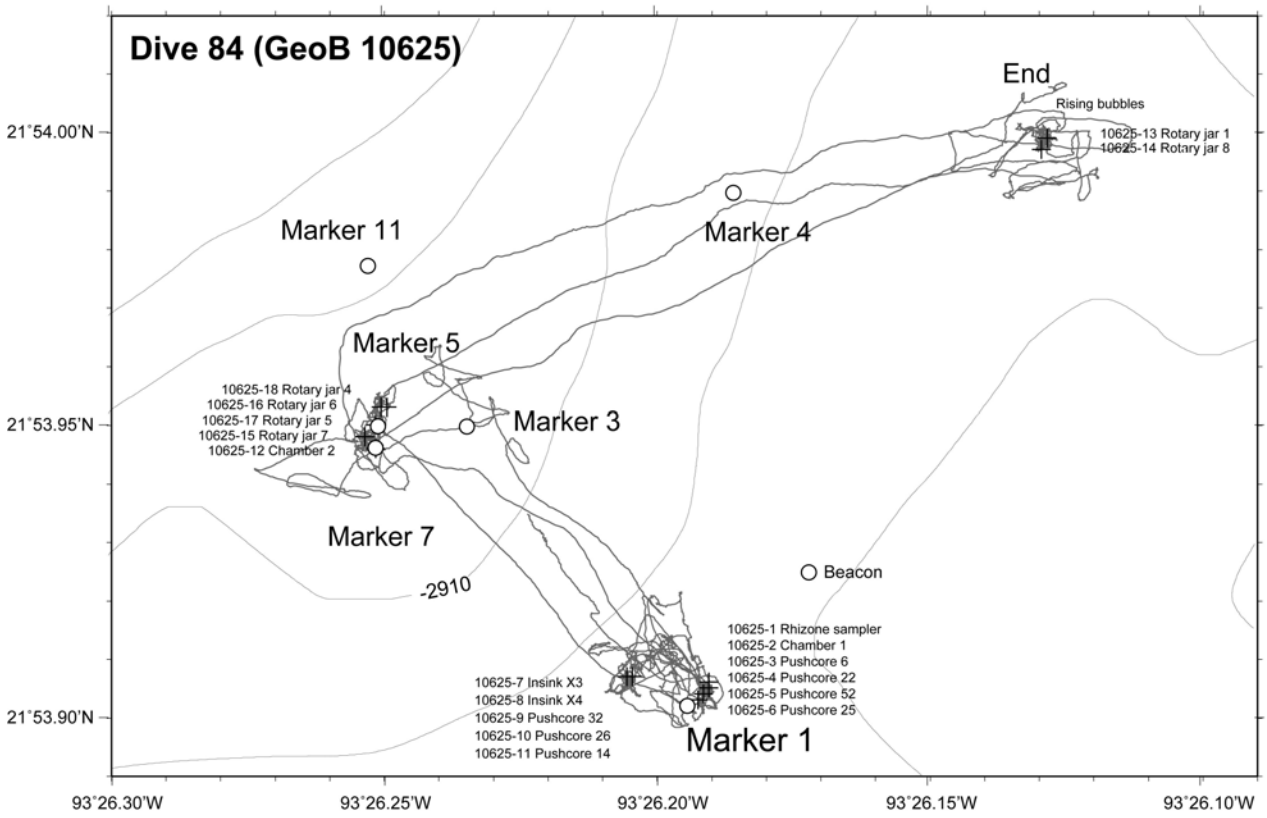

Fig. 49: Tracks and sampling sites documenting the ROV activities during Dive 84.

9 Water Column Work

(C. Ott, B. Böckel, S. Kasten, K. Enneking, T. Wilhelm)

During Sub-leg M67/2a 6 CTD stations were performed between 2456 and 3544 m water depths (Station list, see Appendix 1). A rosette with 24 12-L-Niskin bottles was attached and water from different depths was collected for biological and chemical investigations.

9.1 Coccolithophore Communities

(B. Böckel, C. Ott)

Coccolithophores, marine unicellular, flagellate algae (Prymnesiophyceae) play an important role as main primary producers in today´s oceans. They are characterized by a cell-wall covering, a coccosphere, of coccoliths, minute calcite scales, which are readily preserved as fossils, thus forming a major component of fine-grained deep-sea sediments. Coccolithophores show distinct biogeographic distribution patterns, defining broad latitudinal zones according to their ecological preferences. The basic understanding of modern ecological affinities of the species is essential for palecological studies using coccolith assemblages as proxies in the geological record. Their distribution in sediments is relatively well known, but information on their abundance, ecology and physiology in surface waters is still scarce.

Table 10: Surface water samples at a depth of 5m for coccolithophore analysis.

Sample No. (MO/KP)	Date	Time (UTC)	Water Depth (m)	Latitude N	Longitude W	Water Temp. (°C)	Wind Speed (ms^{-1})	Filter Vol (l)
1	20.03.06	20:46		22°03.80	92°51.12	24.5	9.9	0.8
2	21.03.06	12:58		21°54.00	93°26.24	24.4	5.5	2
3	23.03.06	8:40		21°08.99	93°57.02	24.9	6.7	2
4	23.03.06	15:16		20°51.39	94°01,11	25.2	1.0	2
5	23.03.06	21:52		19°57.37	94°00.84	24.4	4.3	2
6	25.03.06	22:17		20°25.90	93°50.26	24.3	7.1	2
7	28.03.06	19:50		21°28.20	93°25.25	24.4	5.1	2
8	30.03.06	17:34	3550	21°57.44	93°55.10	24.2	9.0	2

Therefore, an investigation of the living coccolithophore communities in the Gulf of Mexico was carried out sampling the uppermost water column. In order to study the coccolithophore´s vertical distribution within the photic zone water samples were taken from NISKIN-bottles of the hydrocast at 6 stations from different water depths (10 to 240 m, see Tab. 10). Eight surface water samples were taken from the vessel's membrane pump at about 5 m water-depth mainly at the rosette stations (see Tab. 11). Generally, 2 l of water were filtered through cellulose nitrate filters (25 mm diameter, 0,45 µm pore size) by means of a vacuum pump immediately onboard. Samples were rinsed with fresh-water to avoid the fall out of salt crystals. The filters were dried at 40°C for at least 24h and then kept permanently dry with silica gel in transparent film. Studies on the distribution and composition of the coccolithophore communities will be carried out on the filtered material using the Scanning Electron Microscope (SEM) at the Bremen University.

9.2 Gas Analyses and Chemical Constituents

Table 11: Hydrocast samples for coccolithophore analysis.

Date	Time (UTC)	Station	Sample No. (RP)	Latitude N	Longitude W	Sample Depth	Water Temp. (°C)	Salinity	Filter (l) A	Vol. B	Remarks
20.03.06	14:12	10601-1	I-1	22°08.19	92°45.09	199	15.44	36.01	2.0	0.77	
			I-2			149	17.97	36.39	2.0	2.0	
			I-3			120	19.15	36.47	2.0	2.0	
			I-4			100	20.99	36.51	2.0	2.0	
			I-5			75	22.91	36.48	2.0	1.6	
			I-6			50	23.77	36.49	2.0	1.7	
			I-7			20	24.91	36.27	2.0	2.0	
	14:19		I-8	22°08.12	92°44.78	10	24.92	36.27	1.89	2.0	MP #1: 5m
21.03.06	14:01	10602-1	II-1	21°53.99	93°26.27	213	29,41	34,63	2	2	
			II-2			200	29,41	34,63	2	2	
			II-3			149	29,41	34,63	2	2	
			II-4			119	29,41	34,63	2	2	
			II-5			99	29,41	34,63	2	2	
			II-6			75	29,41	34,637	2	2	
			II-7			50	29,41	34,637	2	2	
			II-8			20	29,41	34,637	2	2	
	14:19		II-9	21°54.01	93°26.25	10	29,41	34,637	2	2	MP #2: 5m
23.03.06	15:30	10603-1	III-1	20°51.38	94°01.11	240	8,35	35,00	2	2	
			III-2			220	13,37	35,70	2	2	
			III-3			200	13,96	35,79	2	2	
			III-4			150	14,33	35,84	2	2	
			III-5			120	16,19	36,12	2	2	
			III-6			100	17,85	36,35	2	2	
			III-7			75	18,97	36,45	2	2	
			III-8			50	20,86	36,52	2	2	
			III-9			20	25,28	36,40	2	2	
	15:47		III-10	20°51.40	94°01.13	10	25,66	36,44	2	2	MP #4: 5m
23.03.06	22:40	10604-1	IV-1	19°57.37	94°00.84	220	13,66	35,73	2	2	
			IV-2			200	14,33	35,83	2	2	
			IV-3			170	15,02	35,95	2	2	
			IV-4			150	16,57	36,19	2	2	
			IV-5			120	17,63	36,34	2	2	
			IV-6			100	19,05	36,47	2	2	
			IV-7			75	20,36	36,51	2	2	
			IV-8			50	22,66	36,47	2	2	
			IV-9			30	23,64	36,45	1.8	2	
			IV-10			20	24,54	36,37	2	2	
	22:49		IV-11	19°57.37	94°00.84	10	25,03	36,41	2	2	MP #5: 5m
28.03.06	19:39	10605-1	V-1	21°28.23	93°25.27	220	13,66	13,66	2	2	
			V-2			200	14,33	14,33	2	2	
			V-3			150	15,02	15,02	2	2	
			V-4			120	16,57	16,57	2	2	
			V-5			100	17,63	17,63	2	2	
			V-6			75	19,05	19,05	2	2	
			V-7			50	20,36	20,36	2	2	
			V-8			20	22,66	22,66	2	2	
	19:46		V-9	21°28.20	93°25.25	10	23,64	23,64	2	2	MP #7: 5m
30.03.06	17:13	10606-1	VI-1	21°57.51	93°55.11	220	22,26	36,58	2	2	
			VI-2			200	23,22	36,58	2	2	
			VI-3			150	23,19	36,58	2	1.6	
			VI-4			120	24,14	36,59	2	2	
			VI-5			100	24,14	36,59	2	2	
			VI-6			75	24,64	36,316	2	2	
			VI-7			50	24,64	36,32	2	2	
			VI-8			20	24,68	36,32	2	2	
	17:21		VI-9	21°57.45	93°55.10	10	24,70	36,32	2	2	MP #8: 5m

Concentrations of methane and other hydrocarbons in the water column were determined by ultrasonic vacuum degassing of water samples. Water samples taken by Niskin bottles (rosette) were transferred through silicone tubes into 1 L glass bottles. Ultrasonic energy applied to the samples led to gas release into the headspace. A volume of 200 µl of gas was taken through a septum for immediate GC analysis. The 200 µl aliquots of the concentrated headspace were analysed for methane and other hydrocarbons using an Agilent Technologies 6890N gas chromatograph equipped with a flame ionisation detector (FID) and a thermal conductivity detector (TCD) (Chapter 13.1).

During this cruise samples from the rosette casts GeoB 10601-1, 10603-1 and 10605-1 were subjected to vacuum ultrasonic degassing and subsequent gas analyses. For each rosette cast samples for gas analyses were distributed over the whole water column depth with a higher sampling resolution chosen close to the seafloor. The methane concentrations determined at all three sites fluctuate around 1 nmol/l and thus do not show any contents above normal background concentrations of methane in seawater.

Additional water samples were taken to determine the concentrations of dissolved barium and other trace metals. Samples taken by Niskin bottles were filtered through 0.2 µm cellulose acetate membrane filters into acid-washed PE-vials and acidified with nitric acid 65% (400 µl HNO_3/100 ml). The samples are stored at 4 °C until ICP-MS analyses at the AWI in Bremerhaven. Samples from a total of 5 rosette/CTD casts were taken, filtered, acidified and stored at 4°C.

10 Autoclave Sampler

(H.-J. Hohnberg)

The **I**n-situ **P**ressure **S**eafloor **S**ampler (IPSS) has been developed with the aim of recovering, preserving and analyzing sediment samples under in-situ conditions of the deep sea. The IPSS, developed in the frame of the METRO project at the University of Bremen, was deployed by a ROV during R/V METEOR Cruise M67/2. Its total weight is 45 kg in air. The samples are recovered at in-situ pressure up to a maximal pressure corresponding to water depths of 2000 m. However, the IPSS is equipped with a valve-system allowing deployment down to 6000 m water depth. After sampling at that depths the pressure barrel is finally closed in the water depth of 2000 m. The IPSS consists of four structural components, which are handled and released during the deployment by the manipulators of the ROV with very simple actions. In addition, the pressure barrel is equipped with a pressure preserving system (accumulator) supporting the sealing of the pressure barrel during the sealing procedure and enabling pressure preservation over several weeks. After the recovery cooling is especially vital for sediment samples that contain gas hydrate. The pressure barrel was checked and approved by the Berlin TÜV (Technischer Überwachungsverein, technical inspection authority of Germany). The TÜV tested the pressure chamber of the IPSS with 300 bar.

The parts of the pressure barrel exposed to inner pressure made of highly firm stainless steel (1.4462, 1.4571) and aluminium alloy (AlMgSi1 F28) have been approved by the TÜV and classified by 3.1b or 3.1a certificates.

Before deployment three structural components have to be spring loaded and the accumulator has to be loaded with compressed air and partly with sea-water. The pressure of the compressed air corresponds to the water depth in which the pressure barrel is sealed. The system is fixed on a ROV and carried down to the seafloor. Sampling and releasing the closing and sealing-mechanism of the IPSS will be done by the manipulators of the ROV. All actions are supported by a video telemetry system of the ROV. One IPSS-deployment has been conducted during M67/2b at position 21°53,956'N; 93°26,247'W in 2900 m water depth during Dive 83.

The IPSS-pressure barrel obtained 1,15 litre asphalt-sample under the pressure of 250 bar. The sample has been degassed and analysed after recovery by Kai Hinrichs and Florence Schubotz.

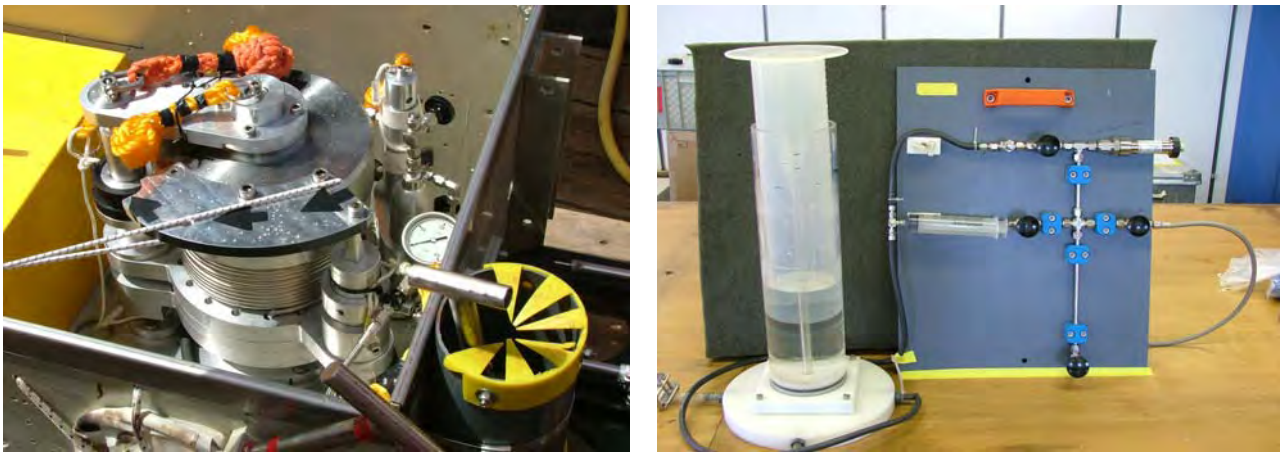

Fig. 50: IPSS fixed in the sample box of the ROV "QUEST" (left); degassing system used for quantitative gas extraction of the samples (right).

11 Geological Sampling

(M. Zabel, M. Dalthorp-Moorhous, A. Gaßner, S. Kasten)

Introduction

One of the main goals on this cruise was to get more information about the driving mechanisms of the asphalt outflow in the southeastern Gulf of Mexico. For this purpose it was planned to sample the whole variety of deposits in the vicinity of typical knoll structures, which already could have been mapped during R/V SONNE Cruise 174 in 2003. Beside the much more precise sampling possibilities of the remotely operated vehicle (ROV) QUEST, especially at small, special restricted structures where oil, gas and fluid flows escape the seafloor, multicorer and gravity corer were deployed to recover longer sequences of all kinds of deposits in the area of the Campeche Knolls. Unfortunately, it was not possible to penetrate an asphalt layer, but the great variety of recovered cores and samples enables among others the examination of the hypothesis that the formation and rise of supercritical water could be the main driving force for these highly dynamic systems (Hovland et al. 2005).

Methods

Marine deposits were recovered by using a multicorer and a gravity corer. The multicorer was equipped with eight large and four small plastic tubes (10 and 6 cm in diameter), each of 60 cm length. Depending on the material of the seafloor, the recovery varied between 0 and 53 cm. This device was deployed at 5 stations. Three times the multicorer was additionally equipped with an online video observation system. The gravity corer had pipe lengths of either 6 or 3 m and was equipped with a weight of 2.5 tons. Depending on the expected material at the sea floor (sediment, asphalt, gas hydrate), the steel tube was lined with a plastic liner or a plastic wrap (GeoB 10610 and GeoB 10612). In any case, the cores were taken as one piece and were sub-sampled on deck or in the Geo-lab immediately after recovery by all scientific groups. In total, with 13 deployments about 49 m of sediment and asphalt sequences were recovered during cruise M67/2 (Tab. 12). Detailed core descriptions (e.g. smear slide sampling or scanning of light reflectance) were not carried out.

Preliminary Results

Samples from GeoB 10606 core were recovered from shallower water depth of about 2300 m, southwestward of the main working area during cruise Leg M67/2b. Sediments consist of hemipelagic mud. The cores show the typical change in colors. So, the iron redox boundary could clearly be identified by the transition from upper brownish to deeper, more grayish tones. To get also undisturbed surface samples from the same location where Gravity Core GeoB 10612-1 was recovered just before (see below), the multicorer was deployed (GeoB 10612-2). Obviously, like documented by analytical results from pore water measurements, the multicorer cores do not fit with the uppermost sediments in the respective gravity core, which supports the great special heterogeneity at the seafloor in this area. Again, sediments consist of undifferentiated hemipelagic mud.

Table 12: Locations of multicorer sampling.

Locations of multicorer sampling

Station	TV	Date* [UTC]	Time* [UTC]	Lat* [°N]	Long* [°W]	Water depth* [m]	Recovery [m]	Remarks	Sub-Sampling Aquat.	Geochem.	Org. Geochem.	Microbiol.
GeoB 10606	no	05.04.2006	11:14	21°14,97	93°49,77	2296	0,35	hemipelagic mud	X		X	X
GeoB 10612-2	no	09.04.2006	17:50	21°54,23	93°25,93	2943	0,53	hemipelagic mud	X		X	X
GeoB 10613	yes	09.04.2006	22:02	21°54,12	93°25,65	2902	0 - 0,20	hemipelagic mud, aspalt piece at the bottom	X		X	X
GeoB 10614	yes	10.04.2006	03:35	21°53,98	93°26,19	2891	0,30	hemipelagic mud	---		---	---
GeoB 10616	yes	10.04.2006	22:51	21°53,92	93°26,17	2897	no		---		---	---

* when bottom contact

Locations of gravity corer sampling

Station	GC (3/6)	Date* [UTC]	Time* [UTC]	Lat* [°N]	Long* [°W]	Water depth* [m]	Recovery [m]	Remarks	Sub-Sampling Aquat.	Geochem.	Org. Geochem.	Microbiol.
M67/2 a												
GeoB 10602-2		21.03.2006	16:05	21°54,01	93°26,24	2884	4,90	hemipelagic mud	X		---	---
GeoB 10605-2		28.03.2006	20:50	21°28,21	93°25,23	2785	5,50	hemipelagic mud	X		---	---
M67/2 b												
GeoB 10607	6	06.04.2006	19:00	21°53,99	93°26,25	2911	6,20	hemipelagic mud,	---		X	---
GeoB 10608	6	06.04.2006	21:36	21°53,90	93°26,35	2897	6,50	hemipelagic mud (returned to sea)	---		---	---
GeoB 10609	6	06.04.2006	23:50	21°5397	93°26,32	2900	6,50	hemipelagic mud (returned to sea)	---		---	---
GeoB 10610	6	07.04.2006	01:58	21°54,25	93°25,88	2964	7,50	hemipelagic mud	X		X	X
GeoB 10612-1	6	09.04.2006	15:40	21°54,23	93°25,91	2926	7,60	hemipelagic mud, viscous oil in cc	X		X	X
GeoB 10618	6	11.04.2006	21:08	21°53,95	93°26,21	2903	1,00	pure asphalt with big pieces of gas hydrate asphalt debris with sediment	---		X	X
GeoB 10623-1	3	14.04.2006	14:03	21°53,96	93°26,22	2882	0,50		---		X	---
GeoB 10623-2	3	14.04.2006	14:50	21°53,56	93°26,22	2895	0,90	pure asphalt	X		X	X
GeoB 10624-1	3	14.04.2006	18:47	21°53,99	93°26,13	2922	1,50	hemipelagic mud, oily mussel shill in cc	X		X	X
GeoB 10624-2	3	14.04.2006	20:58	21°53,99	93°26,15	2923	3,00	-	---		---	---
GeoB 10626	3	16.04.2006	00:30	21°53,99	93°26,13	2914	0	probably gas hydrate	---		---	---
							35,6					

* when bottom contact

During cruise Leg M67/2a, two gravity cores (GeoB 10602-2 and GeoB 10605-2) were retrieved from water depths of 3300 and 2785 meters. Core GeoB 10602-2 was taken from the location of the Chapopote asphalt structure identified on an earlier cruise and GeoB 10605-2 was taken from a site with an active surface oil slick and subsurface knoll as identified through PARASOUND signatures.

The gravity cores exhibit the dark and light gray turbidite layers common in the Gulf of Mexico (Sheppard 1963). The deep basin turbidities consist mainly of gray silts with few foraminifera and

with burrow mottling in the upper portion. Individual turbidities are determined by burrow mottling and subtle color changes rather than grading because most sediments are fine silts (Fig. 51, left). Intermittent layers are characterized by planktonic foraminifera that have sifted down from overlying waters.

The grains of the turbidity layers observed in the cores are largely biogenic in origin and form a nannofossil ooze with varying inputs of clay and quartz. Core GeoB 10602-2 contains a few larger (>2 mm) shell fragments indicating a possibly higher energy level for the turbidity deposition, however the matrix for the surrounding material remained a nannofossil ooze similar to the zones in the core without the larger shell fragments (Fig. 51, right).

Fig. 51: Subtle color changes separated by darker mottling zones indicate turbity layers in Core GeoB 10506-2 (left); Pteropod shell fragment in matrix of nannofossil ooze of Core GeoB 10506-2 at a depth of 118 cm (right).

Gravity Cores GeoB 10607-1, 10608-1, and 10609-1 were taken from the southern inner rim of the Chapopote Knoll (Fig. 8). They consist of light brownish hemipelagic mud, reflecting the oligotrophic character of this region and can be seen as representative for the background of deep-sea sediments. There is not evidence of an influence by upward migration of oil, gas and fluid flows from the deep. Due to the scientific objectives, focusing on inorganic and organic geochemistry, biogeochemistry, biology, and microbiological investigations, Cores GeoB 10608-1 and 10609-1 were not sub-sampled and returned to the sea.

In contrast, very oily sediments were recovered from the northern center of Chapopote Knoll (GeoB 10610-1 and 10612-1, Fig. 52 left). Close to the core catcher sediments contain long streaks of viscous heavy oil (Fig. 52) and have a strong smell of hydrogen sulfide nearly throughout the whole core lengths. Visual differences in the sediment sequences could not be observed.

With Cores GeoB 10618-1 and 10623-2 we succeeded in retrieving asphalt samples, which are ductile to partly viscous and seem to be relatively “fresh”. Both cores show a strong degassing, especially along fine linear structures, which may originate from the shrinking of the asphalt matrix after its outflow. Along these lineaments and within the macroscopic pores of the asphalt, finely distributed gas hydrates were observed (Fig. 53, left). Core 10618-1 contains a big piece of pure, white gas hydrate (Fig. 53, right; Klapp et al. submitted). The recovery of this core was accompanied by a strong rising of gas bubbles to the sea surface. Based on these observations it can be assumed that internal hydrate formation has taken place after deposition of the asphalt. Although the asphalt or rather the asphaltene-rich heavy oil contains hydrogen carbons itself (cf. Chapter 13),

an upward migration of gases from deeper layers cannot be excluded as a source of methane. With Core GeoB 10623-1 only a mixture of asphalt debris and marine sediments was recovered.

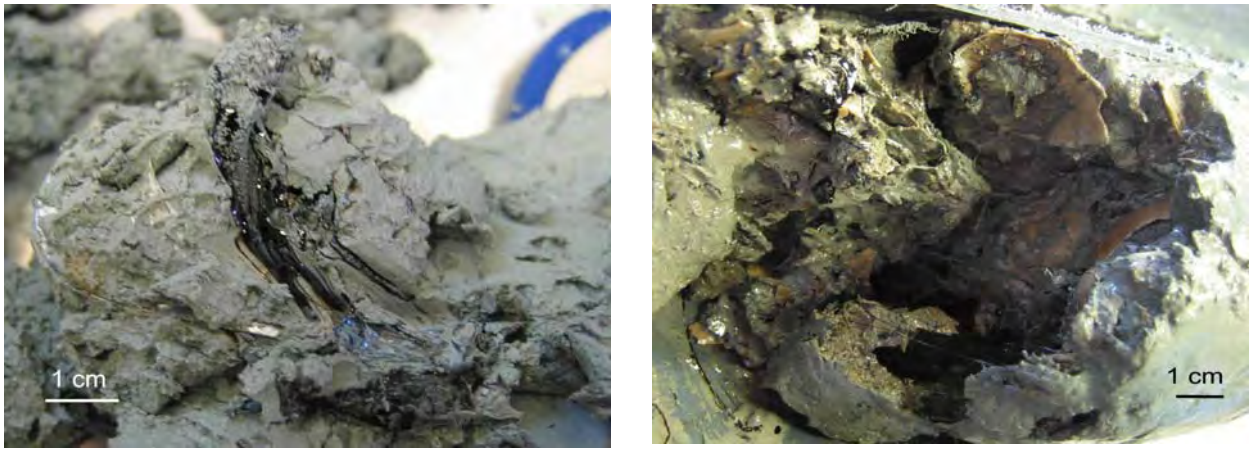

Fig. 52: Long streaks of viscous oil in sediments of Core GeoB 10612-1 (left); Mussel shells at the bottom of Core GeoB 10624-1 interspersed with streaks of viscous heavy oil (right).

Although Gravity Core GeoB 10624-1 was recovered close to Sites GeoB 10618 and 10623, it consists of light brownish hemipelagic mud. A tightly packed layer of mussel shells in about 140 cm sediment depth prevented the deeper penetration of the core. The shells were interspersed with streaks of viscous heavy oil (Fig. 52, right). A strong sulfidic smell indicates intense sulfate reduction coupled, like corroborated by gas measurements (cf. Chapter 13), with anaerobic methane oxidation.

Fig. 53 Finely dispersed gas hydrate along lineaments in asphalt of Core GeoB 10618-1 (left); Piece of gas hydrate in asphalt of Core GeoB 10618-1.

Site GeoB 10626 was at the same position where free gas seepage and outcropping gas hydrates have been observed before in an about 40 to 40 m area during ROV Dive 84. Unfortunately, no samples could be retrieved with the gravity corer. Rising free gas bubbles at the sea surface may indicate that probably gas hydrates have been sampled, but have completely dissolved in the water column.

12 Pore Water Chemistry

(S. Kasten, M. Zabel, A. Gassner, T. Wilhelm and K. Enneking)

12.1 Research Objectives

The focus of geochemical investigations carried out during this cruise in the frame of RCOM projects E1 and E3 was a detailed examination of the influence of oil and asphalt seepage/volcanism on geochemical processes in and at the seafloor as well as the quantification of gas/oil/fluid fluxes across the sediment/water interface. The Campeche Knolls area in the southern Gulf of Mexico is characterized by overall oligotrophic surface water conditions. However, the focused and diffuse seepage/eruption/upward migration of hydrocarbons stimulates high turnover rates of geochemical and biogeochemical processes close to the seafloor – in particular involving the cycling of carbon, sulfur and iron - as also known from other cold seep environments. One of the research objectives therefore is to investigate and quantify processes of mineral formation and dissolution in these hydrocarbon-seepage influenced sites and – together with the organic geochemistry group – determine the potential of diagnostic mineral precipitates to reconstruct hydrocarbon seepage in older geologic sequences. A second major task will be the quantification of fluid/gas fluxes across the sediment/water interface and in this way to identify the significance of these unique hydrocarbon seeps/volcanoes for the carbon cycle and budget in the Gulf of Mexico area.

12.2 Methods of Pore Water Sampling and Analysis

To prevent a warming of the sediments on board the sediment cores were transferred into the cooling room immediately after recovery and maintained at a temperature of about 4°C. Only the gravity cores taken by plastic bags (GeoB 10610-1, GeoB 10612-1) were sampled on deck or in the Geo-lab at ambient temperature. The TV-MUC cores and the ROV push cores were processed within a few hours by means of rhizons (pore size 0.1 µm) or within a glove box under argon atmosphere. Two samples of the supernatant bottom water were taken and filtered for subsequent analyses. The remaining bottom water was carefully removed from the multicorer tube by means of a siphon to avoid destruction of the sediment surface. During subsequent cutting of the core into slices for pressure filtration, pH and Eh measurements were performed with a minimum depth resolution of 1 cm.

Gravity Cores GeoB 10602-2 and GeoB 10605-2 were taken by plastic liners and cut into 1 m segments on deck. From every cut segment surface 5 ml syringe samples of wet sediment were taken for methane analysis. Gravity Cores GeoB 10610-1 and GeoB 10612-1 were taken in tubular plastic film. For the extraction of pore water both rhizon samplers and Teflon-squeezers were used. For the extraction of pore water by pressure filtration and solid-phase sampling the gravity cores were cut lengthwise into two halves and processed in the cooling room in a glove box under argon atmosphere. PH and Eh were determined on the working halves and sediment samples were taken every 25 cm for pressure filtration. The Teflon-squeezers were operated with argon at a pressure gradually increasing up to 5 bar. The pore water was retrieved through 0.2 µm cellulose acetate membrane filters. Depending on the porosity and compressibility of the sediments, the amount of pore water recovered ranged between 5 and 20 ml. Solid phase samples for total digestions,

sequential extractions and mineralogical analyses were taken at 10-cm intervals, kept in gas-tight glass bottles under argon atmosphere and stored at 4 C.

Pore water analyses of the following parameters were carried out during this cruise: Eh, pH, ammonium, alkalinity, phosphate, iron (Fe^{2+}) and hydrocarbons – including methane. Eh and pH were determined with punch-in electrodes before the sediment structure was disturbed by sampling for pressure filtration. Ammonium was measured using a conductivity method. Alkalinity was calculated from a volumetric analysis by tritration of 1 ml of the pore water samples with 0.01 or 0.05 M HCl, respectively. For the analyses of dissolved iron (Fe^{2+}) sub-samples of 1 ml were taken within the glove box or directly from pore water extracted by rhizons, immediately complexed with 50 µl of "Ferrospectral" and determined photometrically. The analysis of phosphate was also performed photometrically.

For further analyses at the University of Bremen and the Alfred Wegener Institute for Polar and Marine Research (AWI) in Bremerhaven, aliquots of the remaining pore water samples were diluted 1:10 and acidified with $HNO_{3\ (suprapure)}$ for determination of cations (Ca, Mg, Sr, K, Ba, S, Mn, Si, B, Li) by ICP-AES and AAS. Additionally, 1.5 ml subsamples of the pore water were added to a ZnAc solution (600 µl) to fix all hydrogen sulfide present as ZnS for later analysis – including sulfur isotopes. Subsamples for sulfate and chloride determinations were diluted 1:100 and stored frozen for ion chromatography (HPLC) analyses at the University of Bremen and the AWI Bremerhaven. Further aliquots of the pore water were taken and stored for $\delta^{18}O$, $\delta^{34}S$ of sulfate, as well as concentrations and $\delta^{13}C$ of DIC and acetate. A complete overview of sampling procedures and analytical techniques used on board and in the laboratories at the University of Bremen is available on http://www.uni-bremen.geochemie.de.

Table 13: Sites investigated geochemically, including parameters analysed on board and aliquots of samples taken and stored for further analyses. * for analyses or further processing in the home lab, ** were taken for org. geochemistry group; vd = vacuum degassing, Ca = Cations, WS = Wet sediment, h = headspace.

Station GeoB	Device	Rhiz. Sam.	PW Squ.	Alk.	NH_4	PO_4	Fe	DIC**	VFA (rh)**	H_2S* (fix.)	$\delta^{34}S$* (sulf.)	$\delta^{34}S$* (HS-)	$\delta^{18}O$*	CH_4* (h)	CH_4 (vd)	SO_4, Cl* (1:100)	Ca.* (1:10)	Water (orig.)	WS.* (cool.)
10601-1	CTD-ROS	---	---	---	---	---	---	---	---	---	---	---	---	---	X (10)	---	---	X (22)	---
10602-1	CTD-ROS	---	---	---	---	---	---	---	---	---	---	---	---	---	---	---	---	X (22)	---
10602-2	GC	---	1 (20)	X	X	X	X	---	---	---	---	---	---	X	---	---	---	---	X
10603-1	CTD-ROS	---	---	---	---	---	---	---	---	---	---	---	---	---	X (10)	---	---	X (22)	---
10604-1	CTD-ROS	---	---	---	---	---	---	---	---	---	---	---	---	---	---	---	---	X (22)	---
10605-1	CTD-ROS	---	---	---	---	---	---	---	---	---	---	---	---	---	X (10)	---	---	X (22)	---
10605-2	GC	---	1 (23)	X	X	X	X	---	---	---	---	---	---	X	---	---	---	---	X
10606-1	MC	2 (19 / 15)	1 (13)	X	X	X	X	X	X	---	---	---	X	---	---	X	X	---	X
10610-1	GC	1 (23)	---	X	X	X	X	X	X	X	---	---	---	X	---	X	X	---	X
10612-1	GC	1 (28)	---	X	X	X	X	X	X	X	X	X	---	X	---	X	X	---	X
10612-2	MC	1 (24)	---	X	X	X	X	X	X	---	---	---	---	---	---	X	X	---	X
10613-1	MC	1 (18)	---	X	X	X	X	X	X	X	---	---	---	---	---	X	X	---	X
10619-5	D82 -PC6R	1 (20)	---	X	X	X	X	---	---	X	---	---	---	---	---	X	---	---	X
10619-11	D82 -PC22R	1 (16)	---	X	X	---	---	---	---	X	---	---	---	---	---	X	X	---	---
10619-12	D82 -PC52	1 (16)	---	X	---	---	---	X	X	---	---	---	---	---	---	X	---	---	---
10624-1	GC	1 (7)	---	X	X	X	X	X	X	X	X	X	X	X	---	X	X	---	X
10625-3	D84, PC6R	1 (12)	---	X	X	X	X	---	---	---	---	---	---	---	---	X	X	---	X
10625-11	D84, PC14	1 (17)	---	X	X	---	---	---	---	X	---	---	---	---	---	X	X	---	---

12.3 Shipboard Results

During this cruise TV-MUC cores from 3 locations, 5 ROV push cores and 5 gravity cores were sampled and investigated in detail for pore water chemistry. In addition, 5 rosette casts (water column samples, c.f. chapter 9) were taken. From Gravity Cores GeoB 10602-2 and GeoB 10605-2 as well as from TV-MUC Core GeoB 10606-1 pore water was extracted by pressure filtration. For all other sediment cores pore water extraction was performed by the rhizon technique. All sites sampled geochemically, including parameters analysed on board as well as aliquots of pore-water and solid-phase samples taken and stored for further analyses at the University of Bremen and at the Alfred Wegener Institute (AWI) in Bremerhaven are listed in Tab. 13.

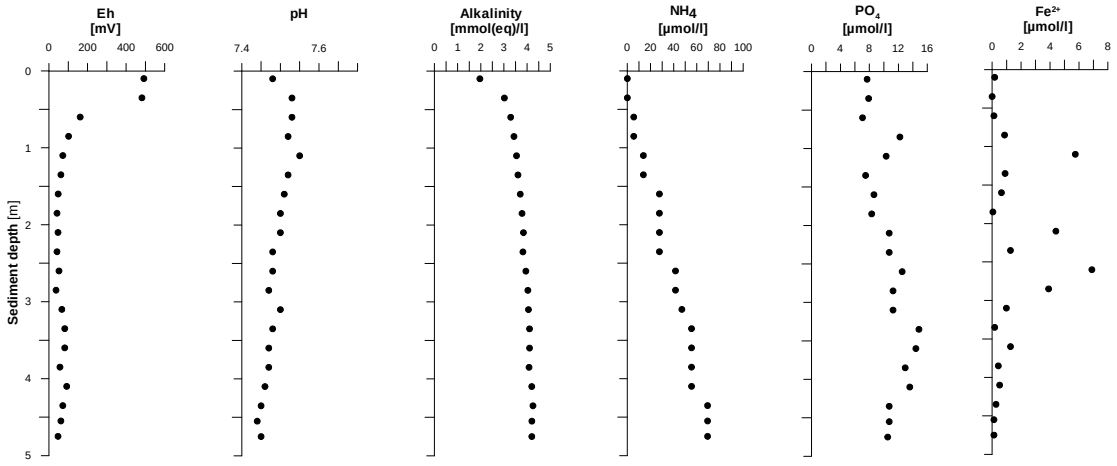

Fig. 54: Pore water concentration profiles of Gravity Ccore GeoB 10602-2 from the Chapopote Knoll area.

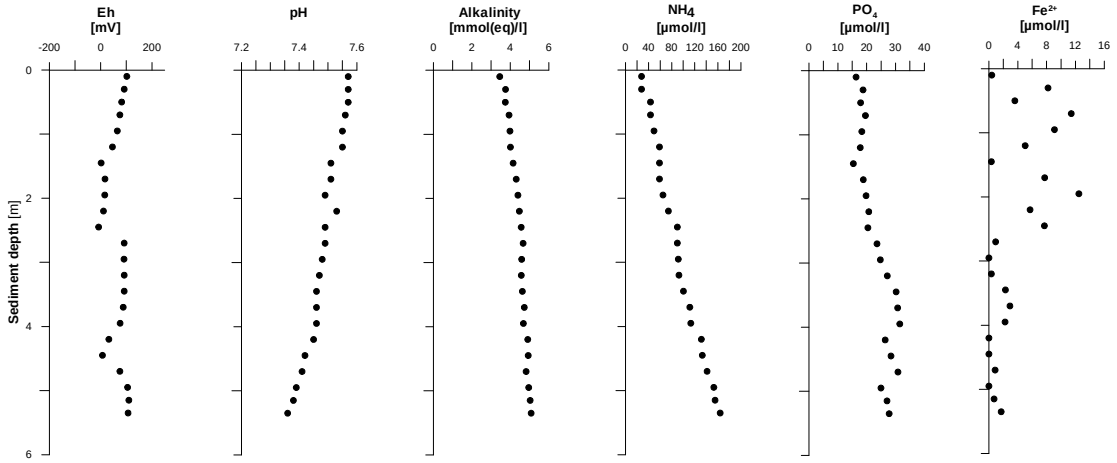

Fig. 55: Pore water concentration profiles of Gravity Core GeoB 10605-2 south of Chapopote where an oil slick was detected.

The two liner Gravity Cores GeoB 10602-2 and GeoB 10605-2 were taken during Leg M67/2a. Core GeoB 10602-2 was retrieved close to the Chapopote Knoll and Core GeoB 10605-2 was sampled south of Chapopote where an oil slick was detected. Both sediment cores did not contain any oil or asphalt and can thus be regarded as reference or background sites for the study area which are not affected by hydrocarbon seepage. At both sites alkalinity is on a relatively low level with maximum values of 4 to 5 mmol(eq)/l. Nutrients in pore water reach concentrations of 70 µmol/l

NH_4 and 15 µmol/l PO_4 in Core GeoB 10602-2 (Fig. 54) and more or less doubled maximum concentrations of 165 µmol/l NH_4 and 31 µmol/l PO_4 in Core GeoB 10605-2 (Fig. 55). In the upper part of both cores dissolved iron irregularly fluctuates with concentrations reaching 7 µmol/l in Core GeoB 10602-2 and about 14 µmol/l in Core GeoB 10605-2. At both stations hydrogen sulfide could not be detected.

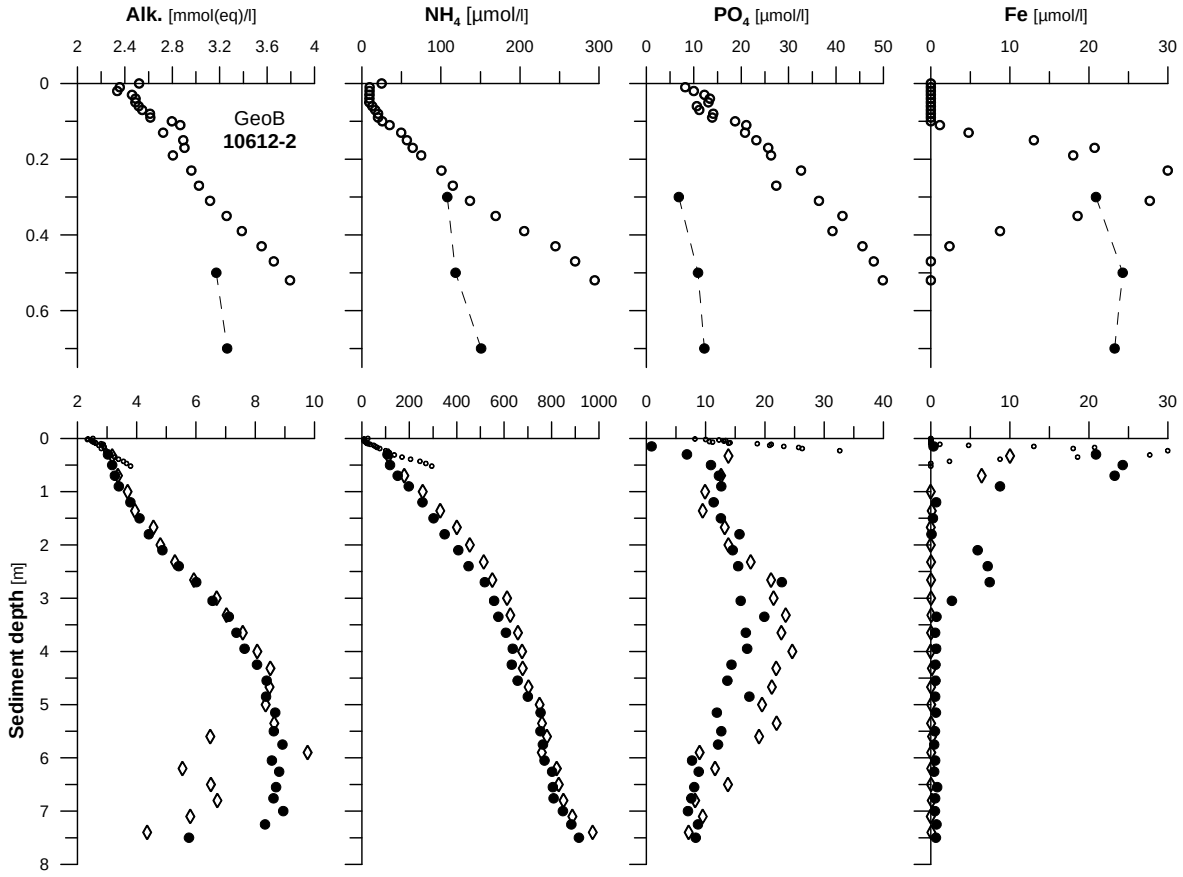

Fig. 56: Pore water concentration profiles for TV-MUC Core GeoB 10612-2 (upper graphs) and the two Gravity Cores GeoB 10610-1 (black dots) and GeoB 10612-1 (diamonds) (lower graphs).

Gravity Cores GeoB 10610-1 and GeoB 10612-1 which were retrieved in tubular plastic film from the north-eastern part of the central depression of the Chapopote Knoll are characterized by high concentrations of hydrogen sulfide and the occurrence of oil in the lowest part of the sampled sediment interval (Fig. 56). Maximum alkalinity values of 9 mmol(eq)/l are found around 6 m sediment depth. A first inspection of the amount of hydrogen sulfide precipitated with Zn-acetate also reveals highest sulfide concentrations at the same depth. Together with the concentrations of methane and other hydrocarbons determined by the organic geochemistry group (c.f., chapter 13) these findings demonstrate that the sulfate/methane reaction zone (SMRZ) is currently located at a sediment depth of about 6 m – obviously driven by the upward diffusive flux of methane (and other hydrocarbons) from the lower oil-containing sediments. Besides elevated levels of alkalinity these two oil cores also show significantly higher concentrations of ammonium of up to 975 µmol/l. The origin or source of these high concentration levels of NH_4 compared to the two background/reference sites described above is still a matter of debate. The pore water data for TV-MUC Core GeoB 10612-2 which was recovered at the same site are depicted in the upper part of

Figs. 56 and 57. The fact that the pore water concentration profiles do not exactly fit to each other may be attributed to the strong spatial/geochemical heterogeneity within the Chapopote Knoll structure.

Geochemical signatures of the MUC cores retrieved from three locations in the study area look significantly different (Fig. 57). Except for phosphate, Core GeoB 10606-1 taken from a water depth of about 2300 m southwest of the main working area is characterized by overall lowest concentrations of the pore water constituents analysed. MUC Core GeoB 10612-2 which was recovered from the site where viscous oil was found a few meters below the sediment surface displays highest ammonium contents of up to 300 µmol/l – in correspondence with the two Gravity Cores GeoB 10610-1 and GeoB 10612-1 from the same area (Fig. 56). This finding suggests that upward seepage of "fresh" oil (and other fluids) possibly supplies nitrogen compounds from the deeper subsurface. TV-MUC Core GeoB 10613-1 originates from a sediment patch between moderately altered asphalt flows on the eastern rim of Chapopote and is characterized by black, sulfidic sediments below a depth of about 7 cm (Fig. 57).

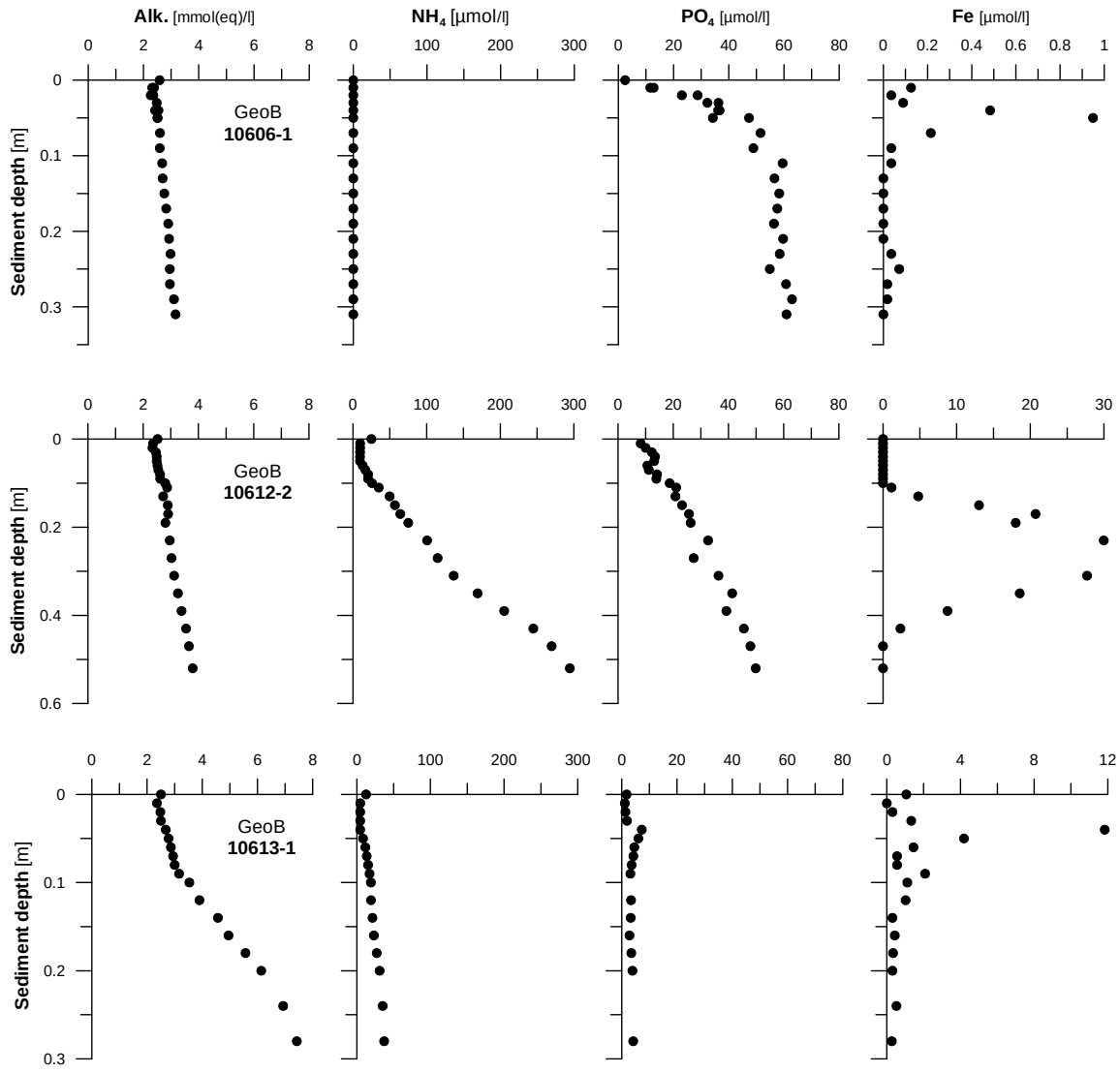

Fig. 57: Pore water concentration profiles of (TV-) MUC Cores GeoB 10606-1, GeoB 10612-2 and GeoB 10613-1.

The 1.6 m long Gravity Core GeoB 10624-1 (Fig. 58) was sampled from the southwestern rim of Chapopote close to sites of relatively fresh asphalt flows and contained a layer of mussel shill at about 1.4 m sediment depth. Due to the low amount of pore water obtained from this core only alkalinity and ammonium could be analysed on board. Compared to the pore water concentration profiles of all other sites the ammonium profile here shows a unique pattern with concentrations decreasing with depth. One possibility to explain this kind of ammonium depth distribution could be a more or less recent/young asphalt flow in the vicinity of this sampling site which might have possibly influenced the geochemical environment of the uppermost sediments. Further and more detailed analyses in the home labs at the University of Bremen and at the AWI in Bremerhaven will be performed to answer this question.

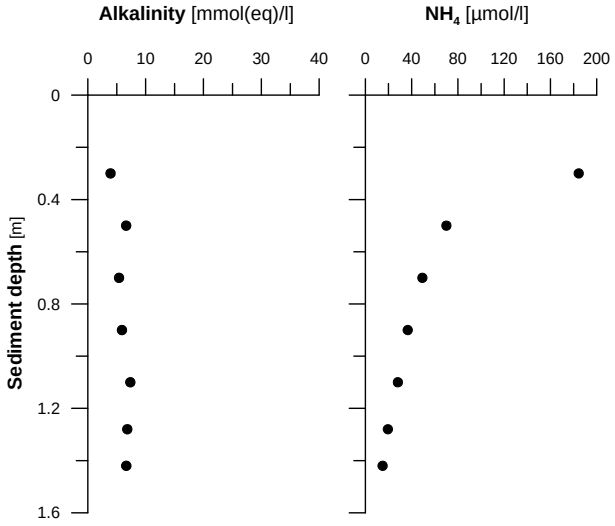

Fig. 58: Pore water concentration profiles of alkalinity and ammonium for Gravity Core GeoB 10624-1.

Push cores taken during ROV Dives 82 and 84 are depicted in Figs. 59 and 60. The three Push Cores PC6R, PC22R and PC52 recovered at site GeoB 10619 (ROV Dive 82) were all oil-stained and sulfidic in the lower part thus implying that the anaerobic oxidation of methane occurs close to the sediment surface induced by an upward supply of oil/hydrocarbons (Fig. 59). Of these three cores, highest alkalinity values were detected in Push Core PC22R suggesting that at this sampling site the SMRZ is located at the most shallow depth. The two push cores retrieved during ROV Dive 84 significantly differ from each other (Fig. 60). Push Core PC6R consists of brown hemipelagic sediments and did not show any indication of oil/hydrocarbon seepage. Pore water data therefore are similar to those of background site GeoB 10606 (Fig. 57). In contrast, Push Core PC14 which was collected from a site with bacterial mats on the sediment surface was heavily stained with oil and sulfidic below a sediment depth below about 2 to 3 cm (Fig. 60). At this site the SMRZ is likely to be located even closer to the sediment surface than sampled with PC22R during ROV Dive 82.

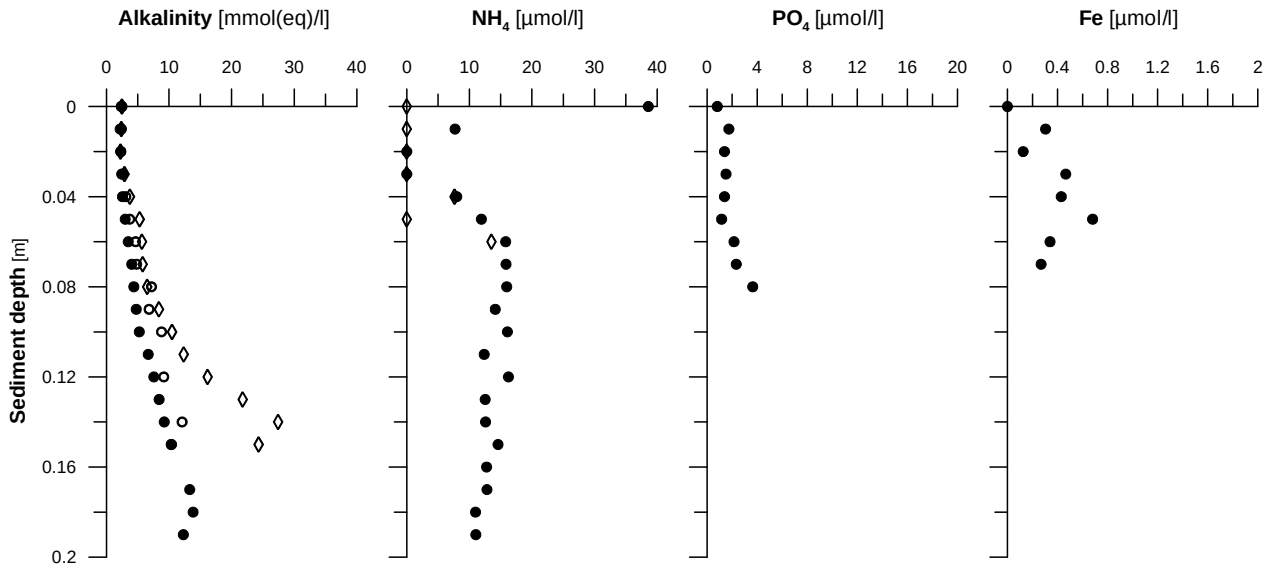

Fig. 59: Pore water concentration profiles of push cores taken during ROV Dive 82 (GeoB 10619). Black dots: PC6R; diamonds: PC22R; open dots: PC52.

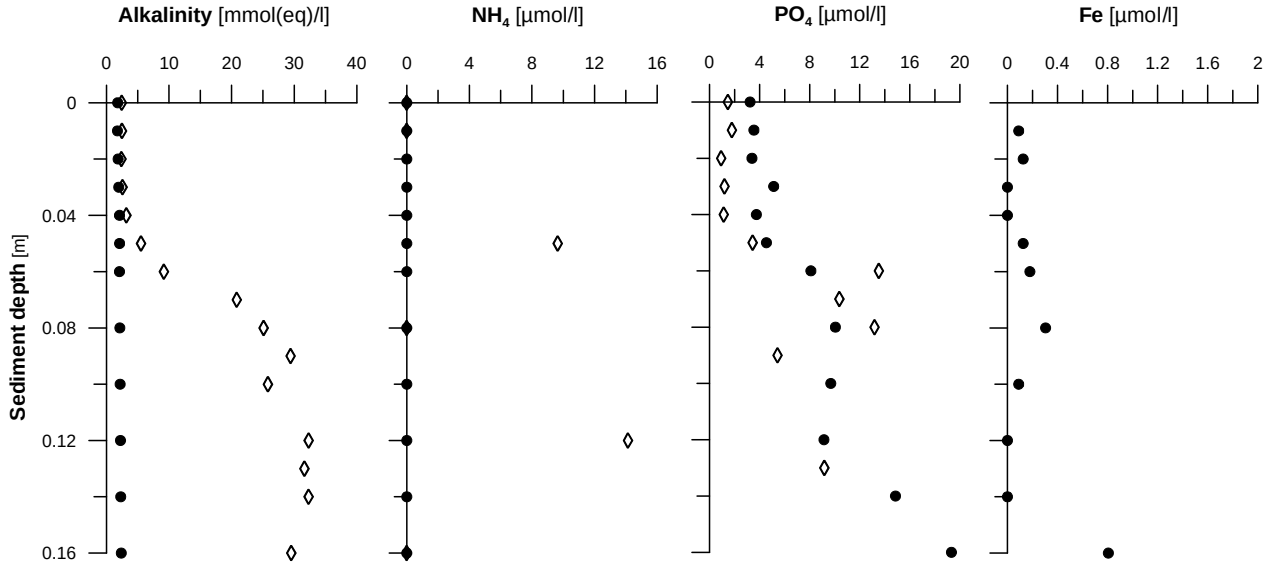

Fig. 60: Pore water concentration profiles of push cores taken during ROV Dive 84 (GeoB 10625). Black dots: PC6R; diamonds: PC14.

13 Organic Geochemistry

(K.-U. Hinrichs and F. Schubotz)

The organic geochemistry program at Chapopote seeks to address two sets of research questions:

(1) What is the origin of "asphalts" that cover the surface of Chapopote, and what mechanism(s) cause "asphalt volcanism"?

(2) How does asphalt volcanism impact the surrounding environment, i.e., what chemicals are leaking from the asphalts? What role do the associated processes play for the local benthic ecosystem? Is the system largely driven by sulfate-dependent methanotrophy or is the oxidation of higher-molecular hydrocarbons and other oil-bearing compounds equally important?

Sampling was designed to understand the interconnections between the unique geological setting that transports hydrocarbon-laden fluids to the surface and the ecosystem of micro- and macrooganisms. Samples consist of (I) solid materials, (II) fluids, and (III) gases (Tab. 14).

(I) Solid samples included sediments, heavy oil (asphalt), and soft tissue from benthic organisms that either host prokaryotic chemosynthetic symbionts or appear to be adapted to extreme environmental conditions at Chapopote by some other means (clams, pogonophora, crabs, sea cucumbers; see biology chapter 15). With these samples, we pursue two main objectives: (1) Asphalt- and oil-bearing materials will be analyzed by combined chromatographic-mass spectrometric approaches in order to identify the oil's source rock and, more importantly, to document compositional changes due to biological, chemical, and physical alteration processes. (2) All solid samples will be analyzed by various molecular and isotopic techniques to specifically target signals from organisms and/or processes related to biological hydrocarbon degradation. This involves analysis of samples for intact polar lipids (Biddle et al., 2006; Sturt et al., 2004), that is, molecular tracers indicative of live prokaryotes, and other microbial biomarkers (e.g., Hinrichs et al., 2000). In addition, sediments will be incubated aerobically and anaerobically to monitor (A) the assimilation of degraded hydrocarbons into biomass using ^{13}C-labeled model compounds (naphthalene and hexadecane) and (B) the diagenetic transformation of carbon with a particular focus on hydrocarbons and volatile fatty acids.

(II) Sampled fluids include porewaters taken for both quantitative and isotopic analysis of volatile fatty acids (VFAs) (Heuer et al., in review) and dissolved inorganic carbon (DIC). These analyses are intended to increase our understanding of the diagenetic transformations of carbon in the Chapopote ecosystem; results will be equally relevant for shorebased biogeochemical and microbiological work. In addition, five seawater samples have been retrieved, three by focused suction using the KIPS sampler (Garbe-Schönberg et al., 2006) and two by Niskin bottles at asphalt-bearing GeoB stations 10617 and 10619 (Tab. 14). The seawater samples are intended for the determination of potential emissions of non-volatile hydrocarbons into the water column and will be studied in Bremen by liquid-liquid extraction followed by gas chromatographic-mass spectrometric analysis.

(III) Gas sampling was designed to provide quantitative, compositional, and isotopic information on gaseous hydrocarbons in both sediments and heavy oils at Chapopote. Together these parameters provide information on the "freshness" of asphalts, the genetic affiliation of the associated heavy oils, and the overprint by diagenetic processes. Gas samples were retrieved from all sites and analyzed onboard for gas quantity and composition. We also analyzed the composition of gases that were released from the new autoclave tool designed by Hans-Jürgen Hohnberg. It

contained a large specimen of fresh asphalt that was retrieved from the seafloor under controlled conditions (see Chapter 10). Additional samples were preserved for isotopic analysis of hydrocarbons and quantification of sorbed hydrocarbons in Bremen. The latter will be combined with compositional analyses of clay mineralogy on a few selected samples for which selected residues have been preserved.

Table 14: List of stations sampled for shipboard and shorebased analysis. Abbreviations: HC-A (hydrocarbons, method A, see text for details), HC-B (hydrocarbons, method B), IPLs, GMB (geomicrobiology experiments, Bremen), DIC ([DIC], δ^{13}C DIC), VFA ([VFA], δ^{13}C VFA), KIPS, BM (Soft tissue, biomass of benthic macrofauna), Asph (pieces of asphalt for chemical characterization), TV-MUC (multicorer equipped with a camera), G (gravity corer), ROV (remotely operated vehicle), PC (push cores).

GeoB-Station	Sample Device	Dive #	Date	HC-A	HC-B	IPLs	GMB	DIC	VFA	KIPS	BM
10606	TV-MUC		05.04.2006		x	x	x	x	x		
10607	G		06.04.2006	x	x	x	x	x	x		
10610	G		07.04.2006	x	x	x		x	x		
10612-1	G		09.04.2006	x	x	x	x	x	x		
10612-2	TV-MUC		09.04.2006	x	x	x	x	x	x		
10613	TV-MUC		09.04.2006	x		x	x	x	x		
10617-1	ROV, Niskin	81	11.04.2006				x			x	
10617-2	ROV, KIPS	81	11.04.2006							x	
10617-3	ROV, KIPS	81	11.04.2006							x	
10617-4	ROV, KIPS	81	11.04.2006							x	
10617-5	ROV, Rotary 4	81	11.04.2006	x							
10617-6	ROV, Rigmaster	81	11.04.2006	x		x	x				
10617-7	ROV, Rotary 5	81	11.04.2006	x							
10618	G		13.04.2006	x		x	x				
10619-3	ROV, Niskin	82	13.04.2006				x				
10619-6	ROV, PC 9	82	13.04.2006		x	x					
10619-8	ROV, PC 25	82	13.04.2006				x				
10619-11	ROV, PC 22	82	13.04.2006				x	x	x		
10619-15	ROV, Rotary 4	82	13.04.2006	x		x					
10619-17	ROV, Rotary 6	82	13.04.2006	x		x	x				
10619-18	ROV, Rotary 6	82	13.04.2006								x
10619-20	ROV, Rotary 6	82	13.04.2006								x
10622-1	ROV, Autoclave	83	14.04.2006	x							
10622-2	ROV	83	14.04.2006								x
10622-3	ROV	83	14.04.2006	x							
10622-4	ROV	83	14.04.2006								x
10623-1	G		14.04.2006	x							
10623-2	G		14.04.2006	x		x					
10624-1	G		14.04.2006	x	x	x		x	x		
10624-2	G		14.04.2006	x							
10625-2	ROV, Chamber 1	84	15.04.2006					x	x		
10625-9	ROV, PC 32	84	15.04.2006	x	x	x					
10625-11	ROV, PC 14	84	15.04.2006				x				
10625-16	ROV, Rotary 6	84	15.04.2006			x					
10625-18	ROV, Rotary 4	84	15.04.2006								

The shipboard analysis program was largely dedicated to the analysis of gaseous hydrocarbons (C_1-C_5) in sediments, oils, asphalts, and hydrate recovered during the two legs of METEOR Cruise M67/2. In particular, the analysis of asphalt samples was expected to provide a better understanding of the mechanisms underlying transport of asphalt material from the subsurface.

13.1 Shipboard Gas Analyses

(F. Schubotz, K.-U. Hinrichs, S. Kasten, K. Enneking, M. Boles)

Methods

Sampling and analysis followed closely the procedures routinely used on the drilling vessel RV JOIDES Resolution, which are outlined in detail by the ODP Leg 201 Shipboard Scientific Party (2003).

Gases were extracted from sediments in either 50-mL (M67/2a) or 20-mL (M67/2b) headspace vials. Three extraction methods were employed, depending on sample type and necessity to obtain results quickly. During Leg M67/2a, 5 mL of wet sediment was sampled with cut-off syringes and extruded into 50-mL headspace vials containing 20 mL of saturated NaCl solution, poisoned with sodium azide solution.

During Leg M67/2b, when the majority of gases were analyzed, 3 to 5 mL of sediment was sampled with cut-off syringes and extruded into a headspace vial with (A) air and (B) air and 5 mL 1N-NaOH. Method A was used for most sites during Leg M67/2b; after vials were sealed with crimp-tops (septa out of silicon with teflon-coating), samples were heated for 20-30 min at 70°C, subsequently cooled to ambient temperature (typically 25°C) and analyzed by gas chromatography. Method B was typically employed for sediment samples that were intended for post-cruise isotopic analysis of the hydrocarbon gases and desorption experiments. For this purpose, samples are placed upside down and frozen until analysis in Bremen. For a few selected sites, method B was used for the shipboard analysis of hydrocarbon concentration, in some instances in parallel with method A to ensure that both protocols lead to comparable results. In those instances, samples were placed on a shaking-table and gently shaken until slurry formation. GC analysis was performed after 24 hours, i.e., the time required for dissolved gas to quantitatively diffuse into the headspace. Sediment samples prepared according to method A were stored for future analysis of the solid phase (mineralogy, bulk elemental composition, etc.). Asphalt-type samples were exclusively analyzed by protocol A.

In addition to standard headspace gas extraction protocols outlined above, we sampled gas from the autoclave experiment. For this purpose, headspace vials were filled with a saturated, aqueous NaCl solution. Gases were sampled with a 50-mL gas-tight syringe and injected into the headspace vials while replacing the salt solution with an equivalent volume of gas. Subsequently, gases were analyzed by GC and stored for transport to Bremen, where isotopic compositions of gaseous hydrocarbons will be determined.

Gas chromatographic analyses:

200 µL of headspace sample was injected with a 250-µL gas-tight syringe into an Agilent 6890N series gas chromatograph (GC) equipped with a flame ionization detector (FID) for detection of gaseous hydrocarbons and a thermal conductivity detector (TCD) for O_2, N_2, and CO_2. While the FID was used routinely, the TCD was only utilized for selected samples. The system was equipped with two columns and injectors: hydrocarbons: Optima 5 capillary column, 50 m x 0.32 mm, film thickness: 5 µm, split/splitless injector set at 180°C; O_2, N_2 and CO_2: Packed column, mol sieve, 60/80 Mesh, EPC purged packed inlet set at 180°C. The oven was programmed from 45°C (4 min) → 15°C/min → 155°C (2 min) → 25°C/min → 240°C (7 min).

Calculation of concentrations

A calibration resulting from injection of known quantities of hydrocarbon gases was applied to calculate the molar fraction in sampled gas mixtures. The system was calibrated for methane with outside air (1.8 ppm), a N18 standard mixture of gaseous hydrocarbons (Air Liquide) with 1000 ppm each of methane, ethane, propane, iso-butane, n-butane, n-pentane, and n-hexane, and pure methane. Concentrations of C_{2+} hydrocarbons were calculated by linear interpolation from the N18 standard since the FID response for hydrocarbons is known to be highly linear.

Hydrocarbon gas concentrations [HC] in the sediment were derived from the headspace concentration by the following equation:

$$[HC] = \chi_M \times P_{atm} \times V_H \times R^{-1} \times T^{-1} \times V_S^{-1} \quad (1)$$

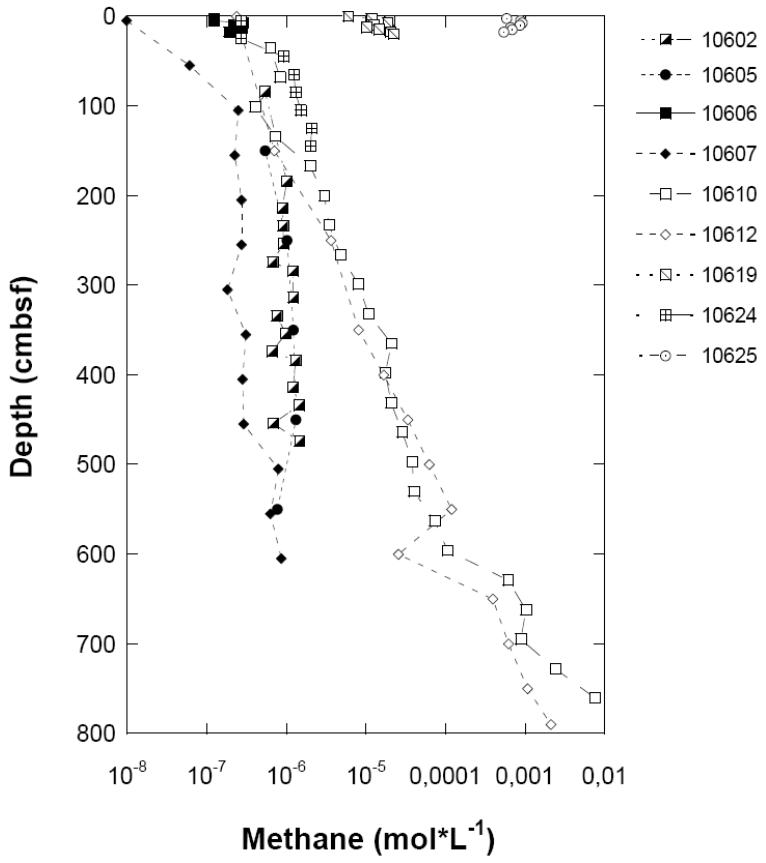

Fig. 61: Concentration profiles of methane at sediment sites occupied during M67/2.

where V_H = volume of the sample vial headspace (for asphalt and hydrate samples, volumes are crude estimates and need to be verified by additional gravimetric measurements in Bremen), V_S = volume of the whole sediment sample, χ_M = molar fraction of hydrocarbon in the headspace gas (obtained from GC analysis), P_{atm} = pressure in the vial headspace (assumed to be atmospheric pressure when the vials were sealed), R = the universal gas constant, T = temperature of the vial headspace in degrees Kelvin.

The detection limit for methane for the entire protocol is estimated to be around 50 nmol*L^{-1} sample and is largely constrained by the presence of methane in air.

Concentrations of hydrogen (M. Boles)

Hydrogen concentrations were measured on board using a Trace Reduction Gas Analyzer RGA3. The sample collection included only gravity cores. 5 mL of sample were collected and placed in a 20-mL headspace vial. After purging the sealed vial with helium, the samples were incubated at 4°C for 96 hrs.

Hydrogen was measured at GeoB Sites 10606 (8 samples) and 10612-1 (11 samples). The sample suite is limited as many of the cores were not good candidates for measurement of hydrogen concentration. Incubation times limited hydrogen analyses at the end of the research cruise. Hydrogen measurements are subject to verification at University of Georgia but the reference core at Site GeoB 10606 shows a baseline of hydrogen concentration, while GeoB 10612-1 shows a peak well above the baseline concentration at a subsurface depth of 1.6 m.

13.2 Preliminary Results

On the basis of concentrations of hydrocarbons, we distinguish three principal environments at Chapopote: (1) hemipelagic sediments not influenced by seepage of oil and gas, (2) hemipelagic sediments impacted by seepage of oil and gas, (3) layered structures of heavy oil, so-called asphalt.

The first environment was sampled at GeoB Sites 10602, and 10605-10607. Here methane concentrations level out at about 1 μmol*L^{-1} wet bulk sediment at subsurface depths of around 4 meter (Fig. 61). In these environments, C_{2+} hydrocarbons were not detected. The second environment is represented by GeoB Sites 10610, 10612, 10619, 10624, and 10625. Here maximum concentrations of methane were three to four orders of magnitude higher than background. Among these sites, we distinguish between settings where methane concentrations appears to be largely controlled by upward-diffusion (Sites 10610, 10612, 10624) and others where upward migration of oil and/or gas results in high methane levels close to the sediment-water interface (Site 10619 and 10625) (Fig. 61). The latter two sites were targeted by push-coring during ROV dives based on visual evidence pointing to high activity.

These hydrocarbon-laden sediments show evidence of high sulfate-dependent turnover of hydrocarbons, e.g., noticeably high levels of H_2S, relatively high concentrations of alkalinity, etc. At GeoB Sites 10610 and 10612, the methane and alkalinity profiles suggest the establishment of a sulfate-methane reaction zone at subsurface depth of about 6 m, i.e., a few meters above oil-bearing sediments that appear to fuel the upward diffusive flux of methane and other hydrocarbons.

Asphalt samples are highly diverse in terms of their content of gaseous hydrocarbons. They usually contain relatively high proportions of C_{2+} hydrocarbons. Highest concentrations of C_2-C_5 hydrocarbons with slightly less than 100 μmol*L^{-1} were observed in two asphalt samples (GeoB 10618 and 10625-16) that, based on their gassy appearance after recovery, were associated with methane hydrate. The other extreme is represented by samples with very low concentrations of methane and higher gaseous hydrocarbons. For example, isolated asphalt pieces that have been sampled with the suction sampler (e.g., samples GeoB 10617-7 and 10619-15; Fig. 62) show strong signs of postdepositional alteration (brittle and porous structure) contain up to four orders of magnitude less hydrocarbons. The relative distribution of individual hydrocarbons in the C_1-C_5 range is highly diverse in asphalts (data not shown, compare next chapter on autoclave experiment). Assuming a single source of oil with a more or less homogenous compound distribution, we interpret this diversity to be reflective of the postdepositional history of the asphalt including the

conditions of sampling. For example, our controlled gas release experiments point to a large potential of fractionation of the gas mixture with the lighter compounds being lost more rapidly. Alternatively, heavy oils are being supplied from various source rocks and/or undergo fractionation processes in the subsurface, which lead to the observed inhomogeneous distribution of hydrocarbons in the subsurface. Shorebased isotopic analysis of hydrocarbon gases will provide additional information on the underlying processes.

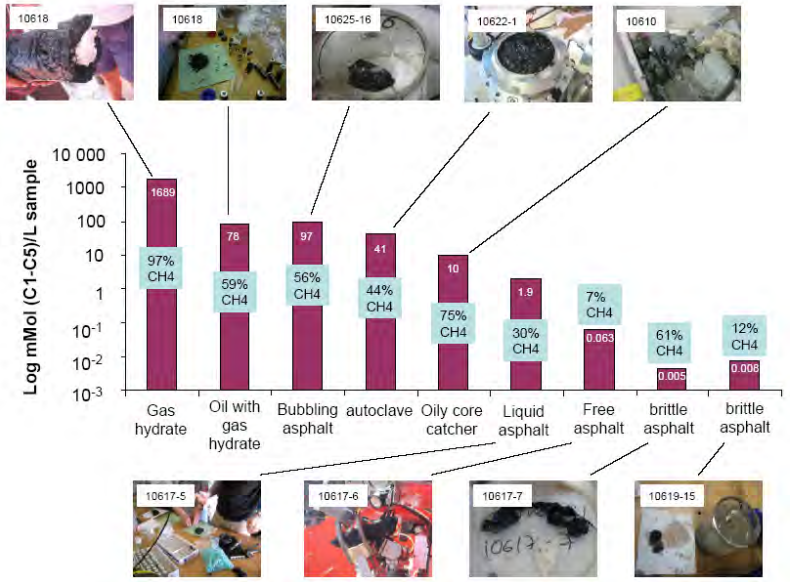

Fig. 62: Total gas contained in various seafloor samples.

During Dive 83, the In-situ Pressure Seafloor Sampler (IPSS; Chapter 10) was successfully deployed and recovered with a sample of 1.15 L of highly elastic asphalt. The goal of the experiment was the quantification of gaseous hydrocarbon in a typical seafloor asphalt sample.

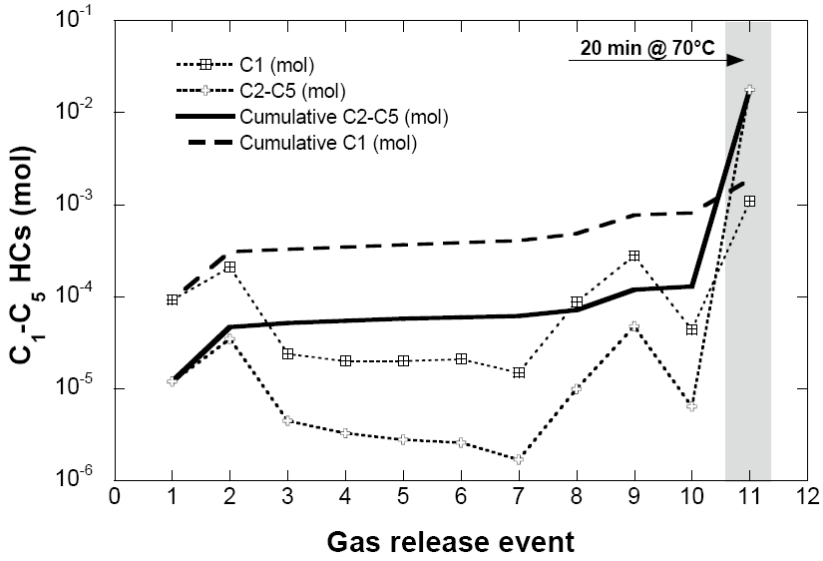

Fig. 63: Sequential release and sampling of gas from asphalt sample contained in IPSS at p_0 of 250 bar through a manifold. Gas concentrations for steps 4 and 10 were interpolated. Step 11, immediately after termination of the experiment, was calculated from the gas composition of a sub-sample heated at 70°C for 20 minutes. For additional details on the relative distribution of hydrocarbons, see Fig. 64.

After return of the IPSS to the ship, the tool was stored for several hours in the cooler at 4°C before the controlled release of gas was initiated. A total of 9.75 L of gas was released. This gas consisted largely of system-internal air, which was introduced through an improperly closed valve. However, no losses of hydrocarbons were caused and the experiment is viewed as being quantitative. A total of 0.94 mmol, or an equivalent of 23 mL of C_1-C_5 hydrocarbon gas, assuming STP conditions and ideal-gas behavior, was released during steps 1-10. Subsequent extraction of gas by short heating of a sub-sample to 70°C (see Methods) released additional hydrocarbon gas. extrapolated to the entire asphalt sample volume, the amount released by heating corresponds to 47 mmol of hydrocarbon gas.

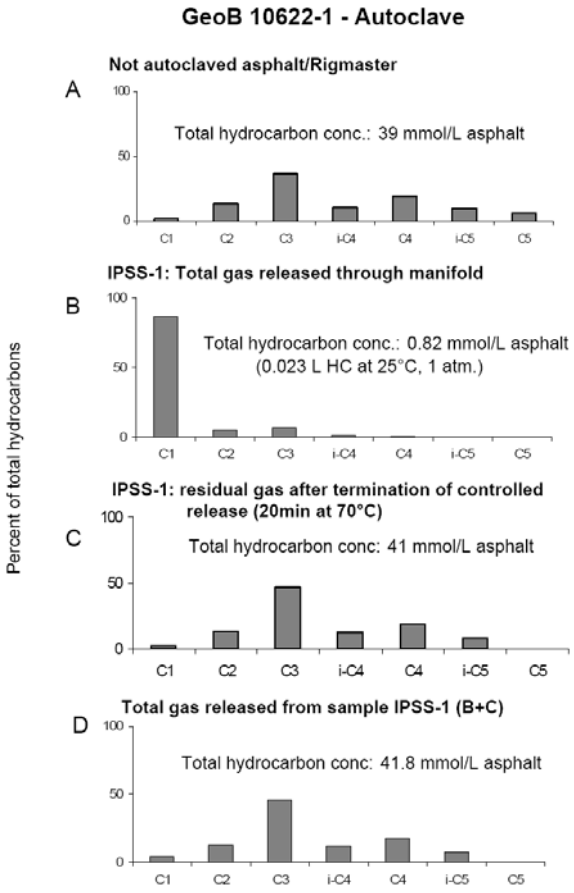

Fig. 64. Distribution of C_1-C_5 hydrocarbons in various subsamples during experiment IPSS-1.

The relative distribution of hydrocarbon released during the two stages of the experiment differed significantly (Fig. 64). While direct release from the IPSS yielded a mixture dominated by methane (Fig. 64, B), the residual gas was strongly dominated by propane (Fig. 64, C), the major hydrocarbon gas in the asphalt sample. Due to the large relative amount, the distribution of the residual gas almost equals that of the total gas in IPSS-1 (Fig. 64, D). Notably, this distribution is almost identical to that in a non-autoclaved sample recovered at the same sampling site (Fig. 64, A). This strongly suggests that the fraction of gas released during the controlled experiment is rather loosely bound and is easily lost during recovery. The residual gas, on the other hand, appears to be dissolved in the inside of the sample and, under conditions at the seafloor, may provide a low, continuous flux of hydrocarbons to fuel the benthic ecosystem.

14 Microbiology

(J. Felden, G. Wegener, M. Bowles, F. Wenzhöfer, A. Boetius)

Sites of hydrocarbon seepage, previously observed at mud volcanoes, gas and oil seeps and gas hydrate-bearing sediments, are often associated with high biological and geochemical activity, including rich chemosynthetic communities and striking build ups of precipitated minerals. In project RCOM E we contribute to questions such as the diversity and coupling of geological and biological processes at seeps and their environmental impact. The work carried out during M67/2b mainly contributes to projects E3 and E4 aiming at the following questions by applying a wide range of methods and tools:

- How do fluid flow, gas and oil ebullition, and mud extrusion influence solute gradients and biogeochemical process rates?
- How are flux, assimilation, and turnover of hydrocarbons linked with biomass build-up and carbon burial at different seep types?
- How are the diversities of microbial communities and carbon-flow patterns linked to regimes of fluid flow and seepage?

Previous work at Campeche Knolls, Gulf of Mexico, led to the discovery of a novel ecosystem associated with asphalt volcanism (MacDonald et al., 2004). In other cold seep environments active hydrocarbon-based microbial ecosystems both within the sediments (Joye et al. 2004) and within hydrate material (Orcutt et al. 2004) were noted. The aims of the current study were to investigate the hydrocarbon-based microbial ecosystems and the microbial interactions with asphalt material at this newly discovered environment, as well as with symbiotic animals.

Studies in the northern Golf of Mexico have shown that the process of sulfate reduction is fueled by the degradation of higher hydrocarbons in sediments, which contain oil. The anaerobic oxidation of methane as further source of sulfide appears to play only a minor role in hydrate and oil bearing habitats. Our main interest was to explore the effect of gas and oil flow on biogeochemical processes and microbial diversity. We measured ex-situ as well as in-situ fluxes and substrate turnovers by focusing on oxygen consumption, sulfate reduction as well as methane oxidation and production. Also we took samples to link geochemical processes and gradients to the distribution of microorganism. Therefore, several methods are used to examine the diversity and function of microbes in the Chapopote ecosystem in relation to this novel geo-bio-system.

14.1 Methods and Materials

Insinc (In-situ incubator)

During this cruise a new *in situ* tool was used to measure sulfate reduction under *in-situ* conditions (Tab.15). Insinc is based on the established method to measure sulfate reduction in push cores. However, with this system the ^{35}S sulfate radiotracer is already injected at the seafloor. The sediment is thereby incubated in the closed incubator system at environmental pressure and temperature. The sulfate reduction reaction is terminated on board by transferring the sediment to ZnAc similar as in the ex-situ method.

Profiler-Module and Benthic Chamber

To investigate in-situ biogeochemical processes two benthic modules, a profiler and a flux chamber, have been constructed for deployment and operation by the ROV. The autonomous profiler module (Wenzhöfer et al., 2000) hosted 2 O_2, 1 temperature (Pt100, UST Umweltsensortechnik GmbH, Geschwenda, Germany), 3 pH and 3 H_2S microsensors. Except from the temperature sensor all electrodes have been constructed in our microsensor laboratory of the MPI in Bremen. Positioned at the sediment surface the profiler gradually moves the sensors downwards in increments of 100 µm for a total distance of 15 - 20 cm and the sensor recordings were stored internally. Afterwards the sensors were moved back to the starting position where they waited until a new measuring cycle is initiated by the ROV. Sensors were calibrated prior to deployment and for the O_2 sensors the readings in the bottom water of know O_2 concentration and in the anoxic sediment was used to cross-check the calibration curves.

Table 15: In-situ tools that were deployed during the ROV dives.

Device	Dive	Date	Station No (GeoB)	Instrument	Time of deployment (h)	Area	Lat. 21°N	Long. 93°W
ROV	82	13.04.2006		Profiler	not deployed due to problems of the lift			
ROV	82	13.04.2006	10619-1	Insinc #1	control without injection of the tracer	Chapopote	53,993'	26,182'
ROV	82	13.04.2006	10619-2	Insinc #2	6,5	Chapopote	53,993'	26,182'
ROV	84	15.04.2006	10625-2	Chamber 1	2,5	Chapopote	53,906'	26,190'
ROV	84	16.04.2006	10625-12	Chamber 2	9,0	Chapopote	53,957'	26,252'
ROV	84	17.04.2006	10625-7	Insinc #3	12,0	Chapopote	53,906'	26,206'
ROV	84	17.04.2006	10625-8	Insinc #4	12,0	Chapopote	53,906'	26,206'

The benthic chamber module is a modified version of the free-falling chamber lander previously used to study benthic processes in the deep-sea (Wenzhöfer and Glud, 2002). This small benthic module consists of a circular chamber, an electronic cylinder, a water sampling system and a battery which can be operated by the ROV. The chamber encloses an area of ca. 283 cm^2 together with 4 -6 l of overlying bottom water. Two oxygen microelectrodes mounted in the chamber lid monitor the concentration change in the enclosed water body while at preprogrammed time intervals 5 water samples (each 50 ml) were retrieved for later analyses of O_2, DIC and other elements. The chamber (Fig. 65) was used to measure fluxes and oxygen consumption at a sedimentary reference site as well as above asphalt (Tab.15).

Ex-Situ

Sulfate reduction and methane oxidation rates: Sediment samples from various gravity cores, multi cores and push cores were investigated for microbially mediated sulfate reduction rates and methane oxidation. In case of multi coring as well as push coring 4 sub cores (Ø 2.5cm), i.e. three biological and one abiological control, were sampled from neighboring cores immediately after recovery. Radio tracer labeled substrate was injected in 1cm intervals through small, silicon sealed

holes. In case of gravity coring 5ml of sediment slurry was sampled with a 0,5-1 m resolution and incubated in rubber stoppered glass tubes. Sediments were incubated with either $^{14}CH_4$ or $^{35}SO_4^{2-}$ for 1-4 days at in situ temperature under anaerobic conditions and then fixed in NaOH and Zn-Ac, respectively, for further measurements of remaining substrate ($^{14}CH_4$, $^{35}SO_4^{2-}$) and product ($^{14}CO_2$, $H_2{}^{35}S$) activity. The ratio of product to substrate activity multiplied with substrate concentrations yields then actual rates. Up to three biological and one abiological control were incubated per site and sediment horizon. The samples will be analyzed in the home laboratory.

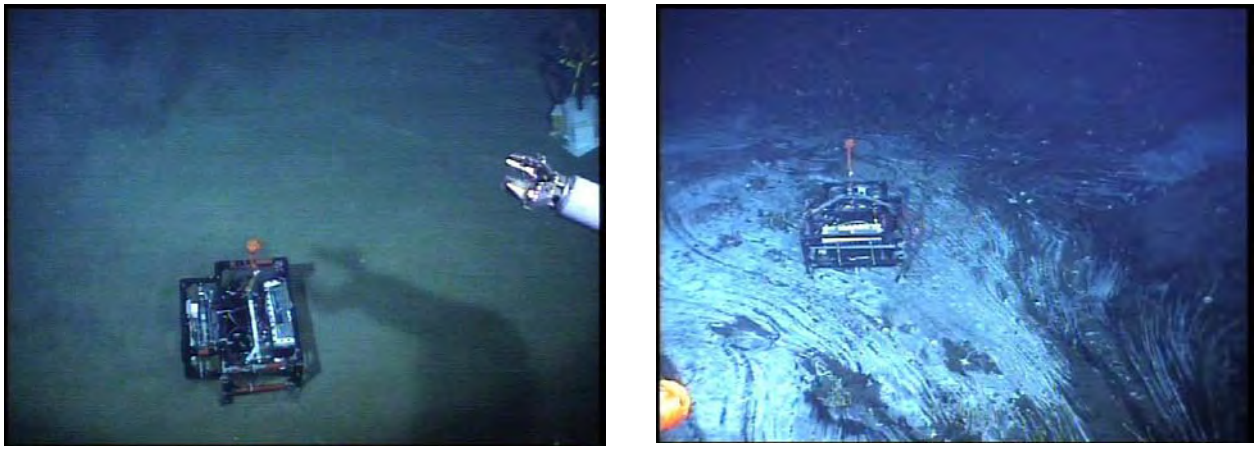

Fig. 65: The two measuring site of the benthic chamber; left: at the reference site, GeoB No: 1625-2; right: on asphalt which is covered with white precipitate, GeoB 1625-12.

Methanogenesis

Sampling on board for methanogenesis rates included samples from multi corer, gravity corer, and push cores. Samples were collected and injected with radio-labeled acetate and bicarbonate. The samples were then incubated at 4°C for an approximate 24 hr period after which the incubation was terminated and the samples were stored. The samples will be processed at the University of Georgia during the summer of 2006.

Bacterial counts

2.5 ml of sediment volume were fixed in 9ml of 2% formalin in sea water for 2 – 4h (Tab. 15).

Fluorescent in situ hybridization (FISH)

2ml of the sediment-formalin suspension (Tab. 15) were centrifuged and supernatant was discarded. The pellet was washed two times in 3 ml 1*PBS-buffer (resuspension, centrifugation, discarding of supernatant). Finally, the pellet was fixed in 2 ml of a 1:1 (v:v) solution of Et-OH:1*PBS (50% final concentrations) and kept at –20°C until further analyses in Bremen.

DNA/RNA

Ca. 4g of fresh sediment was frozen at –20°C until DNA analysis in Bremen (Tab. 15). RNA samples were collected in the same way but frozen at -80 °C.

Microbiology experiments

Sediment and asphalt samples from various sampling devices were transferred to wide mouth glass bottles sealed with gas tight rubber stopper and kept at in situ temperature until further experiments in Bremen.

Table 16: Sediment samples obtained by multiple corer (MUC), ROV Pushcores (PC) and gravity corer (GC). Sediment samples were split into different layers for rate measurements, for total bacterial counts, fluorescence in-situ hybridization (FISH), for microbial diversity analysis (in 2.5 cm horizons, the sample interval was increased to 1m for the GC). The asphalt sample recovered with the rotary sampler (RS) were just partly sampled for rate measurements.

Device	Station No (GeoB)	Date	Dive	Sampled	Site description	Area	Lat. 21°N	Long. 93°W
MUC	10606	05.04.2006			Reference core	Campeche Oil Ridge	19,970'	49,770'
GC	10610	06.04.2006			With oil/ asphaltene in core catcher, sediment less oily	Chapopote	54,250'	25,880'
GC	10612-1	09.04.2006			Some oil on the GC, no oil visible in sediment but sulfidic core catcher	Chapopote	54,230'	25,910'
MUC	10612-2	09.04.2006			Ca 10 cm brownish sediment, then 1-2 cm blackish, then 30 cm greyish	Chapopote	54,230'	25,930'
TV MUC	10613	09.04.2006			Close to asphalt area	Chapopote	54,120'	25,650'
ROV	10617-5	10.04.2006	81	RS 4	Asphalt pieces	Chapopote	53,941'	26,229'
ROV	10617-6	10.04.2006	81		Asphalt piece collected by the ROV manipulator	Chapopote	53,944'	26,229'
GC	10618	11.04.2006			Asphalt with hydrate in core catcher	Chapopote	53,950'	26,210'
ROV	10619-8	13.04.2006	82	PC 25	Oil rich sediment, partially covered with bacterial mats	Chapopote	53,991'	26,183'
ROV	10619-7	13.04.2006	82	PC 10	Oil rich sediment, partially covered with bacterial mats	Chapopote	53,991'	26,183'
ROV	10619-10	13.04.2006	82	PC 56	Oil rich sediment, partially covered with bacterial mats	Chapopote	53,991'	26,183'
ROV	10619-13	13.04.2006	82	PC 36	Oil rich sediment, partially covered with bacterial mats	Chapopote	53,991'	26,183'
ROV	10619-6	13.04.2006	82	PC 9	Very oily with bacteria on the top	Chapopote	53,991'	26,183'
ROV	10619-15	13.04.2006	82	RS 4	Asphalt sample, sediment	Chapopote	53,968'	26,184'
ROV	10619-17	13.04.2006	82	RS 6	Asphalt sample, sediment	Chapopote	53,953'	26,231'
GC	10624-1	14.04.2006			Mussel shell at the bottom o the corer, slightly oily	Chapopote	54,000'	26,160'
ROV	10621-3	14.04.2006	83		Spongelike structure on asphalt piece	Chapopote	53.990'	26.125'
ROV	10625-18	15.04.2006	84	RS 4	Asphalt with white mat	Chapopote	53,957'	26,252'
ROV	10625-16	15.04.2006	84	RS 6	Asphalt with white precipitate	Chapopote	53,957'	26,252'

Bacterial Symbioses

Microscopic observations:

With microscope and binocular microbial organisms from asphalt pieces were investigated. Most pieces of the asphalt pieces were collected with the rotary sampler during the Dive 84 (Tab. 16).

Fig. 66: Sampling of bacterial mats with the rotary sampler, Dive 84.

Symbioses of bacteria with invertebrates:
Tissue samples for analyses of symbiotic associations of tubeworms and mussels were fixed for processing in the home laboratory. The mussels were sectioned and the bacteria-containing gill parts were preserved for microscopical analyses. The foot of the mussel was frozen as well as fixed as negative control. The tubeworm body was sectioned into head, root and trophosome, and preserved for further analyses. DNA samples were frozen at -80°C as well as fixed in 96% Ethanol. Tissues were fixed with 2% Para-formaldehyde and afterwards washed with PBS. These samples will analyzed by ribosomal DNA methods including FISH. Furthermore, the Trump's fixative was used to conserve samples for TEM and SEM.

Table 17: Invertebrate samples for the analyses of symbiotic bacteria.

Device	Dive	Date	Station No (GeoB)	ID #	Taxon	Length [cm]	Area	Lat. 21°N	Long. 93°W
ROV	82	13.04.2006	10619-18	A-1	Siboglinid tubeworm	140,0	Chapopote	53,949'	26,234'
ROV	82	13.04.2006	10619-18	A-2	Siboglinid tubeworm	140,0	Chapopote	53,949'	26,234'
ROV	82	13.04.2006	10619-18	B	Siboglinid tubeworm	140,0	Chapopote	53,949'	26,234'
ROV	83	14.04.2006	10622- 4	4	Siboglinid tubeworm	14,2	Chapopote	53,949'	26,234'
ROV	83	14.04.2006	10622- 4	1	Bathymodiolus	18,9	Chapopote	53,990'	26,124'
ROV	83	14.04.2006	10622- 4	4	Bathymodiolus	9,8	Chapopote	53,990'	26,124'
ROV	83	14.04.2006	10622- 4	11	Bathymodiolus	14,2	Chapopote	53,990'	26,124'
ROV	83	14.04.2006	10622- 4	10	Bathymodiolus	12,6	Chapopote	53,990'	26,124'
ROV	83	14.04.2006	10622- 4	12	Bathymodiolus	2,8	Chapopote	53,990'	26,124'

14.2 Preliminary Results

During the cruise several habitats at Chapopote were investigated visually and a variety of target sites were chosen to obtain surface samples associated with different types of hydrocarbon flow. For the pushcore and multicorer sampling, different sedimentary sites were chosen: 1) a reference site away from Chapopote with hemipelagic sediments (GeoB 10606), 2) a reference site at Chapopote (GeoB 10612), 3) a site next to brittle asphalt with a few tubeworms (GeoB 10613, cores were taken from 1-2 m away from asphalt), 4) one site next to fresher asphalt populated by tubeworm bushes (cores were taken ca 20-50 cm away from the tubeworms and the next asphalt flow) and 5) one highly oily site marked by white precipitates on the seafloor and emanating oil droplets. The asphalt could not be sampled by push coring or multiple coring. Instead samples were obtained by sampling with the ROV and the gravity core. These samples were used for rate measurements to test if the asphalt harbors active microbial communities producing sulfide from hydrocarbon degradation.

The gravity cores were sampled to get an idea on subsurface microbial activities associated with methane or higher hydrocarbon degradation. We subsampled 3 different gravity cores one of which had substantial amounts of oil in the core catcher and smelled sulfidic, indicating ongoing sulfate reduction.

Furthermore we investigated different types of white biogenic mats found on top of asphalt flows. During Dive 83 we detected a white biofilm on top of a piece of asphalt that contained high amounts of large spicules reminiscent of sponge spicules. These white films formed relatively thick crusts around the gas hydrate /flare site on Chapopote. During Dive 84 we also found bacterial mats that were located at the asphalt. Furthermore, the ecosystem of Chapopote supports high biomasses of symbiotic tubeworms anchoring with their roots in crevices of asphalt flows, and in few areas also high biomasses of chemosynthetic mussels (also around the flare site).

In-Situ

Shuttle system:
We had planned to use a shuttle system to deploy our in situ instruments to be able to measure at the seafloor and use all the pushcores for sampling. Unfortunately, during the first deployment the shuttle was lost due to a problem with the cable carrying the floatation spheres, which was not properly disconnected from the winch cable. The shuttle was later recovered by the ROV and ship, but the profiler was damaged, and some floatation was lost. Hence, the shuttle was not further deployed during the cruise.

Insinc:
First tests have shown that the tracer was injected successfully at the seafloor to the sediments of the 20 cm incubator system. Further analyses are done in the home lab including a comparison of in situ and ex situ rates of the same sampling sites.

Profiler-Module and Benthic Chamber:
The Profiler-module was not used due to damage during the first deployment of the shuttle system. Two measurements with the benthic chamber were performed during the Dive 84. Because of

problems with visibility and placing of the chamber by the ROV, the first deployment was too short to get useful measurements. Nevertheless, measurements of the oxygen sensors during the second chamber deployment (GeoB 10625-12) showed high total oxygen consumption of 65.2 nmol m^{-2} d^{-1} at the asphalt site covered with bacterial mat like structure (Fig.67). This is confirmed by the measured oxygen concentrations from the water samples that showed slightly higher total oxygen consumption with 84.5 nmol m^{-2} d^{-1}. In comparison to background oxygen consumption in the GoM, the oxygen consumption by asphalt associated biogeochemical processes is significant higher, but in same range as e.g. for the active Haakon Mosby Mud Volcano seep sites (deBeer et al. 2006). Further analyses including measurements of DIC, H2S, nutrient and fatty acids in the water samples from the chamber will be performed in the home lab.

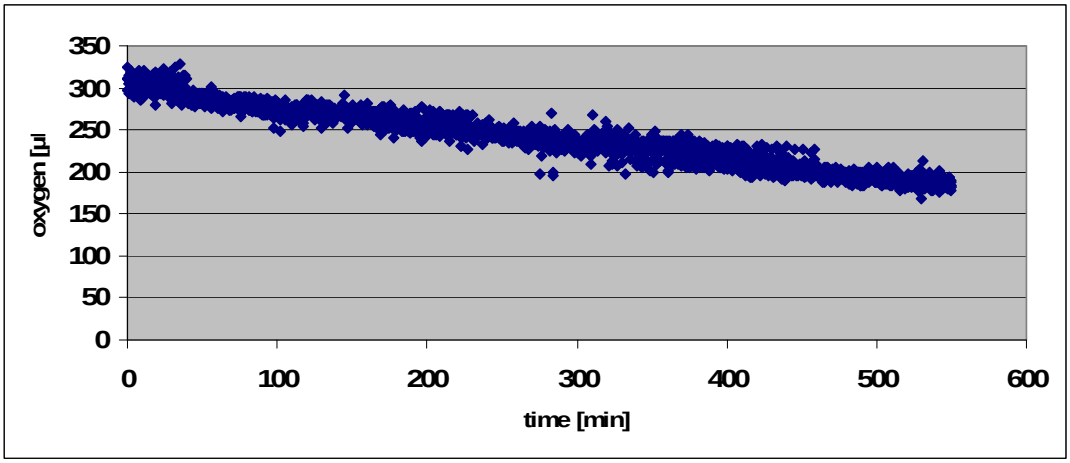

Fig. 67: Oxygen consumption of 2nd camber deployment on the asphalt site.

Ex-Situ:

All measurements of microbial activity as well as identification and distribution of microbes will be done in the home lab.

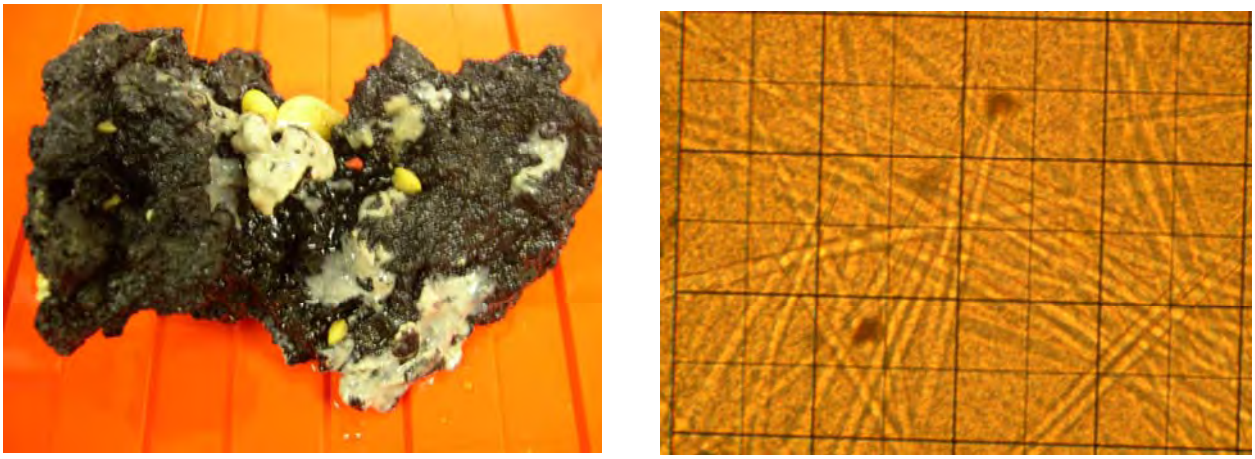

Fig. 68: ROV Dive 83 asphalt sample is covered with white biofilm and mussels (left). Magnification of spicules in the biofilm structure (right)

Bacterial Symbioses:

Samples for the identification of the bacterial symbionts of mussels and tubeworms associated with asphalt will be carried out in the home laboratory. The microscopic observation of biogenic mats on asphalt samples is roughly summarized in the following. During Dive 83 an asphalt piece (Fig. 68,

left) with mussels and a white biofilm was collected. The abundant spicules in the biofilm could be an indication that the white film is formed by sponges (Fig. 68, right). Further analyses in Bremen will be needed test this hypothesis. During Dive 84 asphalt covered by bacterial mats was collected. The observation with higher magnification confirmed the presence of giant filamentous sulfide oxidizers. The bacteria seem to be a Thiotrix typ (Fig. 69) and will be further identified in the home laboratory.

Fig. 69: Dive 84- asphalt with bacterial mat (Thiotrix-typ, left), higher magnification of the bacterial mat (middle) and observation with the microscope (right).

15 Biology

(E. Escobar Briones, A. Gaytán)

Introduction

Cold seeps occur worldwide on the continental margins and subduction zones at depths of 400 and 6000 m. These features are characterized by low temperature anomalies ranging 0.1-0.45°C (Nankai; Boulègue *et al*., 1987) and up to 21°C (Barbados mud volcano; Henry *et al*., 1996), in addition to high methane concentrations (1 to 6 times larger than surrounding water, (MacDonald *et al*., 1989). A total of 71 seep regions had been described until 2005 (Sibuet & Olu, 1998; Escobar-Briones, 2005).

Similarity in the composition of taxa has been recognized among the deep Gulf of Mexico, the accretion prism of Barbados and the Brake Ridge suggesting a potential connectivity at bathyal depths. Species that are shared among sites include *Escarpia laminata*, *Nicomache* sp., *Munidopsis* sp., *Chiridota heheva*, *Ophioctenella aries*, and *Ophioctenella acies* (Cordes *et al*., 2007). The species *Bathymodiolus heckerae*, distributed in these sites under the name of *B. boomerang*, has a close similarity with *Bathymodiolus* sp. A from Nigeria, and with *B. azoricus* and *B. puteoserpentis* from MAR (Cordes *et al*., 2007). Their symbionts are practically identical at the 16S rRNA level and share the same bacterial phylotype with the MAR hydrothermal vent species *B. azoricus* and *B. puteoserpentis*. In contrast the symbionts of *B. brooksii* differ to those of *B. childressi* in spite of co-occurring in the Gulf of Mexico. While species composition varies along discrete segments dominant fauna seems to characterize biogeographical provinces, locations and habitats. These reducing ecosystems and their species are constrained defined ephemeral environments showing a high degree of endemism and in some cases phylogeographic relationships with other reducing environments, such as whale falls and hydrothermal vents.

These contrasting observations lead us to suggest that isolation processes coexist with connectivity (both genetic and hydrographic) processes within the Gulf of Mexico and in deep sea locations of the tropical Atlantic. These two processes have most probably defined the regional diversity over evolutionary history. Considering background faunal components (sponges, echinoderms, crustacean, hydrozoan) that are less explored in this region could provide us a better opportunity of how methane seepage from the seafloor supports animal communities.

Objective

The Mexican participation focused on the structure and function of the benthic community of the asphalt volcano describing the diversity at Chapopote Knoll, recognizing the dominant components and evaluating the proportion of endemics. To accomplish these objectives, the approach of studying the diversity considered different levels of complexity, the scale of landscape /habitat (seep, soft bottom and the hard bottom) and the approach of species diversity.

Field work

The samples were collected in the SW sector of the Gulf of Mexico during R/V METEOR M67/2b (Tab. 1) in academic collaboration of the Research Center Ocean Margins (RCOM) of the University of Bremen, Germany and Texas A & M University in the project "*Fluid seepage of Chile and in the Gulf of Mexico*".

Table 18: M67/2b cruise sampling locations. Abbreviations: Multicorer (MUC), Remotely operated vehicle (ROV), Longitude West (Long W), Latitude N (Lat N).

Station	Sampling device	Date	Long W	Lat N	Depth (m)
10606	MUC	05.04.2006	93.4977	21.1497	2296
10612-2	MUC	09.04.2006	93.2592	21.5423	2943
10613-1	MUC, in asphalt	09.04.2006	93.2565	21.5412	2902
10614-1	MUC	10.04.2006	93.2619	21.5397	2897
10617	Dive 81 ROV	11.04.2006	93.2616	21.5391	2919.2
10619	Dive 82 ROV, scavenger traps and push cores	12.04.2006	93.2616	21.5399	2875
10622	Dive 83 ROV	14.04.2006	93.2508	21.5394	2907
10625	Dive 84 ROV, scavenger traps and push cores	15.04.2006	93.2616	21.5391	2916

Photomosaics

In order to characterize the types of habitats and recognize the dominant components within the habitats we considered to study video and still photographs from transects and the sampling locations recorded during the ROV dives. Only a few videos were processed on board and the frames assembled to photomosaics. These provided a preliminary view of the habitat variability and megafauna that characterizes each habitat (Fig. 70).

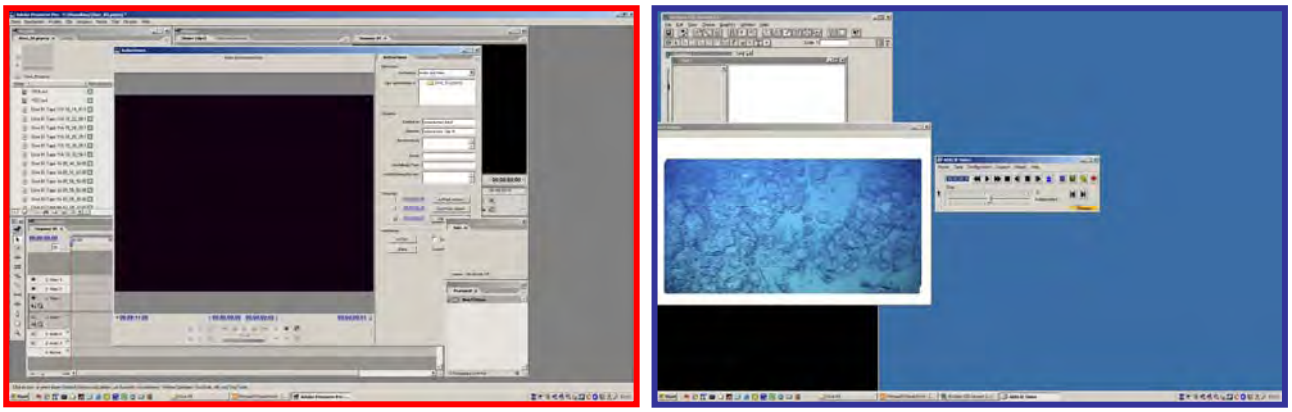

Fig. 70: Strategy used to process the videos into mosaics, edit and assemble the frames.

The mosaics will allow the Biology group to define and delimit habitats and its diversity; it will allow characterizing its complexity and recognizing the dominant megafauna (Fig. 71). The information derived from the mosaics provides basic information to examine the selectivity and preference of occurrence of the dominant megafaunal components.

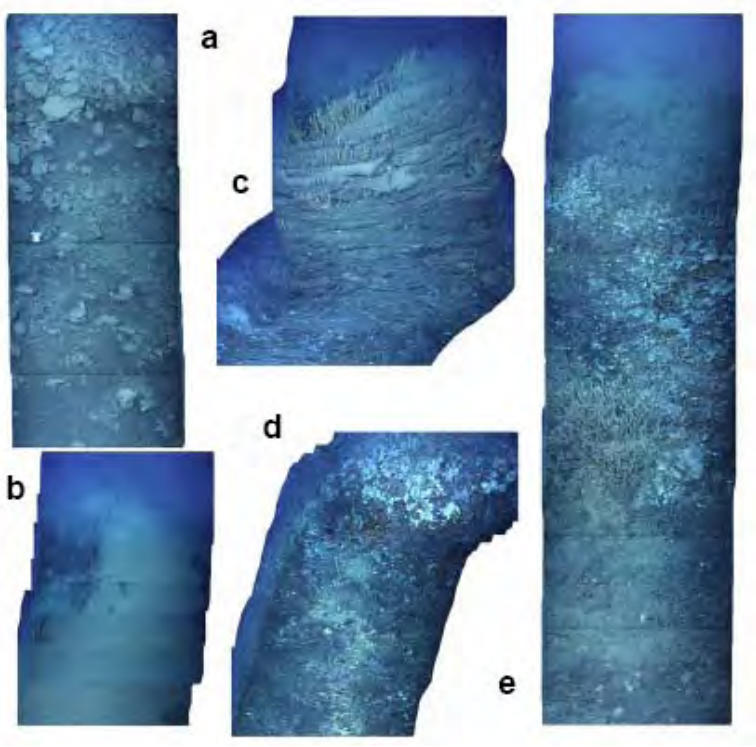

Fig. 71: Examples of habitat diversity recorded from the video processing into photomosaics. **a:** Dive_81 Tape 1A; **b:** Dive_84 Tape 13A; **c:** Dive_81 Tape 2A; **d:** Dive_84 Tape 11A; **e:** Dive_84 Tape 10A.

Collection of megafauna

Megafauna was collected with the ROV Quest by deploying baited traps for scavenger species and for non scavenger fauna and fauna attached to the substrate with the robotic arm and suction device, placed in bins and returned to the surface (Fig. 72). Specimens were photographed upon arrival by keeping them in cold seawater, identified and preserved in most cases with cold 96% ethanol or glutaraldehyde. Specimens collected were shared with other colleagues onboard for different analysis. Tissue and gut samples were extracted from the specimens, before preserving them in ethanol, for geochemical analysis, dried up and where required shared with other colleagues onboard (Appendix 5 for *Munidopsis geyeri*).

Fig. 72: On the left : Scavenger traps deployment in soft sediments. On the right: previous to collection of specimens on the bacterial mat habitat in the asphalt flow.

Processing on board of squat lobsters

Squat lobsters have been considered background fauna in the region and only in some locations these faunal components have been considered typical fauna of reducing/chemosynthetic habitats (i.e. *Munidopsis exuta* Macpherson & Segonzac, 2005). A total of 21 specimens were collected (Appendix 5), photographed, measured and identified onboard as *Munidopsis* cf. *geyeri* (Fig. 73) considering the identification characters described in keys (Pequegnat & Pequegnat, 1970). Specimens were collected both in the soft sediment next to the asphalt flow and on the asphalt flow.

Fig. 73: *Munidopsis geyeri* from the Chapopote location.

Preliminary measurements of characters of taxonomic relevance (Fig. 74) were done onboard and morphological differences were recorded among specimens in characters such as form of rostrum, antennal spine, antennular peduncle, pereiopods, chelipeds and telson (Fig. 75).

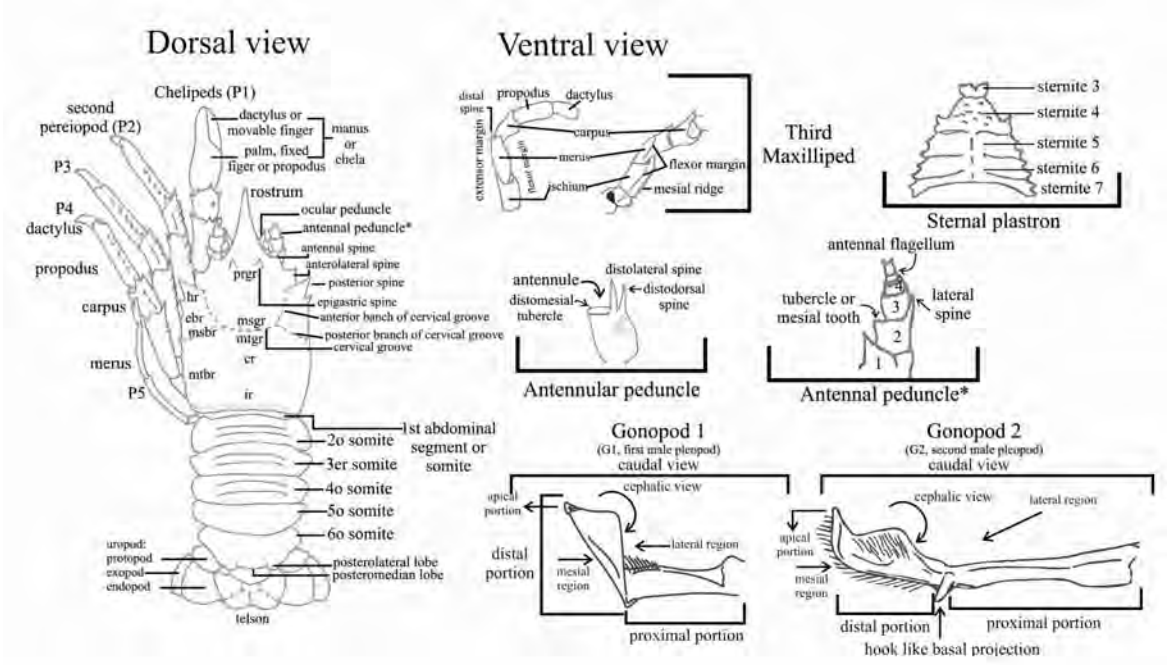

Fig. 74: Characters of taxonomic relevance that were measured in the specimens collected.

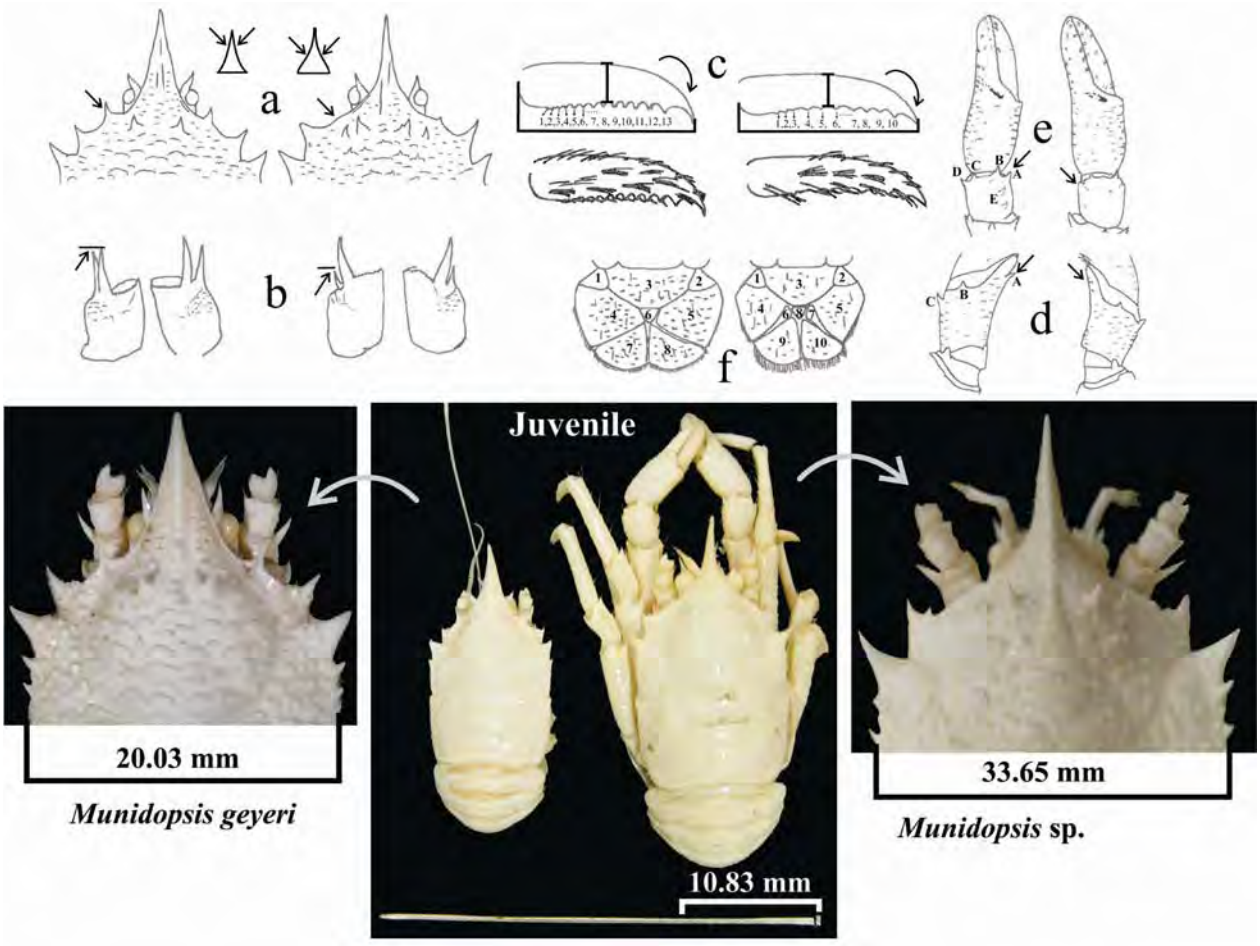

Fig. 75: Main characters that displayed differences among *Munidopsis* specimens from Chapopote Knoll.

Processing on board of holothuroidea

Deep sea cucumber of the genera *Eupentacta, Aslia, Selenkothuria, Psolus, Cucumaria,* use different strategies to feed on the seafloor extracting organic matter, infauna and bacteria from the sediment or hosting bacterial assemblages in mineral nodules in the digestive tract.

Specimens of holothuroidea were collected with the slurp gun, placed in bins and transported to surface. Upon arrival specimens were placed in cold seawater and exposure to light avoided. Specimens were photographed, identified, tissue and gut samples extracted for diet studies using biogeochemical markers and stable isotopes, the rest of the specimen was fixed in 96% ethanol.

The specimens were identified as *Chiridota heheva* through the extraction of spicules in the tentacles. A fraction of tentacle tissue was used for this purpose and eliminated using 18% NaCl. Cones and wheels were observed and measured in at least 10 pieces each (Fig. 76).

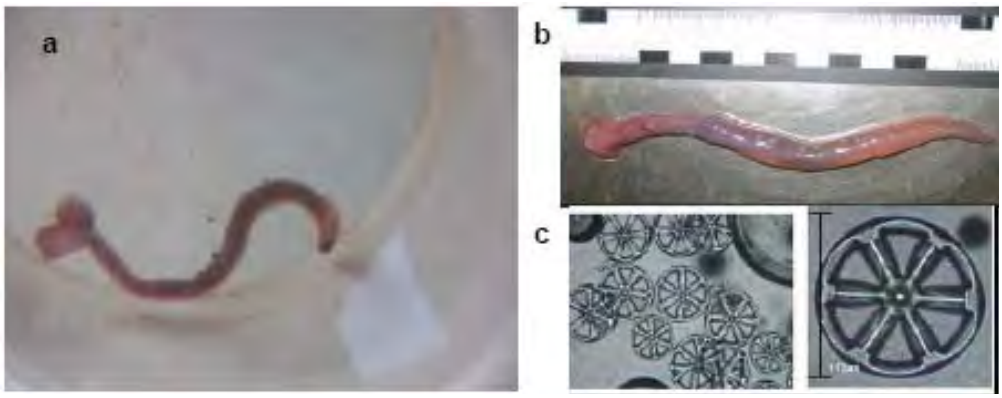

Fig. 76: *Chiridota heheva,* a freshly collected specimen b. specimen processed for the extraction of tissue c. six rays wheels that characterize the genus *Chiridota.*

Chiridota heheva was described by Pawson & Vance (2004) in northern Gulf of Mexico seeps associated to *Bathymodidus sp.* in densities of >60 individuals x5 m^{-2} (Van Dover *et al*., 2000), typical abyssal seafloor off Puerto Rico and in Blake Ridge. Echinoderms are a diversified taxon occurring in seep environments having been described 211 species (Deming & Colwell 1982, Sibuet & Olu, 1998, Goffredia *et. al*., 2004). Echinoderms from both hydrothermal vents and seeps belong to Synaptidae (Juniper & Sibuet, 1987, Desbruyères et al. 2006) and a comparative table of characters is herein included (Tab. 19).

Table 19: Comparison of the *Chiridotas* species found in hydrothermal vents and in methane seeps.

	C. hydrothermica	*C. heheva*
Tentacles		
Number	12	12
Form	lobe	cushion
Processes	fusion	bifurcated
Ring		
Posterior depression	present, deep	present, deep
Dorsal interradial	present	present
Ventral	perforated	without perforation
Dorsal	perforated	split
Spicules		
Form	wheel with 6 rays	wheel with 6 rays
Size	66-202µm	175-177µm
Aggregated in papilae	numerous	numerous
Location	all over	all over
Tentacular spicules		
Form	branched	branched
Longitude	140-250µm	100-202µm
Polianal vesicles	20	20 o more
Ciliar funnels	one	absent
Longitude (mm)	8- 15 cm.	20 cm.
Diameter (mm)	1.3-1.8 cm.	1.5 cm.
Reference	Smirnov *et al.,* 2000	Pawson & Vance 2004

Other taxonomic components collected

Diverse taxa including tubeworms, bivalves, hydroids, peracaridea and caridean crustaceans and sponges (Fig. 77) were collected in hard substrates and habitats. These were shared among colleagues for diverse studies. The relationship of samples of both tubeworms and bivalves is provided in Appendix 6 and 7.

Fig. 77: Other invertebrates collected in rocky substrates at Chapopote Knoll.

Sediment samples

Macrofaunal and meiofaunal samples were obtained from the surficial soft sediment in push core samples retrieved. Additional samples were obtained with the MUC and processed by strata (L1) 0 – 1 cm, (L2) 1.1 – 5 cm, (L3) 5.1 – 10 cm and sieved onboard through 64 and 250 μm mesh size sieves (Fig. 78). Subsamples of each core were frozen to -20°C for elemental composition, $\delta^{13}C$ and $\delta^{15}N$ stable isotopic characterization and grain size. The fate of the cores collected is described in Appendix 8.

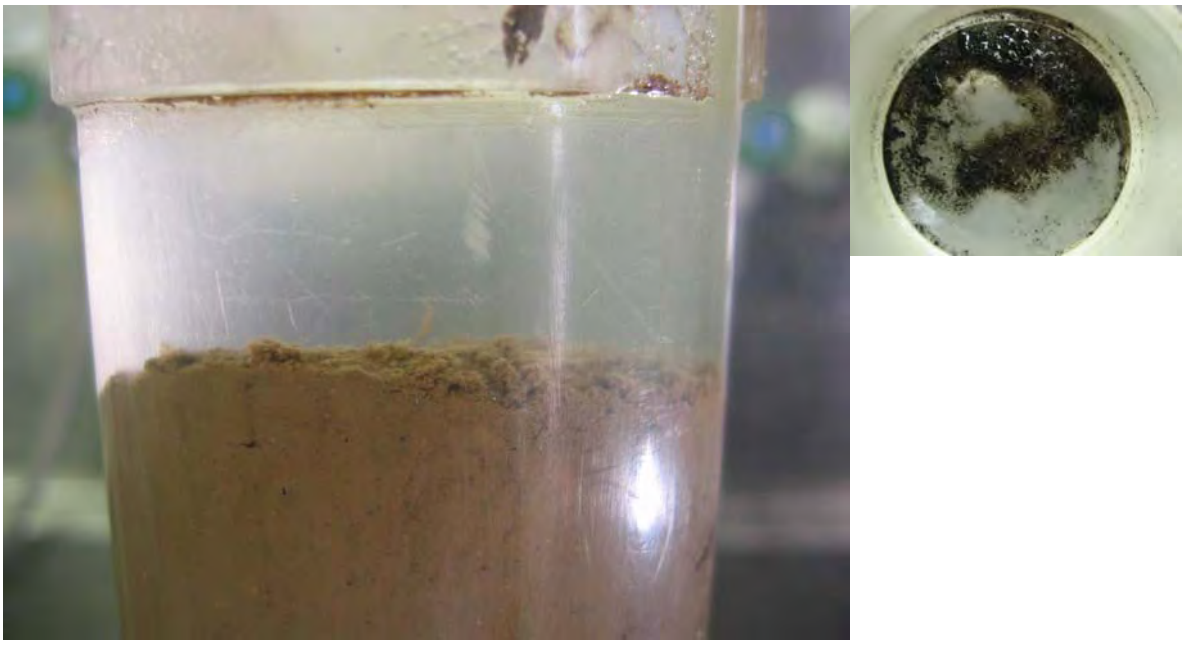

Fig. 78: MUC from a soft sediment habitat in the Chapopote area. Smaller frame shows the sieved sediment from the same sample.

General observations

It is interesting to mention the great regional similarity of the Chapopote chemosynthetic assemblage with hydrothermal vent assemblages where caridean shrimp, Bathymodiolid mussels, and clams dominate in the South Mid-Atlantic Ridge, Caridean shrimp - mainly *Rimicaris exoculat* - and bathymodiolid mussels characterize the Mid-Atlantic Ridge assemblage between Azores Triple Junction and Equator (deep north Atlantic between 2500-3650 m) and Bathymodiolid mussels, amphipods, and caridean shrimp typical of the Azores (shallow north Atlantic between 800-1700 m depth). This relation can be attributed to the palaeographic evolution of the Gulf of Mexico and Caribbean Sea.

16 References

Biddle JF, Lipp JS, Lever M, Lloyd K, Sørensen K, Anderson R, Fredricks HF, Elvert M, Kelly TJ, Schrag D.P., Sogin M.L., Brenchley J.E., Teske A., House C.H., Hinrichs K.-U. (2006) Novel heterotrophic Archaea dominate sedimentary subsurface ecosystems off Peru. Proc. Natl. Acad. Sci. U.S.A., 103, 3846-3851.

Bohrmann G, Schenck S (2004) GEOMAR Cruise Report SO 174, OTEGA II, RV "SONNE". GEOMAR Report 117, Kiel.

Boulègue J, Iiyama JT, Charlou JL, Jedwab J (1987) Nankai Trough, Japan Trench and Kuril Trench: Geochemistry of fluids sampled by submersible « Nautile ». Earth and Planetary Science Letters 83, 363-375.

Cordes EE, Carney SL, Hourdez S, Carney RS, Brooks JM, Fisher CR (2007) Cold seeps of the Gulf of Mexico: Community structure and biogeographic comparisons to Atlantic equatorial belt seep communities. Deep-Sea Research I, 637-653.

de Beer D, Sauter E, Niemann H, Witte U & Boetius A (2006) In situ fluxes and zonation of microbial activity in surface sediments of the Håkon Mosby Mud Volcano. Limnology and Oceanography 51(3): 1315-1331.

Deming JW & Colwell RR (1982) Barophilic bacteria associated with digestive tracts of abyssal holothurians applied and environmental microbiology 44(5):1222-1230.

Desbruyères D, Segonzac M, Bright M (2006) Handbook of deep-sea hydrothermal vent fauna. DENISIA 18, 544pp.

Ding F, Spiess V, Brüning M, Fekete N, Keil H, Bohrmann G (2008) A conceptual model for hydrocarbon accumulation and seepage processes around Chapopote asphalt volcanism site, southern Gulf of Mexico: from a high resolution seismic point of view. J. Geophys. Res., 113, B08404, doi:10.1029/2007JB005484.

Ding F, Spiess V, MacDonald I, Brüning M, Fekete N, Bohrmann G (submitted 11 Aug 2008) Shallow sediment deformation styles in north-western Campeche Knolls, Gulf of Mexico and their controls on the occurrence of hydrocaebon seepage. Marine and Petroleum Geology.

Escobar-Briones E (2005) Energía y mar. Ciencia y Desarrollo. Diciembre, 24-27.

Garbe-Schönberg D, Koschinsky A, Ratmeyer V, Jähmlich H, Westernströer U (2006) KIPS – A new multiport valve-based all-teflon fluid sampling system for ROVs. Abstract. EGU General Assembly in Vienna, Austria.

Goffredia SK, Paull CK, Fulton-Bennett K, Hurtadob LA, Vrijenhoek RC (2004) Unusual benthic fauna associated with a whale fall in Monterey Canyon, California. Deep-Sea Res. I 51: 1295–1306.

Henry P, Le Pichon X, Lallemant S, Lance S, Martin JB, Foucher JP, Fiala-Médioni A, Rostek F, Guilhaumou N, Pranal V, Castrec M (1996) Fluid flow in and around a mud volcano field seaward of the Barbados accretionary wedge: Results from Manon cruise. Journal of Geophysical Research 101, 297-323.

Heuer V, Elvert M, Tille S, Krummen M, Prieto Mollar X, Hmelo LR, Hinrichs K-U (2006) Online $\delta^{13}C$ analysis of volatile fatty acids in sediment/porewater systems by liquid chromatography-isotope ratio-mass spectrometry. Limn. Oceanogr. Meth., 4, 346-357.

Hinrichs K-U, Summons RE, Orphan V, Sylva SP & Hayes JM (2000) Molecular and isotopic analyses of anaerobic methane-oxidizing communities in marine sediments. Org. Geochem., 31, 1685-1701.

Hovland M, MacDonald IR, Rueslåtten H, Johnsen HK, Naehr T and Bohrmann G (2005) Chapopote asphalt volcano, may have been generated by supercritical water. EOS 86 (42): 397-402.

Joye SB, Boetius A, Orcutt BN, Montoya JP, Schulz HN, Erickson MJ and Lugo SK (2004) The anaerobic oxidation of methane and sulfate reduction in sediments from Gulf of Mexico cold seeps. Chem. Geol., 205(3/4): 219-238.

Juniper SK & Sibuet M (1987) Cold seep benthic communities in Japan subduction zones: Spatial organization, trophic strategies and evidence for temporal evolution. Marine Ecology Progress Series 40:115-126.

Klapp SA, Bohrmann G, Kuhs WF, Murshed MM, Heeschen KU, Pape T, Klein H, Techmer K, Abegg F (submitted Dez 2008) Electron-microscopic and X-ray inspection of structure-I and structure-II gas hydrates from the Gulf of Mexico. Marine and Petroleum Geology.

MacDonald IR, Boland GS, Baker JS, Brooks JM, Kennicutt MC II, Bidigare RR (1989) Gulf of Mexico hydrocarbon seep communities. II. Spatial distribution of seep organisms and hydrocarbons at Bush Hill. Marine Biology 101:235-247.

MacDonald IR, Bohrmann G, Escobar E, Abegg F, Blanchon P, Blinova V, Brückmann W, Drews M, Eisenhauer A, Han X, Heeschen K, Meier F, Mortera C, Naehr T, Orcutt B, Bernard B, Brooks J, de Faragó M, (2004) Ashalt volcanism and chemosynthetic life in the Campache Knolls, Gulf of Mexico, Science 304, 999-1002.

Macpherson E, Segonzac M (2005) Species of genus Munidopsis (Crustacea, Decapoda, Galatheidae) from the deep Atlantic Ocean, including cold-seep and hydrothermal vent areas. Zootaxa 1094, 1-60.

Orcutt B, Joye SB, Boetius A, Elvert M, Samarkin V (2005) Molecular biogeochemistry of sulfate reduction, methanogenesis and the anaerobic oxidation of methane at Gulf of Mexico cold seeps. Geochimica et Cosmochimica Acta, 69, 4267-4281.

ODP Leg 201 Shipboard Scientific Party. Explanatory Notes (2003) *In* S.L. D'Hondt, B.B.Jørgensen, D.J. Miller et al., Proc. ODP, Init. Repts., 201 [Online]. http://www-odp.tamu.edu/publications/201_IR/chap_05/chap_05.htm.

Pawson DL & Vance DJ (2004) Chiridota heheva, new species, from Western Atlantic deep-sea cold seeps and anthropogenic habitats (Echinodermata: Holothuroidea: Apodida). Zootaxa 534: 1-12.

Pequegnat LH, Pequegnat WE (1970) Deep-sea anomurans of the subfamily Galatheoidea with description of three new species. In: Contributions on the Biology of the Gulf of Mexico. Texas A&M University of Oceanographic Studies 1, 125-170.

Shepard FP (1963) Submarine Geology. Harper & Row, New York.

Sibuet M, Olu K (1998) Biogeography, biodiversity and fluid dependence of deep-sea cold-seep communities at active and passive margins. Deep-Sea Research II 45, 517-567.

Smirnov AV, Gebruk AV, Galkin SV, Shank T (2000) New species of holothurian (Echinodermata: Holothuroidea) from hydrothermal vent habitats. Journal of the Marine Biological Association of the UK 80:321-328.

Spieß V (1993) Digitale Sedimentographie, Neue Wege zu einer hochauflösenden Akustostratigraphie, FB Geowissenschaften, Universität Bremen, 199 pages.

Sturt HF, Summons RE, Smith KJ, Elvert M, and Hinrichs KU (2004) Intact polar membrane lipids in prokaryotes and sediments deciphered by ESI-HPLC-MS^n – new biomarkers for biogeochemistry and microbial ecology. Rap. Commun. Mass Spectr., 18, 617-628.

Van Dover CL, German CR, Speer KG, Parson LM, Vrijenhoek R (2002) Evolution and biogeography of the deep-sea invertebrates. Science 295(5558), 1252-1257.

Weinrebe W et al. (2006) R/V METEOR Cruise Report M67/1, Chile-Margin-Survey, Talcahuano (Chile) – Balboa (Panama), February 20 – March 13, 2006, IFM-GEOMAR Report No. 7: 80 pages.

Wenzhöfer F, Holby O, Glud RN, Nielsen HK, Gundersen JK (2000) In situ microsensor studies of a shallow water hydrothermal vent at Milos, Greece. Marine Chemistry 69, 43-54.

Wenzhöfer F, Glud RN (2002) Benthic carbon mineralization in the Atlantic: A synthesis based on in situ data from the last decade. Deep-Sea Research I 49(7), 1255-1279.

Appendix 1: Station List

R/V METEOR Cruise M67/2													
							Begin / on seafloor			End / off seafloor			
Date	St. No.	St. No.			Start Sci:	End Sci:	Latitude	Longitude	Water	Latitude	Longitude	Water	Recovery
	GeoB		Instruments	Location	Program	Program	N°	E°	Depth (m)	N°	E°	Depth (m)	Remarks
M67/2a													
20.3	10601	CTD-1	CTD/Ro		11:58	14:19	22°08.118	92°44.782	3327	---	---	---	21 samples
21.3	10602-1	CTD-2	CTD/Ro	Chapopote	13:12	14:19	21°53.99	93°26.25	2906	---	---	---	22 samples
21.3	10602-2	SL-1	G	Chapopote	16:05	16:57	21°54.01	93°26.24	2884	---	---	---	6m Liner
23.3	10603-1	CTD-3	CTD/Ro		14:51	15:47	20°51.384	94°01.108	2456	---	---	---	22 samples
23.3	10604-1	CTD-4	CTD/Ro		22:14	22:52	19°57.373	94°00.845	1346	---	---	---	22 samples
26.3		06-086	Seismic		00:59	05:14	20°22,62	93°48,58	1884	20°21,21'	94°01,98'	2027	
26.3		06-087	Seismic		05:14	08:54	20°21,21	94°01,98	2027	20°12,21'	93°47,19'	1853	
26.3		06-088	Seismic		08:54	11:24	20°12,21	93°47,19	1853	20°07,42'	93°57,84'	1658	
26.3		06-089	Seismic		11:24	14:48	20°07,42	93°57,84	1658	19°52,44'	93°57,94'	1733	
26.3		06-090	Seismic		14:48	16:41	19°52,44	93°57,94	1733	19°45,20'	93°55,06'	1723	
26.3		06-091	Seismic		16:41	17:20	19°45,20	93°55,06	1723	19°46,91'	93°52,43'	1511	
26.3		06-092	Seismic		17:20	18:43	19°46,91	93°52,43	1511	19°53,29'	93°54,69'	1478	
26.3		06-093	Seismic		18:43	19:02	19°53,29	93°54,69	1478	19°53,85'	93°56,12'	1385	
26.3		06-094	Seismic		19:02	21:24	19°53,85	93°56,12	1385	20°04,57'	93°56,57'	1371	
26.3		06-095	Seismic		21:24	22:41	20°04,57	93°56,57	1371	20°06,78'	93°51,63'	1390	
27.3		06-096	Seismic		07:12	08:51	21°04,58	93°56,56	2838	21°07,67'	93°49,50'	2926	
27.3		06-097	Seismic		08:58	10:35	21°08.05	93°49,63	2977	21°13,70'	93°55,71'	3219	
27.3		06-098	Seismic		10:35	11:07	21°13,70	93°55,71	3219	21°15,15'	93°53,64'	3205	
27.3		06-099	Seismic		11:07	12:30	21°15,15	93°53,64	3205	21°11,57'	93°48,34'	3129	
27.3		06-100	Seismic		12:30	13:00	21°11,57	93°48,34	3129	21°13,35'	93°46,57'	3204	
27.3		06-101	Seismic		13:00	14:19	21°13,35	93°46,57	3204	21°18,02'	93°51,61'	3187	
27.3		06-102	Seismic		14:23	14:41	21°18,09	93°51,83	3187	21°17,28'	93°52,71'	3234	
27.3		06-103	Seismic		14:45	16:18	21°17,00	93°52,79	3234	21°12,53'	93°47,68'	3181	
27.3		06-104	Seismic		16:21	18:41	21°12,36	93°47,92	3181	21°10,65'	93°58,86'	3090	
27.3		06-105	Seismic		20:50	03:33	21°07,59	93°56,93	2231	21°13,91'	93°56,82'	3209	
28.3		06-106	Seismic		03:33	04:30	21°13,91	93°56,82	3209	21°16,35'	93°53,70'	3224	
28.3		06-107	Seismic		04:30	06:09	21°16,35	93°53,70	3224	21°12,06'	93°48,17'	3144	
28.3		06-108	Seismic		06:14	06:32	21°12,06	93°47,85	3144	21°13,21'	93°47,27'	3194	
28.3		06-109	Seismic		06:35	07:50	21°13,21	93°47,27	3194	21°17,50'	93°52,09'	3204	
28.3		06-110	Seismic		07:55	11:12	21°17,51	93°52,10	3204	21°24,86'	93°40,53'	3228	
28.3		06-111	Seismic		11:12	14:49	21°24,86	93°40,53	3228	21°27,86'	93°28,00'	3148	
28.3	10605-1	CTD-5	CTD/Ro		18:47	19:46	21°28.23	93°25.26	2760	---	---	---	22 samples
28.3	10605-2	SL-2	G		20:50	21:32	21°28.21	93°25.23	2785	---	---	---	6m Liner
29.3		06-112	Seismic		03:27	08:35	21°41,30	93°26,22	3276	21°56,48'	93°26,33'	3329	
29.3		06-113	Seismic		11:10	14:58	22°04,40	93°27,14	3329	21°41,56'	93°24,65'	3273	
29.3		06-114	Seismic		14:58	16:27	21°41,56	93°24,65	3273	21°48,01'	93°21,25'	3335	
29.3		06-115	Seismic		16:27	18:52	21°48,01	93°21,25	3335	21°55,52'	93°31,51'	3332	
29.3		06-116	Seismic		19:12	23:28	21°56,46	93°30,60	3338	21°56,13'	93°30,92'	3335	
29.3		06-117	Seismic		23:28	00:29	21°56,13	93°30,92	3335	21°55,84'	93°27,57'	3335	
30.3		06-118	Seismic		00:29	01:36	21°55,84	93°27,57	3335	21°52,13'	93°22,33'	3353	
30.3		06-119	Seismic		01:38	04:52	21°52,12	93°22,19	3353	21°57.38'	93°03.95'	3300	
30.3		06-120	Seismic		04:52	05:48	21°57,38	93°03,95	3300	21°58,76'	93°08,63'	3336	
30.3		06-121	Seismic		05:56	07:04	21°58,30	93°08,76	3303	21°52,31'	93°06,21'	3232	
30.3		06-122	Seismic		07:10	07:50	21°52,34	93°05,93	3223	21°55,99'	93°04,31'	3288	
30.3		06-123	Seismic		07:54	08:52	21°56,09	93°04,72	3278	21°54,84'	93°10,82'	3350	
30.3		06-124	Seismic		08:52	10:53	21°54,84	93°10,82	3350	21°55,45'	93°23,69'	3339	
30.3		06-125	Seismic		10:53	12:08	21°55,45	93°23,69	3339	21°52,30'	93°29,97'	3125	
30.3		06-126	Seismic		12:08	13:04	21°52,30	93°29,97	3125	21°51,72'	93°24,66'	3344	
30.3		06-127	Seismic		13:05	14:05	21°51,85	93°24,72	3343	21°54.76'	93°23.06'	3308	
30.3	10605-3	CTD-6	CTD/Ro		17:05	17:22	21°57.54	93°55.12	3544	21°57.45	93°55.08	3444	18 ws; 250 m
M67/2b													
5.4	10606	TV-MUC-1	TV-MUC	Oil Ridge	11:14	12:35	21°14,97	93°49,77	2296	---	---	---	without TV
6.4	10607	SL-3	G	Chapopote	19:00	20:45	21°53,99	93°26,25	2911	---	---	---	bag, 360 cm
6.4	10608	SL-4	G	"	21:36	23:20	21°53,90	93°26,35	2897	---	---	---	bag
6.4	10609	SL-5	G	"	23:50	01:25	21°53,97	93°26,32	2900	---	---	---	bag
7.4	10610	SL-6	G	"	01:58		21°54,25	93°25,88	2964	---	---	---	bag, CC
9.4	10611	TV-S-1	TV-S	Knoll 2139	04:48	08:00	21°38.055	93°26.754	3027	21°39.926	93°26.131	2960	
9.4	10612-1	SL-7	G	Chapopote	15:40	16:31	21°54.23	93°25.91	2926	---	---	---	
9.4	10612-2	TV-MUC-2	TV-MUC	"	17:50	18:55	21°54.230	93°25.927	2943	---	---	---	without TV
9.4	10613	TV-MUC-3	TV-MUC	"	22:02	00:17	21°54.12	93°25.65	2902	21°54.322	93°25.644	2804	
10.4	10614	TV-MUC-4	TV-MUC	"	03:35	04:33	21°53.978	93°26.190	2891	21°53.980	93°26.223	2897	
10.4	10615	Dive 80	ROV	"	17:41	18:45	21°53.920	93°26.152	2840	21°53.917	93°26.146	2904	> 1 hr
10.4	10616	TV-MUC-5	TV-MUC	"	22:51	01:18	21°53.92	93°26.17	2897	21°54.10	93°26.27	2872	no sample
11.4	10617	Dive 81	ROV	"	05:12	16:08	21°53.942	93°26.131	2913	21°53.949	93°26.238	2910	
11.4	10618	SL-6	G	"	21:08	23:05	21°53.95	93°26.21	2903	---	---	---	
12.4	10619	Dive 82	ROV	"	15:50	07:56	21°54.333	93°26.497	2880	21°53.926	93°26.049	2925	> 16 hr
13.4	10620	TV-S-2	TV-S	"	11:43	14:20	21°54.15	93°26.153	2893	21°55.024	93°26.783	2908	
13.4	10621	TV-S-3	TV-S	"	16:56	19:40	21°54.12	93°26.14	2882	21°54.545	93°26.058	2950	
14.4	10622	Dive 83	ROV	"	23:41	11:03	21°53.949	93°26.249	2915	21°53.927	93°26.147	2923	>11 hr
14.4	10623-1	SL-7	G	"	14:03	14:50	21°53.959	93°26.223	2882	---	---	---	3 m
14.4	10623-2	SL-8	G	"	14:50	15:39	21°53.959	93°26.223	2895	---	---	---	3 m
14.4	10624-1	SL-9	G	"	18:47	19:44	21°53.986	93°26.126	2922	---	---	---	3 m
14.4	10624-2	SL-10	G	"	20:58	21:52	21°53.99	93°26.15	2923	---	---	---	3 m
15.4	10625	Dive 84	ROV	"	01:59	20:04	21°53.380	93°26.131	2935	21°53.690	93°26.131	2922	>18 hr
16.4	10626	SL-11	G	"	00:30	01:24	21°53.99	93°26.13	2914	---	---	---	3 m, CC

Abbreviation

G	Gravity corer	**TV-MUC**	TV-multicorer
TV-S	TV sled	**ROV**	Remotely operated vehicle QUEST
CTD/Ro	CTD and rosette		

Appendix 2: Streamer configurations during M67/2a

-GeoB06-086 to 095

Streamer Sections	Acquisition	Distance from the ship (m)	Bird	Position of bird (m)
Stretch	**Stretch**	25 (4)	Digi 5	**72**
Active 1	**Recorded 1**	75	Digi 6	**122**
Active 2	**Recorded 2**	125	Digi 11	**172**
Active 3	**Recorded 3**	175	*(skipped)*	222
Active 4	**Recorded 4**	225	Digi 12	**272**
Active 5	**Recorded 5**	275	*(skipped)*	322
Active 6	**Recorded 6**	325	Digi 13	**372**
Active 7	**Recorded 7**	375	*(skipped)*	422
Active 8	**Recorded 8**	425	Digi 14	**472**
Active 9	**Not Recorded**	475	*(skipped)*	522
Active 10	**Not Recorded**	525	Digi 15	**572**

-GeoB06-096 to 111 and GeoB06-113 to 127

Streamer Sections	Acquisition	Distance from the ship (m)	Bird	Position of bird (m)
Stretch	**Stretch**	25 (4)	Digi 5	**72**
Active 1	**Recorded 1**	75	Digi 6	**122**
Active 2	**Recorded 2**	125	Digi 11	**172**
Active 3	**Recorded 3**	175	*(skipped)*	222
Active 4	**Recorded 4**	225	Digi 12	**272**
Active 5	**Recorded 5**	275	*(skipped)*	322
Active 6	**Recorded 6**	325	Digi 13	**372**
Active 7	**Recorded 7**	375	*(skipped)*	422
Active 8	**Recorded 8**	425	Digi 14	**472**
Active 9	**Not Recorded**	475	*(skipped)*	522
Active 10	**Not Recorded**	525	Digi 15	**572**
Active 11	**Not Recorded**	575	*(skipped)*	622
Active 12	**Not Recorded**	625	*(skipped)*	672

-GeoB06-112

Streamer Sections	Acquisition	Distance from the ship (m)	Bird	Position of bird (m)
Stretch	**On Winch 1**			
Active 1	**On Winch 2**			
Active 2	**On Winch 3**			
Active 3	**On Winch 4**			
Active 4	**On Winch 5**			
Active 5	**On Winch 6**			
Active 6	**On Winch 7**			
Active 7	**On Winch 8**			
Active 8	**On Winch 9**			
Active 9	**Not Recorded**	5	*(skipped)*	52
Active 10	**Recorded 1**	55	Digi 14	**102**
Active 11	**Recorded 2**	105	*(skipped)*	152
Active 12	**Recorded 3**	155	Digi 15	**202**

Appendix 3: Delay times

a. Delay scheme when 4.1 L GI gun was shooting alone

Water depth (m)	Cycle length (ms)	MaMuCS Delay (ms)	Rec. Length (ms)
3750	10000	5000	5000
3375	9500	4500	5000
3000	9000	4000	5000
2625	8500	3500	5000
2250	8000	3000	5000
1875	7500	2500	5000
1500	7000	2000	5000

b. Delay scheme for one GI and one watergun shot

Waterdepth (m)	Watergun delay (ms)	GI gun delay (ms)	MaMuCS delay (ms)	Total step length (ms)	Rec Length (ms)
3375	0	1500	4500	11000	6500
3000	0	1500	4000	10500	6500
2625	0	1500	3500	10000	6500
2250	0	1500	3000	9500	6500
1875	0	1500	2500	9000	6500

c. Delay scheme for one GI and several watergun shots (i.e. as many of the latter during one trigger period as allowed by the water depth).

			Recording Step 1			Recording Step 2		Recording Step 3			
Depth (m)	Delay segments	Delay (ms)	Length of step 1	Digi Bird	Water gun shot 1	Length of step 2	Water gun shot 2	Length of step 3	Water gun shot 3	GI	Mamucs
750	2	1000	1000	0	0	-	-	5700	-	200	0
1125	2	1500	1500	0	0	-	-	5500	-	0	0
1500	2	2000	1500	0	0	-	-	6000	-	0	500
1875	2	2500	1500	0	0	-	-	6500	-	0	1000
2250	3	3000	1500	0	0	1500	0	7000	-	0	0
2625	3	3500	1500	0	0	1500	0	7500	-	0	500
3000	3	4000	1500	0	0	1500	0	8000	-	0	1000
3375	3	4500	1500	0	0	1500	0	10000	0	1500	1500
3750	3	5000	1500	0	0	1500	0	10500	0	1500	2000

Appendix 4: Seismic Profile List

M672a Seismic Profile list - Profile starting and ending point without major turning

	Start of the Profile					End of the Profile				
Profile	Date	time	Lat*	Long	MaMuCS FFN	Date	time	Lat	Long	MaMuCS FFN
GeoB06-086	26.03.06	00:59:42	20°22.63'N	93°48.51'W	1109	26.03.06	03:59:05	20°21.03'N	94°02.82'W	2428
GeoB06-087	26.03.06	04:54:28	20°21.86'N	94°03.60'W	2837	26.03.06	08:44:58	20°12.85'N	93°47.57'W	4747
GeoB06-088	26.03.06	09:14:50	20°11.53'N	93°48.37'W	5003	26.03.06	11:12:28	20°07.87'N	93°57.15'W	6018
GeoB06-089	26.03.06	11:28:06	20°07.19'N	93°57.84'W	6152	26.03.06	14:49:05	19°52.43'N	93°57.94'W	7880
GeoB06-090	26.03.06	15:05:20	19°51.41'N	93°57.59'W	8010	26.03.06	16:36:14	19°45.32'N	93°55.36'W	8780
GeoB06-091	26.03.06	16:43:18	19°45.26'N	93°54.96'W	16	26.03.06	17:13:07	19°46.36'N	93°52.59'W	261
GeoB06-092	26.03.06	17:20:10	19°46.88'N	93°52.42'W	319	26.03.06	18:42:39	19°53.24'N	93°54.67'W	1026
GeoB06-093	26.03.06	18:48:50	19°53.52'N	93°55.04'W	1079	26.03.06	19:02:36	19°53.86'N	93°56.10'W	1197
GeoB06-094	26.03.06	19:10:32	19°54.28'N	93°56.38'W	1265	26.03.06	21:26:07	20°04.66'N	93°56.58'W	2477
GeoB06-095	26.03.06	21:32:36	20°04.99'N	93°56.39'W	2535	26.03.06	22:36:09	20°06.62'N	93°51.97'W	3104
GeoB06-096	27.03.06	07:12:44	21°04.57'N	93°56.59'W	19	27.03.06	08:51:47	21°07.66'N	93°49.55'W	717
GeoB06-097 (Note 1)	27.03.06	08:58:11	21°08.05'N	93°49.59'W	765	27.03.06	09:15:40	21°09.05'N	93°50.73'W	880
GeoB06-098	27.03.06	10:41:28	21°14.01'N	93°55.45'W	510	27.03.06	11:03:34	21°15.13'N	93°53.94'W	642
GeoB06-099	27.03.06	11:08:39	21°15.12'N	93°53.62'W	671	27.03.06	12:26:50	21°11.54'N	93°48.65'W	1157
GeoB06-100	27.03.06	12:32:47	21°11.69'N	93°48.22'W	1191	27.03.06	12:58:51	21°13.24'N	93°46.62'W	1340
GeoB06-101	27.03.06	13:05:30	21°13.71'N	93°46.88'W	1378	27.03.06	14:19:28	21°17.97'N	93°51.54'W	1848
GeoB06-102	27.03.06	14:25:42	21°18.03'N	93°51.97'W	1882	27.03.06	14:41:39	21°17.29'N	93°52.70'W	1969
GeoB06-103	27.03.06	14:49:21	21°16.85'N	93°52.66'W	2011	27.03.06	16:18:30	21°12.55'N	93°47.71'W	2522
GeoB06-104	27.03.06	16:27:29	21°12.15'N	93°48.15'W	2571	27.03.06	18:41:28	21°10.65'N	93°58.81'W	3351
GeoB06-105	28.03.06	01:48:27	21°08.58'N	93°51.53'W	2	28.03.06	03:23:47	21°13.40'N	93°56.86'W	786
GeoB06-106	28.03.06	03:35:40	21°13.97'N	93°56.74'W	881	28.03.06	04:12:20	21°15.64'N	93°54.64'W	1174
GeoB06-107	28.03.06	04:39:11	21°16.07'N	93°53.29'W	1389	28.03.06	06:10:26	21°12.03'N	93°48.14'W	2147
GeoB06-108	28.03.06	06:37:19	21°13.32'N	93°47.48'W	2362	28.03.06	07:45:11	21°17.46'N	93°52.03'W	2938
GeoB06-109 (Note 2)	28.03.06					28.03.06				
GeoB06-110 (Note 3)	28.03.06	07:54:37	21°17.94'N	93°51.92'W	3018	28.03.06	09:38:20	21°21.63'N	93°45.87'W	3809
GeoB06-111	28.03.06	11:17:41	21°24.94'N	93°40.26'W	388	28.03.06	14:48:45	21°27.85'N	93°28.04'W	2024
GeoB06-112	29.03.06	03:22:07	21°41.02'N	93°26.21'W	1	29.03.06	08:34:40	21°56.45'N	93°26.34'W	2418

Continuation Appendix 4

GeoB06-113	29.03.06	11:04:01	22°00.80'N	93°27.13'W	1	29.03.06	14:56:53	21°41.66'N	93.24.67'W	1586
GeoB06-114	29.03.06	15:22:15	21°43.08'N	93°23.81'W	1755	29.03.06	16:22:12	21°47.60'N	93°21.15'W	2168
GeoB06-115	29.03.06	16:28:39	21°48.10'N	93°21.33'W	2211	29.03.06	18:51:51	21°55.44'N	93°31.38'W	3175
GeoB06-116	29.03.06	19:28:19	21°56.19'N	93°29.76'W	3418	29.03.06	21:04:19	21°51.56'N	93°23.08'W	4073
GeoB06-117 (Note 4)	29.03.06	21:28:14	21°51.10'N	93°23.80'W		29.03.06	23:26:44	21°55.99'N	93°30.80'W	
GeoB06-118 (Note 5)	30.03.06	00:04:32	21°57.09'N	93°29.42'W	1071	30.03.06	01:34:44	21°52.22'N	93°22.50'W	1587
GeoB06-119	30.03.06	01:39:02	21°52.13'N	93°22.11'W	1611	30.03.06	04:51:47	21°57.34'N	93°04.04'W	2735
GeoB06-120	30.03.06	05:04:34	21°57.93'N	93°04.51'W	2808	30.03.06	05:47:37	21°58.75'N	93°08.58'W	3054
GeoB06-121	30.03.06	05:58:07	21°58.28'N	93°08.74'W	3114	30.03.06	07:04:04	21°52.41'N	93°06.24'W	3503
GeoB06-122	30.03.06	07:11:56	21°52.55'N	93°05.89'W	3548	30.03.06	07:49:34	21°55.90'N	93°04.33'W	3763
GeoB06-123	30.03.06	07:54:49	21°56.09'N	93°04.71'W	3793	30.03.06	08:46:29	21°54.91'N	93°10.05'W	4094
GeoB06-124	30.03.06	08:55:04	21°54.85'N	93°10.96'W	4143	30.03.06	10:51:28	21°55.46'N	93°23.49'W	4827
GeoB06-125	30.03.06	10:58:50	21°55.28'N	93°24.15'W	4869	30.03.06	12:05:06	21°52.45'N	93°29.88'W	5258
GeoB06-126	30.03.06	12:20:06	21°52.17'N	93°28.89'W	5342	30.03.06	13:02:46	21°51.65'N	93°24.78'W	5581
GeoB06-127	30.03.06	13:07:13	21°51.92'N	93°24.82'W	5606	30.03.06	14:07:06	21°54.80'N	93.29.14'W	5954

* the latitude and longitude positions means the ship DGPS position at the given time.

Note 1: MaMuCS broke down at shot 880 and restarted ~ 5 min later with FFN of 1. For all the shots recorded thereafter, a constant 910 is added in the FFN, during the processing. **The start and end point in the profile list is only the first part of the profile. The second part is recorded in the following table.**

Start of the Profile (GeoB06-097, Second Part)					End of the Profile (GeoB06-097, Second Part)				
Date	time	Lat	Long	MaMuCS FFN	Date	time	Lat	Long	MaMuCS FFN
27.03.06	09:21:11	21°09.367'N	93°51.088'W	1	27.03.06	10:32:46	21°13.496'N	93°55.639'W	466

Note 2: Profile recorded with this name is added to Profile GeoB06-108 in the later processing.

Note 3: MaMuCS broke down at shot 3809, and restarted with FFN of 11but broke down again at shot 131. It restarted again with FFN of 40. For all shots recorded between 3809 and 131, their FFN are added by a constant of 3870, For all shots afterwards, their FFN are added by a constant of 4001, during the processing. **The start and end point in the profile list is only the first part of the profile. The second part is recorded in the following table.**

Start of the Profile (GeoB06-110, Second and third Part)					End of the Profile (GeoB06-110, Second and third Part)				
Date	time	Lat	Long	MaMuCS FFN	Date	time	Lat	Long	MaMuCS FFN
28.03.06	09:59:06	21°22.370'N	93°44.681'W	11	28.03.06	10:14:29	21.22.885'N	93°43.826'W	131
28.03.06	10:32:09	21°23.474'N	93°42.863'W	40	28.03.06	11:12:39	21°24.845'N	93°40.562'W	351

Note 4: 4.1L GI generator could not shoot from time to time, 0.7L GI was in water for a short time while the 4.1L GI was on the deck being repaired.

Note 5: The shot 1071 to 1214 is not stored in the sgy file for 118 in the raw data set. It is in the file for 117 instead.

Appendix 5

Species *Munidopsis gereyi*

ID numbers for the guts extracted from the squat lobsters at Chapopote

ID#	Size	Sex	Status
1	Large	Female	
2	Large	Female	gravid
3	Large	Female	gravid
4	Large	Female	gravid
5	Large	Female	gravid
6	Large	Female	gravid
7	Large	Female	gravid
8	Large	Female	gravid
9	Large	Female	gravid
10	Small	Male	
11	Small	Female	
12	Small	Female	
13	Small	Male	juvenile
14	Small	Male	juvenile
15	Large	Male	
16	Large	Male	
17	Large	Male	
18	Small	Male	
19	Small	Male	
20	Small	Male	
21	Small	Male	

Appendix 6

ROV Dive 83 GeoB 106 22-4 14.04.06

Mussels collected with ROV

ID#	Length (cm)	Comments	Name of Scientist	Research to be made
1	18.9	Kidney shaped	Heiko/Nicole/Erik/ Elva/Florence	
2	18.65	Kidney shaped, large	Elva	National Mollusk collection UNAM
3	11.94	Kidney shaped, small	Elva	National Mollusk collection UNAM
4	9.8	Kidney shaped, medium sized	Heiko/Nicole/Erik/ Elva/Florence	
5		Kidney shaped, medium sized	Heiko	
6		Broken	Ian	Genetics
7	4.76	Oval shaped small	Elva	National Mollusk collection UNAM
8	14.1	Oval shaped large	Elva	National Mollusk collection UNAM
9	15.3	Oval shaped large	Elva	National Mollusk collection UNAM
10	12.6	Oval shaped large	Heiko/Nicole/Erik/ Elva/Florence	
11	14.2	Oval shaped large	Heiko/Nicole/Erik/ Elva/Florence	
12	2.8	Oval shaped small, attached to asphalt piece	Nicole/Erik	
13		Oval shaped small, attached to asphalt piece	Antje	
14		Oval shaped small, attached to asphalt piece	Antje	
15		Oval shaped small, attached to asphalt piece	Antje	
16		Oval shaped very small, attached to asphalt piece	Antje	
17		Oval shaped very small, attached to asphalt piece	Antje	
18		Oval shaped very small, attached to asphalt piece	Antje	

Appendix 7

ROV Dive 83 GeoB 106 22-4 14.04.06

Tube worms collected with ROV

ID#	Length (cm)	Comments	Name of Scientist	Research to be made
1	61	very good specimen	H. Sahling/G. Bohrmann	
2	67	very good specimen	Escobar	Museum Archive
3	86		I. MacDonald	for Eric Cordes
4	75		Dublier/Peckmann/Schubotz	Symbionts, Biomarker, Tube taphonomy
5	57	Bent	Escobar	Museum Archive
6	62		I. MacDonald	for Eric Cordes
7	87		Escobar	Museum Archive
8	69		H. Sahling/G. Bohrmann	
9	67		I. MacDonald	for Eric Cordes
10	59		Escobar	Museum Archive
11	90		I. MacDonald	for Eric Cordes
12	90		I. MacDonald	for Eric Cordes
13	62		Escobar	Museum Archive
4	54	Empty only tube	H. Sahling/G. Bohrmann	
15	45	Broken	Escobar	Isotopes
16	33	Only a fragment		
17	51			
18	38	Only a fragment	Escobar	Isotopes
19	22	Only a fragment		
20	30	Small	S. Kasten	Fossil record

Appendix 8

ROV push cores sampled for biology (UNAM)

Biomarker / DNA (Antje, Kai):	1
SRR and AOM, ex-situ (Antje, Marshall):	3
Incubation (Kai):	1
Rhizons (Matthias, Elva):	2
(pore water, including 2 ml for acetate benthic fauna)	
Pore water squeezer (Sabine, Thomas)	1
(pore water, including 3 ml for DIC, anoxic solid phase)	
Gases (Kai, Sabine), Benthic fauna (Elva)	1
Core for Marshall	1
---	---
SUM	**10**

Publications of this series:

No. 1 **Wefer, G., E. Suess and cruise participants**
Bericht über die POLARSTERN-Fahrt ANT IV/2, Rio de Janeiro - Punta Arenas, 6.11. - 1.12.1985.
60 pages, Bremen, 1986.

No. 2 **Hoffmann, G.**
Holozänstratigraphie und Küstenlinienverlagerung an der andalusischen Mittelmeerküste.
173 pages, Bremen, 1988. (out of print)

No. 3 **Wefer, G. and cruise participants**
Bericht über die METEOR-Fahrt M 6/6, Libreville - Las Palmas, 18.2. - 23.3.1988.
97 pages, Bremen, 1988.

No. 4 **Wefer, G., G.F. Lutze, T.J. Müller, O. Pfannkuche, W. Schenke, G. Siedler, W. Zenk**
Kurzbericht über die METEOR-Expedition No. 6, Hamburg - Hamburg, 28.10.1987 - 19.5.1988.
29 pages, Bremen, 1988. (out of print)

No. 5 **Fischer, G.**
Stabile Kohlenstoff-Isotope in partikulärer organischer Substanz aus dem Südpolarmeer (Atlantischer Sektor). 161 pages, Bremen, 1989.

No. 6 **Berger, W.H. and G. Wefer**
Partikelfluß und Kohlenstoffkreislauf im Ozean.
Bericht und Kurzfassungen über den Workshop vom 3.-4. Juli 1989 in Bremen.
57 pages, Bremen, 1989.

No. 7 **Wefer, G. and cruise participants**
Bericht über die METEOR - Fahrt M 9/4, Dakar - Santa Cruz, 19.2. - 16.3.1989.
103 pages, Bremen, 1989.

No. 8 **Kölling, M.**
Modellierung geochemischer Prozesse im Sickerwasser und Grundwasser.
135 pages, Bremen, 1990.

No. 9 **Heinze, P.-M.**
Das Auftriebsgeschehen vor Peru im Spätquartär. 204 pages, Bremen, 1990. (out of print)

No. 10 **Willems, H., G. Wefer, M. Rinski, B. Donner, H.-J. Bellmann, L. Eißmann, A. Müller, B.W. Flemming, H.-C. Höfle, J. Merkt, H. Streif, G. Hertweck, H. Kuntze, J. Schwaar, W. Schäfer, M.-G. Schulz, F. Grube, B. Menke**
Beiträge zur Geologie und Paläontologie Norddeutschlands: Exkursionsführer.
202 pages, Bremen, 1990.

No. 11 **Wefer, G. and cruise participants**
Bericht über die METEOR-Fahrt M 12/1, Kapstadt - Funchal, 13.3.1990 - 14.4.1990.
66 pages, Bremen, 1990.

No. 12 **Dahmke, A., H.D. Schulz, A. Kölling, F. Kracht, A. Lücke**
Schwermetallspuren und geochemische Gleichgewichte zwischen Porenlösung und Sediment im Wesermündungsgebiet. BMFT-Projekt MFU 0562, Abschlußbericht. 121 pages, Bremen, 1991.

No. 13 **Rostek, F.**
Physikalische Strukturen von Tiefseesedimenten des Südatlantiks und ihre Erfassung in Echolotregistrierungen. 209 pages, Bremen, 1991.

No. 14 **Baumann, M.**
Die Ablagerung von Tschernobyl-Radiocäsium in der Norwegischen See und in der Nordsee.
133 pages, Bremen, 1991. (out of print)

No. 15 **Kölling, A.**
Frühdiagenetische Prozesse und Stoff-Flüsse in marinen und ästuarinen Sedimenten.
140 pages, Bremen, 1991.

No. 16 **SFB 261 (ed.)**
1. Kolloquium des Sonderforschungsbereichs 261 der Universität Bremen (14.Juni 1991):
Der Südatlantik im Spätquartär: Rekonstruktion von Stoffhaushalt und Stromsystemen.
Kurzfassungen der Vorträge und Poster. 66 pages, Bremen, 1991.

No. 17 **Pätzold, J. and cruise participants**
Bericht und erste Ergebnisse über die METEOR-Fahrt M 15/2, Rio de Janeiro - Vitoria,
18.1. - 7.2.1991. 46 pages, Bremen, 1993.

No. 18 **Wefer, G. and cruise participants**
Bericht und erste Ergebnisse über die METEOR-Fahrt M 16/1, Pointe Noire - Recife,
27.3. - 25.4.1991. 120 pages, Bremen, 1991.

No. 19 **Schulz, H.D. and cruise participants**
Bericht und erste Ergebnisse über die METEOR-Fahrt M 16/2, Recife - Belem, 28.4. - 20.5.1991. 149 pages, Bremen, 1991.

No. 20 **Berner, H.**
Mechanismen der Sedimentbildung in der Fram-Straße, im Arktischen Ozean und in der Norwegischen See. 167 pages, Bremen, 1991.

No. 21 **Schneider, R.**
Spätquartäre Produktivitätsänderungen im östlichen Angola-Becken: Reaktion auf Variationen im Passat-Monsun-Windsystem und in der Advektion des Benguela-Küstenstroms. 198 pages, Bremen, 1991. (out of print)

No. 22 **Hebbeln, D.**
Spätquartäre Stratigraphie und Paläozeanographie in der Fram-Straße. 174 pages, Bremen, 1991.

No. 23 **Lücke, A.**
Umsetzungsprozesse organischer Substanz während der Frühdiagenese in ästuarinen Sedimenten. 137 pages, Bremen, 1991.

No. 24 **Wefer, G. and cruise participants**
Bericht und erste Ergebnisse der METEOR-Fahrt M 20/1, Bremen - Abidjan, 18.11.- 22.12.1991. 74 pages, Bremen, 1992.

No. 25 **Schulz, H.D. and cruise participants**
Bericht und erste Ergebnisse der METEOR-Fahrt M 20/2, Abidjan - Dakar, 27.12.1991 - 3.2.1992. 173 pages, Bremen, 1992.

No. 26 **Gingele, F.**
Zur klimaabhängigen Bildung biogener und terrigener Sedimente und ihrer Veränderung durch die Frühdiagenese im zentralen und östlichen Südatlantik. 202 pages, Bremen, 1992.

No. 27 **Bickert, T.**
Rekonstruktion der spätquartären Bodenwasserzirkulation im östlichen Südatlantik über stabile Isotope benthischer Foraminiferen. 205 pages, Bremen, 1992. (out of print)

No. 28 **Schmidt, H.**
Der Benguela-Strom im Bereich des Walfisch-Rückens im Spätquartär. 172 pages, Bremen, 1992.

No. 29 **Meinecke, G.**
Spätquartäre Oberflächenwassertemperaturen im östlichen äquatorialen Atlantik. 181 pages, Bremen, 1992.

No. 30 **Bathmann, U., U. Bleil, A. Dahmke, P. Müller, A. Nehrkorn, E.-M. Nöthig, M. Olesch, J. Pätzold, H.D. Schulz, V. Smetacek, V. Spieß, G. Wefer, H. Willems**
Bericht des Graduierten Kollegs. Stoff-Flüsse in marinen Geosystemen. Berichtszeitraum Oktober 1990 - Dezember 1992. 396 pages, Bremen, 1992.

No. 31 **Damm, E.**
Frühdiagenetische Verteilung von Schwermetallen in Schlicksedimenten der westlichen Ostsee. 115 pages, Bremen, 1992.

No. 32 **Antia, E.E.**
Sedimentology, Morphodynamics and Facies Association of a mesotidal Barrier Island Shoreface (Spiekeroog, Southern North Sea). 370 pages, Bremen, 1993.

No. 33 **Duinker, J. and G. Wefer (ed.)**
Bericht über den 1. JGOFS-Workshop. 1./2. Dezember 1992 in Bremen. 83 pages, Bremen, 1993.

No. 34 **Kasten, S.**
Die Verteilung von Schwermetallen in den Sedimenten eines stadtbremischen Hafenbeckens. 103 pages, Bremen, 1993.

No. 35 **Spieß, V.**
Digitale Sedimentographie. Neue Wege zu einer hochauflösenden Akustostratigraphie. 199 pages, Bremen, 1993.

No. 36 **Schinzel, U.**
Laborversuche zu frühdiagenetischen Reaktionen von Eisen (III) - Oxidhydraten in marinen Sedimenten.189 pages, Bremen, 1993.

No. 37 **Sieger, R.**
CoTAM - ein Modell zur Modellierung des Schwermetalltransports in Grundwasserleitern. 56 pages, Bremen, 1993. (out of print)

No. 38 **Willems, H. (ed.)**
Geoscientific Investigations in the Tethyan Himalayas. 183 pages, Bremen, 1993.

No. 39 **Hamer, K.**
Entwicklung von Laborversuchen als Grundlage für die Modellierung des Transportverhaltens von Arsenat, Blei, Cadmium und Kupfer in wassergesättigten Säulen. 147 pages, Bremen, 1993.

No. 40 **Sieger, R.**
Modellierung des Stofftransports in porösen Medien unter Ankopplung kinetisch gesteuerter Sorptions- und Redoxprozesse sowie thermischer Gleichgewichte. 158 pages, Bremen, 1993.

No. 41 **Thießen, W.**
Magnetische Eigenschaften von Sedimenten des östlichen Südatlantiks und ihre paläozeanographische Relevanz. 170 pages, Bremen, 1993.

No. 42 **Spieß, V. and cruise participants**
Report and preliminary results of METEOR-Cruise M 23/1, Kapstadt - Rio de Janeiro, 4.-25.2.1993. 139 pages, Bremen, 1994.

No. 43 **Bleil, U. and cruise participants**
Report and preliminary results of METEOR-Cruise M 23/2, Rio de Janeiro - Recife, 27.2.-19.3.1993 133 pages, Bremen, 1994.

No. 44 **Wefer, G. and cruise participants**
Report and preliminary results of METEOR-Cruise M 23/3, Recife - Las Palmas, 21.3. - 12.4.1993 71 pages, Bremen, 1994.

No. 45 **Giese, M. and G. Wefer (ed.)**
Bericht über den 2. JGOFS-Workshop. 18../19. November 1993 in Bremen. 93 pages, Bremen, 1994.

No. 46 **Balzer, W. and cruise participants**
Report and preliminary results of METEOR-Cruise M 22/1, Hamburg - Recife, 22.9. - 21.10.1992. 24 pages, Bremen, 1994.

No. 47 **Stax, R.**
Zyklische Sedimentation von organischem Kohlenstoff in der Japan See: Anzeiger für Änderungen von Paläoozeanographie und Paläoklima im Spätkänozoikum. 150 pages, Bremen, 1994.

No. 48 **Skowronek, F.**
Frühdiagenetische Stoff-Flüsse gelöster Schwermetalle an der Oberfläche von Sedimenten des Weser Ästuares. 107 pages, Bremen, 1994.

No. 49 **Dersch-Hansmann, M.**
Zur Klimaentwicklung in Ostasien während der letzten 5 Millionen Jahre: Terrigener Sedimenteintrag in die Japan See (ODP Ausfahrt 128). 149 pages, Bremen, 1994.

No. 50 **Zabel, M.**
Frühdiagenetische Stoff-Flüsse in Oberflächen-Sedimenten des äquatorialen und östlichen Südatlantik. 129 pages, Bremen, 1994.

No. 51 **Bleil, U. and cruise participants**
Report and preliminary results of SONNE-Cruise SO 86, Buenos Aires - Capetown, 22.4. - 31.5.93 116 pages, Bremen, 1994.

No. 52 **Symposium: The South Atlantic: Present and Past Circulation.**
Bremen, Germany, 15 - 19 August 1994. Abstracts. 167 pages, Bremen, 1994.

No. 53 **Kretzmann, U.B.**
^{57}Fe-Mössbauer-Spektroskopie an Sedimenten - Möglichkeiten und Grenzen. 183 pages, Bremen, 1994.

No. 54 **Bachmann, M.**
Die Karbonatrampe von Organyà im oberen Oberapt und unteren Unteralb (NE-Spanien, Prov. Lerida): Fazies, Zyklo- und Sequenzstratigraphie. 147 pages, Bremen, 1994. (out of print)

No. 55 **Kemle-von Mücke, S.**
Oberflächenwasserstruktur und -zirkulation des Südostatlantiks im Spätquartär. 151 pages, Bremen, 1994.

No. 56 **Petermann, H.**
Magnetotaktische Bakterien und ihre Magnetosome in Oberflächensedimenten des Südatlantiks. 134 pages, Bremen, 1994.

No. 57 **Mulitza, S.**
Spätquartäre Variationen der oberflächennahen Hydrographie im westlichen äquatorialen Atlantik. 97 pages, Bremen, 1994.

No. 58 **Segl, M. and cruise participants**
Report and preliminary results of METEOR-Cruise M 29/1, Buenos-Aires - Montevideo, 17.6. - 13.7.1994
94 pages, Bremen, 1994.

No. 59 **Bleil, U. and cruise participants**
Report and preliminary results of METEOR-Cruise M 29/2, Montevideo - Rio de Janiero 15.7. - 8.8.1994. 153 pages, Bremen, 1994.

No. 60 **Henrich, R. and cruise participants**
Report and preliminary results of METEOR-Cruise M 29/3, Rio de Janeiro - Las Palmas 11.8. - 5.9.1994. Bremen, 1994. (out of print)

No. 61 **Sagemann, J.**
Saisonale Variationen von Porenwasserprofilen, Nährstoff-Flüssen und Reaktionen in intertidalen Sedimenten des Weser-Ästuars. 110 pages, Bremen, 1994. (out of print)

No. 62 **Giese, M. and G. Wefer**
Bericht über den 3. JGOFS-Workshop. 5./6. Dezember 1994 in Bremen.
84 pages, Bremen, 1995.

No. 63 **Mann, U.**
Genese kretazischer Schwarzschiefer in Kolumbien: Globale vs. regionale/lokale Prozesse.
153 pages, Bremen, 1995. (out of print)

No. 64 **Willems, H., Wan X., Yin J., Dongdui L., Liu G., S. Dürr, K.-U. Gräfe**
The Mesozoic development of the N-Indian passive margin and of the Xigaze Forearc Basin in southern Tibet, China. – Excursion Guide to IGCP 362 Working-Group Meeting "Integrated Stratigraphy". 113 pages, Bremen, 1995. (out of print)

No. 65 **Hünken, U.**
Liefergebiets - Charakterisierung proterozoischer Goldseifen in Ghana anhand von Fluideinschluß - Untersuchungen. 270 pages, Bremen, 1995.

No. 66 **Nyandwi, N.**
The Nature of the Sediment Distribution Patterns in ther Spiekeroog Backbarrier Area, the East Frisian Islands. 162 pages, Bremen, 1995.

No. 67 **Isenbeck-Schröter, M.**
Transportverhalten von Schwermetallkationen und Oxoanionen in wassergesättigten Sanden. - Laborversuche in Säulen und ihre Modellierung -. 182 pages, Bremen, 1995.

No. 68 **Hebbeln, D. and cruise participants**
Report and preliminary results of SONNE-Cruise SO 102, Valparaiso - Valparaiso, 95.
134 pages, Bremen, 1995.

No. 69 **Willems, H. (Sprecher), U.Bathmann, U. Bleil, T. v. Dobeneck, K. Herterich, B.B. Jorgensen, E.-M. Nöthig, M. Olesch, J. Pätzold, H.D. Schulz, V. Smetacek, V. Speiß. G. Wefer**
Bericht des Graduierten-Kollegs Stoff-Flüsse in marine Geosystemen.
Berichtszeitraum Januar 1993 - Dezember 1995. 45 & 468 pages, Bremen, 1995.

No. 70 **Giese, M. and G. Wefer**
Bericht über den 4. JGOFS-Workshop. 20./21. November 1995 in Bremen. 60 pages, Bremen, 1996. (out of print)

No. 71 **Meggers, H.**
Pliozän-quartäre Karbonatsedimentation und Paläozeanographie des Nordatlantiks und des Europäischen Nordmeeres - Hinweise aus planktischen Foraminiferengemeinschaften.
143 pages, Bremen, 1996. (out of print)

No. 72 **Teske, A.**
Phylogenetische und ökologische Untersuchungen an Bakterien des oxidativen und reduktiven marinen Schwefelkreislaufs mittels ribosomaler RNA. 220 pages, Bremen, 1996. (out of print)

No. 73 **Andersen, N.**
Biogeochemische Charakterisierung von Sinkstoffen und Sedimenten aus ostatlantischen Produktions-Systemen mit Hilfe von Biomarkern. 215 pages, Bremen, 1996.

No. 74 **Treppke, U.**
Saisonalität im Diatomeen- und Silikoflagellatenfluß im östlichen tropischen und subtropischen Atlantik. 200 pages, Bremen, 1996.

No. 75 **Schüring, J.**
Die Verwendung von Steinkohlebergematerialien im Deponiebau im Hinblick auf die Pyritverwitterung und die Eignung als geochemische Barriere. 110 pages, Bremen, 1996.

No. 76 **Pätzold, J. and cruise participants**
Report and preliminary results of VICTOR HENSEN cruise JOPS II, Leg 6,
Fortaleza - Recife, 10.3. - 26.3. 1995 and Leg 8, Vítoria - Vítoria, 10.4. - 23.4.1995.
87 pages, Bremen, 1996.

No. 77 **Bleil, U. and cruise participants**
Report and preliminary results of METEOR-Cruise M 34/1, Cape Town - Walvis Bay, 3.-26.1.1996.
129 pages, Bremen, 1996.

No. 78 **Schulz, H.D. and cruise participants**
Report and preliminary results of METEOR-Cruise M 34/2, Walvis Bay - Walvis Bay, 29.1.-18.2.96
133 pages, Bremen, 1996.

No. 79 **Wefer, G. and cruise participants**
Report and preliminary results of METEOR-Cruise M 34/3, Walvis Bay - Recife, 21.2.-17.3.1996.
168 pages, Bremen, 1996.

No. 80 **Fischer, G. and cruise participants**
Report and preliminary results of METEOR-Cruise M 34/4, Recife - Bridgetown, 19.3.-15.4.1996.
105 pages, Bremen, 1996.

No. 81 **Kulbrok, F.**
Biostratigraphie, Fazies und Sequenzstratigraphie einer Karbonatrampe in den Schichten der Oberkreide und des Alttertiärs Nordost-Ägyptens (Eastern Desert, N'Golf von Suez, Sinai).
153 pages, Bremen, 1996.

No. 82 **Kasten, S.**
Early Diagenetic Metal Enrichments in Marine Sediments as Documents of Nonsteady-State Depositional Conditions. Bremen, 1996.

No. 83 **Holmes, M.E.**
Reconstruction of Surface Ocean Nitrate Utilization in the Southeast Atlantic Ocean Based on Stable Nitrogen Isotopes. 113 pages, Bremen, 1996.

No. 84 **Rühlemann, C.**
Akkumulation von Carbonat und organischem Kohlenstoff im tropischen Atlantik: Spätquartäre Produktivitäts-Variationen und ihre Steuerungsmechanismen. 139 pages, Bremen, 1996.

No. 85 **Ratmeyer, V.**
Untersuchungen zum Eintrag und Transport lithogener und organischer partikulärer Substanz im östlichen subtropischen Nordatlantik. 154 pages, Bremen, 1996.

No. 86 **Cepek, M.**
Zeitliche und räumliche Variationen von Coccolithophoriden-Gemeinschaften im subtropischen Ost-Atlantik: Untersuchungen an Plankton, Sinkstoffen und Sedimenten. 156 pages, Bremen, 1996.

No. 87 **Otto, S.**
Die Bedeutung von gelöstem organischen Kohlenstoff (DOC) für den Kohlenstoffffluß im Ozean.
150 pages, Bremen, 1996.

No. 88 **Hensen, C.**
Frühdiagenetische Prozesse und Quantifizierung benthischer Stoff-Flüsse in Oberflächensedimenten des Südatlantiks. 132 pages, Bremen, 1996.

No. 89 **Giese, M. and G. Wefer**
Bericht über den 5. JGOFS-Workshop. 27./28. November 1996 in Bremen. 73 pages, Bremen, 1997.

No. 90 **Wefer, G. and cruise participants**
Report and preliminary results of METEOR-Cruise M 37/1, Lisbon - Las Palmas, 4.-23.12.1996.
79 pages, Bremen, 1997.

No. 91 **Isenbeck-Schröter, M., E. Bedbur, M. Kofod, B. König, T. Schramm & G. Mattheß**
Occurrence of Pesticide Residues in Water - Assessment of the Current Situation in Selected EU Countries. 65 pages, Bremen 1997.

No. 92 **Kühn, M.**
Geochemische Folgereaktionen bei der hydrogeothermalen Energiegewinnung. 129 pages, Bremen 1997.

No. 93 **Determann, S. & K. Herterich**
JGOFS-A6 "Daten und Modelle": Sammlung JGOFS-relevanter Modelle in Deutschland.
26 pages, Bremen, 1997.

No. 94 **Fischer, G. and cruise participants**
Report and preliminary results of METEOR-Cruise M 38/1, Las Palmas - Recife, 25.1.-1.3.1997,
with Appendix: Core Descriptions from METEOR Cruise M 37/1. Bremen, 1997.

No. 95 **Bleil, U. and cruise participants**
Report and preliminary results of METEOR-Cruise M 38/2, Recife - Las Palmas, 4.3.-14.4.1997. 126 pages, Bremen, 1997.

No. 96 **Neuer, S. and cruise participants**
Report and preliminary results of VICTOR HENSEN-Cruise 96/1. Bremen, 1997.

No. 97 **Villinger, H. and cruise participants**
Fahrtbericht SO 111, 20.8. - 16.9.1996. 115 pages, Bremen, 1997.

No. 98 **Lüning, S.**
Late Cretaceous - Early Tertiary sequence stratigraphy, paleoecology and geodynamics of Eastern Sinai, Egypt. 218 pages, Bremen, 1997.

No. 99 **Haese, R.R.**
Beschreibung und Quantifizierung frühdiagenetischer Reaktionen des Eisens in Sedimenten des Südatlantiks. 118 pages, Bremen, 1997.

No. 100 **Lührte, R. von**
Verwertung von Bremer Baggergut als Material zur Oberflächenabdichtung von Deponien - Geochemisches Langzeitverhalten und Schwermetall-Mobilität (Cd, Cu, Ni, Pb, Zn). Bremen, 1997.

No. 101 **Ebert, M.**
Der Einfluß des Redoxmilieus auf die Mobilität von Chrom im durchströmten Aquifer. 135 pages, Bremen, 1997.

No. 102 **Krögel, F.**
Einfluß von Viskosität und Dichte des Seewassers auf Transport und Ablagerung von Wattsedimenten (Langeooger Rückseitenwatt, südliche Nordsee). 168 pages, Bremen, 1997.

No. 103 **Kerntopf, B.**
Dinoflagellate Distribution Patterns and Preservation in the Equatorial Atlantic and Offshore North-West Africa. 137 pages, Bremen, 1997.

No. 104 **Breitzke, M.**
Elastische Wellenausbreitung in marinen Sedimenten - Neue Entwicklungen der Ultraschall Sedimentphysik und Sedimentechographie. 298 pages, Bremen, 1997.

No. 105 **Marchant, M.**
Rezente und spätquartäre Sedimentation planktischer Foraminiferen im Peru-Chile Strom. 115 pages, Bremen, 1997.

No. 106 **Habicht, K.S.**
Sulfur isotope fractionation in marine sediments and bacterial cultures. 125 pages, Bremen, 1997.

No. 107 **Hamer, K., R.v. Lührte, G. Becker, T. Felis, S. Keffel, B. Strotmann, C. Waschkowitz, M. Kölling, M. Isenbeck-Schröter, H.D. Schulz**
Endbericht zum Forschungsvorhaben 060 des Landes Bremen: Baggergut der Hafengruppe Bremen-Stadt: Modelluntersuchungen zur Schwermetallmobilität und Möglichkeiten der Verwertung von Hafenschlick aus Bremischen Häfen. 98 pages, Bremen, 1997.

No. 108 **Greeff, O.W.**
Entwicklung und Erprobung eines benthischen Landersystemes zur *in situ*-Bestimmung von Sulfatreduktionsraten mariner Sedimente. 121 pages, Bremen, 1997.

No. 109 **Pätzold, M. und G. Wefer**
Bericht über den 6. JGOFS-Workshop am 4./5.12.1997 in Bremen. Im Anhang: Publikationen zum deutschen Beitrag zur Joint Global Ocean Flux Study (JGOFS), Stand 1/1998. 122 pages, Bremen, 1998.

No. 110 **Landenberger, H.**
CoTReM, ein Multi-Komponenten Transport- und Reaktions-Modell. 142 pages, Bremen, 1998.

No. 111 **Villinger, H. und Fahrtteilnehmer**
Fahrtbericht SO 124, 4.10. - 16.10.199. 90 pages, Bremen, 1997.

No. 112 **Gietl, R.**
Biostratigraphie und Sedimentationsmuster einer nordostägyptischen Karbonatrampe unter Berücksichtigung der Alveolinen-Faunen. 142 pages, Bremen, 1998.

No. 113 **Ziebis, W.**
The Impact of the Thalassinidean Shrimp *Callianassa truncata* on the Geochemistry of permeable, coastal Sediments. 158 pages, Bremen 1998.

No. 114 **Schulz, H.D. and cruise participants**
Report and preliminary results of METEOR-Cruise M 41/1, Málaga - Libreville, 13.2.-15.3.1998. Bremen, 1998.

No. 115 **Völker, D.J.**
Untersuchungen an strömungsbeeinflußten Sedimentationsmustern im Südozean. Interpretation sedimentechographischer Daten und numerische Modellierung. 152 pages, Bremen, 1998.

No. 116 **Schlünz, B.**
Riverine Organic Carbon Input into the Ocean in Relation to Late Quaternary Climate Change. 136 pages, Bremen, 1998.

No. 117 **Kuhnert, H.**
Aufzeichnug des Klimas vor Westaustralien in stabilen Isotopen in Korallenskeletten. 109 pages, Bremen, 1998.

No. 118 **Kirst, G.**
Rekonstruktion von Oberflächenwassertemperaturen im östlichen Südatlantik anhand von Alkenonen. 130 pages, Bremen, 1998.

No. 119 **Dürkoop, A.**
Der Brasil-Strom im Spätquartär: Rekonstruktion der oberflächennahen Hydrographie während der letzten 400 000 Jahre. 121 pages, Bremen, 1998.

No. 120 **Lamy, F.**
Spätquartäre Variationen des terrigenen Sedimenteintrags entlang des chilenischen Kontinentalhangs als Abbild von Klimavariabilität im Milanković- und Sub-Milanković-Zeitbereich. 141 pages, Bremen, 1998.

No. 121 **Neuer, S. and cruise participants**
Report and preliminary results of POSEIDON-Cruise Pos 237/2, Vigo – Las Palmas, 18.3.-31.3.1998. 39 pages, Bremen, 1998

No. 122 **Romero, O.E.**
Marine planktonic diatoms from the tropical and equatorial Atlantic: temporal flux patterns and the sediment record. 205 pages, Bremen, 1998.

No. 123 **Spiess, V. und Fahrtteilnehmer**
Report and preliminary results of RV SONNE Cruise 125, Cochin – Chittagong, 17.10.-17.11.1997. 128 pages, Bremen, 1998.

No. 124 **Arz, H.W.**
Dokumentation von kurzfristigen Klimaschwankungen des Spätquartärs in Sedimenten des westlichen äquatorialen Atlantiks. 96 pages, Bremen, 1998.

No. 125 **Wolff, T.**
Mixed layer characteristics in the equatorial Atlantic during the late Quaternary as deduced from planktonic foraminifera. 132 pages, Bremen, 1998.

No. 126 **Dittert, N.**
Late Quaternary Planktic Foraminifera Assemblages in the South Atlantic Ocean: Quantitative Determination and Preservational Aspects. 165 pages, Bremen, 1998.

No. 127 **Höll, C.**
Kalkige und organisch-wandige Dinoflagellaten-Zysten in Spätquartären Sedimenten des tropischen Atlantiks und ihre palökologische Auswertbarkeit. 121 pages, Bremen, 1998.

No. 128 **Hencke, J.**
Redoxreaktionen im Grundwasser: Etablierung und Verlagerung von Reaktionsfronten und ihre Bedeutung für die Spurenelement-Mobilität. 122 pages, Bremen 1998.

No. 129 **Pätzold, J. and cruise participants**
Report and preliminary results of METEOR-Cruise M 41/3, Vítoria, Brasil – Salvador de Bahia, Brasil, 18.4. - 15.5.1998. Bremen, 1999.

No. 130 **Fischer, G. and cruise participants**
Report and preliminary results of METEOR-Cruise M 41/4, Salvador de Bahia, Brasil – Las Palmas, Spain, 18.5. – 13.6.1998. Bremen, 1999.

No. 131 **Schlünz, B. und G. Wefer**
Bericht über den 7. JGOFS-Workshop am 3. und 4.12.1998 in Bremen. Im Anhang: Publikationen zum deutschen Beitrag zur Joint Global Ocean Flux Study (JGOFS), Stand 1/ 1999. 100 pages, Bremen, 1999.

No. 132 **Wefer, G. and cruise participants**
Report and preliminary results of METEOR-Cruise M 42/4, Las Palmas - Las Palmas - Viena do Castelo; 26.09.1998 - 26.10.1998. 104 pages, Bremen, 1999.

No. 133 **Felis, T.**
Climate and ocean variability reconstructed from stable isotope records of modern subtropical corals (Northern Red Sea). 111 pages, Bremen, 1999.

No. 134 **Draschba , S.**
North Atlantic climate variability recorded in reef corals from Bermuda. 108 pages, Bremen, 1999.

No. 135 **Schmieder, F.**
Magnetic Cyclostratigraphy of South Atlantic Sediments. 82 pages, Bremen, 1999.

No. 136 **Rieß, W.**
In situ measurements of respiration and mineralisation processes – Interaction between fauna and geochemical fluxes at active interfaces. 68 pages, Bremen, 1999.

No. 137 **Devey, C.W. and cruise participants**
Report and shipboard results from METEOR-cruise M 41/2, Libreville – Vitoria, 18.3. – 15.4.98. 59 pages, Bremen, 1999.

No. 138 **Wenzhöfer, F.**
Biogeochemical processes at the sediment water interface and quantification of metabolically driven calcite dissolution in deep sea sediments. 103 pages, Bremen, 1999.

No. 139 **Klump, J.**
Biogenic barite as a proxy of paleoproductivity variations in the Southern Peru-Chile Current. 107 pages, Bremen, 1999.

No. 140 **Huber, R.**
Carbonate sedimentation in the northern Northatlantic since the late pliocene. 103 pages, Bremen, 1999.

No. 141 **Schulz, H.**
Nitrate-storing sulfur bacteria in sediments of coastal upwelling. 94 pages, Bremen, 1999.

No. 142 **Mai, S.**
Die Sedimentverteilung im Wattenmeer: ein Simulationsmodell. 114 pages, Bremen, 1999.

No. 143 **Neuer, S. and cruise participants**
Report and preliminary results of Poseidon Cruise 248, Las Palmas - Las Palmas, 15.2.-26.2.1999. 45 pages, Bremen, 1999.

No. 144 **Weber, A.**
Schwefelkreislauf in marinen Sedimenten und Messung von in situ Sulfatreduktionsraten. 122 pages, Bremen, 1999.

No. 145 **Hadeler, A.**
Sorptionsreaktionen im Grundwasser: Unterschiedliche Aspekte bei der Modellierung des Transportverhaltens von Zink. 122 pages, 1999.

No. 146 **Dierßen, H.**
Zum Kreislauf ausgewählter Spurenmetalle im Südatlantik: Vertikaltransport und Wechselwirkung zwischen Partikeln und Lösung. 167 pages, Bremen, 1999.

No. 147 **Zühlsdorff, L.**
High resolution multi-frequency seismic surveys at the Eastern Juan de Fuca Ridge Flank and the Cascadia Margin – Evidence for thermally and tectonically driven fluid upflow in marine sediments. 118 pages, Bremen 1999.

No. 148 **Kinkel, H.**
Living and late Quaternary Coccolithophores in the equatorial Atlantic Ocean: response of distribution and productivity patterns to changing surface water circulation. 183 pages, Bremen, 2000.

No. 149 **Pätzold, J. and cruise participants**
Report and preliminary results of METEOR Cruise M 44/3, Aqaba (Jordan) - Safaga (Egypt) – Dubá (Saudi Arabia) – Suez (Egypt) - Haifa (Israel), 12.3.-26.3.-2.4.-4.4.1999. 135 pages, Bremen, 2000.

No. 150 **Schlünz, B. and G. Wefer**
Bericht über den 8. JGOFS-Workshop am 2. und 3.12.1999 in Bremen. Im Anhang: Publikationen zum deutschen Beitrag zur Joint Global Ocean Flux Study (JGOFS), Stand 1/ 2000. 95 pages, Bremen, 2000.

No. 151 **Schnack, K.**
Biostratigraphie und fazielle Entwicklung in der Oberkreide und im Alttertiär im Bereich der Kharga Schwelle, Westliche Wüste, SW-Ägypten. 142 pages, Bremen, 2000.

No. 152 **Karwath, B.**
Ecological studies on living and fossil calcareous dinoflagellates of the equatorial and tropical Atlantic Ocean. 175 pages, Bremen, 2000.

No. 153 **Moustafa, Y.**
Paleoclimatic reconstructions of the Northern Red Sea during the Holocene inferred from stable isotope records of modern and fossil corals and molluscs. 102 pages, Bremen, 2000.

No. 154 **Villinger, H. and cruise participants**
Report and preliminary results of SONNE-cruise 145-1 Balboa – Talcahuana, 21.12.1999 – 28.01.2000. 147 pages, Bremen, 2000.

No. 155 **Rusch, A.**
Dynamik der Feinfraktion im Oberflächenhorizont permeabler Schelfsedimente. 102 pages, Bremen, 2000.

No. 156 **Moos, C.**
Reconstruction of upwelling intensity and paleo-nutrient gradients in the northwest Arabian Sea derived from stable carbon and oxygen isotopes of planktic foraminifera. 103 pages, Bremen, 2000.

No. 157 **Xu, W.**
Mass physical sediment properties and trends in a Wadden Sea tidal basin. 127 pages, Bremen, 2000.

No. 158 **Meinecke, G. and cruise participants**
Report and preliminary results of METEOR Cruise M 45/1, Malaga (Spain) - Lissabon (Portugal), 19.05. - 08.06.1999. 39 pages, Bremen, 2000.

No. 159 **Vink, A.**
Reconstruction of recent and late Quaternary surface water masses of the western subtropical Atlantic Ocean based on calcareous and organic-walled dinoflagellate cysts. 160 pages, Bremen, 2000.

No. 160 **Willems, H. (Sprecher), U. Bleil, R. Henrich, K. Herterich, B.B. Jørgensen, H.-J. Kuß, M. Olesch, H.D. Schulz,V. Spieß, G. Wefer**
Abschlußbericht des Graduierten-Kollegs Stoff-Flüsse in marine Geosystemen. Zusammenfassung und Berichtszeitraum Januar 1996 - Dezember 2000. 340 pages, Bremen, 2000.

No. 161 **Sprengel, C.**
Untersuchungen zur Sedimentation und Ökologie von Coccolithophoriden im Bereich der Kanarischen Inseln: Saisonale Flussmuster und Karbonatexport. 165 pages, Bremen, 2000.

No. 162 **Donner, B. and G. Wefer**
Bericht über den JGOFS-Workshop am 18.-21.9.2000 in Bremen: Biogeochemical Cycles: German Contributions to the International Joint Global Ocean Flux Study. 87 pages, Bremen, 2000.

No. 163 **Neuer, S. and cruise participants**
Report and preliminary results of Meteor Cruise M 45/5, Bremen – Las Palmas, October 1 – November 3, 1999. 93 pages, Bremen, 2000.

No. 164 **Devey, C. and cruise participants**
Report and preliminary results of Sonne Cruise SO 145/2, Talcahuano (Chile) - Arica (Chile), February 4 – February 29, 2000. 63 pages, Bremen, 2000.

No. 165 **Freudenthal, T.**
Reconstruction of productivity gradients in the Canary Islands region off Morocco by means of sinking particles and sediments. 147 pages, Bremen, 2000.

No. 166 **Adler, M.**
Modeling of one-dimensional transport in porous media with respect to simultaneous geochemical reactions in CoTReM. 147 pages, Bremen, 2000.

No. 167 **Santamarina Cuneo, P.**
Fluxes of suspended particulate matter through a tidal inlet of the East Frisian Wadden Sea (southern North Sea). 91 pages, Bremen, 2000.

No. 168 **Benthien, A.**
Effects of CO_2 and nutrient concentration on the stable carbon isotope composition of C37:2 alkenones in sediments of the South Atlantic Ocean. 104 pages, Bremen, 2001.

No. 169 **Lavik, G.**
Nitrogen isotopes of sinking matter and sediments in the South Atlantic. 140 pages, Bremen, 2001.

No. 170 **Budziak, D.**
Late Quaternary monsoonal climate and related variations in paleoproductivity and alkenone-derived sea-surface temperatures in the western Arabian Sea. 114 pages, Bremen, 2001.

No. 171 **Gerhardt, S.**
Late Quaternary water mass variability derived from the pteropod preservation state in sediments of the western South Atlantic Ocean and the Caribbean Sea. 109 pages, Bremen, 2001.

No. 172 **Bleil, U. and cruise participants**
Report and preliminary results of Meteor Cruise M 46/3, Montevideo (Uruguay) – Mar del Plata (Argentina), January 4 – February 7, 2000. Bremen, 2001.

No. 173 **Wefer, G. and cruise participants**
Report and preliminary results of Meteor Cruise M 46/4, Mar del Plata (Argentina) – Salvador da Bahia (Brazil), February 10 – March 13, 2000. With partial results of METEOR cruise M 46/2. 136 pages, Bremen, 2001.

No. 174 **Schulz, H.D. and cruise participants**
Report and preliminary results of Meteor Cruise M 46/2, Recife (Brazil) – Montevideo (Uruguay), December 2 – December 29, 1999. 107 pages, Bremen, 2001.

No. 175 **Schmidt, A.**
Magnetic mineral fluxes in the Quaternary South Atlantic: Implications for the paleoenvironment. 97 pages, Bremen, 2001.

No. 176 **Bruhns, P.**
Crystal chemical characterization of heavy metal incorporation in brick burning processes. 93 pages, Bremen, 2001.

No. 177 **Karius, V.**
Baggergut der Hafengruppe Bremen-Stadt in der Ziegelherstellung. 131 pages, Bremen, 2001.

No. 178 **Adegbie, A. T.**
Reconstruction of paleoenvironmental conditions in Equatorial Atlantic and the Gulf of Guinea Basins for the last 245,000 years. 113 pages, Bremen, 2001.

No. 179 **Spieß, V. and cruise participants**
Report and preliminary results of R/V Sonne Cruise SO 149, Victoria - Victoria, 16.8. - 16.9.2000. 100 pages, Bremen, 2001.

No. 180 **Kim, J.-H.**
Reconstruction of past sea-surface temperatures in the eastern South Atlantic and the eastern South Pacific across Termination I based on the Alkenone Method. 114 pages, Bremen, 2001.

No. 181 **von Lom-Keil, H.**
Sedimentary waves on the Namibian continental margin and in the Argentine Basin – Bottom flow reconstructions based on high resolution echosounder data. 126 pages, Bremen, 2001.

No. 182 **Hebbeln, D. and cruise participants**
PUCK: Report and preliminary results of R/V Sonne Cruise SO 156, Valparaiso (Chile) - Talcahuano (Chile), March 29 - May 14, 2001. 195 pages, Bremen, 2001.

No. 183 **Wendler, J.**
Reconstruction of astronomically-forced cyclic and abrupt paleoecological changes in the Upper Cretaceous Boreal Realm based on calcareous dinoflagellate cysts. 149 pages, Bremen, 2001.

No. 184 **Volbers, A.**
Planktic foraminifera as paleoceanographic indicators: production, preservation, and reconstruction of upwelling intensity. Implications from late Quaternary South Atlantic sediments. 122 pages, Bremen, 2001.

No. 185 **Bleil, U. and cruise participants**
Report and preliminary results of R/V METEOR Cruise M 49/3, Montevideo (Uruguay) - Salvador (Brasil), March 9 - April 1, 2001. 99 pages, Bremen, 2001.

No. 186 **Scheibner, C.**
Architecture of a carbonate platform-to-basin transition on a structural high (Campanian-early Eocene, Eastern Desert, Egypt) – classical and modelling approaches combined. 173 pages, Bremen, 2001.

No. 187 **Schneider, S.**
Quartäre Schwankungen in Strömungsintensität und Produktivität als Abbild der Wassermassen-Variabilität im äquatorialen Atlantik (ODP Sites 959 und 663): Ergebnisse aus Siltkorn-Analysen. 134 pages, Bremen, 2001.

No. 188 **Uliana, E.**
Late Quaternary biogenic opal sedimentation in diatom assemblages in Kongo Fan sediments. 96 pages, Bremen, 2002.

No. 189 **Esper, O.**
Reconstruction of Recent and Late Quaternary oceanographic conditions in the eastern South Atlantic Ocean based on calcareous- and organic-walled dinoflagellate cysts. 130 pages, Bremen, 2001.

No. 190 **Wendler, I.**
Production and preservation of calcareous dinoflagellate cysts in the modern Arabian Sea. 117 pages, Bremen, 2002.

No. 191 **Bauer, J.**
Late Cenomanian – Santonian carbonate platform evolution of Sinai (Egypt): stratigraphy, facies, and sequence architecture. 178 pages, Bremen, 2002.

No. 192 **Hildebrand-Habel, T.**
Die Entwicklung kalkiger Dinoflagellaten im Südatlantik seit der höheren Oberkreide. 152 pages, Bremen, 2002.

No. 193 **Hecht, H.**
Sauerstoff-Optopoden zur Quantifizierung von Pyritverwitterungsprozessen im Labor- und Langzeit-in-situ-Einsatz. Entwicklung - Anwendung – Modellierung. 130 pages, Bremen, 2002.

No. 194 **Fischer, G. and cruise participants**
Report and Preliminary Results of RV METEOR-Cruise M49/4, Salvador da Bahia – Halifax, 4.4.-5.5.2001. 84 pages, Bremen, 2002.

No. 195 **Gröger, M.**
Deep-water circulation in the western equatorial Atlantic: inferences from carbonate preservation studies and silt grain-size analysis. 95 pages, Bremen, 2002.

No. 196 **Meinecke,G. and cruise participants**
Report of RV POSEIDON Cruise POS 271, Las Palmas - Las Palmas, 19.3.-29.3.2001. 19 pages, Bremen, 2002.

No. 197 **Meggers, H. and cruise participants**
Report of RV POSEIDON Cruise POS 272, Las Palmas - Las Palmas, 1.4.-14.4.2001. 19 pages, Bremen, 2002.

No. 198 **Gräfe, K.-U.**
Stratigraphische Korrelation und Steuerungsfaktoren Sedimentärer Zyklen in ausgewählten Borealen und Tethyalen Becken des Cenoman/Turon (Oberkreide) Europas und Nordwestafrikas. 197 pages, Bremen, 2002.

No. 199 **Jahn, B.**
Mid to Late Pleistocene Variations of Marine Productivity in and Terrigenous Input to the Southeast Atlantic. 97 pages, Bremen, 2002.

No. 200 **Al-Rousan, S.**
Ocean and climate history recorded in stable isotopes of coral and foraminifers from the northern Gulf of Aqaba. 116 pages, Bremen, 2002.

No. 201 **Azouzi, B.**
Regionalisierung hydraulischer und hydrogeochemischer Daten mit geostatistischen Methoden. 108 pages, Bremen, 2002.

No. 202 **Spieß, V. and cruise participants**
Report and preliminary results of METEOR Cruise M 47/3, Libreville (Gabun) - Walvis Bay (Namibia), 01.06 - 03.07.2000. 70 pages, Bremen 2002.

No. 203 **Spieß, V. and cruise participants**
Report and preliminary results of METEOR Cruise M 49/2, Montevideo (Uruguay) - Montevideo, 13.02 - 07.03.2001. 84 pages, Bremen 2002.

No. 204 **Mollenhauer, G.**
Organic carbon accumulation in the South Atlantic Ocean: Sedimentary processes and glacial/interglacial Budgets. 139 pages, Bremen 2002.

No. 205 **Spieß, V. and cruise participants**
Report and preliminary results of METEOR Cruise M49/1, Cape Town (South Africa) - Montevideo (Uruguay), 04.01.2001 - 10.02.2001. 57 pages, Bremen, 2003.

No. 206 **Meier, K.J.S.**
Calcareous dinoflagellates from the Mediterranean Sea: taxonomy, ecology and palaeoenvironmental application. 126 pages, Bremen, 2003.

No. 207 **Rakic, S.**
Untersuchungen zur Polymorphie und Kristallchemie von Silikaten der Zusammensetzung $Me_2Si_2O_5$ (Me:Na, K). 139 pages, Bremen, 2003.

No. 208 **Pfeifer, K.**
Auswirkungen frühdiagenetischer Prozesse auf Calcit- und Barytgehalte in marinen Oberflächen-sedimenten. 110 pages, Bremen, 2003.

No. 209 **Heuer, V.**
Spurenelemente in Sedimenten des Südatlantik. Primärer Eintrag und frühdiagenetische Überprägung. 136 pages, Bremen, 2003.

No. 210 **Streng, M.**
Phylogenetic Aspects and Taxonomy of Calcareous Dinoflagellates. 157 pages, Bremen 2003.

No. 211 **Boeckel, B.**
Present and past coccolith assemblages in the South Atlantic: implications for species ecology, carbonate contribution and palaeoceanographic applicability. 157 pages, Bremen, 2003.

No. 212 **Precht, E.**
Advective interfacial exchange in permeable sediments driven by surface gravity waves and its ecological consequences. 131 pages, Bremen, 2003.

No. 213 **Frenz, M.**
Grain-size composition of Quaternary South Atlantic sediments and its paleoceanographic significance. 123 pages, Bremen, 2003.

No. 214 **Meggers, H. and cruise participants**
Report and preliminary results of METEOR Cruise M 53/1, Limassol - Las Palmas – Mindelo, 30.03.2002 - 03.05.2002. 81 pages, Bremen, 2003.

No. 215 **Schulz, H.D. and cruise participants**
Report and preliminary results of METEOR Cruise M 58/1, Dakar – Las Palmas, 15.04..2003 – 12.05.2003. Bremen, 2003.

No. 216 **Schneider, R. and cruise participants**
Report and preliminary results of METEOR Cruise M 57/1, Cape Town – Walvis Bay, 20.01. – 08.02.2003. 123 pages, Bremen, 2003.

No. 217 **Kallmeyer, J.**
Sulfate reduction in the deep Biosphere. 157 pages, Bremen, 2003.

No. 218 **Røy, H.**
Dynamic Structure and Function of the Diffusive Boundary Layer at the Seafloor. 149 pages, Bremen, 2003.

No. 219 **Pätzold, J., C. Hübscher and cruise participants**
Report and preliminary results of METEOR Cruise M 52/2&3, Istanbul – Limassol – Limassol, 04.02. – 27.03.2002. Bremen, 2003.

No. 220 **Zabel, M. and cruise participants**
Report and preliminary results of METEOR Cruise M 57/2, Walvis Bay – Walvis Bay, 11.02. – 12.03.2003. 136 pages, Bremen 2003.

No. 221 **Salem, M.**
Geophysical investigations of submarine prolongations of alluvial fans on the western side of the Gulf of Aqaba-Red Sea. 100 pages, Bremen, 2003.

No. 222 **Tilch, E.**
Oszillation von Wattflächen und deren fossiles Erhaltungspotential (Spiekerooger Rückseitenwatt, südliche Nordsee). 137 pages, Bremen, 2003.

No. 223 **Frisch, U. and F. Kockel**
Der Bremen-Knoten im Strukturnetz Nordwest-Deutschlands. Stratigraphie, Paläogeographie, Strukturgeologie. 379 pages, Bremen, 2004.

No. 224 **Kolonic, S.**
Mechanisms and biogeochemical implications of Cenomanian/Turonian black shale formation in North Africa: An integrated geochemical, millennial-scale study from the Tarfaya-LaAyoune Basin in SW Morocco. 174 pages, Bremen, 2004. Report online available only.

No. 225 **Panteleit, B.**
Geochemische Prozesse in der Salz- Süßwasser Übergangszone. 106 pages, Bremen, 2004.

No. 226 **Seiter, K.**
Regionalisierung und Quantifizierung benthischer Mineralisationsprozesse. 135 pages, Bremen, 2004.

No. 227 **Bleil, U. and cruise participants**
Report and preliminary results of METEOR Cruise M 58/2, Las Palmas – Las Palmas (Canary Islands, Spain), 15.05. – 08.06.2003. 123 pages, Bremen, 2004.

No. 228 **Kopf, A. and cruise participants**
Report and preliminary results of SONNE Cruise SO175, Miami - Bremerhaven, 12.11 - 30.12.2003. 218 pages, Bremen, 2004.

No. 229 **Fabian, M.**
Near Surface Tilt and Pore Pressure Changes Induced by Pumping in Multi-Layered Poroelastic Half-Spaces. 121 pages, Bremen, 2004.

No. 230 **Segl, M. , and cruise participants**
Report and preliminary results of POSEIDON cruise 304 Galway – Lisbon, 5. – 22. Oct. 2004. 27 pages, Bremen 2004

No. 231 **Meinecke, G. and cruise participants**
Report and preliminary results of POSEIDON Cruise 296, Las Palmas – Las Palmas, 04.04 – 14.04.2003. 42 pages, Bremen 2005.

No. 232 **Meinecke, G. and cruise participants**
Report and preliminary results of POSEIDON Cruise 310, Las Palmas – Las Palmas, 12.04 – 26.04.2004. 49 pages, Bremen 2005.

No. 233 **Meinecke, G. and cruise participants**
Report and preliminary results of METEOR Cruise 58/3, Las Palmas - Ponta Delgada, 11.06 - 24.06.2003. 50 pages, Bremen 2005.

No. 234 **Feseker, T.**
Numerical Studies on Groundwater Flow in Coastal Aquifers. 219 pages. Bremen 2004.

No. 235 **Sahling, H. and cruise participants**
Report and preliminary results of R/V POSEIDON Cruise P317/4, Istanbul-Istanbul , 16 October - 4 November 2004. 92 pages, Bremen 2004.

No. 236 **Meinecke, G. und Fahrtteilnehmer**
Report and preliminary results of POSEIDON Cruise 305, Las Palmas (Spain) - Lisbon (Portugal), October 28th – November 6th, 2004. 43 pages, Bremen 2005.

No. 237 **Ruhland, G. and cruise participants**
Report and preliminary results of POSEIDON Cruise 319, Las Palmas (Spain) - Las Palmas (Spain), December 6th – December 17th, 2004. 50 pages, Bremen 2005.

No. 238 **Chang, T.S.**
Dynamics of fine-grained sediments and stratigraphic evolution of a back-barrier tidal basin of the German Wadden Sea (southern North Sea). 102 pages, Bremen 2005.

No. 239 **Lager, T.**
Predicting the source strength of recycling materials within the scope of a seepage water prognosis by means of standardized laboratory methods. 141 pages, Bremen 2005.

No. 240 **Meinecke, G.**
DOLAN - Operationelle Datenübertragung im Ozean und Laterales Akustisches Netzwerk in der Tiefsee. Abschlußbericht. 42 pages, Bremen 2005.

No. 241 **Guasti, E.**
Early Paleogene environmental turnover in the southern Tethys as recorded by foraminiferal and organic-walled dinoflagellate cysts assemblages. 203 pages, Bremen 2005.

No. 242 **Riedinger, N.**
Preservation and diagenetic overprint of geochemical and geophysical signals in ocean margin sediments related to depositional dynamics. 91 pages, Bremen 2005.

No. 243 **Ruhland, G. and cruise participants**
Report and preliminary results of POSEIDON cruise 320, Las Palmas (Spain) - Las Palmas (Spain), March 08th - March 18th, 2005. 57 pages, Bremen 2005.

No. 244 **Inthorn, M.**
Lateral particle transport in nepheloid layers – a key factor for organic matter distribution and quality in the Benguela high-productivity area. 127 pages, Bremen, 2006.

No. 245 **Aspetsberger, F.**
Benthic carbon turnover in continental slope and deep sea sediments: importance of organic matter quality at different time scales. 136 pages, Bremen, 2006.

No. 246 **Hebbeln, D. and cruise participants**
Report and preliminary results of RV SONNE Cruise SO-184, PABESIA, Durban (South Africa) – Cilacap (Indonesia) – Darwin (Australia), July 08th - September 13th, 2005. 142 pages, Bremen 2006.

No. 247 **Ratmeyer, V. and cruise participants**
Report and preliminary results of RV METEOR Cruise M61/3. Development of Carbonate Mounds on the Celtic Continental Margin, Northeast Atlantic. Cork (Ireland) – Ponta Delgada (Portugal), 04.06. – 21.06.2004. 64 pages, Bremen 2006.

No. 248 **Wien, K.**
Element Stratigraphy and Age Models for Pelagites and Gravity Mass Flow Deposits based on Shipboard XRF Analysis. 100 pages, Bremen 2006.

No. 249 **Krastel, S. and cruise participants**
Report and preliminary results of RV METEOR Cruise M65/2, Dakar - Las Palmas, 04.07. – 26.07.2005. 185 pages, Bremen 2006.

No. 250 **Heil, G.M.N.**
Abrupt Climate Shifts in the Western Tropical to Subtropical Atlantic Region during the Last Glacial. 121 pages, Bremen 2006.

No. 251 **Ruhland, G. and cruise participants**
Report and preliminary results of POSEIDON Cruise 330, Las Palmas – Las Palmas, November 21th – December 03rd, 2005. 48 pages, Bremen 2006.

No. 252 **Mulitza , S. and cruise participants**
Report and preliminary results of METEOR Cruise M65/1, Dakar – Dakar, 11.06.- 1.07.2005. 149 pages, Bremen 2006.

No. 253 **Kopf, A. and cruise participants**
Report and preliminary results of POSEIDON Cruise P336, Heraklion - Heraklion, 28.04. – 17.05.2006. 127 pages, Bremen, 2006.

No. 254 **Wefer, G. and cruise participants**
Report and preliminary results of R/V METEOR Cruise M65/3, Las Palmas - Las Palmas (Spain), July 31st - August 10th, 2005. 24 pages, Bremen 2006.

No. 255 **Hanebuth, T.J.J. and cruise participants**
Report and first results of the POSEIDON Cruise P342 GALIOMAR, Vigo – Lisboa (Portugal), August 19th – September 06th, 2006. Distribution Pattern, Residence Times and Export of Sediments on the Pleistocene/Holocene Galician Shelf (NW Iberian Peninsula). 203 pages, Bremen, 2007.

No. 256 **Ahke, A.**
Composition of molecular organic matter pools, pigments and proteins, in Benguela upwelling and Arctic Sediments. 192 pages, Bremen 2007.

No. 257 **Becker, V.**
Seeper - Ein Modell für die Praxis der Sickerwasserprognose. 170 pages, Bremen 2007.

No. 258 **Ruhland, G. and cruise participants**
Report and preliminary results of Poseidon cruise 333, Las Palmas (Spain) – Las Palmas (Spain), March 1st – March 10th, 2006. 32 pages, Bremen 2007.

No. 259 **Fischer, G., G. Ruhland and cruise participants**
Report and preliminary results of Poseidon cruise 344, leg 1 and leg 2, Las Palmas (Spain) – Las Palmas (Spain), Oct. 20th –Nov 2nd & Nov. 4th – Nov 13th, 2006. 46 pages, Bremen 2007.

No. 260 **Westphal, H. and cruise participants**
Report and preliminary results of Poseidon cruise 346, MACUMA. Las Palmas (Spain) – Las Palmas (Spain), 28.12.2006 – 15.1.2007. 49 pages, Bremen 2007.

No. 261 **Bohrmann, G., T. Pape, and cruise participants**
Report and preliminary results of R/V METEOR Cruise M72/3, Istanbul – Trabzon – Istanbul, March 17th – April 23rd, 2007. Marine gas hydrates of the Eastern Black Sea. 130 pages, Bremen 2007.

No. 262 **Bohrmann, G., and cruise participants**
Report and preliminary results of R/V METEOR Cruise M70/3, Iraklion – Iraklion, 21 November – 8 December 2006. Cold Seeps of the Anaximander Mountains / Eastern Mediterranean. 75 pages, Bremen 2008.

No. 263 **Bohrmann, G., Spiess, V., and cruise participants**
Report and preliminary results of R/V Meteor Cruise M67/2a and 2b, Balboa -- Tampico -- Bridgetown, 15 March -- 24 April, 2006. Fluid seepage in the Gulf of Mexico. Bremen 2008.